Bedrock Geology and Ore Deposits of the Palmer Quadrangle, Marquette County, Michigan

GEOLOGICAL SURVEY PROFESSIONAL PAPER 769

Prepared in cooperation with the Geological Survey Division of the Michigan Department of Natural Resources

Bedrock Geology and Ore Deposits of the Palmer Quadrangle, Marquette County, Michigan

By JACOB E. GAIR

With a section on THE EMPIRE MINE

By TSU-MING HAN, CLEVELAND CLIFFS IRON COMPANY

GEOLOGICAL SURVEY PROFESSIONAL PAPER 769

Prepared in cooperation with the Geological Survey Division of the Michigan Department of Natural Resources

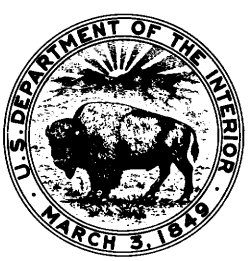

Middle Precambrian metasedimentary rocks of the Marquette synclinorium in the north half of the Palmer quadrangle contain important iron ore deposits and overlie lower Precambrian gneiss exposed to the south

UNITED STATES GOVERNMENT PRINTING OFFICE, WASHINGTON : 1975

UNITED STATES DEPARTMENT OF THE INTERIOR

STANLEY K. HATHAWAY, *Secretary*

GEOLOGICAL SURVEY

V. E. McKelvey, *Director*

Library of Congress Cataloging in Publication Data

Gair, Jacob Eugene, 1922–
Bedrock geology and ore deposits of the Palmer quadrangle, Marquette County, Michigan.

(Geological Survey professional paper ; 769)
Bibliography: p.
Includes index.
Supt. of Docs. no.: I 19.16:769
1. Geology—Michigan—Marquette Co. 2. Iron ores—Michigan—Marquette Co. I. Michigan. Geological Survey Division. II. Title. III. Series: United States. Geological Survey. Professional paper ; 769.
QE126.M35G27 557.44'96 75-619107

For sale by the Superintendent of Documents, U.S. Government Printing Office
Washington, D.C. 20402
Stock Number 024-001-02668-6

CONTENTS

ILLUSTRATIONS

[Plates are in pocket]

TABLES

BEDROCK GEOLOGY AND ORE DEPOSITS OF THE PALMER QUADRANGLE, MARQUETTE COUNTY, MICHIGAN

By JACOB E. GAIR

ABSTRACT

The Palmer quadrangle is in the southeast part of the Marquette iron range, Michigan. The area is underlain mainly by lower Precambrian gneiss and middle Precambrian metasedimentary and metaintrusive rocks. Upper Precambrian (Keweenawan) diabase dikes cut some units of the older Precambrian rocks.

At least two major episodes of deformation and metamorphism have affected rocks in the area. During the first episode, before the beginning of middle Precambrian time, metamorphism reached the amphibolite grade; during the other, the Penokean orogeny, at the close of middle Precambrian time, metamorphism varied in parts of the area from chlorite to biotite grade. Widespread but mild and irregular uplift and erosion also occurred twice during middle Precambrian time, without attendant metamorphism.

Major structural-stratigraphic features are (1) the west-trending, west-plunging Marquette synclinorium of middle Precambrian rocks constituting the Marquette Range Supergroup in the north half of the quadrangle; (2) the Palmer basin—a downfolded, downfaulted outlier of middle Precambrian rocks bordering the synclinorium proper on the south; and (3) the broad uplifted area of lower Precambrian gneiss occupying much of the south half of the quadrangle. In the north half of the quadrangle, the south side of the Marquette synclinorium is deformed into several west-plunging folds, en echelon from northeast to southwest. Steep west-trending faults are associated with these and lesser folds in the synclinorium. The largest fault is the Palmer fault, which marks the south edge of the synclinorium proper for many miles, and which in the central part of the quadrangle separates the Palmer basin from the main part of the synclinorium. Some west-trending faults are cut by faults trending northwest or north-northeast.

The lower Precambrian rocks in the area comprise the Compeau Creek Gneiss, Palmer Gneiss, and dikes of metadiabase. Palmer Gneiss is a mappable unit of comminuted, sericitized, chloritized, silicified, or carbonatized Compeau Creek Gneiss, in shear zones and elsewhere adjacent to the contact of the lower Precambrian gneissic rocks with middle Precambrian rocks.

The formations of the Marquette Range Supergroup are in the Chocolay, Menominee, and Baraga Groups. The Enchantment Lake Formation, Kona Dolomite, and Wewe Slate are definitely recognized formations of the Chocolay Group. The Kona Dolomite and Wewe Slate are northeast of Goose Lake but are not readily correlated as units with most rocks of the Chocolay Group south of Goose Lake. South of the lake, the only identifiable unit in the group is the Enchantment Lake Formation. Other rocks of the group are not divided into formations in that area but may include beds correlative with the Mesnard Quartzite east of the Palmer quadrangle as well as beds equivalent to the Kona and Wewe formations northeast of Goose Lake. Ajibik Quartzite, Siamo Slate, and Negaunee Iron-Formation constitute the Menominee Group, and Goodrich Quartzite is the basal part of the Baraga Group. The base of the Ajibik and Goodrich Quartzites contains local lenses of conglomerate; each of these formations is essentially conformable with the formation beneath it but is separated locally from the underlying unit by an erosional disconformity.

The Enchantment Lake Formation consists mainly of conglomerate, but has minor beds of quartzite, wacke, arkose, slate, and schist. Some of the conglomerate contains dropstones in a matrix of laminated slate and may have formed during glaciation.

The Kona Dolomite consists of interlaminated dolomite and chert, massive dolomite, and subordinate beds of slate, dolomitic quartzite, and quartzite. Algal structures are present in at least three stratigraphic zones. Locally the dolomite is silicified. The Kona Dolomite in the quadrangle has a maximum thickness of 2,500 feet.

The Wewe Slate is mainly gray quartz-sericite slate. The formation is 400–600 feet thick north of Goose Lake.

In the Wewe Hills south of Goose Lake, the undivided Chocolay Group consists principally of slate, impure quartzite, wacke, arkose, and schist. A distinctive lens of sericite-quartz-andalusite-chloritoid-cordierite(?) schist about 300 feet thick occurs in the group along the north slope of the Wewe Hills in sec. 23, T. 47 N., R. 26 W. Other chloritoid-bearing schist occurs adjacent to the Palmer fault one-half mile northeast of the village of Palmer. In the Wewe Hills, the undivided Chocolay Group rests either on lower Precambrian gneiss or more commonly on Enchantment Lake rocks. Divergent attitudes and the absence of mappable marker beds in areas of best exposure preclude an accurate measurement of thickness of the undivided Chocolay Group in the Wewe Hills.

The Ajibik Quartzite consists of vitreous quartzite in the northeast part of the quadrangle, north of Goose Lake, but to the south and southwest it also contains sericitic quartzite and wacke and subordinate sericite slate. Conglomerate at the base of the formation rests on undivided Chocolay rocks in the Marquette synclinorium northeast of Palmer and on lower Precambrian gneiss along the south edge of the Palmer basin. The thickness of the Ajibik in the quadrangle is 450–600 feet.

Major lithologic types of the Siamo Slate are slate, sericitic, chloritic, and feldspathic quartzites, arkose, and graywacke. A bed of siderite-magnetite-iron silicate iron-forma-

tion, the Goose Lake Member, extends continuously for 4–5 miles and is 50–100 feet thick. Ungraded common graywacke beds, several inches to several feet thick, are interpreted to be a result of short-distance transportation of sediment in submarine mudflows that allowed little opportunity for differential settling of clastic grains. The maximum thickness could be as much as 3,000 feet; the minimum thickness in the synclinorium proper is 1,000 feet. In the south part of the Palmer basin the Siamo virtually disappears or forms an unmappable zone not more than a few tens of feet thick between Ajibik Quartzite and Negaunee Iron-Formation.

The Negaunee Iron-Formation is metasedimentary rock which contains (1) siderite, magnetite, iron silicates, and chert, or (2) mixtures of hematite, magnetite, and chert. The Negaunee is the source of iron ore mined in the quadrangle. The iron minerals and chert may form monomineralic laminae or may be intermixed in thin layers, the assemblages differing in practically infinite variety from layer to layer. Thicker layers commonly have granules of silicate, carbonate, magnetite, hematite, or chert. Clastic sediment is present in the iron-formation in the south part of the synclinorium and in the Palmer basin.

The iron-formation is classified by facies on the basis of the dominant iron mineral as carbonate, oxide (magnetite or hematite), silicate, and as mixed facies of carbonate-magnetite, carbonate-silicate, magnetite-silicate, and carbonate-magnetite-silicate. A small part of the iron-formation contains riebeckite and (or) aegirinaugite. Iron minerals may be of primary, diagenetic, or low-grade metamorphic origin. Anomalous grunerite in the nominally low-grade metamorphic zone formed by contact metamorphism during the intrusion of mafic sills into the iron-formation.

Characteristics of the iron-formation are noted in the axial sector of the Marquette synclinorium, in the Empire-south limb sector, and in the Palmer basin. In the axial sector, the iron-formation is intruded by four thick sills of metadiabase which divide the iron-formation into stratigraphic segments. The lowermost sill, the Tracy sill, is 1,100–1,200 feet above the base of the iron-formation. The iron-formation has a maximum thickness of about 3,500 feet in the northeast part of the Empire-south limb sector and thicknesses of 450–1,300 feet in the Palmer basin. The lower 900–1,000 feet of iron-formation in the axial sector is thinly laminated and dominantly sideritic, and contains subordinate silicate and magnetite. The lower 100 feet contains beds of slate in a gradational zone above the Siamo. The upper 150–200 feet of iron-formation below the Tracy sill is characterized by granular and nongranular layers, ½–4 inches thick, rich in minnesotaite, magnetite, and chert. Much of the iron-formation beneath the Tracy sill is oxidized to secondary hematite and goethite and has been partially leached of chert within 1,000–1,500 feet down from the surface.

The Empire mine provides most of the data on the iron-formation in the Empire-south limb sector. Principal varieties contain assemblages of magnetite-chert-carbonate, magnetite-carbonate-silicate-chert, and chert-carbonate. Numerous shallow-water and preconsolidation slump structures are present in the iron-formation. Residual "islands" mainly of siderite-chert are present in parts of magnetite-rich beds and indicate secondary derivation of the magnetite, probably by oxidation-replacement of siderite-chert beds during diagenesis.

The iron-formation in the west half of the Palmer basin is largely jaspilite (cherty hematitic oxide facies), or assemblages of magnetite-chert and magnetite-carbonate-chert, and oxidized iron-formation probably derived from varieties rich in magnetite and carbonate. In the east half of the Palmer basin, iron-formation is extensively oxidized to secondary hematite and goethite. The preoxidation rock probably was rich in carbonate and (or) magnetite. Magnetite-carbonate iron-formation is the dominant variety at the southeast end of the basin. Clastic sediment is common in the iron-formation in the central, south-central, and southeast parts of the basin.

The iron-formation is believed to have formed by chemical precipitation of the principal iron minerals and silica gel. The alternation of different iron minerals in layers may reflect the effect of the precipitation of one iron mineral on the subsequent precipitation of a second iron mineral. Some magnetite—possibly large amounts—also formed by replacement of ferrous iron minerals during diagenesis, and most iron silicate probably formed by metamorphism of an earlier silicate mineral. Some silicate probably also formed by reactions between iron carbonate or iron oxide and chert or clastic quartz during diagenesis. Recrystallized (metamorphosed) hematite has probably been formed both from primary hematite and from iron oxide derived by the oxidation of ferrous iron minerals prior to regional metamorphism. Clastic sedimentation during deposition of the iron-formation is attributed to disturbances caused by faulting along the south edge of the Palmer basin and Marquette synclinorium in zones marked by Palmer Gneiss. The fault movements are believed to have been an early stage of the deformation that culminated during the Penokean orogeny at the end of middle Precambrian time.

The Goodrich Quartzite consists mainly of quartzite of varying composition and basal lenses of conglomerate. Minor amounts of monazite containing radioactive thorium are present in the formation. Boulders and smaller angular fragments of jaspilitic iron-formation are a part of the conglomerate. The thickness of the Goodrich in the quadrangle is 1,000–1,400 feet, but because of erosion, the total original thickness is unknown. East of the village of Palmer, a lens of metamorphosed mafic pyroclastic rock and vitrophyric flow rock at least several hundred feet thick occupies an equivalent stratigraphic position to the Goodrich, above the Negaunee Iron-Formation. The deposition of the Goodrich was preceded by slight local uplift and erosion of parts of the area; locally the Negaunee remained submerged and is overlain by the Goodrich without an intervening erosion surface.

Intrusive rocks in the quadrangle are sills and dikes of metadiabase and dikes of diabase. The metadiabase is of early and middle Precambrian age, predating Penokean metamorphism, and the diabase is of late Precambrian age. North-trending dikes in the lower Precambrian gneiss that end at the south edge of the Palmer basin probably are of early Precambrian age. Dikes of highly altered chloritic and sericitic rock that cut the Negaunee Iron-Formation probably were metadiabase prior to alteration that is believed to be associated with oxidation of the iron-formation.

Quartz veins and brecciated quartz and silicified rock are common along fractures and fault zones, particularly along the Palmer fault and in many linear zones in the Wewe Hills in sec. 23, T. 47 N., R. 26 W. The most conspicuous quartz vein extends about 5,500 feet southeast from the west edge of the quadrangle at the line between T. 46 N., and T. 47 N. No known metallization is associated with vein quartz

in the quadrangle, except for small occurrences of specular hematite in the Wewe Hills. Dolomite-quartz veins are found in a few places in the Palmer Gneiss and the north part of the Compeau Creek Gneiss. Patchy concentrations of pyrite occur in two places, one in gneiss adjacent to a metadiabase dike, and the other in Ajibik quartzite at the south edge of the Palmer basin.

Major west- to northwest-plunging folds within the Marquette synclinorium include anticlines under the Kona Hills and Wewe Hills, the Goose Lake syncline between those anticlines, an anticline under the Ajibik Hills southwest of the Wewe Hills anticline, the syncline between the Ajibik Hills and Wewe Hills anticline, broad synclines separated by narrow anticlines or faults in secs. 7 and 18, T. 47 N., R. 26 W., and sec. 13, T. 47 N., R. 27 W., and tight fault-bounded synclines between broader anticlines in secs. 5 and 8, T. 47 N., R. 26 W. Two of the tight fault-bounded synclines are sites of the important Athens and Tracy ore bodies. The eastern part of the Palmer basin is occupied by a poorly defined east-west syncline, the south limb of which is complexly folded into a second-order doubly plunging syncline in the SW¼ sec. 27, T. 47 N., R. 26 W. The northwest-plunging Isabella syncline is a major subsidiary fold in the western part of the Palmer basin.

Major faults are associated with folding of the Marquette synclinorium. The axial part of the synclinorium is extensively sliced by east-west faults. The Palmer basin is bounded on the north by the Palmer fault, and is dissected by the major Volunteer, Richmond, and Warner Creek faults. Much of the south margin of the basin is a fault or shear zone.

Foliation in the Compeau Creek Gneiss trends east to southeast, and in general is discordant with the fault-bounded south edge of the Marquette synclinorium and Palmer basin.

Most iron mining in the quadrangle dates from 1870. Major categories of ore are taconite ore and hard and soft ore and intermediate semihard ore. The hard and soft types compositionally encompass Bessemer and non-Bessemer ore, siliceous ore, and manganiferous ore. Total production to date has been about 90 million tons, which includes 14 million tons of siliceous ore and 25 million tons of pellets made from taconite ore. Of about a dozen mines in the quadrangle that have produced more than 1 million tons of iron ore each, only one was in operation in 1972. Ore mined before 1963 consisted entirely of iron oxide concentrated by natural processes. Since 1963, taconite ore taken at the Empire mine, from which magnetite is concentrated artifically and pelletized, has been a major part of production from the quadrangle. The Tracy mine where the last mining of natural (soft) iron ore was done in the quadrangle, was closed in January 1971.

Bodies of soft ore are localized in upward-opening structural traps, mainly synclines and troughs made by dike intersections with tilted iron-formation or by slate faulted against tilted iron-formation. Ore is underlain by relatively impermeable slate, intrusive rock, or parts of the iron-formation. Dikes or slate faulted against iron-formation commonly form barriers on the upper side of which soft ore has accumulated. Bodies of hard ore invariably have formed just under the erosional contact between the iron-formation and Goodrich Quartzite. Hard ore was concentrated substantially, if not entirely, before regional metamorphism.

Soft ore probably formed during the Paleozoic-Keweenawan interval, 600 million to 900 million years ago. Available evidence indicates that soft ore was formed by (1) the action of supergene ground water which caused oxidation of ferrous iron minerals of the preore iron-formation, principally siderite; (2) leaching of chert and its replacement by secondary hematite and goethite; and (3) removal of large amounts of CO_2. A deep gypsiferous zone in areas of oxidized iron-formation and soft ore east and southeast of Negaunee apparently is distributed in the configuration of a former land surface or water table. Evidence for hypogene ground water is equivocal, and its possible effects appear to be minor—principally the deposition of some clay minerals and manganese oxide in vugs and cracks in oxidized iron-formation and soft ore.

Hard ore is believed to have formed by oxidation and enrichment of carbonate iron-formation to soft ore during a period of middle Precambrian weathering followed by metamorphism during Penokean orogeny, which caused the soft ore to recrystallize to hard ore. Some local enrichment of ore may have been caused by the mobilization of connate or bonded water in oxidized iron-formation and soft ore during Penokean metamorphism.

The monazite content of the Goodrich Quartzite constitutes a large low-grade thorium resource. The total estimated quantity of thorium is 169,500 tons, but much of it probably will never be recoverable because of its wide dispersion and deep burial.

INTRODUCTION

LOCATION, EXTENT, AND ACCESSIBILITY OF AREA

The Palmer 7½-minute quadrangle is a few miles east and southeast of the central part of the Marquette iron range, east-central Marquette County, in the northern peninsula of Michigan (lat 46°22′30″–46°30′ N. and long 87°30′–87°37′30″ W.; fig. 1). The quadrangle occupies an area of about 51 square miles in most of T. 47 N., R. 26 W., and adjoining parts of T. 46 N., R. 26 W., and T. 47 N., R. 27 W. On the east, north, and west it is bordered respectively by the Sands, Negaunee, and Ishpeming 7½-minute quadrangles. The northeast corner of the Palmer quadrangle is 5 miles southwest of the city of Marquette, the county seat and a major iron-ore port on Lake Superior. The quadrangle is named for the village of Palmer in the west-central part of the area. Part of the iron-mining city of Negaunee, site of the first discovery of iron ore in the Lake Superior region, is in the northwestern part of the quadrangle. The large low-grade Empire iron (taconite) mine is just northwest of Palmer. Railroads and good highways connect Negaunee and Palmer to Marquette and to the iron-ore port of Escanaba on Lake Michigan. Few places in the quadrangle are farther than 1 mile from drivable roads.

TOPOGRAPHY AND DRAINAGE

Much of the Palmer quadrangle is characterized by relatively rugged knobby topography and is covered by a dense second-growth forest. Elevations

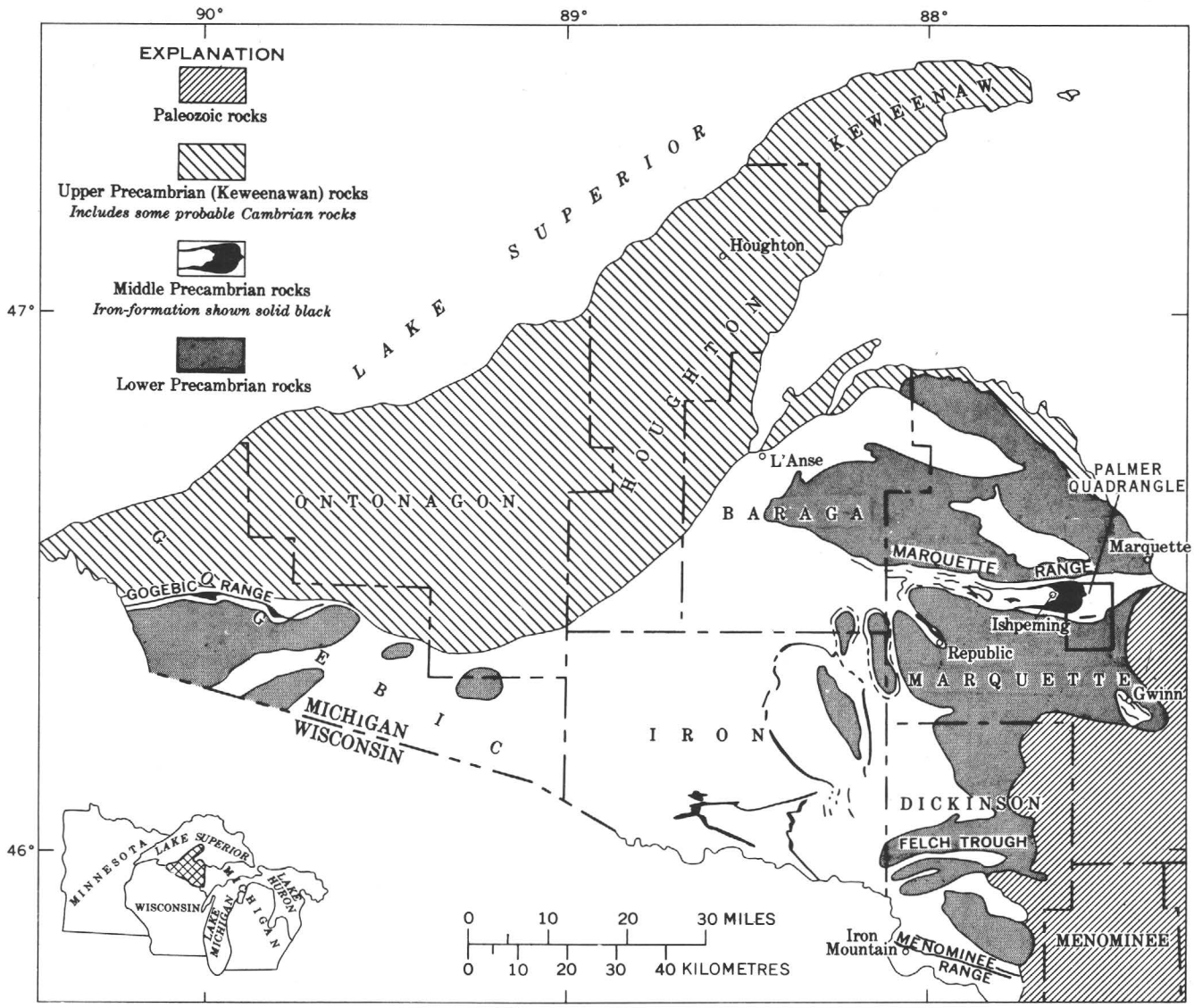

FIGURE 1.—Geologic sketch map of western part of northern peninsula of Michigan, showing location of Palmer quadrangle.

range from about 1,160 feet above sea level near the southeast corner to about 1,780 feet 1½ miles northwest of Palmer. The most prominent rises are the Kona Hills in the northeastern part of the quadrangle, the Wewe Hills and their westward extension between Goose Lake in sec. 14, T. 47 N., R. 26 W., and the village of Palmer (including unnamed hill in NW ¼ sec. 28–NE ¼ sec. 29 called Ajibik Hills by Van Hise and Bayley in 1897, and now called "Hendrickson Bluff" by local residents), ridges extending from sec. 10 to sec. 20, T. 47 N., R. 26 W., the belt of hills reaching 3 miles south from Negaunee, and the broad east-west belt of hills south of Palmer. Part of an extensive sand plain in the Sands quadrangle to the east continues into the east-central part of the Palmer quadrangle.

The area is entirely within the Lake Michigan drainage basin, and drainage has a distinctive southeastward grain. The largest stream is the East Branch of the Escanaba River, which forms in the south-central part of the quadrangle from the confluence of Warner and Schweitzer Creeks. The Goose Lake system drains much of the north-central and eastern parts of the quadrangle. Small swamps occur at widely different elevations in much of the area.

PRESENT INVESTIGATION

The mapping of the Palmer quadrangle is part of a continuing program by the U.S. Geological Survey, in cooperation with the Michigan Department of Natural Resources, to remap the Marquette iron

range on modern topographic base maps, for publication at 1:24,000 scale.

The first phase of the mapping was done in the Marquette and Sands quadrangles at the eastern end of the iron range between 1957 and 1960 (Gair and Thaden, 1968). The Negaunee and Palmer quadrangles, immediately west of the Marquette and Sands quadrangles, respectively, are the next areas in which mapping has been completed. Fieldwork in the Palmer quadrangle, including ground magnetometer surveys covering approximately 8 square miles, was done between 1961 and 1968 and required about 28 man months. An additional 3–4 man months was spent studying drill core.

In most of the quadrangle, mapping was done directly on topographic sheets enlarged to 1:12,000 scale. The field compilation was reduced to 1:24,000 for publication (pl. 1). All known outcrops have been plotted on the map. Outcrops were located by pace and compass traverses from known points and by reference to topographic features. Most traversing in the northern half of the quadrangle was done with the aid of a sundial compass.

Many references to specific locations are given in the following pages, in feet and direction from a section corner; for example, 850N–2550E of a southwest corner or 500S–1800W of a northeast corner.

Ground magnetic surveys have been made in the north-central part of the quadrangle and in the Palmer area at 1:6,000 scale. Structural data at the New Richmond open-pit mine have been plotted on a planetable base map of the pit, at 1:1,200 scale.

A detailed geologic map of a part of sec. 19, T. 47 N., R. 26 W., at 1:2,400 scale has been obtained from the Cleveland Cliffs Iron Co.

DRILL DATA

Drill data from logs and cores were of immense help in determining the distribution of the iron-formation and some adjacent rock units, and in studying iron-formation lithology.

Nearly 900 holes of record have been drilled from the surface in the quadrangle since the beginning of mining, in addition to countless holes from underground mine workings. Surface drill-hole locations are plotted on plate 1. An index map (pl. 8) and data sheets (at the end of the report) contain records of all surface drill holes and the following data if available: drill-hole number keyed to an arbitrary drill-hole location number (DHL), name of company, name of exploration if any, footage to ledge, total footage, type of rock at ledge, and dip and direction of drill hole.

ACKNOWLEDGMENTS

Kenneth L. Wier of the U.S. Geological Survey made a survey in 1963 of about 4½ square miles in the north-central part of the quadrangle with a Jalander magnetometer. S. Roger Kirkpatrick and Jack A. Hallberg assisted me with fieldwork in the area of dominantly lower Precambrian gneiss in the southern half of the quadrangle during the summers of 1963 and 1965, respectively.

The cooperation of the Cleveland Cliffs Iron Co., Jones and Laughlin Steel Corp., and U.S. Steel Corp. is gratefully acknowledged. These companies permitted entry to properties and examination of drill cores, drilling records, and maps. Part of the geology shown in the E½ sec. 7, T. 47 N., R. 26 W. (see pl. 1), is based on data supplied by the Jones and Laughlin Steel Corp.

GEOLOGIC SETTING

The north half of the Palmer quadrangle straddles the axial part and south limb of the west-trending, west-plunging Marquette synclinorium. The south half of the quadrangle contains mainly lower Precambrian gneissic and granitoid rocks which form the basement for metasedimentary and intrusive rocks of middle Precambrian age within the synclinorium. Lower and middle Precambrian rocks are cut by diabase dikes of late Precambrian (Keweenawan) age.

The sequence of middle Precambrian metasedimentary rocks in the quadrangle, from oldest to youngest, is Enchantment Lake Formation, Kona Dolomite, Wewe Slate, Ajibik Quartzite, Siamo Slate, Negaunee Iron-Formation, and Goodrich Quartzite. These formations are assigned to the Chocolay, Menominee, and Baraga Groups. The groups in turn form part of the Marquette Range Supergroup (Cannon and Gair, 1970), which is equal to "Animikie Series" of James (1958), but in accordance with later provisions of the Code of Stratigraphic Nomenclature (Am. Comm. Stratig. Nomenclature, 1961), "series" is now called "supergroup." The substitution of the supergroup term, "Marquette Range," for the terms "Huronian" and "Animikie" formerly applied to these rocks is a plan, consistent with present stratigraphic knowledge, to limit named supergroups to geographic districts of the Lake Superior region, within which correlations are reasonably certain. The Marquette Range Supergroup is restricted to middle Precambrian rocks on the south shore of Lake Superior. The positions of these formations relative to older and younger rocks of adjoining areas is shown in figure 2.

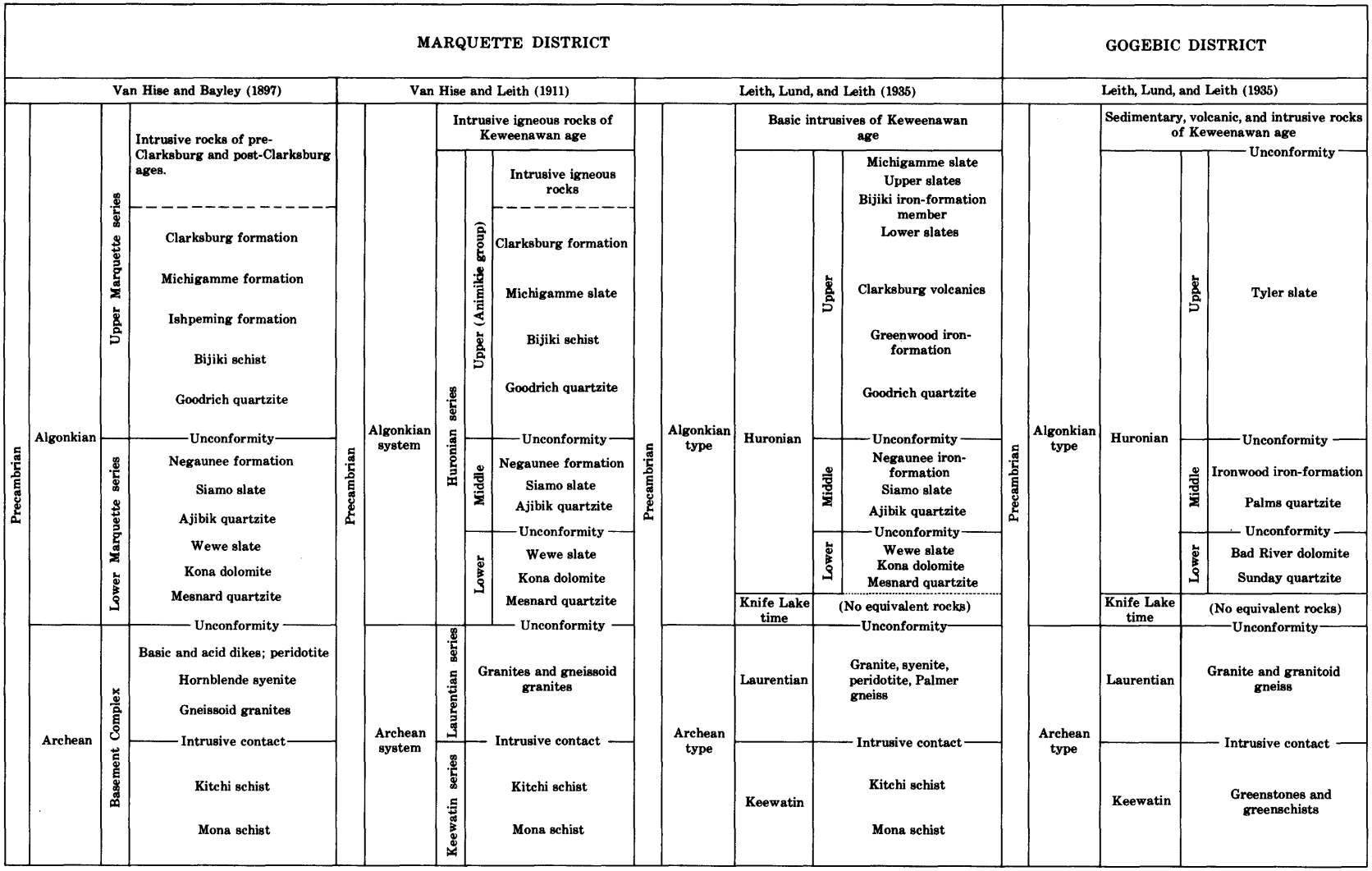
MARQUETTE DISTRICT
GOGEBIC DISTRICT
Van Hise and Bayley (1897)
Van Hise and Leith (1911)
Leith, Lund, and Leith (1935)
Leith, Lund, and Leith (1935)
Precambrian
Algonkian
Upper Marquette series
Intrusive rocks of pre-Clarksburg and post-Clarksburg ages.
Clarksburg formation
Michigamme formation
Ishpeming formation
Bijiki schist
Goodrich quartzite
Unconformity
Lower Marquette series
Negaunee formation
Siamo slate
Ajibik quartzite
Wewe slate
Kona dolomite
Mesnard quartzite
Unconformity
Archean
Basement Complex
Basic and acid dikes; peridotite
Hornblende syenite
Gneissoid granites
Intrusive contact
Kitchi schist
Mona schist
Precambrian
Algonkian system
Intrusive igneous rocks of Keweenawan age
Huronian series
Upper (Animikie group)
Intrusive igneous rocks
Clarksburg formation
Michigamme slate
Bijiki schist
Goodrich quartzite
Unconformity
Middle
Negaunee formation
Siamo slate
Ajibik quartzite
Unconformity
Lower
Wewe slate
Kona dolomite
Mesnard quartzite
Unconformity
Archean system
Laurentian series
Granites and gneissoid granites
Intrusive contact
Keewatin series
Kitchi schist
Mona schist
Precambrian
Algonkian type
Basic intrusives of Keweenawan age
Huronian
Upper
Michigamme slate
Upper slates
Bijiki iron-formation member
Lower slates
Clarksburg volcanics
Greenwood iron-formation
Goodrich quartzite
Unconformity
Middle
Negaunee iron-formation
Siamo slate
Ajibik quartzite
Unconformity
Lower
Wewe slate
Kona dolomite
Mesnard quartzite
Knife Lake time
(No equivalent rocks)
Unconformity
Archean type
Laurentian
Granite, syenite, peridotite, Palmer gneiss
Intrusive contact
Keewatin
Kitchi schist
Mona schist
Precambrian
Algonkian type
Sedimentary, volcanic, and intrusive rocks of Keweenawan age
Unconformity
Huronian
Upper
Tyler slate
Unconformity
Middle
Ironwood iron-formation
Palms quartzite
Unconformity
Lower
Bad River dolomite
Sunday quartzite
Knife Lake time
(No equivalent rocks)
Unconformity
Archean type
Laurentian
Granite and granitoid gneiss
Intrusive contact
Keewatin
Greenstones and greenschists

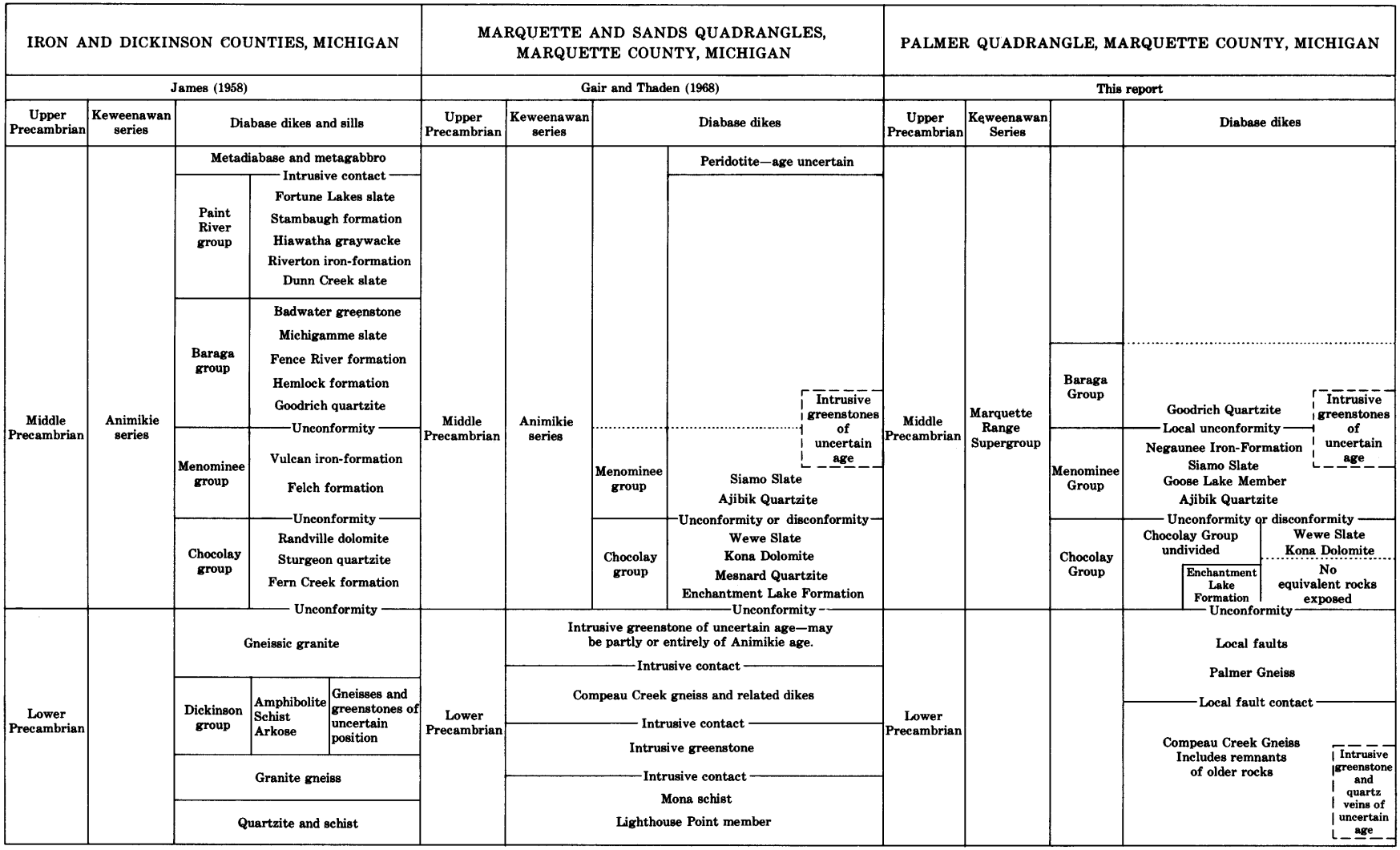

FIGURE 2.—Correlation chart of Precambrian rocks in parts of northern Michigan.

In the north half of the quadrangle, the south side of the Marquette synclinorium is bent into several west-plunging folds arranged en echelon from northeast to southwest. The folds widen the belt of Negaunee Iron-Formation to about 4 miles at the west edge of the quadrangle. Steep west-trending faults are associated with the folds. The largest, the Palmer fault, extends across the quadrangle from the south edge of the Wewe Hills in secs. 23 and 24, T. 47 N., R. 26 W., to the north side of Palmer Lake in sec. 25, T. 47 N., R. 27 W. Many west-trending folds and faults are cut by northwest-trending faults.

Geologic features may be grouped into several structural-stratigraphic-physiographic units, some of which extend eastward into the Sands quadrangle and help prove continuity with the geology of that area mapped earlier in the present program (Gair and Thaden, 1968). Continuity to the east is established by (1) areas of lower Precambrian gneiss underlying the extensive sand plain south of the Wewe Hills and adjoining the sand plain on the south, (2) the broad anticlinal area of Kona Dolomite underlying the Kona Hills northeast of Goose Lake in sec. 13, T. 47 N., R. 26 W., and (3) the west-trending belt of Ajibik Quartzite and Siamo Slate dipping northward toward the axis of the synclinorium on the north flank of the Kona Hills in secs. 11 and 12, T. 47 N., R. 26 W. In the Wewe Hills, south of Goose Lake, lower middle Precambrian slates, impure quartzites, conglomerates, and associated metasedimentary rocks overlie updomed lower Precambrian gneiss unconformably. The stratigraphic position of these rocks is established as lower middle Precambrian (Chocolay Group) by the underlying gneiss and overlying Ajibik Quartzite. Except for basal conglomerate in this sequence, which can be correlated with the Enchantment Lake Formation, the rocks in the Wewe Hills are generally unlike those characteristic of any of the other formations of the Chocolay Group to the northeast. Nevertheless, most rocks in the middle Precambrian of the Wewe Hills have counterparts in the Chocolay Group to the northeast, except for the carbonate rock of the Kona Dolomite, which is not present in the Wewe Hills. None of the rocks of the Chocolay Group in the Wewe Hills above the basal Enchantment Lake conglomerate is readily mapped as a stratigraphic unit corresponding to the Mesnard, Kona, or Wewe formations to the northeast. The rocks in the Wewe Hills above the Enchantment Lake and beneath the Ajibik may be equivalent to all or only to part of this sequence, and hence are assigned to the Chocolay Group without designation as to formation.

One of the most important structural features in the quadrangle and an outstanding feature of the entire Marquette iron range is the Palmer basin. Displacement downward to the south on the Palmer fault has somewhat isolated a large synclinal, canoe-shaped block of middle Precambrian rock south of the main part of the Marquette synclinorium. However, part of the north limb has been lost along the Palmer fault and the west end of the canoe-shaped syncline has been disrupted by the west-southwest-trending Volunteer fault. Furthermore, the central part of the canoe-shaped syncline is cut by the northwest-trending Richmond fault northeast of which altered lower Precambrian gneiss has been raised to the bedrock surface (Davis, 1965, p. 12–14).

Approximately the northwest quarter of the quadrangle, north of the Palmer fault, is occupied mainly by, from oldest to youngest, Siamo Slate, Negaunee Iron-Formation, and Goodrich Quartzite, and by mafic sill-like intrusive bodies in the broad core or axial area of the Marquette synclinorium. In passing from the north limb across the axis of the synclinorium to the south limb in this area, the Negaunee Iron-Formation strikes generally southeast to south to southwest and dips westward. Steep faults trending roughly westward and northwestward are common. A significant part of the iron-ore production of the Marquette range has come from this part of the quadrangle.

METAMORPHISM

Lower Precambrian rocks were regionally metamorphosed to amphibolite grade before middle Precambrian time, 2.6 billion years ago or earlier, probably at the same time that granitization occurred in the Compeau Creek Gneiss. During Penokean metamorphism at the close of middle Precambrian time about 1.9 billion years ago, middle Precambrian rocks were metamorphosed progressively to the chlorite and biotite grades and some of the already-metamorphosed lower Precambrian rocks were retrograded. The isograd between the chlorite and biotite zones trends southeast across the Marquette synclinorium near the city of Ishpeming (James, 1955, pl. 1), crosses the quadrangle boundary west of Palmer and extends irregularly eastward across the quadrangle, with the chlorite zone to the north and the biotite zone to the south (isograd not shown on pl. 1). The Penokean metamorphism was at the level of the upper biotite zone in most of

the two south tiers of sections in the quadrangle. During intrusion of middle Precambrian diabase sills into the Negaunee Iron-Formation in the area between the towns of Negaunee and Palmer, grunerite formed locally by contact metamorphism, and during the subsequent Penokean chlorite-grade metamorphism, it was retrograded in places to assemblages of quartz, magnetite, and iron carbonate.

LOWER PRECAMBRIAN ROCKS

COMPEAU CREEK GNEISS

DISTRIBUTION

Compeau Creek Gneiss forms the bulk of the lower Precambrian basement rock that occupies most of the south half of the quadrangle and a few small areas in the Wewe Hills between the Palmer basin and Goose Lake. The gneiss has been named for exposures along Compeau Creek in the Marquette 7½-minute quadrangle north of the Marquette synclinorium and has been correlated with gneiss south of the synclinorium in the Sands quadrangle because of similar rocks and structural relations (Gair and Thaden, 1968, p. 18). The main belt of gneiss in the Palmer quadrangle is continuous with that in the Sands quadrangle to the east.

COMPONENTS

The gneiss consists of foliated granite, massive nonfoliated granite, pegmatite, and layered rock—amphibolite and biotite schist and lighter colored probably granitized modifications of the dark-layered gneiss. The granitic rocks are biotitic, chloritic, or leucocratic. The term "granite" is used here as a general descriptive name encompassing a broad range of light-colored quartz-feldspar rocks having a granitoid texture and compositions of tonalite, granodiorite, quartz monzonite, and true granite. These varieties of granite are identified by the ratio of plagioclase to potassic feldspar (Gair and Thaden, 1968, table 9). Tonalite, which contains more than seven-eighths plagioclase, is the most abundant variety of granitic rock, whereas true granite, which contains more than two-thirds potassic feldspar, is rare. However, pegmatite, which is abundant in some parts of the gneiss, is rich in microcline or microcline-perthite and is true granite or quartz monzonite. The varieties of granite generally cannot be identified in the field and have not been mapped separately, but zones containing much dark gneiss are shown separately on plate 1.

Amphibolite and biotite schist commonly are interlayered with or pass along the strike of beds into lighter colored layered granitic gneiss or into foliated or nonfoliated granite. Foliated and nonfoliated massive granites surround zones of layered gneiss and are by far the most abundant part of the formation. Layered gneiss is commonly cut by dikes and veins of granite and pegmatite. In places, foliated granite is truncated by nonfoliated massive granite, and both the layered gneiss and nonlayered granite are cut by pegmatite and quartz veins. Gradations from foliated or massive granite into pegmatite are common. In a few places, one pegmatite cuts another.

LAYERED GNEISS

GENERAL FEATURES AND DISTRIBUTION

Layered gneiss is found principally in the northern and eastern parts of the area of Compeau Creek Gneiss. It occurs in the midst of nonlayered granite, in poorly defined irregular patches which generally have a southeastward elongation and together compose a roughly southeast-trending belt reaching from the west edge of the quadrangle west of the village of Palmer to the vicinity of the southeast corner of the quadrangle (pl. 1). Locally the layered gneiss trends north or northeast as in the SE¼ secs. 32 and 33, and at the east side of the Palmer basin in the NE¼ sec. 26 and the NW¼ sec. 35, T. 47 N., R. 26 W.

The layered gneiss consists of dark-green to black amphibolite and biotite schist, gray biotitic and chloritic quartz-feldspar rocks (granodiorite and tonalite), and green to dark-green rock of uncertain origin that may be metagraywacke, mafic crystal metatuff, or cataclastically deformed amphibolite. The dark-layered rock appears to be more abundant than the light-colored varieties. However, the light-colored types are not readily distinguished from nonlayered granitic rocks on weathered surfaces, so undoubtedly are present but unrecognized in many places and may be more abundant than the dark types. Only the readily recognized dark-layered varieties are shown differently from the rest of the formation on plate 1. Modes are listed in table 1. Only dark varieties are described in the following paragraphs on layered rocks. The light-colored granitic types differ little from foliated nonlayered granitic rock—mainly in having a more pronounced gathering of biotite, chlorite, and quartz-feldspar in layers—so these rocks are not described separately from the other granitic rocks.

AMPHIBOLITE

Much of the dark-layered gneiss shown on plate 1 consists of dark-green to black amphibolite. The

TABLE 1.—*Modes (volume percent),*

	1	2	3	4	5	6	7	8	9	10	11	12	13	14	15	16	17
Quartz	44.5	41.9	41.6	37.2	48.0	24.0	41.4	23.8	53.0	20.4	33.8	46.5	36.8	33.4	44.2	40.0	33.2
Plagioclase [1]	[2] 55.4	---	52.6	47.2	[3] 51.6	10.0	54.2	62.8	45.6	46.8	64.0	46.8	57.4	40.1	45.2	50.6	58.6
Microline	---	---	---	Tr	---	---	Tr	.9	---	---	---	---	---	---	---	---	---
Myrmekite	---	---	---	---	---	---	---	---	---	---	---	---	---	---	---	---	---
Muscovite-sericite	---	---	---	---	---	---	---	---	---	---	---	[4] 34.7	3.8	---	---	---	8.2
Hornblende	---	---	---	---	---	---	---	---	---	---	---	---	---	---	---	---	---
Biotite	---	---	.4	15.6	.4	53.8	4.6	12.5	---	2.2	---	---	.4	---	---	9.2	Tr
Chlorite	---	---	5.4	---	---	3.4	---	---	.4	12.0	1.0	1.8	1.4	22.1	10.0	---	---
Carbonate	---	---	---	Tr	Tr	3.0	---	---	---	15.0	.6	---	---	.4	---	Tr	.4
Epidote	---	---	---	---	Tr	4.6	---	---	1.0	2.8	---	---	---	---	---	---	---
Apatite	---	---	---	---	---	Tr	---	---	---	---	---	---	---	---	---	---	---
Sphene	---	---	---	---	---	---	---	---	---	---	---	---	---	---	---	---	---
Zircon	---	---	---	---	---	---	Tr	---	---	---	---	---	---	---	---	---	---
Opaque	---	---	---	---	---	---	Tr	---	---	.8	---	Tr	Tr	4.0	.6	---	---
Other	---	[5] 58.1	---	---	---	---	---	---	---	---	---	---	---	---	---	---	---

[1] Albite or oligoclase in most hornblende-poor rock; andesine in amphibolite.
[2] Plagioclase is almost entirely sericitized.
[3] Plagioclase is An_{32-37}.
[4] All or most of sericite replaces plagioclase.
[5] Slightly sericitized plagioclase is separated by well-alined lenses of chlorite.

1. JG–89–65; leucotonalite; 1,150N–1,740W of SE. cor. 25–47–27.
2. JG–97–65; chloritic tonalite; 370S–80W of NE. cor. 34–47–26.
3. JG–106–65; tonalite; 800S–2,600W of NE. cor. 36–47–27.
4. JG–107–65; biotitic tonalite; 2,150S–800W of NE. cor. 36–47–27.
5. JG–110–65 (1), tonalite—cuts biotite schist, JG–110–65 (2), see No. 6; 340S–400W of NE. cor. 5–46–26.
6. JG–110–65 (2), layered biotite schist—cut by tonalite, JG–110–65 (1), see No. 5; 350S–400W of NE. cor. 5–46–26.
7. JG–114–65; tonalite; 1,500S–1,570W of NE. cor. 3–46–26.
8. JG–55A–66; foliated biotitic tonalite; 2,250S–2,400E of NW. cor. 7–46–26.
9. JG–71–66 (1); leucotonalite—cuts carbonate-chlorite schist, JG–71–66 (2), see No. 10; 1,760N–1,700W of SE. cor. 17–46–26.
10. JG–71–66 (2); carbonate-chlorite schist—cut by leucotonalite, JG–71–66 (1), see No. 9; 1,760N–1,700W of SE. cor. 17–46–26.
11. JG–40A–67; leucotonalite; 960S–1,240W of NE. cor. 33–47–26.
12. JG–41B–67; sericitized tonalite; 550N–900E of SW. cor. 23–47–26.
13. JG–41C–67; tonalite; 550N–900E of SW. cor. 23–47–26.
14. JG–108–61; foliated chloritic tonalite; 100S–2,000W of NE. cor. 26–47–26.
15. JG–109–61; foliated chloritic tonalite; 1,600N–1,600W of SE. cor. 23–47–26.

weathered rock may have a black and white "salt and pepper" speckled appearance. Beds of amphibolite range from about a foot to several hundred feet in thickness and generally have internal layering a fraction of an inch to several inches thick. Representative modes, in volume percent, are listed in table 1, Nos. 29–31. The amphibolite consists mainly of hornblende and oligoclase-andesine and their alteration products, biotite, chlorite, carbonate, epidote, and sericite. Hornblende is pleochroic from deep green or brown-green to pale yellow or tan. The plagioclase varies from biaxially negative grains with indices of refraction below N_o of quartz (1.54) to biaxially positive grains with indices of refraction equal to or somewhat higher than N_o of quartz. Magnetite and ilmenite, which is rimmed by leucoxene or sphene, are common accessory minerals. About 10–15 percent quartz is present in some samples. Generally no distinction can be made in thin section between possible primary and later quartz. Locally, the hornblende and plagioclase are extensively altered, particularly where they are markedly elongated and alined. The plagioclase generally is slightly saussuritized or sericitized, but along some shear zones it has been extensively saussuritized, sericitized, chloritized, or carbonatized. The hornblende tends to be replaced slightly by biotite and epidote or by chlorite. Biotite grades to chlorite in places, so chlorite that appears to replace hornblende directly may have passed through an intermediate biotite stage. In one sample of possible altered amphibolite from near 2,000S–2,000E, NW. cor. sec. 6, T. 46 N., R. 26 W., the hornblende is intergrown with aggregates of epidote and sphene that may be pseudomorphous replacements of plagioclase. Some dark-layered gneiss, as for example some near 550N–900E, SW. cor. sec. 23, and 650S–400W, NE. cor. sec. 31, T. 47 N., R. 26 W., consists principally of partly saussuritized plagioclase and blocky aggregates of biotite and epidote, biotite and carbonate, biotite, epidote, and carbonate, chlorite, chlorite and epidote, or chlorite and carbonate. The aggregates merge in places, causing plagioclase to appear to "float" in a matrix of the aggregate minerals. The aggregates are about the same size as the plagioclase crystals (or hornblende crystals in typical amphibolite) and with the plagioclase form a fabric similar to amphibolite's. Such rocks probably are altered amphibolite, but their primary origin is unknown.

BIOTITE SCHIST

Zones or layers of dark-green to black biotite-quartz schist ranging from a fraction of an inch to several feet in thickness are widespread in the belt of amphibolite and other layered gneiss that reaches from west of the village of Palmer to the vicinity of the southeast corner of the quadrangle. Perhaps the most notable occurrences are near 2,200S–1,800W, NE. cor. sec. 10, T. 46 N., R. 26 W., and in the cliff along the north side of the East Branch of the Escanaba River just northwest of the southeast corner of the same section. There and elsewhere, the schist has been injected by granite and frays out into thin biotite seams in the granite. Some of the schist along the East Branch is studded with metasomatic feld-

Compeau Creek Gneiss, Palmer quadrangle.

18	19	20	21	22	23	24	25	26	27	28	29	30	31	32	33	34	35	36	37
32.0	47.1	40.0	32.0	31.8	36.0	37.8	27.0	34.4	38.5	29.0	8.6	0.4	---	7.8	31.3	22.6	5.2	21.5	5.7
67.4	37.7	47.0	42.0	40.4	---	35.6	27.6	40.8	25.4	37.0	81.0	48.4	47.7	19.4	22.4	18.2	35.0	29.5	28.2
---	8.5	8.6	18.8	20.0	26.0	19.8	45.0	24.2	34.3	25.4	---	---	---	---	---	---	---	---	---
---	---	---	---	---	---	---	---	---	---	---	---	---	---	---	---	---	---	---	---
---	3.1	---	---	---	[4]38.0	---	Tr	Tr	Tr	---	---	---	---	---	---	Tr	---	---	---
---	---	---	---	---	---	---	---	---	---	---	---	41.4	47.2	60.8	---	---	---	---	---
.6	3.6	2.4	6.9	7.8	---	6.8	.4	.6	1.3	8.0	---	.8	.9	Tr	31.9	4.4	---	26.5	64.0
---	---	1.8	---	---	---	---	---	---	Tr	---	5.6	2.8	.5	---	5.4	50.4	39.0	8.7	.7
---	---	Tr	Tr	---	---	---	---	---	---	---	4.8	.4	.8	Tr	---	2.8	7.5	10.5	---
---	---	---	---	---	---	---	---	---	Tr	---	---	4.8	.8	10.0	---	---	10.0	---	1.2
---	---	Tr	---	---	---	---	---	---	---	---	---	---	---	---	---	---	---	---	---
---	---	---	---	---	---	---	---	---	---	---	---	---	.9	Tr	---	1.2	2.5	1.5	---
---	---	Tr	---	---	---	---	---	---	---	---	---	---	---	---	---	---	---	---	---
---	---	---	---	---	---	---	---	---	---	---	---	1.0	1.2	2.2	---	---	.7	1.5	---
---	---	---	---	---	---	---	---	---	---	---	---	---	---	---	8.8	---	---	---	---

16. RK–3A–63; foliated tonalite; 1,600S–2,840W of NE. cor. 1–46–27.
17. RK–21–63; leucotonalite; 2,400S–800W of NE. cor. 4–46–26.
18. RK–21A–63; leucotonalite, 2,400S–800W of NE. cor. 4–46–26.
19. JG–112–65; foliated granodiorite; 1,200N–1,200W of SE. cor. 33–47–26.
20. JG–115–65; granodiorite; 1,670S–770W of NE. cor. 3–46–26.
21. RK–3–63; granodiorite; 1,600S–2,840W of NE. cor. 1–46–27.
22. JG–119–65; biotite granodiorite; 370N–2,800E of SW. cor. 11–46–26.
23. JG–113–65; foliated sericitized quartz monzonite, 1,100N–1,100W of SE. cor. 33–47–26.
24. JG–55–66; foliated quartz monzonite; 2,250S–2,400E of NW. cor. 7–46–26.
25. JG–45–64; quartz monzonite; 2,100S–1,900E of NW. cor. 5–46–26.
26. JG–113A–65; sericitized quartz monzonite; 1,100N–1,100W of SE. cor. 33–47–26.
27. JG–125–65; quartz monzonite; 2,400S–1,700W of NE. cor. 8–46–26.
28. JG–55B–66; foliated quartz monzonite; 2,250S–2,400E of NW. cor. 7–46–26.
29. RK–8–63; albite syenite; 370S–200W of NE. cor. 1–46–27.
30. JG–61–64; amphibolite; 1,860S–1,800W of NE. cor. 32–47–26.
31. JG–63–64; amphibolite; 2,100N–2,400W of SE. cor. 32–47–26.
32. JG–111–65; amphibolite; 200N–1,620E of SW. cor. 33–47–26.
33. JG–88–65; quartz-plagioclase-biotite schist; 1,970N–2,970W of SE. cor. 25–47–27.
34. JG–105–65; well-layered microclastic chlorite-quartz-plagioclase rock; 180S–400W of NE. cor. 36–47–27.
35. JG–108–65; well-layered microclastic chlorite-plagioclase rock; 250S–1,950W of NE. cor. 26–47–26.
36. RK–17–63; well-layered microclastic plagioclase-biotite-quartz rock; 2,000S–400W of NE. cor. 31–47–26.
37. RK–20–63; well-layered microclastic biotite-plagioclase rock; 1,050S–800E of NW. cor. 4–46–26.

spar augen, is cut by veins of granite, and, as elsewhere, frays out into thin biotitic seams in granite. These remnant seams of biotite in granite result in a layered granite gneiss.

METAGRAYWACKE(?), METATUFF(?), OR CATACLASTIC AMPHIBOLITE(?)

Dark-green well-layered microclastic rock of uncertain origin occurs in several places in the northern part of the Compeau Creek Gneiss south of Palmer. The dark rock is interbedded with and cut by veins or dikes of granite in most exposures. The principal occurrences are in a narrow southeast-trending belt almost entirely on the north side of Michigan Highway 35, between 1,800S–1,000W, NE. cor. sec. 31, T. 47 N., R. 26 W., and 1,000S–800E, NW. cor. sec. 4, T. 46 N., R. 26 W. Other occurrences are in the vicinity of 200S–400W, NE. cor. sec. 36, T. 47 N., R. 27 W., and 400S–2,000W, NE. cor. sec. 26, T. 47 N., R. 26 W.

The dark rock is characterized by ½- to 2-inch beds in which an open framework of clastlike grains of plagioclase, and, in some beds, quartz, "float" in a matrix or groundmass of chlorite, chlorite-quartz, biotite, or biotite-carbonate (table 1, Nos. 33–36). Plagioclase grains generally are quite fresh, equant, and have albite twinnings. Many such grains are sharply angular, and their boundaries break irregularly across crystallographic surfaces or twin planes. Some are ragged from marginal replacement by the metamorphic growth of biotite or chlorite of the groundmass. Quartz grains are grossly equant and rounded, but, in detail, grain boundaries tend to be ragged and to have small reentrants or concavities which suggest that existing grain surfaces resulted from secondary overgrowths of quartz or were irregularly replaced by biotite or chlorite. Biotite or chlorite of the groundmass or matrix is generally somewhat elongated and alined parallel to the layers, but the fabric does not appear to be severely deformed.

Lamey (1935) evidently considered the well-layered dark rock along Michigan Highway 35 as relict from normal lower Huronian (lower part of Marquette Range Supergroup here) metasedimentary rocks that have been modified by granite intrusion. However, several features rule out a correlation of the well-layered dark rock with middle Precambrian bedded rocks. The rock along Michigan Highway 35 differs markedly from known lower middle Precambrian rocks in the area in having a combination of mafic composition and abundant clastlike grains of plagioclase. Neither of these features, furthermore, is attributable to granitization of the known types of lower middle Precambrian sedimentary rock. Also, evidence from mapping throughout the eastern part of the Marquette synclinorium rules out granite intrusions younger than the middle Precambrian rocks in that area. The dark rock along Michigan Highway 35 conforms with southeastward structural trends in bordering granite and amphibolite to the north and south, and diverges sharply from the eastward trend of the

nearest middle Precambrian metasedimentary rock in the south part of the Palmer basin.

The well-layered dark rock thus appears clearly to be part of the basement gneiss. On mineralogic and textural evidence, it could perhaps equally well have been:

(1) Graywacke—a sedimentary precursor of at least some granite and gneiss in the "southern complex," as were beds of the Dickinson Group, 30–40 miles to the southwest (James and others, 1961, p. 13–21).

(2) Mafic crystal tuff, perhaps closely related to mafic volcanic flows from which amphibolite in the gneiss might be derived.

(3) Amphibolite or its parent volcanic(?) rock that was deformed by cataclasis, followed by recrystallization of more finely comminuted parts of the rock.

GRANITIC ROCK

GENERAL FEATURES AND DISTRIBUTION

Granitic rock forms most outcrops of Compeau Creek Gneiss. It is dominant over layered granitic gneiss in most exposures containing the layered rock and is present in many outcrops containing amphibolite. Granitic rock is probably even more abundant than amphibolite in the amphibolite-rich belt described above. The granitic rock is slightly to moderately well foliated in much of the area, but in large parts of secs. 9, 15, and 16, and the east halves of secs. 8 and 17, T. 46 N., R. 26 W., it is generally massive, nonfoliated, and leucocratic. Partly altered syenitic rock described by Davis (1965, p. 12–14) near the west quarter corner of sec. 28, T. 47 N., R. 26 W., is correlated here with Compeau Creek Gneiss.

DESCRIPTION

The unweathered granitic rocks are light gray to very pale salmon gray, the color varying with the amount of accessory biotite or chlorite. They generally weather to a light pink, salmon, or dark gray, and rounded glaciated outcrop surfaces generally are coated with a dark-gray to black film. The colors observed in most places have been affected by weathering and probably do not represent identifiable varieties of the granite. A bright salmon color is particularly distinctive of some of the granite, but on new fractures this color grades inward from the weathered surface to light-gray rock. Likewise, the common pinkish and dark-gray surface colors grade into light-gray unweathered granite. Therefore, it seems likely that most fresh granitic rock is a rather uniform light gray, and compositional varieties cannot be identified by the color of fresh or weathered rock.

Most of the granitic rock in the Palmer quadrangle is equigranular and medium grained (grain sizes, 0.1–2.0 mm). In parts of the massive nonfoliated granite in the mid-south part of the main belt of Compeau Creek Gneiss, grain sizes commonly range from 1 to 5 mm. Markedly inequigranular granite containing tabular phenocrysts or metacrysts (augen) of microcline or albite, 2–3 cm long or longer, are known in only a few small areas, notably in a zone between 850S–1,700E and 600S–3,500E of the NW. cor. sec. 17, T. 46 N., R. 26 W., and in an outcrop at 1,100N–2,180W of the SE. cor. sec. 8, T. 46 N., R. 26 W. Such rock becomes abundant west of the Palmer quadrangle (G. C. Simmons, W. F. Cannon, U.S. Geol. Survey, oral communs., 1968). It is common in roadcuts along Michigan Highway 95 north of Republic about 20 miles to the west and is an important part of the lower Precambrian Margeson Creek Gneiss, 15–20 miles southwest of Republic (Gair and Wier, 1956, p. 18–25).

Modes of granite and foliated gneissic granite are shown in table 1; compositions of layered granitic gneiss are essentially similar to these. Plagioclase (An_{0-20} in different samples) is dominant over potassic feldspar in most of the area, and quartz content is high. Grains are anhedral. Potassic feldspar is almost entirely microcline, and most is of medium grain size, as is the plagioclase and quartz with which it is intergrown in typical granitic textures. Small amounts of primary biotite are present in much of the granite, and monazite, zircon, and opaque minerals are minor accessory minerals. Some granite contains chlorite analogous in form and distribution to the more common biotite, and biotite in places is partly retrograded to chlorite, so it is likely that chloritic granite was originally biotitic. Plagioclase nearly everywhere is clouded and slightly sericitized or chloritized and in places is extensively replaced by sericite or sericite and chlorite. Some plagioclase is replaced by biotite. Strong alteration of plagioclase generally has taken place near the edges of conspicuous outcrop areas bordering long narrow valleys that probably mark major shear zones. Microcline, in striking contrast to plagioclase, is remarkably fresh. The unaltered condition of microcline might suggest that it had been added to the rock during or after alteration of the plagioclase, but on the other hand, prealteration potassic feldspar might have been spared sericitization because of its composition. The presence of microcline next to plagioclase grains, showing all stages of sericitization from slight to complete, suggests that

microcline did not form as an accompaniment to sericitization of plagioclase. Shears and fractures, which may have formed at the same time that the plagioclase was being altered, in places break microcline crystals into pieces and suggest that microcline was present prior to alteration of the plagioclase. During low-grade regional and local shearing metamorphism, such microcline apparently was present but was not susceptible to alteration (Gair and Simmons, 1968, p. D191). In addition to sericite and chlorite—the principal products of alteration—some altered granite also contains small amounts of secondary carbonate, epidote, and (or) leucoxene-sphene. In thin section, the foliated granitic rock typically has shears along the edges of the larger feldspar grains and in the groundmass. Quartz commonly is somewhat elongated in the direction of shearing and evidently recrystallized readily during deformation. Shears commonly hold concentrations of sericite, chlorite, and fine-grained (granulated?) quartz and may cut through some large feldspar crystals, as noted above for microcline. A general correlation exists between the spacing and extent of shears and the degree of alteration of plagioclase.

ORIGIN

Field relations suggest that the amphibolite and biotite schist are metamorphosed remnants of earlier rock—possibly mafic volcanic flows and graywacke—digested during the intrusion of granite. Laminae of biotite or hornblende in banded gneiss commonly fray into and are truncated by felsic material, so that the amount of mafic material appears to be inversely proportional to the amount of felsic material. Layered parts of the Compeau Creek Gneiss commonly are surrounded by foliated granitic gneiss with which the layers are conformable. Amphibolite may fray out into streaky seams of biotite in a mass of quartz-feldspar. The biotite evidently is derived from hornblende, or both minerals had a common ancestor in the pregranitized country rock. In many places there is a gradation from coarse-grained nonfoliated leucocratic granite to medium-grained foliated gray biotitic granite to layered feldspar-biotite gneiss to biotite schist or amphibolite. The intermediate rocks appear to be uncompleted stages in the digestion of the biotite schist or amphibolite by granite. In one outcrop where such gradations have been observed, both tonalite and quartz monzonite are present (table 1, Nos. 8, 21, 25), and in another such outcrop, tonalite and granodiorite are present (table 1, Nos. 14, 19). Apparently two (or more?) intergradational varieties of granitic rock can form during the replacement of dark country rock by felsic magma.

Massive leucocratic granite which is almost free of inclusions or lenses of banded gneiss and amphibolite occupies large parts of secs. 9, 15, and 16, and the east halves of secs. 8 and 17, T. 46 N., R. 26 W. The area of massive granite gives way laterally to granite gneiss and to amphibolite. The massive granite truncates foliated granite gneiss in places and may have formed later than the foliated granite, or be a final stage of intrusion of the same granite and perhaps marks a center of intrusion in the area.

Leucocratic high-silica tonalite near the north edge of the exposed basement rock, about 1,000W–900S of NE. cor., sec. 33, T. 47 N., R. 26 W. (Gair and Simmons, 1968, table 1, No. 9) probably formed by local remobilization or selective melting of more normal tonalite. The tonalite—essentially a quartz-albite rock containing 79.8 percent silica (for example, see table 1, No. 11, listing mode of one thin section)—surrounds discontinuous layers of dark metaigneous rock, apparently chloritized amphibolite. The plagioclase is not sericitized as it invariably is to some extent in other tonalite in the area; so the albite may be syntectonic or may postdate deformation and regional metamorphism.

PALMER GNEISS

HISTORY OF NAME

The Palmer Gneiss was named by Van Hise and Bayley (1895, p. 514; 1897, p. 211–218) for schistose and gneissic rocks near the village of Palmer that occur in narrow belts between lower Precambrian ("Archean") gneiss—the Compeau Creek Gneiss of this report—and middle Precambrian (Huronian, Animikie) metasedimentary rocks (pl. 1, Gair and Simmons, 1968). The name Palmer Gneiss has been used commonly by some geologists for all the lower Precambrian gneiss within several miles south and southeast of Palmer, but such usage clearly was not the intent of Van Hise and Bayley. They considered the Palmer Gneiss to be comminuted, sericitized, and partly silicified modifications of normal "Archean" gneiss. In practice, though, they found it difficult to distinguish some Palmer Gneiss, probably the silicified variety, from somewhat sheared and altered Ajibik Quartzite. Furthermore, intergradations exist between the Palmer Gneiss and less modified parts of the Compeau Creek Gneiss, so that both types inadvertently were lumped together in places during the early work, and possibly also during the present study. Van Hise and Leith (1911, p. 255–256), evidently acknowledging the practical difficulty of separating some of the altered gneiss and quartzite, de-

cided that the Palmer Gneiss properly included both—that is, rocks of early and middle Precambrian ages.

Lamey (1935) believed that parts of the Palmer Gneiss were remnants of Huronian sedimentary formations; two of these, the Mesnard Quartzite and the Kona Dolomite, he extended from the northeast into the area southeast of Palmer where they had not been previously recognized. Lamey thought that the sedimentary rocks had been altered and partly replaced by post-middle Precambrian (post-Huronian) granite, an outgrowth of his earlier conclusion (1931, 1933, 1934) that most or all of the granitic rock bordering the south side of the Marquette syncline is of post-Huronian age. Tyler and others (1940, p. 1436, 1455, 1461) followed Lamey's view.

Davis (1965, p. 87) returned to the interpretation of Van Hise and Bayley. He specifically recognized effects of retrograde metamorphism and suggested that the term "phyllonite" was applicable to parts of the altered gneiss. Gair and Simmons (1968) corroborated these findings and restricted Palmer Gneiss to lower Precambrian granitoid and gneissic rocks that have been sericitized, chloritized, carbonatized, or silicified, and form comparatively narrow belts between "normal" Compeau Creek Gneiss and middle Precambrian metasedimentary rock.

DISTRIBUTION

The principal exposures of Palmer Gneiss are found in east-west belts along the south side of the Palmer basin and the Marquette synclinorium proper, across the north part of sec. 33, T. 47 N., R. 26 W., and in the bluff northwest of Palmer Lake in the central part of sec. 25, T. 47 N., R. 27 W. Other exposures similarly situated in the geologic section are in the SW¼ sec. 23, in the south-central part of sec. 30, in the NE¼ sec. 31, and in the NW¼ sec. 34, T. 47 N., R. 26 W. Palmer Gneiss also occurs in the Wewe Hills uplift between the Palmer basin and Goose Lake, in a rather broad irregular west-northwest-trending zone bordering the Compeau Creek Gneiss in the central part of sec. 23.

DESCRIPTION

The following description of Palmer Gneiss closely corresponds with that in Gair and Simmons (1968). The rock consists largely of green, gray, and tan schist and, in places, associated pale-olive-green or tan massive quartz-sericite rock. The schist probably originated by the comminution of once coarser grained rocks and could be termed phyllonite (Knopf, 1931, p. 14–19). Some of the schist has well-developed layers, ¼–2 inches thick, particularly in the bluff northwest of Palmer Lake. Locally, the schist contains conformable pods as much as several feet thick and stringers of granitic rock or feldspar-chlorite gneiss. In a few places, small granitic or pegmatitic blobs or stringers, less than a foot long and less than an inch thick, cut the foliation of the schist.

The schist consists mainly of highly variable proportions of sericite, aluminous chlorite, fine-grained quartz, and dolomite. Variations in the proportions of these minerals undoubtedly reflect original compositional variations in the parent rock. In many places along the south margin of the Palmer basin, beds and lenses of schist have been replaced by fine-grained quartz. Veins of quartz or dolomite are especially common in carbonate-chlorite schist in the NE¼ sec. 33, T. 47 N., R. 26 W. Large brown-weathering podlike masses of coarse dolomite or dolomite and quartz are also especially common in this area. They transect and wedge into the schistosity of the rock. The largest pods are about 20 feet long and 3 feet wide. Quartz-sericite rock characteristically contains rudely blocky or less well-defined areas of very fine grained nearly pure sericite separated by knots or subparallel ribbons of coarse-grained quartz (Gair and Simmons, 1968, fig. 6). The knots stand out on weathered surfaces and are easily mistaken for detrital grains, but in thin section they are irregular in outline, lack detrital form, and are interconnected by roughly subparallel thin quartz veins. The knots are probably analogous to lenses and nests of recrystallized quartz that Knopf (1931, p. 18–19) considered to be "particularly characteristic of phyllonites."

ORIGIN

Many remnants of plagioclase in the Palmer Gneiss are extensively sericitized and surrounded by patches of sericite probably derived from the original grains of plagioclase. The common blocky aggregates of sericite are probably thoroughly replaced crystals of plagioclase. Microcline is present in some of the rock and is fresh even where plagioclase has been completely replaced. Whether the fresh microcline was emplaced in the rock after alteration of the plagioclase or whether it predates the sericitization and was spared alteration because of its potassic composition is unknown. In a few thin sections of carbonate-chlorite schist, carbonate grades into remnants of feldspar, and west of the quadrangle in the east-central part of sec. 26, T. 47 N., R. 27 W. partly altered gneiss, occurring between chlorite-

quartz-carbonate schist of the Palmer Gneiss to the north and hornblende gneiss to the south, contains partly chloritized biotite and partly carbonatized feldspar (Gair and Simmons, 1968). Chloritization of mafic minerals and sericitization and carbonatization of plagioclase were important in the formation of the schist of the Palmer Gneiss.

Strong shearing of the schist is indicated by subparallel ribbons of recrystallized quartz and well-alined mica and chlorite. Conformable stringers and pods of granite and feldspar-chlorite gneiss in the schist are interpreted as remnants of the parent rock, similar to those described by Becke (1909). In some places, especially in sec. 23, T. 47 N., R. 26 W., large tabular crystals of feldspar have been completely sericitized but are undeformed. Sericitization evidently was not necessarily accompanied or preceded by shearing, and in occurrences such as in sec. 23, the sericite may be derived from material formed by the alteration of plagioclase in a regolith on the pre-middle Precambrian land surface.

The brown-weathering pods of dolomite or dolomite and quartz common in some of the Palmer Gneiss closely resemble carbonate-quartz pods found in a few places in the Compeau Creek Gneiss south of the Palmer basin. Such pods therefore are clearly derived by alteration of the "normal" gneiss. The CaO, MgO, and SiO_2 could have been supplied entirely from the surrounding rocks.

Chemical analyses of dolomite-chlorite-quartz-sericite (dark) and quartz-sericite (light) varieties of Palmer Gneiss (Gair and Simmons, 1968) indicate similarities with amphibolitic and felsic parts of the Compeau Creek Gneiss, respectively.

The petrographic and chemical evidence for the derivation of the Palmer Gneiss by the alteration of Compeau Creek Gneiss, plus the distribution of the Palmer Gneiss in narrow belts along the contact between lower and middle Precambrian rocks and the strong schistosity of the Palmer Gneiss in most places, suggest one or a combination of the following modes of origin:

(1) Shearing and alteration during faulting of middle Precambrian rocks against lower Precambrian rocks at the close of middle Precambrian time.

(2) Passage of aqueous solutions along the contact between lower and middle Precambrian rocks.

(3) Alteration of a regolith, with or without shearing, during folding at the close of middle Precambrian time.

MIDDLE PRECAMBRIAN ROCKS—MARQUETTE RANGE SUPERGROUP

CHOCOLAY GROUP

The Chocolay Group contains the oldest rocks of middle Precambrian age in the Marquette Range Supergroup and is equivalent to the lower Huronian and lower Animikie of earlier reports (James, 1958, p. 35). The Chocolay Group in the Palmer quadrangle consists of Enchantment Lake Formation, Kona Dolomite, and Wewe Slate, but in the Wewe Hills south of Goose Lake the group may also include rocks equivalent to sub-Kona beds other than the Enchantment Lake Formation to the northeast.

ENCHANTMENT LAKE FORMATION

The Enchantment Lake Formation was named by Gair and Thaden (1968, p. 27) for a unit of interbedded conglomerate, graywacke, wacke, arkose, and slate at the base of the Chocolay Group in the eastern part of the Marquette Range. In the Palmer quadrangle, the Enchantment Lake Formation is present only in the Wewe Hills, south of Goose Lake, and consists largely of conglomerate. Conglomerate occurs widely in the lower part of the Chocolay Group in sec. 22 and the W½ sec. 23, adjacent to (overlying) lower Precambrian gneiss. Minor arkose, quartzite, quartz-sericite schist, and slate are interbedded with the conglomerate in places. The correlation of these rocks with the Enchantment Lake Formation to the east is based on the conglomeratic lithology and stratigraphic position. Nonconglomeratic rocks adjacent to lower Precambrian gneiss, but not closely associated with conglomerate, as in places in the SW¼ sec. 22, and in the W½ sec. 23, may also be equivalent to the Enchantment Lake Formation. However, as the Enchantment Lake may be lenticular (Gair and Thaden, 1968, p. 27) rather than a continuous sheet on the basement rocks, and as the nonconglomeratic rocks in question cannot be mapped into the conglomerate, such rocks are included with the undivided Chocolay Group.

DISTRIBUTION

Conglomerate occurs in numerous outcrops in sec. 22 and the W½ sec. 23. Most exposures are adjacent to areas of Compeau Creek Gneiss, within a few hundred feet stratigraphically of the gneiss. In some places conglomerate is directly in contact with gneiss; elsewhere, lenses of interbedded conglomerate-quartzite or conglomerate-quartzite-slate border the gneiss, but which of these types is in contact with the gneiss is problematical and may differ from place to place. Almost all other occurrences of con-

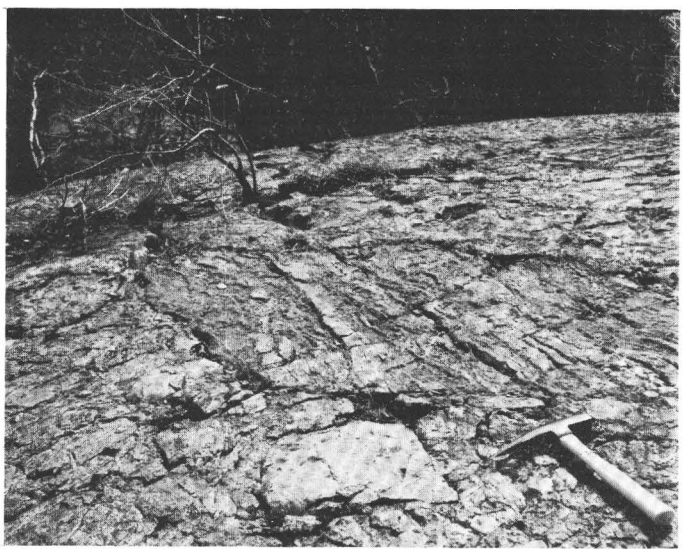

A

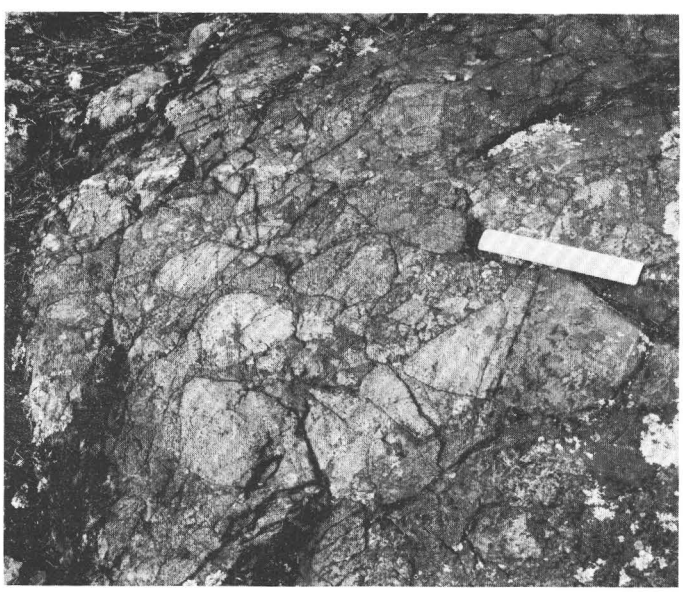

B

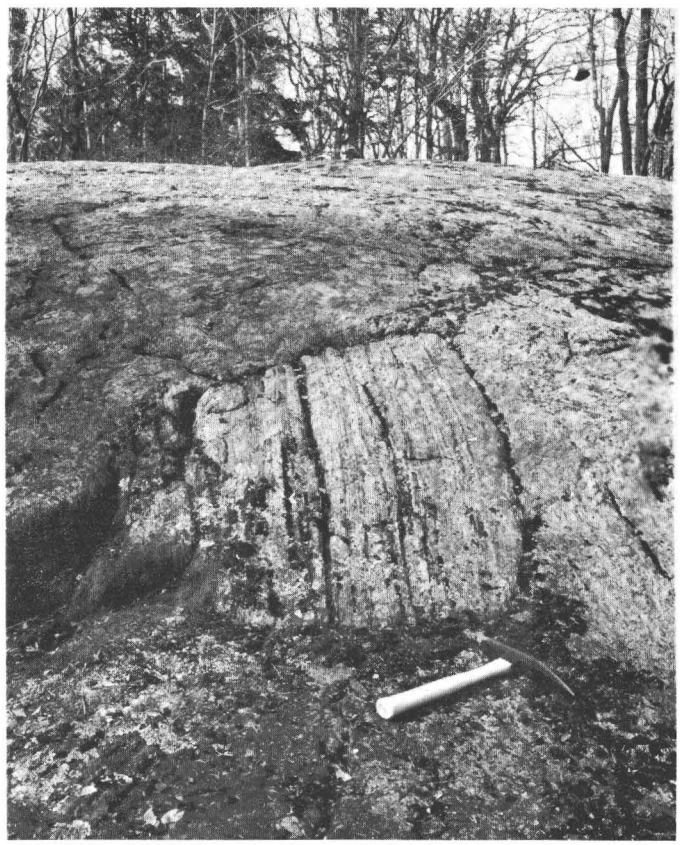

C

FIGURE 3.—Conglomerate in Enchantment Lake Formation. (Locations measured from SW. cor. sec. 22, T. 47 N., R. 26 W.) *A*, Tightly packed boulder conglomerate. Above hammerhead is lozenge-shaped boulder of layered gneiss, about 6 feet in maximum dimension. Location near 2,500N–2,700E. *B*, Tightly packed cobble conglomerate. Cobbles and pebbly matrix consist of granitic gneiss. Scale is 7 in. long. Location near 2,500N–2,100E. *C*, Angular boulder of layered gneiss in tightly packed boulder conglomerate. Location near 2,550N–2,500E.

glomerate farther removed from known areas of gneiss in the Wewe Hills can be reasonably inferred to overlie gneiss closely, or to border gneiss buried under Pleistocene glacial deposits. Conglomerate in the east-central part of sec. 22 occurs about 1,000 feet east and northeast of the nearest exposures of gneiss. This area occupies a saddle between uplifts of the gneiss to the east and west; so gneiss may occur at shallow depths beneath the exposure of conglomerate. Gneiss is inferred to extend into the NE¼ sec. 22 from sec. 23, across an area of no exposures that is bordered by exposed conglomerate dipping away from the area.

DESCRIPTION

Excellent descriptions of the conglomerate have been given by Van Hise and Bayley (1897, p. 275–280).

Conglomerates immediately adjacent to the Compeau Creek Gneiss in the west-central part of sec. 23 are generally less distinctive than elsewhere in the area. Pale-tan or salmon-colored cobbles and pebbles of altered foliated gneiss, sericitic quartzite, and sericitic cherty rock commonly are separated by a similarly colored matrix of foliated quartz-sericite-feldspar, which tends to obscure the fragments. Some of the feldspathic quartzite and conglomerate adjacent to gneiss in the west-central part of sec. 23 are easily mistaken for gneiss and generally can be

distinguished from gneiss with certainty only where distinct widely scattered pebbles can be found in them.

A large outcrop in the central part of sec. 22 that is elongated west-northwest, and centers approximately at 2,600N–3,200W, SE. cor. of the section contains spectacular exposures of boulder conglomerate with closely packed blocks of gneiss as much as 10 feet across (fig. 3). Because of abundant feldspar or feldspar-rich fragments, much of the conglomerate is arkosic. Thicknesses of 100–200 feet of coarse conglomerate are present in several other prominent outcrops in the central and east-central parts of sec. 22. Rounded cobbles of gneiss, 6 inches or less in diameter, are especially abundant in outcrops centering approximately at 3,000N–1,000W, 1,900N–1,500W, and 2,400N–2,000W, SE. cor. of the section.

The spectacular boulder conglomerate in the central part of sec. 22 passes downward rather abruptly into interbedded quartzite and sericite slate between 2,300N–2,800W and 2,300N–3,200 W of the SE. cor. of the section. On strike 300 feet to the southeast and for another 700 feet farther southeast, however, the coarse conglomerate grades downward through a zone less than 50 feet thick along the southwest side of the outcrop into a finer grained, more loosely packed conglomerate resembling varved dropstone conglomerate in which angular and subrounded pebbles and cobbles of gneiss are scattered in a matrix of green laminated slate (fig. 4*A*). Weathered surfaces of the slate have a delicate pattern of regularly alternating dark and lighter colored laminae. The dark laminae range from about 0.2 to 1 mm in thickness and contain mainly mixtures of clay-sized chlorite, biotite, and quartz, and silt-sized quartz. The lighter colored laminae range in thickness from about 0.5 to 2 mm and consist largely of clay-sized particles. The dark layers are faintly graded in places. Locally, the slate laminae are depressed beneath rock fragments or are disrupted and contorted between the fragments. The concentration of fragments dispersed in the slate decreases downward, and at the southeast end of the exposures near 1,700N–2,200W, SE. cor. sec. 22, uncontorted green laminated slate dips evenly northeast beneath the conglomerate. A chemical analysis of the slate matrix from the above exposure (table 2) is fairly similar to Nanz' (1953) average of 33 Precambrian slates, except for having more Na_2O than K_2O.

About 3,000 feet to the southeast, in the SW¼ sec. 23, a similiar sequence of virtually identical loosely packed conglomerate and green laminated

A

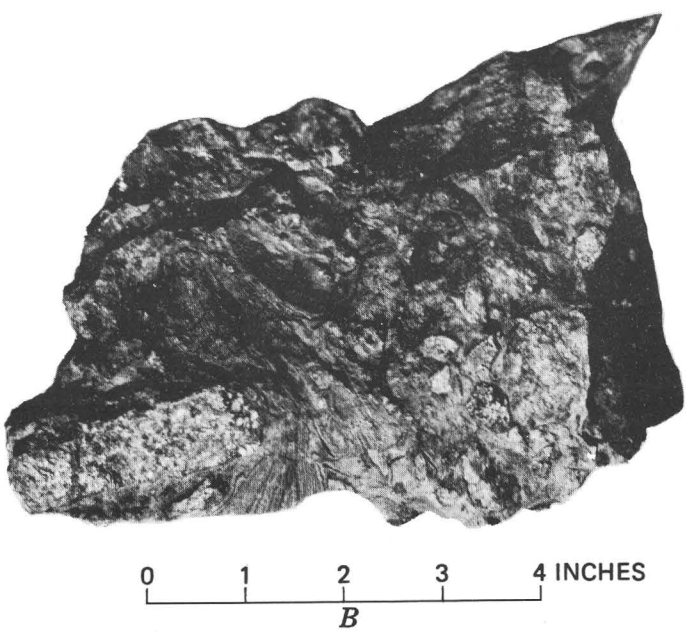

B

FIGURE 4.—Slate-conglomerate in Enchantment Lake Formation. *A*, Cobbles and pebbles of granitic gneiss "float" in laminated slate, as in varved dropstone conglomerate. Location near 1,700N–2,200W of SE. cor. sec. 22, T. 47 N., R. 26 W. *B*, Angular cobbles and pebbles of granitic gneiss "float" in laminated slate, as in varved dropstone conglomerate. Some slate layers contorted between cobbles. Location near 1,200N–600E of SW. cor. sec. 23, T. 47 N., R. 26 W.

slate (fig. 4*B*) rests on Compeau Creek Gneiss to the east. Because of the observed relationship in the SW¼ sec. 23, a similar relationship of the conglomerate-slate sequence to underlying gneiss is postulated in the south-central part of sec. 22. Hence, gneiss is inferred to extend along the valley bottom

immediately southwest of the slate-conglomerate exposures in sec. 22.

TABLE 2.—*Chemical analysis, in percent, of laminated slate-forming matrix of slate-conglomerate, Enchantment Lake Formation*

[Standard chemical analysis by S. M. Berthold, U.S. Geol. Survey. Sample JG–27–67; location, 1,700N–2,250W of SE. cor. sec. 22, T. 47 N., R. 26 W.]

SiO_2	60.28	H_2O^+	2.45
Al_2O_3	18.29	H_2O^-	.07
Fe_2O_3	1.10	TiO_2	.54
FeO	5.70	P_2O_5	.18
MgO	3.20	MnO	.06
CaO	.48	CO_2	.05
Na_2O	4.50		
K_2O	2.90	Total	99.80

The rather abrupt change on strike northwestward from slate and loosely packed slate-conglomerate near 2,400W–2,000N to interbedded quartzite and slate directly under the coarse conglomerate near 2,800W–2,300N in sec. 22 may be normal—a facies change—or may be a result of local shearing-out of gradational conglomerate between the coarse conglomerate and the quartzite-slate during folding.

Some of the conglomerate in secs. 22 and 23 forms pebble zones, 1 inch to several feet in thickness, which are interbedded with quartzite. Pebbles generally are rounded, less than 2 inches in diameter, and consist principally of vein quartz and gneiss and to a lesser extent of quartzite, greenstone, and quartz-sericite schist. Clasts of feldspar, as much as several millimeters in diameter, are abundant in parts of the pebble conglomerate. These pebble layers evidently are similar to those described by Ovenshine (1970) in glacial deposits at Glacier Bay, Alaska.

POSSIBLE GLACIAL AFFINITIES

The boulder conglomerate in the central part of sec. 22 is the most spectacular in the area and the most difficult to explain. It grades downward from a jumbled mass of tightly packed angular boulders and cobbles (fig. 3) through loosely packed cobbly and pebbly slate-conglomerate (fig. 4) into slate or interbedded slate and quartzite. To the southeast in sec. 23, the slate rests on gneiss or on arkose immediately above gneiss. The "floating" pebbles and larger fragments in a laminated fine-grained matrix, and the upward sequence above an erosional unconformity from slate or quartzite to loosely packed slate-conglomerate to massive tightly packed boulder conglomerate is similar to relationships in part of the Gowganda Formation in the Blind River district of Ontario (Collins, 1925, p. 65–67; Jackson, 1965). Any satisfactory explanation of the boulder conglomerate in sec. 22 must account for a gradation contrary to that in normal depositional sequences and for the "floating" cobbles and pebbles of gneiss in a matrix of laminated slate in the intermediate zone between the coarse conglomerate above and the slate below.

Deposits containing materials with tremendous differences in grain size are now generally attributed to mud flows (Crowell, 1957), to analogous landslides, or to glacial deposition (Pettijohn, 1949, p. 222). The Gowganda, which is a notable example of Precambrian rock characterized by great discrepancies in grain size, is now generally attributed to glaciation (Ovenshine, 1965, p. 165–180). The Fern Creek Formation of southern Dickinson County, Mich., is considered equivalent to the Enchantment Lake Formation (Gair and Thaden, 1968). Some conglomerate in the Fern Creek has been classified as tillite by Pettijohn (1943), who also related to glaciation the closely associated laminated argillite containing scattered cobbles. In the Gowganda, the combination of varvelike stratified argillite and isolated erratics (dropstones) is considered to be particularly consistent with a glacial origin (Jackson, 1965, p. 878–881).

The Na_2O/K_2O ratio of greater than 1 in the slate matrix of the slate-conglomerate (table 2) is characteristic of abraded poorly weathered sediment (Pettijohn, 1957, p. 345) and is consistent with ratios in the argillaceous matrix of conglomerates in the Gowganda (Pettijohn and Bastron, 1959) and in the Reany Creek Formation north of the Marquette synclinorium, parts of which may be of glacial origin (Puffett, 1969). Such abraded, sodium oxide-rich sediments might equally well be a product of rapid fluvial deposition, landslides, or glaciation. Fluvial deposition, however, does not explain the tremendous differences in grain size.

The debouching of a local mountain glacier or a landslide into a depositional basin where mud was being laid down over gneiss might explain equally well the huge blocks overlying cobbly and pebbly slate-conglomerate and slate. However, the sequence of cobbly and pebbly conglomerate in a laminated slate matrix overlying laminated slate is not equally well explained by mud flow or glaciation. Although the laminated slate is considerably disturbed between some cobbles, segments of slate being folded on themselves and slightly faulted, the sets of laminae have retained much of their continuity. In places, furthermore, laminae have been bent downward beneath "floating" pebbles but retain continuity from one side of the pebble to the other. These features would seem to preclude an origin by mud flow. Therefore, the sequence in the Enchantment Lake Formation in the central part of sec. 22 is in-

terpreted as representing essentially three stages of deposition, as follows:

1. Thinly laminated muds—possibly varve deposits—were laid down on a floor of gneiss under a shallow body of water.
2. Onset or continuation of local glaciation on nearby land area; ice-rafted cobbles and pebbles were dropped into accumulating body of laminated muds.
3. Local glacier expanded into the shallow body of water; morainal blocks of gneiss were shoved over conglomerate formed in stage 2 or were carried out on floating end of ice and dumped as ice melted.

Stages 1 and 2 are also represented in the exposures of conglomerate in the SW¼ sec. 23.

KONA DOLOMITE

NAME, VARIETIES, AND DISTRIBUTION

The Kona Dolomite was named by Van Hise and Bayley (1895, p. 523) for the Kona Hills in secs. 12 and 13, T. 47 N., R. 26 W., in parts of the Palmer and Sands quadrangles. The formation was described most recently in the Marquette and Sands quadrangles (Gair and Thaden, 1968, p. 37–45) where dolomite and interlaminated chert-dolomite are characteristic, and quartzose dolomite, quartzite, and slate constitute a substantial part of the formation. Estimates of thickness vary between 1,200 and 2,500 feet. In the Palmer quadrangle, approximately the upper 1,000 feet of the formation is exposed in the Kona Hills northeast of Goose Lake. The rocks are gently folded; they strike generally northward and dip westward at low angles. Laminated maroon, salmon-colored, and buff dolomite are major rock types. Red, pink, and flesh-colored chert is interlaminated with the dolomite in many outcrops in the SW¼ sec. 12 and the NW¼ sec. 13. Massive dolomite is subordinate to laminated varieties and occurs mainly in the upper 100 feet of the formation, in a small syncline in the SW¼NW¼ sec. 13 and the adjoining part of sec. 14. Maroon slate in layers generally not more than a few feet thick is interbedded with dolomite, mainly about 600 to 1,000 feet below the top of the formation in sec. 13, within 1,500 feet west of the edge of the quadrangle. Algal structures generally similar to those in the Marquette and Sands quadrangles are known from six places representing at least three different stratigraphic horizons. Many small occurrences of silicified dolomite—jasperoid—are present in the SW¼ sec. 12 and in the adjacent part of sec. 11, and in a few places algal structures have been selectively silicified. Silicified dolomite is the only known representative of the formation south of Goose Lake.

THICKNESS

Marker units are not apparent in the Kona Dolomite; so the thickness of the formation in the quadrangle cannot be measured directly from surface data. Thickness determinations are also inaccurate because the upper contact of the formation is not closely located along the east side of Goose Lake adjacent to the area where determinations of thickness are least complicated by folding. The mapped width of the Kona along west-trending fold axes in secs. 11–12 and 13–14, corrected for an axial plunge of 15°, gives a thickness of about 1,000 feet between the assumed base of the overlying Wewe Formation and the east edge of the quadrangle. Approximately 230 feet of dolomite is exposed in the cliff next to the southeast arm of Goose Lake.

Inadequate exposures generally precluded accurate determinations of the full thickness of the Kona in the Marquette and Sands quadrangles, except between Little Pelesier and Carp River Lakes in the latter quadrangle, where the thickness was determined to be 1,200 feet (Gair and Thaden, 1968, p. 37). Marker beds were found by extensive drilling done by private interests after the work cited above, and the total combined thickness of the Kona in the Palmer and Sands quadrangles is about 2,500 feet; this suggests that the formation between Little Pelesier and Carp River Lakes has been reduced by bedding faults that were not detected during the mapping.

DESCRIPTION

The rocks in the Kona are the same in the Palmer quadrangle as in the Marquette and Sands quadrangles (Gair and Thaden, 1968, p. 37–40).

Dolomite beds in the Kona consist of virtually pure dolomite in recrystallized mosaics. Grain diameters are generally less than 0.3 mm. In zones without interlaminated chert, beds range from an inch or two to several feet in thickness; they generally are internally laminated. In laminated chert and dolomite, beds range from about ½ inch to 2 inches in thickness. Laminae are both planar and lenticular. Quartz clasts as large as 0.2 mm in diameter are scattered through some layers of dolomite. Commonly, laminae of extremely fine-grained pure dolomite alternate with laminae containing mixtures of dolomite and silty quartz. Contacts between the layers in places are scoured or deformed by preconsolidation slumping. The silty layers commonly have

a "cut and fill" relationship with the layers of pure dolomite, and tiny dikes of the silty material may extend into the pure dolomite layers. Angular and partly rounded fragments of dolomite in many layers are mixed with nonoolitic dolomite granules. Such rock resembles somewhat the clastic Randville Dolomite in Dickinson County, Mich. (Bayley and others, 1966, p. 35–36). Clastic dolomite forms a considerable part of the Randville and was attributed to erosion along local shorelines during deposition of the formation. The fragments in the Kona, in contrast, are irregularly distributed between thin dolomite laminae, even within areas the size of a thin section, so probably represent very restricted effects of wave action, currents, and slumping on partly consolidated material.

Colors of fresh dolomite typically are lavender, maroon, salmon, and pink, and weathered surfaces are yellowish tan, rusty or chocolate brown, buff, or nearly white. Chert laminae are red, pink, salmon, or flesh colored. They may be primary or may be jasperoid replacements of selected dolomite beds, but are interpreted as primary wherever they are persistent, regular in thickness, and strictly conformable with alternating dolomite laminae. Slate beds consist of mixtures of sericite, quartz, iron oxide, and dolomite, and generally are maroon. Colors are produced principally by the tan carbonate combined with varied mixtures of very fine grained, red, brown, and black iron oxides disseminated within and between grains of dolomite.

Dolomite beds in several places contain scattered coarse euhedral bright salmon-red metacrysts of hematitic dolomite. The principal locations of such rock, measured in feet from the SW. cor. sec. 12, are at 2,160S–300W (in sec. 14), 900N–350E, 1,300N–650E, and 1,950N–1,150E (in sec. 12). These localities are near the main occurrences of silicified dolomite, and the red carbonate euhedra probably were recrystallized from surrounding dolomite by the solutions that produced silicification.

Quartzite and dolomitic quartzite are minor components of the formation in the Palmer quadrangle; only one occurrence of quartzite and two of dolomitic quartzite are known. An 8- to 10-foot bed of pink quartzite is interlayered with dolomite, 2,900S–800E of the NW. cor. sec. 13. Dolomitic quartzite is at 850N–2,550E and at 2,030S–500E of the same corner. The first occurrence is a 2- to 3-foot cross-bedded layer in nearly the lowest part of the Kona exposed in the quadrangle; the other is a small outcrop in the syncline containing massive dolomite near the top of the formation.

ALGAL STRUCTURES

Certain domical, swirly, or bulbous concentrically laminated features in Precambrian dolomite are generally considered to be stromatolitic growths representing algal colonies (Walcott, 1914; Twenhofel, 1919; Rezak, 1957; James and others, 1961; Bayley and others, 1966, p. 35). Such features are common in the Kona Dolomite in the Marquette and Sands quadrangles (Gair and Thaden, 1968, p. 41–42), and have been found in six outcrops representing several different stratigraphic zones in the Palmer quadrangle (fig. 5).

The illustrations show the typical growth of algal domes or bulbs from a bedding surface. Domes and bulbs presumably represent separate algal colonies which grew in contact with one another as well as in isolated masses. Domes are circular to oval in plan, and of varying size in different outcrops, ranging in width from about 1 inch to 6 feet. Figure 5*D* shows that a planar section such as a bedding surface could cut arches of greatly varying width in the same dome, depending on the level of erosion.

To date, stromatolites have been classified by American paleontologists arbitrarily on form differences (Riedel, 1953; Rezak, 1957, p. 130–131). Many algal forms in the Kona resemble species of *Collenia* illustrated by Walcott (1914). Twenhofel (1919) named the species *Collenia kona* from a single occurrence south of Marquette, but many other forms are also found in the Kona which are not identified in the present report.

SILICIFIED DOLOMITE

Small areas of silicified dolomite are exposed in many outcrops in secs. 11 and 12, T. 47 N., R. 26 W. Immediately south, in secs. 13 and 14, silicified dolomite is relatively uncommon. Silicification of dolomite is recognized where dolomite beds grade directly into beds of cherty quartz, where remnant patches of bedded dolomite are surrounded by cherty quartz, and where isolated outcrops of bedded cherty quartz entirely similar to known silicified dolomite occur in or adjacent to mapped areas of Kona Dolomite. Silicified dolomite seems to be more common in the upper 100 feet or so of the formation than in underlying beds in the Palmer quadrangle, although the best single exposure in the quadrangle, north of Goose Lake, is approximately 800–900 feet below the top of the formation, near 550N–2,100E of SW. cor. sec. 12. In contrast, beds lower in the formation are extensively silicified in the Marquette and Sands quadrangles (Gair and Thaden, 1968, p. 42–

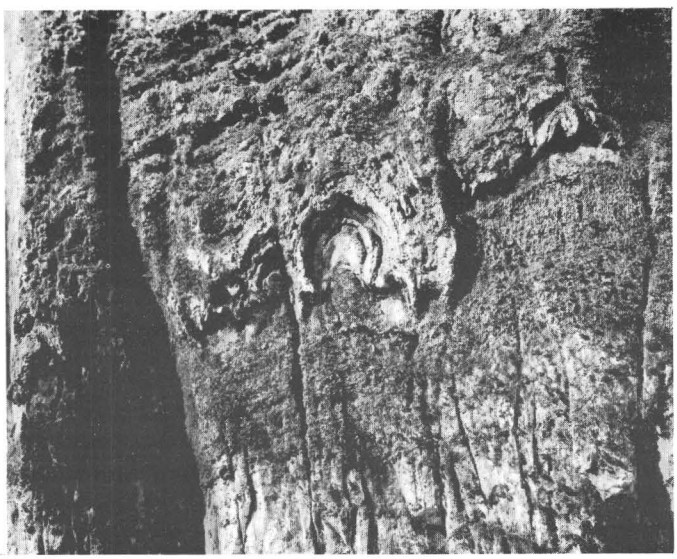

A

B

C

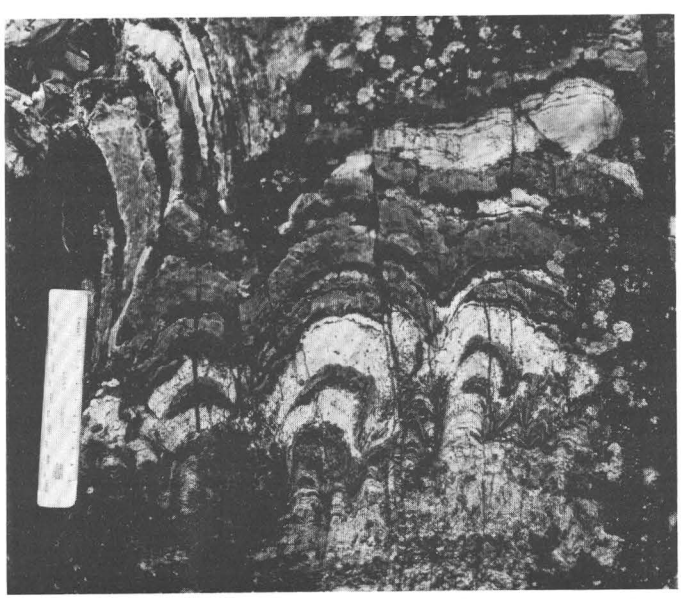

D

FIGURE 5.—Algal structures in laminated dolomite and chert, Kona Dolomite. (Locations measured from SW. cor. sec. 12, T. 47 N., R. 26 W.) *A*, Bulbous forms rise from single bedding surface. Algal bed slightly faulted in right third of photograph. Massive dolomite underlies algal bed. 550N–2,160E. *B*, Bulbous forms rise from single bedding surface underlain by massive dolomite. 700N–2,400E. *C*, Domed and bulbous forms rise from single bedding surface, which is underlain by zone of thin cusped laminae. Cusps probably also are algal structures. Same locality as *B*. *D*, Note great variation in size of arches within individual domed "colonies." Large arches have thicker layers. Length of scale 7 inches. Same locality as *B*.

44). Several large outcrops of brecciated cherty quartz just south of Goose Lake are mapped as silicified Kona Dolomite. Those rocks are similar to much silicified Kona in the Marquette and Sands quadrangles.

Silicified dolomite, jasperoid (Lovering, 1962; Gair and Thaden, 1968, p. 43–44), is very fine grained compact quartz. Characteristic colors of jasperoid in the Palmer quadrangles are pink flesh colored, shades of red, or banded red and white, depending on the amount of finely disseminated hematite. Associated vein quartz is generally coarser grained and white. At magnifications of $\times$500 to

A

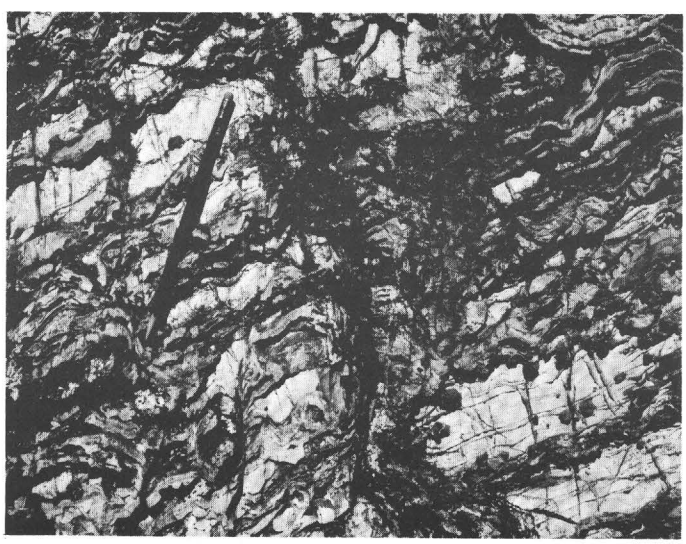

B

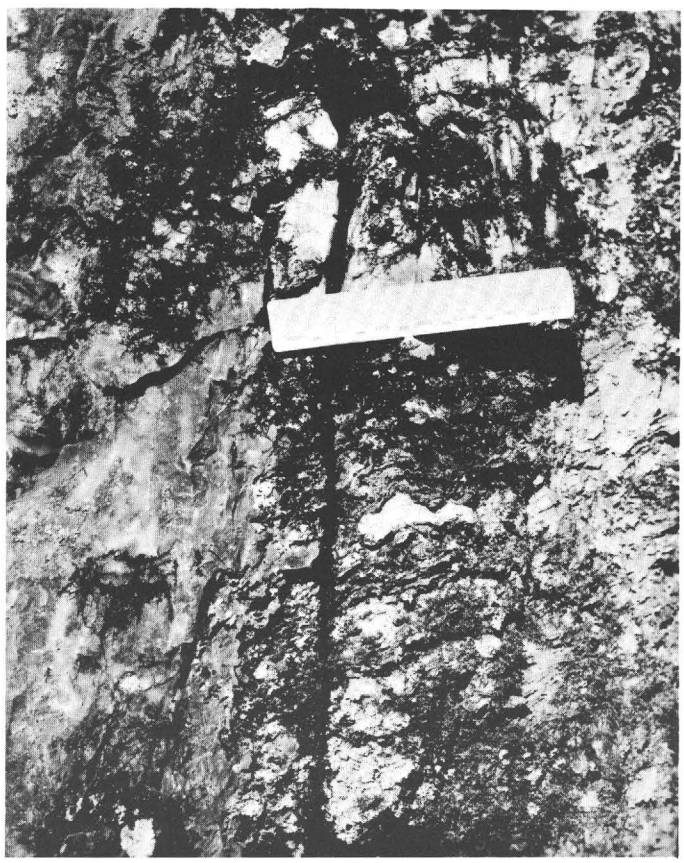

C

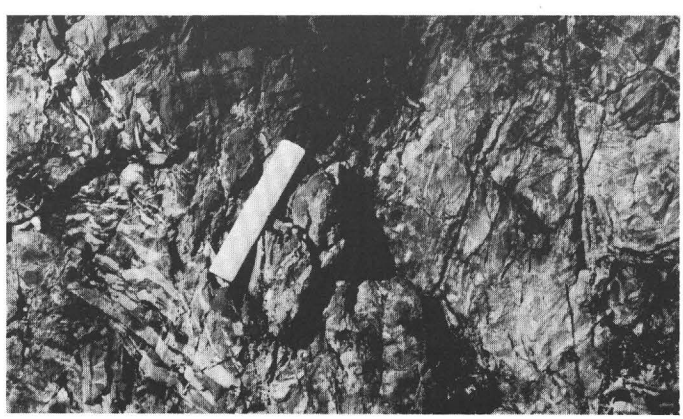

D

FIGURE 6.—Silicified Kona Dolomite, 550N–2,100E of SW. cor. sec. 12, T. 47 N., R. 26 W. *A*, Dolomite passes along bedding into red, massive jasperoid. Remnants of laminated dolomite are surrounded by jasperoid to the left of the hammer. Cherty material interbedded with dolomite may be partly primary and partly secondary (jasperoid). *B*, Area in right-central part of *A*. Irregular pinching and swelling red, cherty laminae and isolated nodules are at least partly secondary. The cherty laminae coalesce along some crosscutting cracks into masses of jasperoid, such as near the pencil point. *C*, Area immediately above the hammerhead in *A*. Shows sharp boundary between jasperoid and areas of dolomite. Cherty laminae that enclose isolated lenses of dolomite are probably largely secondary (jasperoid). Scale is 7 inches long. *D*, Red- and white-banded jasperoid. Red bands (dark) are silicified dolomite, and white bands may represent unmodified layers of primary chert. Scale is 7 inches long.

×800 in thin section, small open clusters of tiny carbonate grains are visible in places in the jasperoid. Apparently the clusters are relicts of the presilicification dolomite.

Jasperoid consists mainly of secondary silica, so is discriminated conceptually from chert which is considered primary, but often the two types cannot be distinguished. In places where massive jasperoid passes abruptly along bedding into interlaminated cherty quartz and dolomite (fig. 6), the evidence is

incontrovertible that the dolomite beds have been replaced by red jasperoid. Chertlike layers between unreplaced dolomite beds may be largely primary, partly primary and partly secondary, or mainly secondary, and thus, in a sense, may be extensions from the main mass of jasperoid. The cherty layers in the dolomitic area shown in figure 6*B* appear to be partly or entirely secondary because of their irregular pinching and swelling and the local truncation of dolomite layers. With total silicification of dolomite beds, cherty beds merge with and tend to become indistinguishable from the secondary quartz of the jasperoid. However, red- and white-banded jasperoid (fig. 6*D*) may be silicified dolomite-chert in which the red bands originally were dolomite layers and the white bands are essentially unmodified original chert layers.

Small algal growths that somewhat resemble cup corals in plan view have been selectively replaced by red cherty quartz near 2,500S–400W of NE. cor. sec. 14, and the silicified forms have been partly weathered out of the less resistant dolomite (fig. 7). Selective silicification of algal structures contemporaneous with sedimentation or diagenesis has been reported from Mississippian limestones in Montana and Utah (Bissell, 1959, p. 160). Coarse euhedral metacrysts of carbonate in the dolomite rock have the same red color as the silicified algal forms and may have been recrystallized from dolomite of the host rock by the same solutions that caused silicification.

Much of the silicification of the Kona in the eastern part of the Marquette and Sands quadrangles was related to the movement of silica-bearing solutions along faults (Gair and Thaden, 1968, p. 44). Silicification in the western part of those quadrangles and some in the Kona Hills in the Palmer quadrangle, on the other hand, appears to be unrelated to faults and may have taken place at the post-Precambrian erosion surface, as proposed for other areas around Lake Superior by Leith (1925). Near the east end of the Marquette range, slippage zones that formed along the contact between the Kona and underlying Mesnard Quartzite during regional folding provided a major access route for silica-bearing solutions (Gair and Thaden, 1968, p. 44). The location of about half the occurrences of silicification dolomite in the Palmer quadrangle near the top of the Kona suggests that slippage zones between the Kona and the overlying Wewe Slate may also have aided silicification. Silicification of the Kona Dolomite south of Goose Lake probably was localized by the fault that passes along the southeast arm of the lake.

The passage of layers of dolomite into layers of

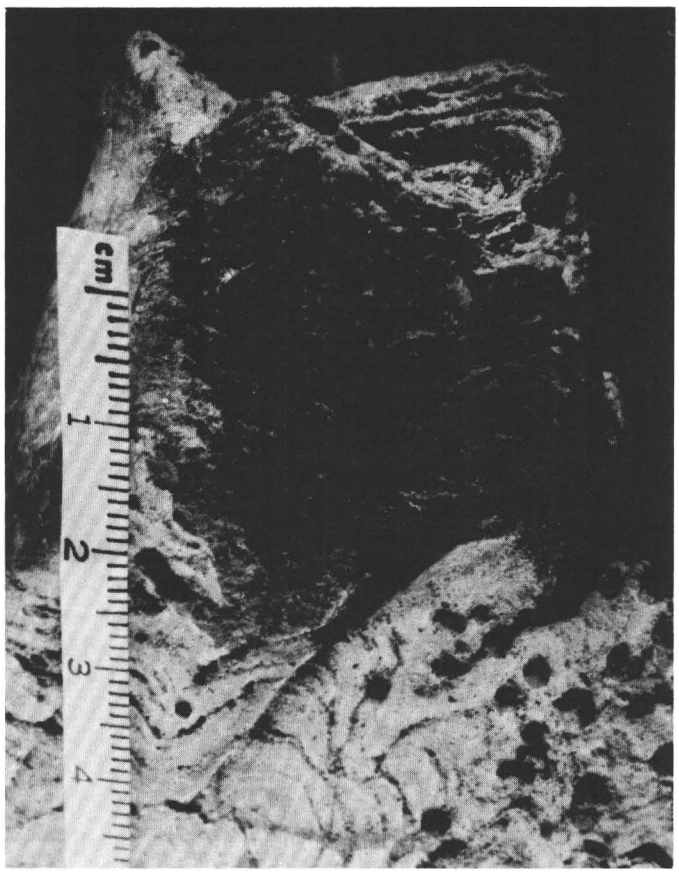

A

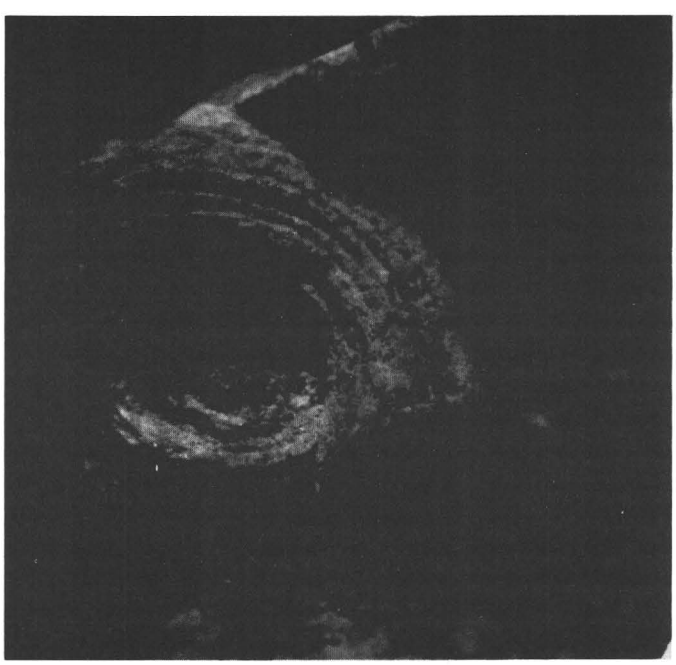

B

FIGURE 7.—Selectively silicified algal growth in dolomite. *A*, Side view. Note coarse (red) metacrysts of dolomite. *B*, Top view.

red jasperoid with no change in thickness and with internal laminations preserved in places, indicates a particle-by-particle exchange between carbonate and silica.

Silicified dolomite in partly silicified outcrops may be sharply limited by bedding surfaces or localized along cross fractures (fig. 6*A*, *B*). These avenues facilitated the movement of silica close to sites of replacement. Breccia zones also were important passageways for silica-bearing solutions, as shown by the fact that silicified parts of the dolomite commonly are brecciated.

CONDITIONS OF DEPOSITION

The Kona represents an accumulation of rather pure carbonate mud, layers of silica gel, and subordinate beds of well-sorted quartz sand. Fossil algal structures, scattered grains of detrital quartz, intraformational fragmental and granular structural features, and cut-and-fill structural features indicate deposition of the Kona in shallow water. The lithology of the Kona, its shallow-water depositional environment, and its association with the conformably underlying rather pure Mesnard Quartzite east of the report area indicates that it is virtually a classic example of stable shelf deposit. The carbonate in the formation is almost pure dolomite, and there is no textural evidence of replacement; so it is not known whether the original carbonate was calcite or dolomite.

WEWE SLATE

Wewe Slate was named for the Wewe Hills in secs. 23 and 24, T. 47 N., R. 26 W., south of Goose Lake (Van Hise and Bayley, 1895, p. 530 ff). Van Hise and Leith (1911, pl. 17) reassigned the rocks of the type area of the Wewe to the sub-Kona Mesnard Quartzite, but they retained "Wewe Slate" for rocks similar to those in the type area that directly overlay Kona Dolomite north and northeast of Goose Lake. In the present report, Wewe Slate is used essentially in that sense, for rocks underlain by Kona Dolomite and overlain by Ajibik Quartzite. Wewe Slate thus restricted occurs only north and northeast of Goose Lake in secs. 11 and 12, T. 47 N., R. 26 W. Rocks exposed in the Wewe Hills that originally were assigned to the Wewe Slate and later to the Mesnard Quartzite by Van Hise and his coworkers are now assigned mainly to the Chocolay Group without designation as to formation, or to the Enchantment Lake Formation at the base of the Chocolay Group. Wewe Slate probably underlies much of the Goose Lake topographic basin between high ground occupied by Kona Dolomite to the east and Ajibik Quartzite to the west.

The Wewe Slate is mainly fine-grained fissile gray argillaceous rock—typical slate of the Lake Superior district. In the NW¼ sec. 12, most outcrops are of gray and blue-gray mixtures of quartz and sericite. Chlorite and dusty hematite and leucoxene are typical minor components. Some of the slate is faintly laminated, and some contains thin silty layers.

The Wewe Slate has a maximum thickness of about 400 feet in sec. 12 and is roughly 500–600 feet thick immediately north of Goose Lake, on the basis of estimated average dips and widths of mapped belts of the formation.

CHOCOLAY GROUP, UNDIVIDED

Many exposures in the Wewe Hills—the type area for the Wewe Slate of Van Hise and Bayley (1895, 1897)—are assigned in the present report to the Chocolay Group without designation as to formation. These rocks occur between lower Precambrian gneiss or the immediately overlying Enchantment Lake Formation and Ajibik Quartzite and are stratigraphically equivalent to part or all of the type Chocolay Group at the east end of the Marquette district. The Chocolay there consists of Enchantment Lake, Mesnard, Kona, and Wewe formations (Gair and Thaden, 1968). In the Wewe Hills, the undivided Chocolay Group contains much impure quartzite, in addition to slate. On the other hand, clean vitreous quartzite and dolomite, which are major rock types in the Mesnard and Kona Formations in the type section of the Chocolay, are minor or absent in the undivided Chocolay Group in the Wewe Hills, indicating pinchouts or facies changes between the two areas. Some of the rocks of the undivided Chocolay Group, particularly slate close to the contact with Ajibik Quartzite, must correspond to the Wewe Slate north of Goose Lake. Stratigraphically lower in the group, the wedge of brecciated silicified Kona Dolomite south of the southeast arm of Goose Lake (p. 20) appears to strike toward and to be conformable with schist and slate a short distance to the west and northwest in sec. 23; the latter rocks may be of similar age to the Kona, although of different sedimentary facies.

DISTRIBUTION OF ROCK TYPES

In the Wewe Hills and adjoining hills in secs. 21, 22, 27, and 28, T. 47 N., R. 26 W., the undivided Chocolay Group consists mainly of quartz-sericite rocks containing varied amounts of chert and iron oxides. The iron oxides are mainly finely granular or dusty hematite, magnetite in isolated octahedra, or martite, and locally make up as much as several

percent of the rock. Some of the rocks are virtually free of iron oxides and are tan, olive green, or light gray, but the ferruginous content generally produces blue-black, dark-maroon, or dark-red weathered surfaces. Most of these rocks are massive impure quartzite or wacke and seemingly have no internal structure or only a slight schistosity; some, on the other hand, are schist and some are slate. Thin beds of conglomerate are present in a few places above the Enchantment Lake Formation of the lower part of the group. These varieties of rock have not been mapped separately because they generally are closely interbedded and not readily distinguished from one another on weathered surfaces.

The many divergent positions of bedding in secs. 22 and 23 indicate small-scale complex folding, which would further complicate any effort to project the different rock types between outcrops. The absence of mappable marker beds and the complicated folding preclude an accurate measurement of original thickness.

A lens of aluminous pelitic schist about 300 feet thick in the north part of sec. 23 contains porphyroblasts of andalusite, chloritoid, and cordierite(?).

Chloritoid-bearing quartz-sericite schist and conglomeratic schist occur beneath Ajibik Quartzite along the steep south-facing slope of the prominent hill known locally as Hendrickson Bluff (called Ajibik Hills in U.S. Geol. Survey Monograph 28) in the NW¼ sec. 28 and the NE¼ sec. 29, T. 47 N., R. 26 W.

Fracture and breccia zones in quartzite, cemented by coarse-grained and cherty vein quartz and specular hematite, and areas of ferruginous silicified slate are very common in secs. 23 and 24. A conspicuous zone of brecciated slate impregnated by vein quartz extends northwest across the W½ sec. 22 (fig. 8). The principal occurrences of breccia and associated vein quartz are shown on plate 1 (qv). The more conspicuous and linear occurrences, at least, appear to be associated with faults.

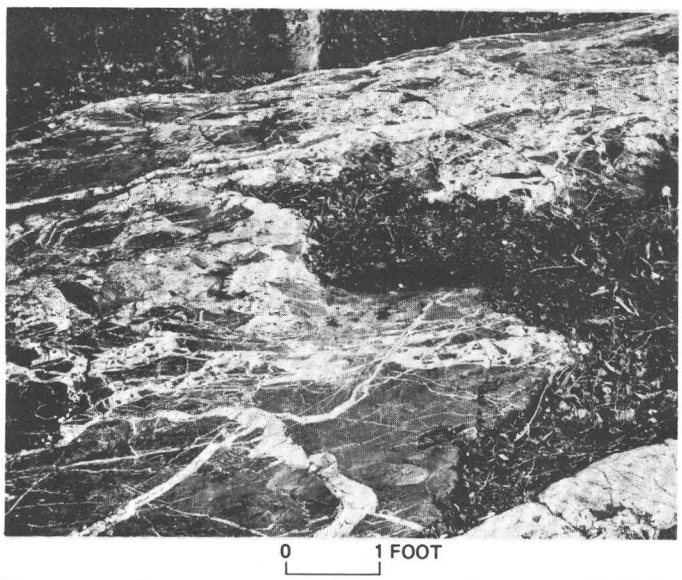

FIGURE 8.—Brecciated slate, Chocolay Group, undivided; cracks between breccia fragments filled with white vein quartz. Adjacent to inferred fault, near 2,200N–1,450E of SW. cor. sec. 22, T. 47 N., R. 26 W.

QUARTZITE, WACKE, SLATE, AND SCHIST

Ferruginous sericitic quartzite, wacke, slate, and schist are dominant in the undivided Chocolay Group in the Wewe Hills area. They form abundant exposures along the top and north slope of the hills in secs. 23 and 24, T. 47 N., R. 26 W., and constitute most of the exposures of the group, other than conglomerate, in secs. 21, 22, 27, and 28. Many individual outcrops consist entirely of quartzite, wacke, or slate, but the rocks are interlayered in many other exposures. Beds and lenses range from a fraction of an inch to many feet in thickness. Rock types are not shown on plate 1, except for relatively pure quartzite, conglomerate, and andalusite-chloritoid-cordierite(?) schist.

Fresh quartzite is colorless to gray or gray green, depending on impurities. Relatively pure quartzite weathers white, but impure quartzite and wacke weather to shades of red, red brown, or brown. Relatively pure quartzite contains more than 95 percent quartz in detrital grains and overgrowths. Such rock occurs mainly in the W½ sec. 24, in the eastern part of the Wewe Hills; it is mapped separately on plate 1, but because of its limited extent and uncertain stratigraphic position, it is not classified as a formation but is shown as a lithologic variety within the undivided Chocolay Group. The impure quartzite generally contains mixtures of detrital and cherty quartz, sericite, and finely granular iron oxide. Quartz detritus is subangular to subrounded and is generally inequigranular, ranging in size from about 0.05 to 0.7 mm. Overgrowths are common on quartz grains and in most such grains, preovergrowth outlines are marked by opaque dusty rims or narrow clusters of sericite or carbonate. Sericite is intergrown with cherty quartz of the matrix or forms thin seams between clastic grains of quartz. Quartz generally composes 85–95 percent of the rock. The typical light-gray fresh quartzite contains very minor amounts of dusty iron oxides, which in the weathered rinds are greatly concentrated to as much as several percent. Aggregates of finely granular iron oxide in the weathered quartzite are mainly

hematite and cause the dark-reddish-brown surface color of the impure quartzite in most exposures.

Wacke is similar in makeup to the impure quartzite, except that it has relatively abundant sericite—15 percent or more—and correspondingly smaller amounts of detrital quartz. Quartz grains "float" in the sericite-rich matrix.

Slate in the undivided Chocolay Group is light gray, green, or pale olive green and weathers to brown, red brown, bluish black, maroon, tan, or brownish green. It is composed largely of sericite and quartz. Finely laminated slate forms the matrix of slate-conglomerate in secs. 22 and 23, beneath massive conglomerate, and is a mixture of chlorite and quartz plus minor biotite or stilpnomelane and clastic feldspar.

Mottled gray-salmon-colored quartz-sericite schist is the dominant rock type in the Chocolay rocks in the NW¼ sec. 28 and the NE¼ sec. 29. The schist locally contains poorly defined concentrations of pebbles of slate, vein quartz, and gneiss in the NE¼ sec. 29. Most pebbles are less than one-half inch in diameter. An outcrop centered near 1,500S–450W of the NE. cor. sec. 29, is of slate-conglomerate—scattered pebbles and cobbles and one boulder 6–8 feet in diameter—of granitic gneiss in a matrix of green slate. Some of the schist in the NE¼ sec. 29 contains porphyroblasts of chloritoid (fig. 9). Van Hise and Bayley (1897, Atlas Sheet 32) evidently interpreted this rock as lower Precambrian ("Archean") gneiss, and indeed much of the nearby quartz-sericite schist strongly resembles parts of the Palmer Gneiss. The conglomerate, however, indicates that the rock is of detrital origin. The large pieces of gneiss in the conglomerate suggest closeness to the source; so possibly this rock is equivalent to the Enchantment Lake Formation.

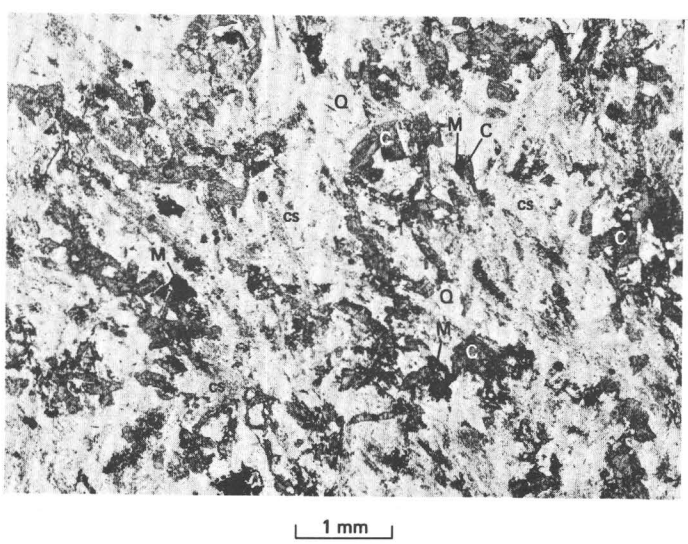

FIGURE 9.—Photomicrograph of schist consisting of porphyroblasts of chloritoid (C), quartz clasts (Q), and irregular patches of dusty opaque, possibly magnetite (M), in chert-sericite (cs) matrix, undivided Chocolay Group. JG–25–62, short distance north of Palmer fault, near 1,700S–500W of NE. cor. sec. 29, T. 47 N., R. 26 W. Plane-polarized light.

Carbonate, chlorite, biotite, feldspar, tourmaline, and leucoxene are common minor components in the Chocolay rocks.

ANDALUSITE-CHLORITOID-CORDIERITE(?) SCHIST

A lens 300 feet thick of knotty gray rusty-weathered quartz-sericite schist in the undivided Chocolay Group contains more or less altered porphyroblasts of andalusite and chloritoid, and of an unidentified mineral, possibly altered or incipient cordierite [1] (fig. 10). The lens extends east-west for about one-half mile across the north part of sec. 23, T. 47 N., R. 26 W., just north of a zone of brecciated and recemented vein quartz that is inferred to mark a fault. There is no indication that brecciation or excessive shearing extended from the inferred fault into the porphyroblastic schist.

Porphyroblasts of andalusite and possible cordierite and their alteration products compose 8–34 percent of measured thin sections. With allowances for probable sampling bias of porphyroblast-rich zones in the schist, the average estimated volume of porphyroblasts is 15 percent. Chloritoid and its replacement minerals make up 5 percent or less of the volume of the schist.

Most of the porphyroblasts of andalusite and possible cordierite contain retrograde mixtures of sericite, pyrophyllite, chlorite, kaolinite, quartz, and (or) dusty hematite.[2] Chloritoid is both in isolated grains and poikiloblastically enclosed in some grains of andalusite and possible cordierite. Most original prisms of chloritoid are now pseudomorphs rich in chlorite, hematite, or both. Sericite rims are common around the porphyroblasts of possible cordierite (fig. 10).

The associations andalusite-chloritoid and cordierite-chloritoid are reported in aluminous rocks from a number of locations in the world (Halferdahl, 1961, table 24). Intergrowths of chloritoid with these two minerals evidently are rare. Chloritoid first forms at very low metamorphic grades but evidently can also develop or persist at moderate

[1] Andalusite identified optically and by X-ray; chloritoid identified optically and by form; unknown porphyroblasts tentatively identified as cordierite by John Green of University of Minnesota at Duluth from form and general appearance (written commun., 1966), but X-ray patterns indicate only matrix minerals or retrograde alteration products.

[2] X-ray identification of andalusite and alteration minerals by A. J. Gude, U.S. Geological Survey.

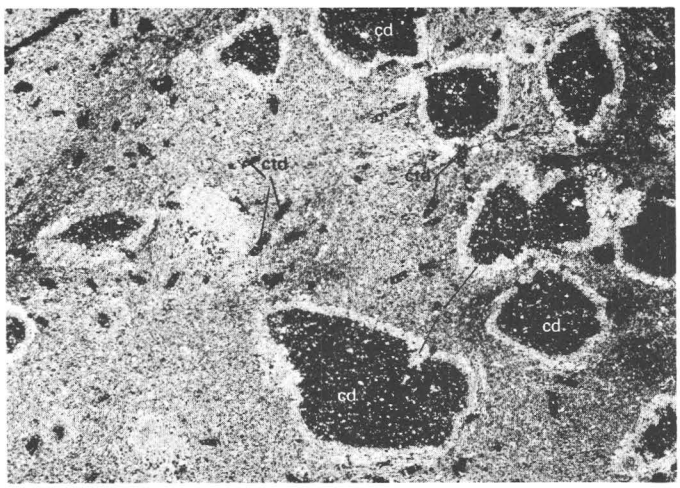

A

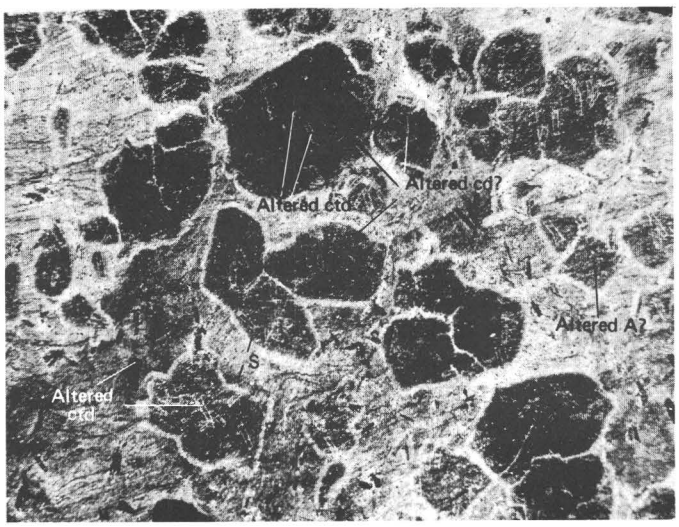

C

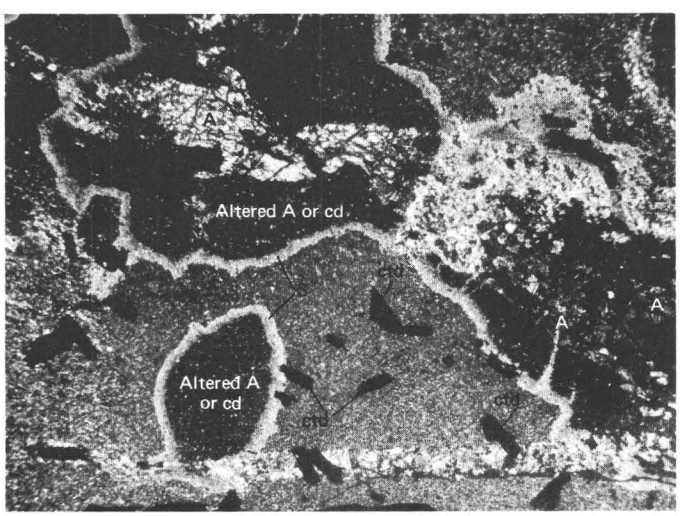

B

FIGURE 10.—Photomicrographs of porphyroblast-bearing schist, undivided Chocolay Group. (Locations measured from SW. cor. sec. 23, T. 47 N., R. 26 W.) *A*, Chloritoid-cordierite(?) schist. Porphyroblasts of chloritoid (ctd) and possible cordierite (cd) set in matrix of quartz and sericite. Cordierite(?) grains rimmed by sericite (S). Chloritoid extensively replaced by chlorite and hematite. Crossed polarizers. JG–32–61, near 4,500N–3,650E. *B*, Andalusite-chloritoid-cordierite(?) schist. Porphyroblasts of altered andalusite (A), chloritoid (ctd), and cordierite(?) (cd) set in quartz-sericite matrix. Andalusite remnants within altered porphyroblasts of andalusite or cordierite(?). Crossed polarizers. JG–55–61, near 4,500N–2,050E. *C*, altered hematite-stained andalusite-chloritoid-cordierite(?) schist. Pseudomorphs of chloritoid (ctd) poikiloblastically enclosed within altered porphyroblasts of andalusite (A) or cordierite (cd). Plane-polarized light. JG–33–61, near 4,100N–3,700E.

grades in association with andalusite or cordierite. Whether intergrowths are equilibrium assemblages is an open question. The sharply defined chloritoid prisms, poikiloblastic within andalusite (and cordierite?), suggest either simultaneous growth of the host and enclosed minerals, or later (retrograde) growth of the enclosed chloritoid by alteration of the host.

The aluminous schist in sec. 23 (table 3) is compositionally suitable for the development of andalusite, chloritoid, and cordierite. Andalusite probably formed by prograde dehydration reactions involving kaolinite, sericite, or pyrophyllite. Cordierite may have formed by prograde dehydration reactions between any of the latter minerals and chlorite. A prograde reaction between chlorite and sericite to form cordierite would be the reverse of the retrograde reaction forming pinite, a common alteration product of cordierite. Chloritoid may be a result of the prograde reaction of kaolinite, chlorite, and water, or of retrograde hydration reactions involving andalusite or cordierite.

Rocks surrounding the porphyroblastic schist in sec. 23 are of low regional metamorphic grade, which in the absence of nearby intrusive bodies, indicates that the schist too formed at relatively low temperature. Despite the suggestion of higher grade given by the presence of andalusite and cordierite(?), possibly these minerals form at relatively low temperature under certain conditions. Experimental data suggest an overlap in the P-T fields of andalusite and chloritoid below a pressure of a few

kilobars at 300°–400°C (Clark and others, 1957, p. 637–638; Clark, 1961; Halferdahl, 1961, fig. 15; Miyashiro, 1961, figs. 4, 5) and from experimental data, Schreyer and Yoder (1959) extrapolated a low P-T field for cordierite. According to Thompson (1955, fig. 2, p. 90–96), hydration-dehydration reactions during metamorphism take place at different P-T conditions near open fissures than in closed systems. The zone of brecciated and recemented vein quartz south of the schist in sec. 23 is interpreted as the site of a fault and may have been an open fissure system during metamorphism of the schist. Thompson showed that in an open system of fissures through which water could escape from rocks undergoing metamorphism, the temperature of dehydration reactions would decrease as pressure is increased, opposite to the effect in a closed system. Retrograde alterations of porphyroblasts can be explained by P-T changes in the direction of present day conditions that necessarily followed prograde metamorphism.

TABLE 3.—*Chemical analysis of porphyroblast-bearing schist, undivided Chocolay Group, sec. 23, T. 47 N., R. 26 W*

[Standard analysis by S. M. Berthold, U.S. Geol. Survey. Sample JG–24–67. Location, 4,500N–3350E of SW. cor. sec. 23, T. 47 N., R. 26 W]

SiO_2	67.52	H_2O^+	3.94
Al_2O_3	19.80	H_2O^-	.14
Fe_2O_3	5.02	TiO_2	.33
FeO	.25	P_2O_5	.13
MgO	.21	MnO	.00
CaO	.10	CO_2	.05
Na_2O	.52		
K_2O	2.24	Total	100.25

AGE RELATIONS

Northeast of the Wewe Hills, in the eastern part of the Marquette iron range, the Wewe Slate underlies Ajibik Quartzite and overlies Kona Dolomite, which in turn overlies Mesnard Quartzite. In the Wewe Hills, rocks of the undivided Chocolay Group underlie the Ajibik and either rest directly on a basement of lower Precambrian ("Archean") granitic gneiss or on conglomeratic Enchantment Lake Formation, which in turn lies directly on gneiss. Van Hise and Bayley (1895, 1897) considered the entire pre-Ajibik sedimentary sequence in the Wewe Hills to be one formation equivalent to the post-Kona slate to the northeast, and they named the formation for the Wewe Hills. They explained the absence of the Mesnard and Kona in the Wewe Hills as a result of the area being above water during deposition of the Mesnard and Kona to the northeast. Accordingly, subsidence of lower Precambrian rocks in the Wewe Hills and sedimentation on them did not begin until Wewe time, as the middle Precambrian sea transgressed westward. Gneissic rocks in the Wewe Hills and Kona Dolomite to the northeast then became covered by the contiguous deposits of mud and associated materials.

Van Hise and Leith (1911, pl. 17) reassigned the Wewe Slate in the Wewe Hills to the sub-Kona Mesnard Quartzite but retained Wewe Slate to the northeast where it directly overlies Kona Dolomite. Curiously, this major change in their map was not discussed in the text. It therefore is conjectured that despite the lack of lithologic resemblance of typical white-weathering vitreous Mesnard Quartzite and impure quartzite and most other rocks in the Wewe Hills, the change was made because of the analogous relationships of the Mesnard and the rocks in the Wewe Hills to subjacent lower Precambrian rocks. The change placed Mesnard immediately beneath Ajibik Quartzite in the western part of the Wewe Hills, and by implication required the pinchout or erosional truncation of at least many hundreds of feet of Kona Dolomite and Wewe Slate in a distance of about 3,000 feet between the Kona Hills northeast of Goose Lake and the western Wewe Hills.

Erosion is known to have followed deposition of the Chocolay Group and preceded deposition of the Ajibik Quartzite; so possibly a substantial part of the Chocolay, including carbonate facies of the Kona Dolomite, was removed by that erosion in the Wewe Hills. Indeed, erosional truncation is one possible explanation for the absence of Chocolay rocks farther west in the Marquette district. Nevertheless, the absence of fragments of dolomite and the scanty fragments of silicified dolomite in basal Ajibik conglomerate in the Wewe Hills indicates that if deposition took place in that area during Kona time, carbonate was not significant as it was to the east. Possibly carbonate is rare or absent in the Wewe Hills because the area was generally emergent, as Van Hise and Bayley thought, so that little or no deposition occurred during Kona time, or because only noncarbonate (nearshore?) deposits accumulated there during Kona time. The alternatives that the undivided Chocolay Group in the Wewe Hills may be (1) of post-Kona age, equivalent only to the Wewe Slate farther east; (2) an undetermined (lower) part of the full Chocolay section, remaining after erosion; or, (3) lithologic variants of the type Chocolay section, stratigraphically equivalent to all or part of that section farther east, probably cannot be evaluated without time or horizon markers in the rocks.

The lithologic similarity and probable similar stratigraphic position of slate closely underlying Ajibik Quartzite in the western Wewe Hills and of Wewe Slate between the Ajibik and the Kona north of Goose Lake indicate a probable correlation of

these slates. Because of this probable correlation and the difficulty of mapping stratigraphic units in the Wewe Hills, the original interpretation of Van Hise and Bayley was followed during much of the present work (Gair, 1968). However, much of the rock previously considered to be Wewe Slate in the Wewe Hills is here assigned to the Chocolay Group without designation as to formation, in recognition of the uncertain correlation of most outcrops.

MENOMINEE GROUP

The formations of the Menominee Group in the Palmer quadrangle are the Ajibik Quartzite, the Siamo Slate, and the Negaunee Iron-Formation. The Ajibik and Siamo together correspond stratigraphically to the Felch Schist in the type area of the group in Dickinson County (James and others, 1961, p. 36–39), and the Negaunee is equivalent to the Vulcan Iron-Formation in that area.

AJIBIK QUARTZITE

NAME, DISTRIBUTION, AND THICKNESS

The Ajibik Quartzite was named by Van Hise and Bayley (1895, p. 540–554) for the Ajibik Hills in secs. 28 and 29, T. 47 N., R. 26 W., ½–1 mile northeast of Palmer. The hills are not named on the present topographic map, but the cliff along their south side is called Hendrickson Bluff by local inhabitants. North of Goose Lake, the formation consists largely of light-colored rather pure vitreous quartzite. South and southwest of the lake, in a belt bordering the Wewe Hills, the formation contains both vitreous quartzite and less pure quartzite and wacke having a matrix of sericite and some cherty quartz, and, in places, a little chlorite. Both kinds of quartzite occur in the type area. The only outcrop of the Ajibik on the east margin of the Palmer basin is white-weathering vitreous quartzite, but at the southeast end and along the south side of the basin, most of the Ajibik consists of mixtures of detrital quartz, sericite, chlorite, and chert, and is darker. Much of the Ajibik there is a quartz wacke. Vitreous Ajibik Quartzite has been faulted up into the central part of the Palmer basin in the SW¼ sec. 28. On the south flank of the Marquette synclinorium, northwest of Palmer in the hill lying just north of the center of sec. 30, T. 47 N., R. 26 W., cherty, sericitic, and chloritic quartzite and wacke are the principal kinds of rock. Subordinate sericitic slate is also present. The rock in that area has been considerably deformed and fractured by movement along the Palmer fault and contains veins and other secondary deposits of quartz. Andalusite and chloritoid have formed in some beds. Conglomerate is present at the base of the Ajibik in some localities (fig. 11) and confirms and extends earlier evidence (Van Hise and Bayley, 1895, p. 550; 1897, p. 294, 307; Van Hise and others, 1905; Gair and Thaden, 1968, p. 48) of erosion just prior to the deposition of the formation. The pre-Ajibik erosion evidently was widespread. Northeast of the Palmer basin, the Ajibik overlies undivided Chocolay rocks, but around the margins of the basin and to the west along the south flank of the Marquette synclinorium, it directly overlies lower Precambrian rocks. The differences in sub-Ajibik rock may have been caused by the pre-Ajibik erosion and truncation of successively older formations from east to west across the area, or by the transgression of the Ajibik onto lower Precambrian rocks that had previously been above sea level. At the northeast corner of the Palmer basin and to the north, the Ajibik is overlain conformably by a considerable thickness of Siamo Slate, but in the rest of the basin, the Siamo either is very thin or nonexistent, and the Ajibik is in contact or nearly so with the Negaunee Iron-Formation. The Ajibik is distinguished from lithologically similar rock in the Chocolay Group principally by its proximity to overlying Siamo Slate or Negaunee Iron-Formation. Drill holes that pass through the base of the iron-formation along the south side of the basin generally enter greenish graywacke that is more akin to parts of the Siamo than to the Ajibik. It is therefore likely that the Ajibik, as mapped in parts of that area, includes an unexposed thin upper zone of Siamo-type rock. Near the west edge of the quadrangle and in quadrangles to the west (G. C. Simmons, W. F. Cannon, oral commun., 1970), the Ajibik and Siamo generally cannot be mapped separately. In the NW¼NW¼ sec. 33, T. 47 N., R. 26 W., vitreous Ajibik Quartzite is interbedded with and grades upward into magnetite-rich iron-formation.

The maximum thickness of the Ajibik in the Palmer quadrangle, derived from mapped widths of the formation in several places and corrected for dip, is approximately 450 to 600 feet. The formation is closely delimited both above and below in only one place in the area, near the SE. cor. sec. 16, T. 47 N., R. 26 W. For an assumed dip of 30°, the thickness there is 470 feet. The outcrop of Ajibik in the SW¼ sec. 11 is about 1,100 feet wide perpendicular to the strike, but the unit is not closely delimited either above or below. For an assumed average dip of 25°, the exposed rock is 450 feet thick, and the thickness between the mapped contacts is about 600 feet. On the nose of the anticline in the west-central part of sec. 21, T. 47 N., R. 26 W., the width of Ajibik from the well-defined base of the formation to the top of

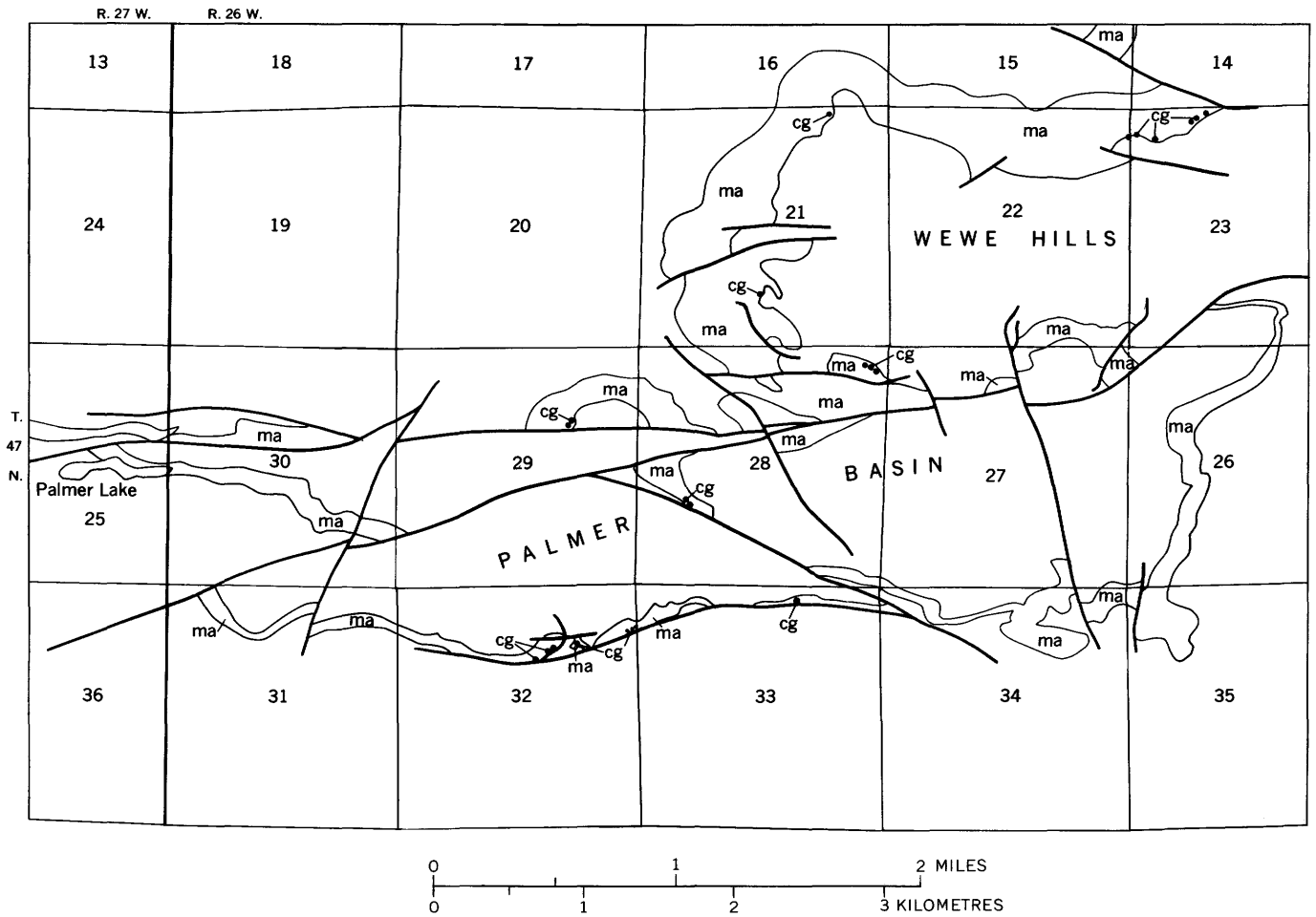

FIGURE 11.—Sketch map showing distribution of basal conglomerate in the Ajibik Quartzite in part of the Palmer quadrangle. ma, Ajibik Quartzite; cg, conglomerate.

the uppermost outcrop is about 1,300 feet, representing a thickness of 530 feet, if the dip is taken as 25°. The thickness in that area between the upper and lower mapped contacts is 620 feet.

CONGLOMERATE

NORTH OF PALMER BASIN

The most conspicuous occurrence of basal Ajibik conglomerate in the quadrangle is a narrow outcrop, 300 feet long, centered at 1,450 feet east-southeast of the NW. cor. sec. 23, T. 47 N., R. 26 W. Angular fragments of red chert, tan and dark slates, knotty andalusite-chloritoid-cordierite(?) rock, quartz-sericite schist, quartzite, and vein quartz range in size from less than an inch to several feet. Several of these types of rock are common in exposures of the undivided Chocolay Group to the southeast. The largest fragment seen in the outcrop is a 3- to 4-foot boulder of laminated red and white silicified dolomite (jasperoid). Laminae are folded and cut by veins of white quartz and are truncated by the edge of the boulder. Folding, silicification, and veining of original dolomite in this case must have taken place before deposition of the Ajibik.

Other outcrops of Ajibik conglomerate north of the Palmer basin are small and contain thicknesses of not more than a few feet, except for an exposure west of Hendrickson Bluff and just north of the Palmer basin northeast of Palmer, at 1,700S–1,500W, NE. cor. sec. 29. The outcrop there is about 100 feet long and 20 feet wide; the conglomerate contains pebbles and cobbles of vein quartz and pebbles of quartz-sericite schist, but is separated from the underlying schist in the existing exposures by a bed of vitreous quartzite 5–10 feet thick, so is not strictly basal at the present land surface. The minor occurrences of conglomerate consist mainly of pebbles of quartz or quartzite in a wacke or slate matrix. South of the NE. cor. sec. 22 (fig. 11), a bed of basal Ajibik conglomerate, 1–3 feet thick, contains fragments of quartzite or vein quartz as large as cobble size. The conglomerate overlies seri-

citic and quartz-sericitic slate with a probable discordance in trend of 25°–30°, on the basis of somewhat uncertain bedding surfaces above and below the contact. To the east in sec. 23, a bed of cobbly quartzitic conglomerate, 1–2 feet thick, appears to truncate underlying slate at an angle of about 90°. However, the contact between that conglomerate and the slate may be a fault. Near the base of the Ajibik in the NE¼ sec. 21, a mass of cobbly quartzite a few feet across—quartzite cobbles in a matrix of sericitic quartzite or wacke—occurs in an outcrop of ferruginous vitreous quartzite. In the south-central part of sec. 21, T. 47 N., R. 26 W., pebbles of vein quartz and sericite-quartz rock like that in underlying Chocolay rocks occur in a matrix of schistose sericitic quartzite. In the northeast part of sec. 28, pebbles of tan slate and a siltite, less than one half inch in size, occur in a dark-bluish slaty matrix, in a bed a few feet thick. The slaty conglomerate is underlain by slate (Chocolay Group, undivided) and overlain by vitreous quartzite.

PALMER BASIN

The principal occurrences of basal conglomerate in the Ajibik in the Palmer basin are adjacent to lower Precambrian gneiss along the south margin in the NE¼ sec. 32, and in Ajibik that has been upfaulted in the central part of the basin, in the west-central part of sec. 28 (fig. 11). In sec. 32, fragments in pebbly and cobbly schistose conglomerate or in pebbly quartz-chlorite wacke are largely pink-weathering granitoid rock, as much as 6 inches in diameter, and certain vaguely defined cobbles as much as 1 foot across. The conglomerate in the west-central part of sec. 28 consists of pebbles, cobbles, and boulders as much as 1 foot in size, of chert, quartzite, and vein quartz surrounded by a matrix of vitreous quartzite. Conglomerate has been seen at the base of the formation also in sec. 33 (fig 11). At the southeast end of the basin, near 600S–1,150E, NW. cor. sec. 35, scattered quartz pebbles as much as one-half inch in size occur in sericitic quartzite well above the base of the Ajibik, and would seem to have no relation to pre-Ajibik erosion.

QUARTZITE, WACKE, AND SLATE

Colorless, light-gray or gray-tan, light-pink, and red vitreous quartzite composes most of the formation north of the Palmer basin and is virtually identical to quartzite in the Ajibik in the Marquette and Sands quadrangles (Gair and Thaden, 1968). The description in the report on those quadrangles applies also for most of the Ajibik north of the Palmer basin and for minor pure quartzite parts of the formation in the basin.

Along the south margin of the Palmer basin, and along the south flank of the Marquette synclinorium, ½–¾ mile northwest of Palmer, massive and schistose quartzite and wacke composed mainly of sericite, chert, chlorite, and clastic quartz are typical of the Ajibik (figs. 12, 13). In the Wewe Hills north of the east half of the Palmer basin, such rock is subordinate to vitreous quartzite. Small amounts of

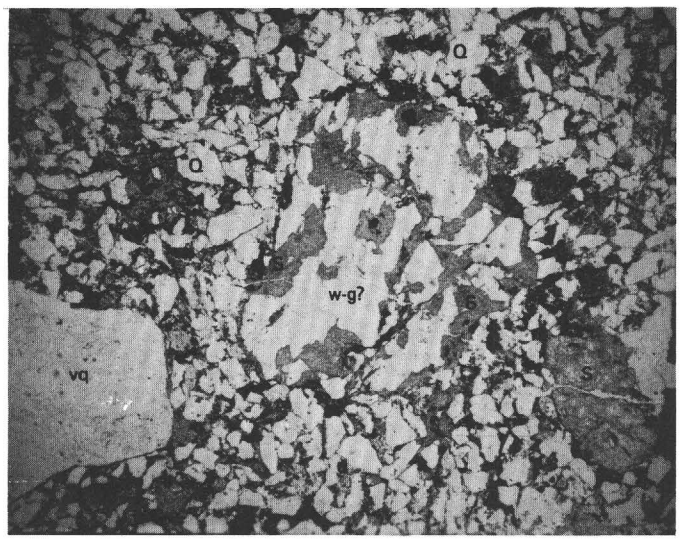

A

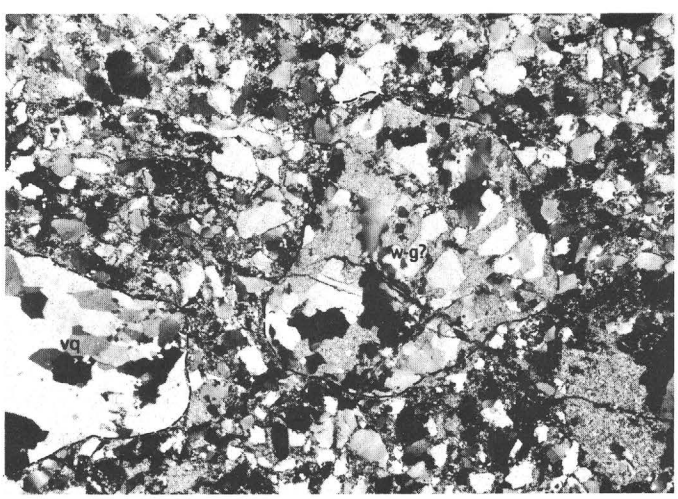

B

FIGURE 12.—Photomicrographs of quartz-sericite wacke, Ajibik Quartzite. Clastic quartz (Q) and rock fragments loosely packed in matrix consisting mainly of sericite (S). Rock fragments shown are of vein quartz (vq) and quartz-sericite wacke or completely sericitized granite (w-g?). *A*, Plane-polarized light; *B*, Crossed polarizers. JG–102–64, 1,000S–1,900W of NE. cor. sec. 34, T. 47 N., R. 26 W.

FIGURE 13.—Photomicrograph of strongly foliated and brecciated quartz-sericite wacke, Ajibik Quartzite near Palmer fault. Elongated clastic quartz grains (Q) "float" in sericite matrix. Some drag along breccia crack (bc). Crossed polarizers. JG–21D–66, 2,100S–1,700E of NW. cor. sec. 30, T. 47 N. ,R. 26 W.

sericite-rich slate are interbedded with these rocks. Minor amounts of dusty hematite(?) are common in the argillaceous parts of the wacke, slate, and impure quartzite. Such Ajibik rocks that contain substantial amounts of materials other than clastic quartz are generally light shades of gray, greenish gray, or tan, and weather light gray, gray, gray-green, brownish gray, or salmon. Clastic quartz ranges in amount from a few percent to about 90 percent, and in size from about 0.1 to 5.0 mm. Small clasts generally are subrounded or rounded; larger ones are angular. Intermixed sericite, chert, and chlorite typically compose the matrix of clastic beds, and also are the principal constituents of beds of schistose wacke. Wacke composed essentially of a dominant matrix of sericite and subordinate "floating" subrounded and rounded clasts of quartz is particularly well developed in the north-central part of sec. 34, and in the NW¼ sec. 35, T. 47 N., R. 26 W.

On the south margin of the Palmer basin in the NW¼NW¼ sec. 33, magnetite is an important component of the matrix of wacke and impure quartzite in a transition zone about 20–50 feet wide between the Ajibik and the overlying Negaunee Iron-Formation. In that zone, beds of magnetite-bearing quartzite and wacke, as much as 4 inches thick, alternate with inch-thick and thinner layers rich in magnetite and reddish hematitic chert. Clastic grains there are as much as a quarter of an inch in diameter. Farther west, between 1,200S–1,500S and 1,200E–1,800E of the NW. cor. sec. 32, interbedding of vitreous clastic quartzite and reddish hematite-chert iron-formation is common near the top of the Ajibik.

ANDALUSITE- AND CHLORITOID-BEARING ROCKS

On the south side of the Palmer basin, andalusite and chloritoid occur in some beds rich in sericite, pyrophyllite, and kaolinite, some of which may also contain chlorite and cherty quartz, near 1,400S–2,300W and 1,200S–2,050W of the NE. cor. sec. 32. Chloritic pseudomorphs of chloritoid(?) are present in some of the cherty sericitic Ajibik Quartzite in the NW¼ sec. 35, and the adjoining part of sec. 26 (fig. 14). Preliminary identification of andalusite and chloritoid were made by microscope, and each was confirmed, along with kaolinite and pyrophyllite, in separate X-ray patterns by T.E.C. Keith, U.S. Geological Survey. At the first two localities in sec. 32 mentioned above, pyrophyllite is also present in coarse "books" with quartz in veins cutting the Ajibik near irregular patches of pyritic mineralization. Chloritoid is locally abundant in cherty sericite-chlorite-quartz wacke near 800S–1,600W of the NE. cor. sec. 31. Lamey (1935, p. 1145–46) found andalusite and chloritoid in the same belt of Ajibik Quartzite, and Davis (1965, p. 10) reported andalusite in drill core, cutting probable Ajibik in the north-central part of sec. 32. One-half to three-fourths of a mile northwest of Palmer in the N½ sec. 30, and immediately north of the Palmer fault, some schistose sericitic quartzite, wacke, and slate of the Ajibik contain porphyroblasts of andalusite, chloritoid, or both (fig. 14).

These minerals typically occur in parts of the rock (table 4) rich in sericite, sericite and cherty quartz, or sericite, chlorite, and quartz. In a sample of Ajibik schist from southeast of Palmer, however, chloritoid is virtually restricted to ragged patches of nearly pure cherty quartz that are scattered through a "matrix" of evenly mixed sericite and cherty quartz. Prisms of chloritoid in places are poikilitically enclosed in andalusite. Andalusite porphyroblasts commonly have been partly retrograded to

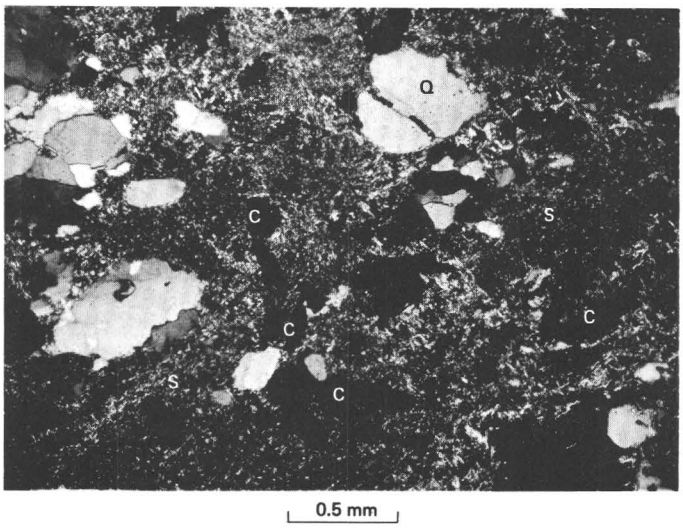

A

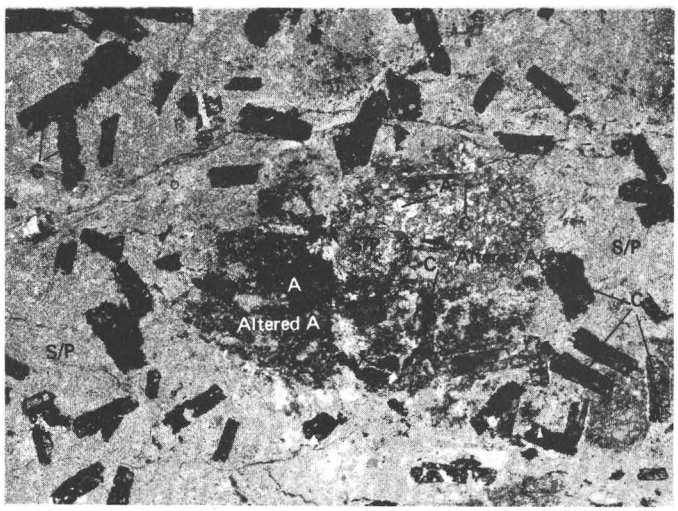

C

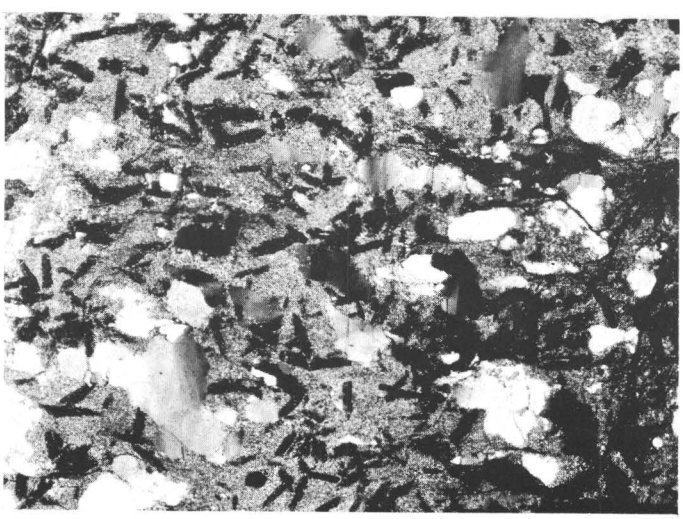

B

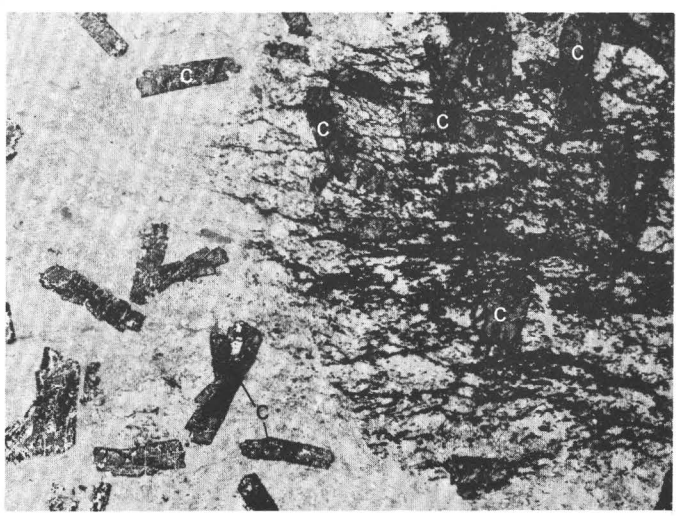

D

FIGURE 14.—Photomicrographs of chloritoid-bearing Ajibik Quartzite. *A*, Quartz-sericite wacke containing chloritic pseudomorphs of chloritoid(?) (C) and grains of clastic quartz (Q) in matrix rich in sericite (S). Crossed polarizers. JG–93–65, 200N–600E of SW. cor. sec. 26, T. 47 N., R. 26 W. *B*, Chloritoid (C)-rich quartz-sericite wacke. Crossed polarizers. JG–21E–66, 3,100N–1,700E of SW. cor. sec. 30, T. 47 N., R. 26 W. *C*, Andalusite-chloritoid schist. Some prisms of chloritoid (C) poikiloblastically enclosed in extensively altered large porphyroblast of andalusite. Remnants of andalusite (A) surrounded by sericite (S) and (or) pyrophyllite (P). Crossed polarizers. JG–22–66, 3,250N–1,700E of SW. cor. sec. 30, T. 47 N., R. 26 W. *D*, Sericite-chloritoid schist. Porphyroblasts of chloritoid (C) are set in matrix consisting largely of sericite. Hematite produced by oxidation-weathering is concentrated in and emphasizes foliation surfaces. Chloritoid formed later than the foliation. Plane-polarized light. JG–22C–66, 3,250N–1,750E of SW. cor. sec. 30, T. 47 N., R. 26 W.

mixtures of pyrophyllite, sericite(?), and quartz; chloritoid has been partly oxidized to red-brown hematite by weathering.

Conditions of origin appear to have been similar to those of the andalusite-chloritoid-cordierite(?) schist in the undivided Chocolay Group discussed earlier (p. 26). Andalusite formed in aluminous rocks adjacent to faults, under conditions of relatively low grade metamorphism, and the chloritoid grew during a later stage of the metamorphism,

after schistosity and andalusite had formed. Some chloritoid developed retrogressively from andalusite. The growth of andalusite may have been promoted by the loss of water along nearby faults.

TABLE 4.—*Chemical analysis of chloritoid-bearing sericitic schist, Ajibik Quartzite*

[Standard chemical analyses by S. M. Berthold, U.S. Geol. Survey. Sample JG-19-67. Location, 3,200N-1,850E of SW. cor. sec. 30, T. 47 N., R. 26 W.]

SiO_2	75.31	H_2O^+	2.76
Al_2O_3	17.26	H_2O^-	.18
Fe_2O_3	1.11	TiO_2	.61
FeO	1.00	P_2O_5	.21
MgO	.29	MnO	.00
CaO	.26	CO_2	.00
Na_2O	.79		
K_2O	.75	Total	100.53

EROSIONAL DISCONTINUITY AT BASE OF FORMATION

The widespread occurrences of conglomerate at the base of the Ajibik south of Goose Lake (fig. 11) and the occurrences of Ajibik conglomerate in the Sands quadrangle (Gair and Thaden, 1968, p. 47) and near Negaunee (Van Hise and others, 1905; Puffett, 1974) suggest an area-wide erosional discontinuity and confirm the division by Van Hise and others (1905) of the original Marquette series into two units—their lower and middle Huronian rocks—separated by an erosional unconformity. North of Goose Lake, the map pattern indicates that, as in the Marquette and Sands quadrangles (Gair and Thaden, 1968, p. 48), the Ajibik is practically concordant with the underlying beds, or at most, forms a very low-angle unconformity with them. In the Wewe Hills south of Goose Lake, on the other hand, nonsystematic small-scale folding is characteristic of the Chocolay rocks but is not reflected in the Ajibik, so there is considerable local structural discordance between the Ajibik and underlying formations in that area. This may have been caused by limited pre-Ajibik uplift and deformation in the Wewe Hills that perhaps also explains the more numerous occurrences of conglomerate south of Goose Lake than to the north and northeast. On the other hand, the nonsystematic small-scale folds may have formed during Penokean orogeny as a reflection of irregular doming of basement rocks beneath the Wewe Hills. The detailed effects of such irregular doming could have died out upward into the more general fold around the hills made by the Ajibik Quartzite.

North of the Palmer basin, Ajibik conglomerate rests on undivided Chocolay rocks but in the Palmer basin and to the west, such conglomerate directly overlies lower Precambrian basement rock. Whether the pre-Ajibik erosion indicated by the conglomerate stripped middle Precambrian metasedimentary rock from the basement in the area of the Palmer basin and westward, or whether that area was above sea level during pre-Ajibik deposition is not known.

CORRELATION AND AGE

Lithology and stratigraphic associations indicate that the Ajibik Quartzite is correlative with the Palms Quartzite of the Gogebic Range (Van Hise and Leith, 1911, p. 229–230, 598; Aldrich, 1929, p. 82–89), and stratigraphic associations indicate equivalency with the lower part of the Felch Schist of Dickinson County (James and others, 1961, p. 36–37). The widespread erosion that took place just before and up to the deposition of the Ajibik was brought about by slight uplift in the northeast part of the Palmer quadrangle and gentle folding and uplift south from the Goose Lake area. The presence of conglomerate over a 10-mile interval from the Sands quadrangle (Gair and Thaden, 1968, p. 47–48) suggests erosion of regional extent. The hiatus between Ajibik and underlying rocks, therefore, probably corresponds to that between the Palms Quartzite and underlying Bad Water Dolomite and between Felch Schist and Randville Dolomite, separating rocks of the lower and middle parts of the Marquette Range Supergroup.

SIAMO SLATE

The Siamo Slate was named by Van Hise and Bayley (1895, p. 554) for the Siamo Hills (not named on latest topographic map of U.S. Geol. Survey) near the west end of Teal Lake. The formation is conformable with Ajibik Quartzite below and Negaunee Iron-Formation above. It is mapped from the top of massive light-colored quartzite (Ajibik) to the stratigraphically lowest bed of Negaunee Iron-Formation. Major rock types in the Siamo are slate, sericitic, chloritic, and feldspathic quartzite, and graywacke. Arkose is common in a limited zone in the upper part of the formation about a mile southeast of the city of Negaunee. A bed of ferruginous magnetic rock, the Goose Lake Member, is 50–100 feet thick and is continuous for 4–5 miles, and other thinner unmappable ferruginous beds occur in slate generally within about 100 feet stratigraphically above or below the Goose Lake Member. Quartz-sericite schist containing porphyroblasts of andalusite and chloritoid a short distance north of the Palmer fault near 1,400S–1,200E of the NW. cor. sec. 28, T. 47 N., R. 26 W., appears to overlie Ajibik Quartzite and is interpreted as a part of the Siamo Slate. The quartz-sericite lithology and proximity to the Palmer fault rather than the strati-

graphic unit are believed to be critical factors in the development of the porphyroblasts, as discussed in the preceding sections of the report.

STRATIGRAPHIC ZONES AND THICKNESS

From its base upward, the Siamo can be divided into a lower slate unit, the ferruginous Goose Lake Member, a middle slate unit, a medium-grained quartzite-arkose-graywacke unit, and an upper slate unit. The upper part of the clastic unit in places is equivalent to the upper slate unit. The boundaries of the zones are poorly known and are not shown on plate 1. The zones are of uncertain thickness in most of the area, except for the lowest zone and the Goose Lake Member overlying that zone. The Goose Lake Member is represented in pl. 1 chiefly by a line marking the magnetic anomaly which is the principal means of locating the member.

Exposures of the Siamo are clustered in several areas. Parts of the lower and middle slates are well exposed in the S½ sec. 3, N½ sec. 10, and in the central part of sec. 15, T. 47 N., R. 26 W. Numerous outcrops of the upper slate and the quartzite-arkose-graywacke unit occur ½–1½ miles east and southeast of Negaunee in parts of secs. 4, 5, 8, and 9, and in the SE¼ sec. 17. Graywacke is the dominant type of rock in the upper 200–300 feet of the formation in clusters of outcrops in the north-central part of sec. 20, and in the N½ sec. 30 and the adjoining part of sec. 19.

Lower slate: Contains beds of graywacke; approximately 500–600 feet thick; thickness computed from mapped width and estimated average dip in the SE¼ sec. 10, the east-central part of sec. 15, and the adjoining east-central part of sec. 20 and west-central part of sec. 21.

Goose Lake Member: Unit traced magnetically for 4–5 miles northeast from point about one-half mile north of village of Palmer; estimated thickness of 50–100 feet is based on magnetic data (Gair and Wier, 1964).

Middle slate: Contains beds of graywacke; poorly exposed; highly conjectural thickness of 1,000–1,500 feet is estimated from "reasonable" guesses about structure in the S½ sec. 9 and the NW¼ sec. 15, T. 47 N., R. 26 W. Most of the estimated thickness may be illusory and exaggerated because of very low dips, repetition of beds by folding, or flowage of slate into the axial part of the synclinorium during folding.

Quartzite-arkose-graywacke: Unit contains beds of slate; south of middle of sec. 20, T. 47 N., R. 26 W., this unit appears to extend upward to the top of the formation, so in part is stratigraphically equivalent to the upper slate; approximately 500–600 feet thick exclusive of beds equivalent to the upper slate; thickness computed from mapped width and average dip on southwest limb of large second-order fold south of the Tracy fault in the NE¼ sec. 8, T. 47 N., R. 26 W., but no allowance made for possible isoclinal folds on that limb. Numerous outcrops present in secs. 5, 6, and 9, but folding is too complicated and continuity of horizons is too uncertain to compute the thickness there.

Upper slate: Contains beds of graywacke; located in northern part of quadrangle and evidently does not continue south of the middle sec. 20, T. 47 N., R. 26 W.; approximately 200–300 feet thick; thickness computed in E½ sec. 5, from mapped widths and average dips, but no allowance made for possible isoclinal folds.

Drill holes that pass from Negaunee Iron-Formation into the Siamo in the northwest part of the quadrangle commonly cut clusters of white chert laminae in the uppermost few feet of the Siamo. The chert laminae alternate with layers of green chloritic slate (fig. 15) and appear to have heralded the end of Siamo deposition and the beginning of iron-rich sedimentation.

Van Hise and Bayley (1897, p. 322) reported a thickness of 1,250 feet for the Siamo Slate, measured on the north limb of the synclinorium near Teal Lake, but they stated that because of possible undetected folds, the true thickness might be about 600 feet or less. Along a northwest-trending line

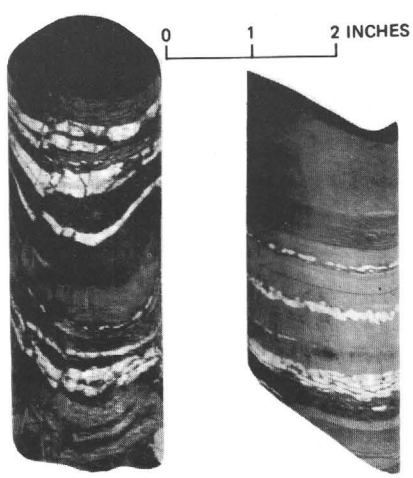

FIGURE 15.—Drill-core samples of interlaminated green slate and white chert, top of Siamo Slate, few feet below contact with Negaunee Iron-Formation. LEFT: JG–106C–66, drill-hole location 221, from 591 feet; collar approximately 1,900S–280W of NE. cor. sec. 7, T. 47 N., R. 26 W. RIGHT: JG–96S–66, drill-hole location 232, from 2,100 feet; collar approximately 2,100N–1,250E of SW. cor. sec. 7, T. 47 N., R. 26 W.

across the central part of sec. 20 and the adjoining west-central part of sec. 21, T. 47 N., R. 26 W., the computed thickness of Siamo is 1,000 feet. Along that line, the lower slate unit has a thickness of about 500 feet, consistent with its thickness elsewhere, but the units above the Goose Lake Member are much thinner than they appear to be 2 miles to the north in the axial part of the synclinorium. The middle slate unit, which is not exposed, must have a thickness of about 300 feet, and the quartzite-arkose-graywacke—equivalent here in part also to the upper slate unit farther north—is only about 200 feet thick. The 1,000–1,500 feet thickness estimated for the middle slate in the S½ sec. 9, W⅓ sec. 10, and in the NW¼ sec. 15 may indeed reflect a thicker primary deposit than exists between the same horizons to the southwest in secs. 20–21, or as already noted, it may be largely an illusory thickness. Likewise, the apparent 500–600 feet of quartzite-arkose-graywacke in the NE¼ sec. 8 may exceed the true thickness because of undetected isoclinal folds. The maximum thickness of the Siamo therefore may be as much as 3,100 feet, but the suggested indeterminate factors may have caused great exaggerations of original thickness. A failure to recognize folds because of the lack of exposures, particularly in the middle slate, and a lack of marker beds in the well-exposed parts of the Siamo may be prime causes of error.

CONTACT RELATIONS

The base of the Siamo Slate is exposed in three places. The best evidence that the Siamo is conformable with the underlying Ajibik is seen in a roadcut on Michigan Highway 35, in the NW¼ sec. 11, T. 47 N., R. 26 W., about 2,000 feet south of County Road 480. A gradation occurs there in a stratigraphic distance of approximately 50 feet, from white-weathering vitreous Ajibik Quartzite, through massive chloritic quartzite, alternating layers of chloritic quartzite and chloritic slate, into chloritic slate containing scattered lenses of quartzite less than an inch thick. In the central part of the Palmer basin, the base of the formation—alternating graywacke and slate and chloritic quartzite and slate—appears to be in conformable contact with vitreous Ajibik Quartzite in two of three exposures in the SW¼ sec. 28. At the northwesternmost of the three exposures, however, there is an angular discordance of Ajibik and Siamo beds, which is interpreted here to be the result of a local fault. At the old Gilmore prospect, near the S¼ cor. sec. 23, T. 47 N., R. 26 W., some 8–10 feet of gray sericitic-chloritic Siamo quartzite, in beds 2–3 feet thick, rests conformably on colorless vitreous Ajibik Quartzite. The Siamo in secs. 23 and 28 is the only part of the formation exposed in the Palmer basin. As noted earlier, however (p. 29), several drill holes along the south margin of the basin cut Siamo-type graywacke which probably forms a thin layer between the Ajibik and the Negaunee but which it is not practical to map separately from the Ajibik. Thus, the Siamo thins drastically south from the main part of the synclinorium to the south side of the Palmer basin.

The upper contact of the Siamo Slate is exposed at 1,680N–1,600W, SE. cor. sec. 5; at 1,750S–2,100E, NW. cor. sec. 8; at a number of places in the north-central part of sec. 20; at several places near the south edge of the Empire mine in sec. 19; and, at one place in the NW¼ sec. 30. At the exposures in sec. 20 and in several drill holes in secs. 7 and 8, slate or graywacke of the Siamo and iron-formation of the Negaunee alternate through a thickness of as much as 100 feet in a gradational contact zone. The Negaunee-Siamo contact in such places is arbitrarily placed at the base of the lowest iron-formation.

The Goose Lake Member is exposed in only a few places. Exposures are present in the SE¼ secs. 3 and 16, and in the NE¼ secs. 10 and 15.

SLATE

Slate of the Siamo includes both laminated and nonlaminated green, gray, and gray-green argillaceous rocks. Most of the laminated variety occurs in the lower slate unit. Nonlaminated rock of the middle slate unit is known principally from occurrences just above the Belleview "sill" in secs. 3, 4, and 10, T. 47 N., R. 26 W.; most of this rock is a structureless argillite and can be called slate only in the broadest sense used by geologists of the Canadian Shield for any fine-grained pelitic rock. Slate in the upper unit and beds in the quartzite-arkose-graywacke zone are generally poorly laminated but may have a strong fissility parallel to bedding. True slaty cleavage is found only very locally.

Most of the slate is composed of fine-grained mixtures of chlorite, chert, and sericite, through which are scattered quartz clasts and in some layers, feldspar clasts, ranging in size from about 0.05 to 0.5 mm. Laminations generally result from the concentration of larger grains in layers. Chlorite and cherty quartz are present in roughly equal amounts and compose about 70–80 percent of the material in the rock.

Stilpnomelane is common in parts of the lower slate near the Goose Lake Member, in the middle

slate, and in the uppermost part of the formation. X-ray identification of the stilpnomelane has been made by Norman Herz and Eleanora R. Iberall of the U.S. Geological Survey. Amounts of stilpnomelane vary from a few percent to about half the material in some layers. Stilpnomelane generally occurs in or near sideritic rock in the lower slate, or in the upper part of the formation in secs. 17 and 20—the part of the Siamo that contains thin layers of magnetic iron-formation.

Mineral assemblages in metadiabase that intrudes the Siamo and in many layers of the Siamo indicate the chlorite zone of metamorphism.

Thin unmapped siderite-rich layers and layers of iron-formation consisting of siderite and mixed stilpnomelane and chert are present in the lower slate unit in the east-central part of sec. 10. Magnetite euhedra are scattered through the mixed layers and in a few places coalesce to form discrete laminae. The ferruginous layers commonly are identifiable in the field by their tendency to weather rusty brown and by thinly striped layering brought out by the weathering.

QUARTZITE, ARKOSE, AND GRAYWACKE

Most exposures of quartzite, arkose, and graywacke in the Siamo occur in secs. 4, 5, 8, 9, 20, and 30, T. 47 N., R. 26 W. These rocks typically form gray, greenish-gray, and tan beds, 3 inches to several feet thick, but in many exposures layering cannot be seen in the thicker beds particularly. Beds rarely are graded, and ripple marks or cross-stratification have not been seen. Sole markings are present in places. Layers of slate are common between sandy beds. In the transition zone between Ajibik Quartzite and Siamo Slate exposed on Michigan Highway 35 in the SW¼NW¼ sec. 11, beds of gray-green chloritic quartzite, 3–10 inches thick, alternate with generally thinner beds of chloritic slate. The quartzite, arkose, and graywacke are gradational in composition and texture and similar in color; field distinctions generally cannot be made between graywacke and the chloritic quartzite and arkose.

Quartzites of the Siamo are green, gray green, light tannish gray, or pale green; they vary from compact, quartzose, and vitreous, containing 90–95 percent sand grains, to less compact rock in which sand grains make up about 85 percent of the material. Such rocks are gradational into and interbedded with graywacke, which contains more than 15 percent of matrix. Chlorite is the principal matrix mineral; sericite, chert, carbonate, and secondary brown iron oxide are generally subordinate if present. The matrix of the quartzite typically is in the form of randomly oriented seams between sand grains; in places the rock is deformed and matrix seams are strongly alined. Sand grains consist principally of parts of single crystals of quartz, but in some layers as much as 15 percent of the grains are microcline and plagioclase. Plagioclase grains are more or less altered to sericite and clay minerals. Minor chert clasts are present in a few places. The sand grains range in size from about 0.05 to 2.0 mm, but most are less than 0.8 mm; the larger grains generally are well rounded, whereas the smaller are angular to subrounded. Grains larger than 0.8 mm form less than 10 percent of the clasts and are scattered among the smaller detrital grains. Quartz clasts generally are marginally replaced by chlorite of the matrix, and in places the clasts have been enlarged by quartz overgrowths.

With increases in the amount of feldspar to more than 25 percent of the sandy material, feldspathic quartzite grades into arkose. Arkose in the Siamo is light gray, light tan, or light salmon and is generally similar in texture and appearance to the less chloritic varieties of quartzite.

In this report, green, gray-green, and gray sandy rocks in the Siamo that contain more than 15 percent of matrix are considered to be graywacke, which differs from quartzite and arkose principally in having a higher proportion of matrix to sand grains. Matrix constituents are similar to those in the quartzite and arkose. However, biotite is part of the matrix of some graywacke, particularly in secs. 20 and 23. Biotite in sec. 20 may have originated during regional metamorphism or it may be a contact metamorphic product of the intrusion of the Belleview metadiabase; that in sec. 23 may be metamorphic or it may be clastic, derived from nearby lower Precambrian gneiss. Sand grains generally "float" in the matrix. From place to place such grains may be entirely of quartz, quartz and feldspar up to about half feldspar, or mixtures of these minerals with small amounts of rock fragments, clastic chert, and clastic muscovite, and a trace of zircon. Rock fragments are generally angular pieces of chloritic or sericitic slate; some are of impure quartzite and vein quartz. Rock fragments are of about the same size as the coarser of the other sand grains and generally make up less than 1 percent of the detrital material. About half of a graywacke bed at 1,180S–2,650W of the NE. cor. sec. 20, T. 47 N., R. 26 W., in the Negaunee-Siamo transition zone, consists of a chlorite-chert matrix and granules of chlorite. Most of the other ma-

terial is clastic quartz. Clastic quartz grains are 0.12–0.3 mm in diameter, and granules are slightly elongated and reach 0.4 mm in maximum dimension. Carbonate granules and magnetite are minor constituents. This graywacke is interbedded with strongly magnetic iron-formation and with slate having the same constituents as the graywacke but in far different proportions. Foliated graywacke at 600S–2,150W, NE. cor. sec. 20, contains elongated and well-alined quartz clasts, most of which are 0.2–0.4 mm in maximum dimension. A strongly alined foliated matrix of sericite, chlorite, and biotite or stilpnomelane makes up about 45 percent of the rock. The ends of the elongate sand grains fray out into the foliation of the matrix as a result possibly of recrystallization of the sand grains, overgrowths of secondary quartz, or the growth of alined matrix minerals into the corroded ends of sand grains.

A bed of graywacke near 1,700N–1,950W of the SE. cor. sec. 3, T. 47 N., R. 26 W., contains numerous chips of dark-blue-gray slate and constitutes a type of intraformational or sharpstone conglomerate. Slate-chip graywacke is common in Siamo graywacke in the Negaunee quadrangle (W. P. Puffett, oral commun., 1968), and such graywacke is also found in other areas (Pettijohn, 1957, p. 302). The slate chips are probably a product of the breaking up, immediately before the deposition of the graywacke, of layers of mud by drying and cracking on mudflats (Shrock, 1948, p. 257), by wave action in shallow water during the deposition of the graywacke, or by the submarine slumping of partially consolidated graywacke (sand-mud) and interbedded shale (mud). Clastic dikes of graywacke cut slate in a few places in the Siamo (fig. 16) and provide evidence of a type of preconsolidation slumping in which partially consolidated laminated shale was disrupted, and segments of it were isolated by the movement of unconsolidated graywacke.

Above the basal Siamo described earlier in this section at the old Gilmore iron prospect, just south of the S1/4 cor. sec. 23, T. 47 N., R. 26 W., thin beds of graywacke are interbedded with chert, ferruginous chert, quartzite, and cherty chloritic quartzite. In the laminated graywacke and chert, chlorite is associated almost exclusively with clastic quartz in the graywacke, and the chert is virtually devoid of chlorite. Apparently the deposition of detrital quartz and chlorite (or the premetamorphic analogue of chlorite) of the graywacke alternated with the chemical precipitation of some layers of chert, and practically no overlap of the two processes took place.

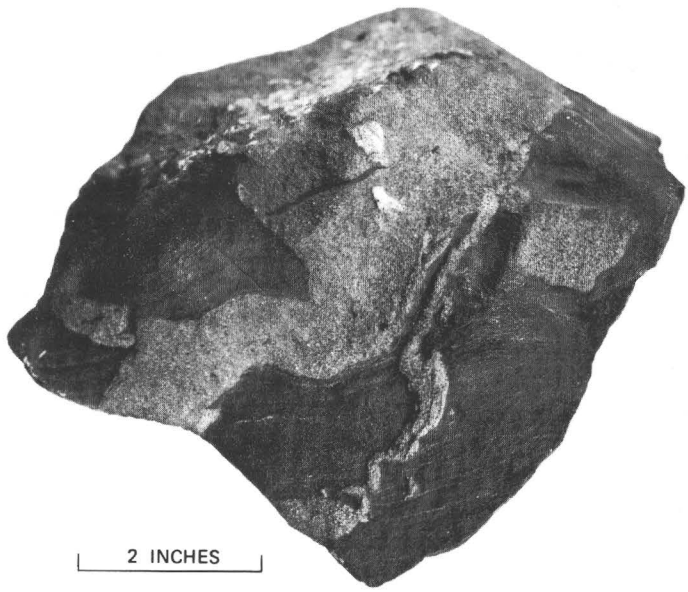

FIGURE 16.—Dikes of graywacke cutting slate, Siamo Slate. Segment of slate isolated in graywacke, at left. JG–123–62, 1,850S–2,100W of NE. cor. sec. 20, T. 47 N, R. 26 W.

IRON-FORMATION (GOOSE LAKE MEMBER)

The iron-formation is exposed in the SE1/4 sec. 3, NE1/4 secs. 10 and 15, SE1/4 sec. 16, and the south-central part of sec. 20. The name Goose Lake was first used for the rock by Tyler and Twenhofel (1952); in the present report the name is applied to exposures near the upper end of Goose Lake in the NE1/4 sec. 15, and to similar rocks exposed along the magnetic belt passing through the outcrops in sec. 15.

The iron-formation of the Goose Lake Member is a green to dark gray-green laminated rock that weathers rusty brown or striped rusty brown and white. Weathering therefore commonly emphasizes the laminated structure.

The principal minerals are siderite, chert, magnetite, chlorite, and stilpnomelane.[3] Secondary brown iron oxide is a common byproduct of the weathering of siderite, chlorite, and stilpnomelane. Typical laminated structure is produced by the concentration of separate minerals or by variations in the proportions of mixtures of the minerals (fig. 17). Layers of chert or chert-carbonate generally contain a light sprinkling of tiny needles of a brownish silicate, probably stilpnomelane, alined at large angles to the layers. Scattered carbonate and magnetite crystals reach 0.03 mm in size, but most grains are less than 0.01 mm. Poorly defined granules, about 0.1 mm in diameter, are present in some layers of chert or mixed chert and

[3] X-ray identification of stilpnomelane and siderite by Norman Herz and Eleanora R. Iberall, U.S. Geol. Survey.

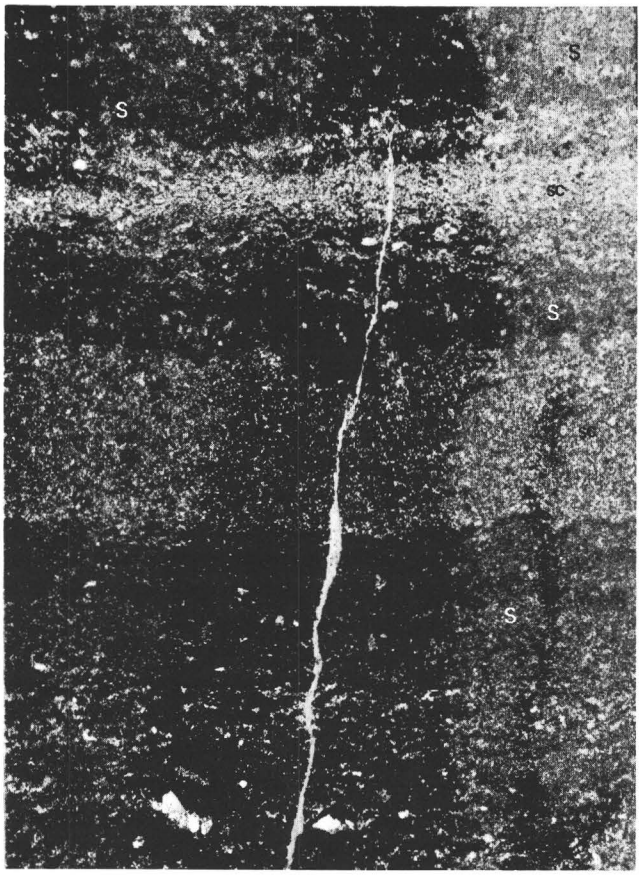

A

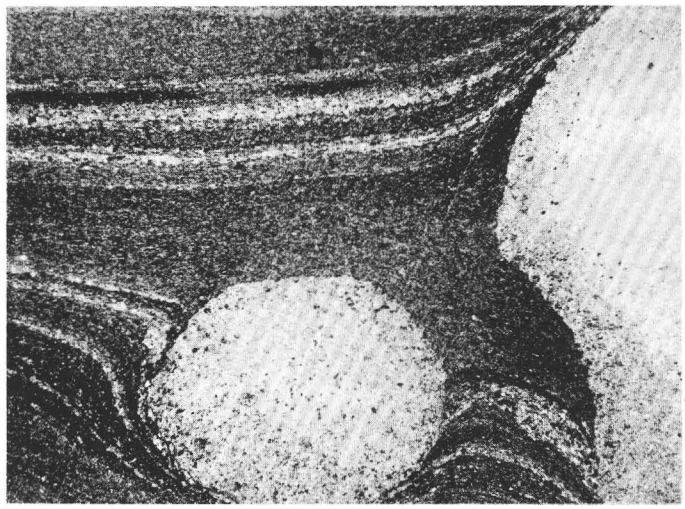

B

FIGURE 17.—Photomicrographs of Goose Lake Member of Siamo Slate. Crossed polarizers. *A*, Laminated siderite-chert iron-formation. Laminae are rich in siderite (S) and intergrown siderite and chert (sc). Secondary brown iron oxide (opaque) derived by oxidation of siderite adjacent to crosscutting crack. JG–47–62, 1,900S–1,470W of NE cor. sec. 10, T. 47 N., R. 26 W. *B*, Laminated siderite-magnetite-chlorite-chert iron-formation. Pebbles of sideritic chert indented thin laminae during deposition or compaction. JG–3–62, 1,880N–1,140W of SE. cor. sec. 16, T. 47 N., R. 26 W.

siderite. In at least one place, well-rounded and irregular pebbles of sideritic chert are impacted in thinly laminated siderite-magnetite-chert-chlorite iron-formation (fig. 17*B*). The cherty pebbles indicate shallow-water deposition during which a chert bed that had become partly solidified (dried?) was broken and reworked, or contracted into separate knots during drying.

Chemical analyses of typical samples of the iron-formation are given in table 5. Analyses 1 and 2 are of fresh and oxidized forms of similar, but not exactly the same, primary rock from the same outcrop. The oxidized rock is rich in secondary ferric oxide—hematite or goethite. The principal results of weathering and oxidation in these two samples is a great reduction in the amount of FeO and a corresponding increase in Fe_2O_3, a loss in CO_2, and an increase in H_2O. Analysis 3 is of weathered magnetite-stilpnomelane iron-formation in which magnetite has been partly oxidized to hematite. Analysis 4 is of relatively fresh siderite-magnetite-chlorite-chert iron-formation from the same vicinity and of about the same composition and appearance as the host rock of the chert-pebble iron-formation shown in figure 17*B*.

TABLE 5.—*Chemical analyses and densities, iron-formation, Goose Lake Member of Siamo Slate*

[Rapid rock analyses by P. Elmore, S. D. Botts, G. Chloe, L. Artis, and H. Smith, U.S. Geol. Survey]

	1	2	3	4
SiO_2	36.2	44.7	41.2	43.5
Al_2O_3	1.7	3.1	3.7	5.3
Fe_2O_3	5.2	27.4	35.8	13.7
FeO	31.0	8.7	9.7	20.8
MgO	3.2	2.4	1.7	1.7
CaO	.57	.34	.09	.32
Na_2O	.12	.10	.25	1.2
K_2O	.52	.47	1.2	1.4
H_2O^-	.94	2.0	1.8	.51
H_2O^+	1.9	5.2	4.3	2.0
TiO_2	.07	.13	.12	.22
P_2O_5	.39	.27	.21	.24
MnO	1.3	1.0	.30	.58
CO_2	17.0	4.4	<.05	8.5
Total	100.00	100.00	100.00	100.00
Density	3.16	2.96	3.09	3.09

1. JG–51A–62; slightly oxidized siderite-chlorite-chert iron-formation; 2,100S–1,470W of NE. cor. sec. 10, T. 47 N., R. 26 W.
2. JG–51–62; oxidized siderite-chlorite-chert iron-formation; 2,100S–1,470W of NE. cor. sec. 10, T. 47 N., R. 26 W.
3. JG–30A–62; oxidized stilpnomelane-magnetite iron-formation; 540S–770W of NE. cor. sec. 15, T. 47 N., R. 26 W.
4. JG–4–62; siderite-magnetite-chlorite-chert iron-formation; 1,830N–900W of SE. cor. sec. 16, T. 47 N., R. 26 W.

SIGNIFICANCE OF UNGRADED BEDS OF GRAYWACKE

Typical graywacke has graded beds (Kuenen and Migliorini, 1950), which are attributed to rapid deposition from turbidity currents in deep water just beyond the bottom of a continental or other long submarine slope.

In the Siamo, the common lack of graded graywacke beds indicates that deposition of the beds involved very little differential settling. The poor sorting, as in the classic examples, indicates rapid transport and no significant reworking following initial deposition. Large clasts are well rounded, probably because they spent less time in suspension and more time rolling along streambeds and sea bottom during transport than did the finer grained more angular particles. The absence of differential settling during deposition suggests either that most Siamo graywacke was (1) deposited directly and precipitously where streams having steep gradients entered the sea; or (2) in the manner of typical graywacke, was carried downslope from initial shallow-water depositional sites, but was carried in and deposited from relatively dense submarine mudflows rather than from turbidity currents. The common interbedding of laminated slate with the graywacke indicates recurring quiet deposition that tends to rule out the first possibility. Perhaps turbidity currents generally begin as submarine mudflows which become diluted only while travelling long distances, such as down continental slopes. Halting the process at an early stage after a submarine mudflow had moved a short distance and destroyed any original density stratification of the unconsolidated graywacke sediment would cause redeposition virtually concurrent with the halting of the mudflow, and little or no differential settling. It is therefore proposed that the ungraded Siamo graywacke formed similarly to typical graywacke but in a shallow restricted marine basin in which submarine mudflows could move only short distances, and turbidity currents did not develop.

NEGAUNEE IRON-FORMATION

GENERAL FEATURES

The Negaunee Iron-Formation is iron-rich metasedimentary rock stratigraphically above Siamo Slate or Ajibik Quartzite and below Goodrich Quartzite. The term "Negaunee Formation" was evidently first used by Wadsworth (1892, 1893) for both the iron-rich rocks of the present Menominee Group, widely exposed in and south of the city of Negaunee, and the overlying iron-poor metasedimentary rocks of the present Baraga Group. Van Hise and Bayley (1895, 1897), and Van Hise and Leith (1911) restricted "Negaunee formation" to the iron-rich rocks, and Leith, Lund, and Leith (1935) changed the name of the unit to "Negaunee iron-formation," the term now in general use.

The Negaunee Iron-Formation in the eastern part of the Marquette Range is, for convenience of presentation, here divided into four sectors. These are named for appropriate parts of the Marquette synclinorium and, in two of the sectors, for the largest mines in the area: (1) Maas-Mather-north limb (named for the Maas mine in Negaunee quadrangle and Mather mine on the north limb of the synclinorium in Ishpeming, Negaunee, and Negaunee SW. quadrangles), (2) axial part of synclinorium, (3) Empire-south limb (named for the Empire mine in the Palmer quadrangle), and (4) Palmer basin (fig. 18). Inasmuch as the Maas-Mather-north limb sector is outside the Palmer quadrangle to the north and northwest, it is not considered further in this report. The broad axial sector occupies much of the northwestern part of the quadrangle from the south part of the city of Negaunee to the north edge of the Empire mine.

Because of many exposures and extensive drilling and mining operations, the distribution of the iron-formation is rather well known in much of the area. An aeromagnetic survey (Case and Gair, 1965) and ground magnetic surveys made in parts of the main area of iron-formation by the Cleveland Cliffs Iron Co. and Jones and Laughlin Steel Corp., and in the Palmer basin by the author, have provided supplemental data on the location of the iron-formation. The iron-formation has been the immediate source of iron ore mined from places within the quadrangle since the middle of the 19th century. Major mines in the quadrangle have been the Athens, Jackson, Mary Charlotte, and Tracy in the axial sector, and the old Volunteer, Isabella, Star West, Platt, Old Richmond, Moore, and New Richmond in the Palmer basin. Of these, only the Empire and Tracy were in operation during most of the work on this report. The Tracy mine closed early in 1971. Lower workings of the operating Mather mine (9th–12th levels) following the dip of the north limb, extend about 800 feet into the north part of the quadrangle at depths greater than about 2,500 feet.

THICKNESS

The thickness of the iron-formation varies in different parts of the area. It is about 450 feet thick one-half mile south of the village of Palmer, about 1,300 feet thick in the deep central part of the Palmer basin near the northeast corner of

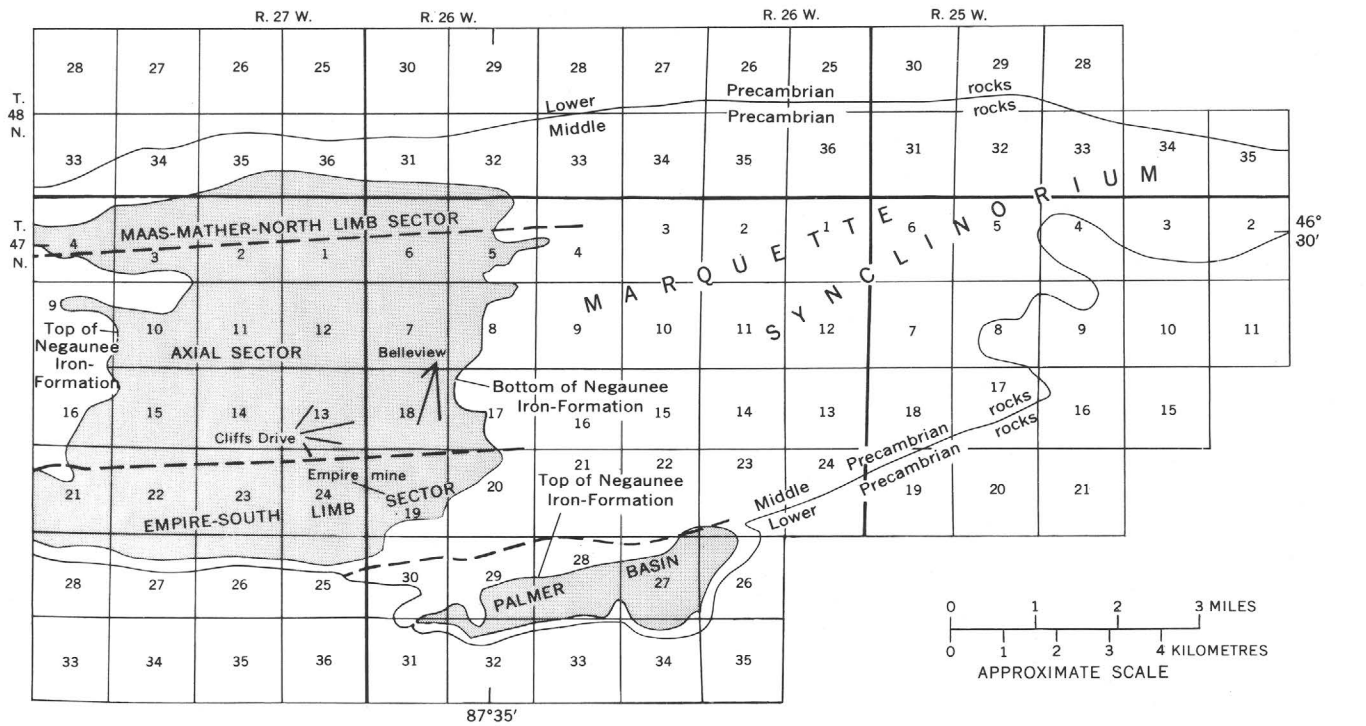

FIGURE 18.—Sectors of Negaunee Iron-Formation in eastern part of Marquette iron range. Patterned area underlain chiefly by Negaunee Iron-Formation (includes large areas of intrusive metadiabase).

Palmer, about 3,500 feet thick in the Empire-south limb sector, 1–2 miles northwest of Palmer, and about 2,500 feet thick in the axial part of the synclinorium, ½–1½ miles south of the city of Negaunee. In the Palmer basin, thicknesses of the iron-formation have been measured in individual diamond drill cores that cut the entire section from the Goodrich Quartzite hanging wall to the Ajibik-Siamo footwall. In the south half of the axial sector —the Belleview-Cliffs Drive area (fig. 18)—in the northwestern part of the quadrangle, thickness has been determined by combining measurements of drill core with mapped widths of iron-formation corrected for dip, between mafic sills used as markers. Essentially unrepeated segments of iron-formation are believed to be delimited between the main sills. Because of the absence of distinctive narrow horizon markers in the iron-formation, however, the possibility of repetition of beds and some exaggeration of thicknesses on local thrust faults cannot be ruled out within individual segments of iron-formation between unfaulted stretches of sill rock. The common variations in the mapped width of belts of iron-formation between sills may be explained by local faulting, crosscutting by the sills, or variations in the dip of the iron-formation.

Major sills which delimit the measured segments of iron-formation in the Belleview-Cliffs Drive part of the axial sector are, in upward order, the Tracy sill, the Summit Mountain sill, the Partridge Creek sill, and the Suicide sill (Gair and Simmons, 1970; this report, p. 121 and pl. 1). Thicknesses of iron-formation and locations of several measured segments are as follows:

Segment and location	*Type of measurement*	*Thickness (feet)*
1. Top of Siamo Slate to base of Tracy sill, sec. 7, T. 47 N., R. 26 W.	Several diamond-drill cores.	1,100–1,200
2. Top of Tracy sill to base of Summit Mountain sill, sec. 18 and S½ sec. 7, T. 47 N., R. 26 W.	Diamond-drill cores and mapped width, corrected for dip.	120–340
3. Top of Summit Mountain sill to base of Partridge Creek sill, SW¼ sec. 7, T. 47 N., R. 26 W.	Mapped width, corrected for dip.	70–140
Belt of iron-formation between branches of Partridge Creek sill, SE¼ sec. 12, T. 47 N., R. 27 W.	Mapped width, corrected for dip.	150
4. Top of Partridge Creek sill to base of Suicide sill, SE¼ sec. 12, T. 47 N., R. 27 W.	Mapped width, corrected for dip.	900
Total		2,340–2,730

The Tracy sill thins south of sec. 7 and evidently pinches out near the south edge of sec. 18 or in the north part of sec. 19, T. 47 N., R. 26 W. Farther south, in the Empire-south limb sector of the synclinorium (fig. 18), the span of iron-formation from the top of the Siamo to the base of the Summit Mountain sill is uninterrupted by sills. In that area, furthermore, the iron-formation thickens greatly. In the Belleview-Cliffs Drive area, the maximum combined thickness of the iron-formation and metadiabase below the Summit Mountain sill is about 1,750 feet, but the same stratigraphic interval along a northwest-trending line through the Empire mine contains about 3,000 feet of iron-formation.

Although the Goodrich Quartzite is exposed in the Jackson mine area near the northwest corner of the quadrangle, and the Negaunee-Siamo contact has been found by drilling and mining in the Mather mine 2,600–3,000 feet almost directly below the Goodrich, numerous faults of unknown displacement preclude a measurement of true thickness in that area.

The original thickness of the Negaunee Iron-Formation is not known because the upper limit of the iron-formation nearly everywhere is an erosional surface. The thicknesses given above from the Palmer basin represent the total existing section between the Goodrich Quartzite and Ajibik-Siamo rock. The measurements from the principal area of iron-formation in the Marquette synclinorium proper, on the other hand, are less than the full existing thickness by an undetermined amount representing the uppermost part of the Negaunee Iron-Formation —the part overlying the Suicide sill, which occurs only to the west in the Ishpeming quadrangle.

It is not certain if pre-Goodrich erosion alone produced the variations in thickness enumerated above, or if they are partly depositional. The angular discordance between beds of Goodrich Quartzite and immediately underlying iron-formation is virtually zero to a few degrees in the few places where the relationship can be seen, which suggests that changes in thickness resulting from erosion should be more gradual than they are. The more abrupt differences in thickness, such as between the south flank and center of the Palmer basin, and between the Palmer basin and the Empire-south limb sector of the Marquette synclinorium, are therefore probably largely depositional differences.

MINERALS IN THE IRON-FORMATION, PALMER QUADRANGLE

MAGNETITE

Magnetite (Fe_3O_4) is the most abundant iron oxide of depositional or diagenetic origin in the Negaunee Iron-Formation. It occurs typically in discrete thin layers, interlaminated with chert, siderite, and iron silicates, or intergrown with one or more of these minerals. It is an important matrix mineral in some beds of graywacke. Magnetite occurs in isolated octahedra and in closely packed aggregates of octahedra, most of which are between 0.01 mm and 0.05 mm in diameter. It is identified by its attraction to a hand magnet or magnetized needle and by its characteristic octahedral form, light-gray color (in reflected light), and moderate reflectivity.

HEMATITE

Hematite (α-Fe_2O_3) locally is an important primary mineral in the Negaunee Iron-Formation. It is identified by its red color and streak, by its tabular form, and by characteristic high reflectivity and strong pleochroism in polished section. Hematite generally is intergrown or interlaminated with chert. Vast quantities of hematite resulting from postdepositional and postdiagenetic (secondary) oxidation occur in the iron-formation, as red earthy replacements of the primary iron minerals, magnetite, siderite, and silicates. The primary or secondary origin of much premetamorphic (recrystallized) hematite is problematical.

MARTITE

Martite (Fe_2O_3) is an important mineral in all parts of the iron-formation originally rich in magnetite. It is crystalline ferric oxide occupying magnetitelike octahedra or is associated with magnetite in such octahedra. Optically, it is identical with specular hematite, having high reflectivity and strong pleochroism. All proportions of martite to magnetite exist in martite-bearing octahedra, from tiny amounts on marginal rims and patches to virtually entire octahedra of martite, in which there are tiny ragged "islands" of magnetite. No doubt martite formed by oxidation replacement of magnetite. If it can be assumed that the octahedral magnetite grains formed during regional metamorphism, martite postdates metamorphism.

GOETHITE

Goethite (α-FeO(OH)) is an abundant mineral in the Negaunee Iron-Formation; it is entirely of secondary origin, an earthy product of the postmetamorphic oxidation and hydration of siderite and iron silicates. It is recognized by its yellow-brown color and by its characteristic reflectivity, pleochroism, yellow-red internal reflection, and pitted appearance in polished section.

IRON CARBONATE

Sideritic carbonate (ideally $FeCO_3$, but invariably also contains a total of about 20 percent $CaCO_3$, $MgCO_3$, and $MnCO_3$ in solid solution) is perhaps the most common primary mineral in the Negaunee Iron-Formation. It occurs widely in primary association with all other abundant minerals of the formation except hematite. It is readily recognized as a carbonate mineral by luster and gray to tan color, by the characteristic appearance of carbonate in thin section, and by hardness, and as sideritic carbonate by the bulk chemical composition of rocks in which it is dominant (table 6), by index of refraction, N_0, well above 1.800, staining from hematitic and goethitic oxidation products, and X-ray patterns.[4] Grain sizes typically range from 0.01-0.03 mm. Coarser grained secondary ankeritic carbonate, kutnahorite—the manganese analogue of dolomite, and dolomite occur in parts of the iron-formation, generally in scattered grains near veins or mafic intrusive bodies, or in thin seams along bedding.

MINNESOTAITE

Minnesotaite ($(Fe,Mg)_3Si_4O_{10}(OH)_2$; see Gruner, 1944b, p. 370; James, 1966, p. W8–W9) is the most abundant iron silicate in the Negaunee Iron-Formation. It may form nearly pure layers, as much as 4 inches thick, in places consisting of granules of minnesotaite or minnesotaite-magnetite in a minnesotaite matrix. It commonly is intergrown with sideritic carbonate, stilpnomelane, magnetite, or chert. Minnesotaite is recognized by its flaky form, pale-green color, birefringence, and slight to nonexistent pleochroism in conjunction with its mineral associations. Grain sizes generally are less than 0.03 mm.

STILPNOMELANE

Stilpnomelane ($(OH)_4(K,Na,Ca)_{0-1}(Fe,Mg,Al)_{7-8}Si_8O_{23-24}\cdot(H_2O)_{2-4}$; see Gruner, 1944a, 1946; James, 1966, p. W9) is probably a close second in abundance among the iron silicate minerals of the Negaunee Iron-Formation. The mineral generally is intergrown with sideritic carbonate, magnetite, or minnesotaite. Identification is based on mineral associations, platy or flaky form, brown or green color, and strong pleochroism and birefringence. It is generally distinguishable from minnesotaite by its brown or deep-green color. The mineral resembles biotite, although it appears to lack the characteristic "birds-eye shimmer" of biotite. Grain size commonly is less than 0.05 mm. Positive identification has been made by X-ray.

[4] X-ray identification by T. E. C. Keith, U.S. Geol. Survey.

CHLORITE

Chlorite ($(Mg,Fe)_6(OH)_8Si_4O_{10}$ to $(Mg,Fe)_4Al_2(OH)_8Si_2Al_2O_{10}$) is a minor iron silicate in the iron-formation, except very locally in beds of graywacke, in association with small aggregates of clastic quartz, or in argillaceous beds in the transitional zone between the iron-formation and underlying Siamo Slate. In relatively few places, minor chlorite is intergrown with sideritic carbonate or magnetite and chert. Most of the chlorite is deep green, has low birefringence, and is probably the iron-rich variety, thuringite.

GRUNERITE

Grunerite ($Fe_7(OH)_2Si_8O_{22}$) is locally abundant in the iron-formation in the belt northwest of the village of Palmer, near mafic intrusive bodies, and is attributed to contact metamorphism. Layers of nearly pure grunerite may alternate with layers rich in magnetite, carbonate, or minnesotaite, and porphyroblasts of grunerite are imprinted over aggregates of minnesotaite or carbonate. In places, grunerite-bearing iron-formation is cut by veinlets of grunerite. Grunerite has been identified by its pale gray-green color, amphibole form, moderately strong birefringence, lack of pleochroism, and extinction angle (standard optical tests), and by X-ray. Blades of grunerite commonly range from 0.1 mm to 5 mm in length.

RIEBECKITE

Riebeckite ($Na_2Fe^{+2}{}_3Fe^{+3}{}_2(OH)_2Si_8O_{22}$) or soda hornblende, which has rarely been reported from iron-formation of North America, has been found in two areas in the Negaunee Iron-Formation of the Palmer quadrangle. It occurs in a narrow stratigraphic zone for a distance of at least three quarters of a mile in magnetite-carbonate-chert iron-formation in the Empire mine (sec. 19, T. 47 N., R. 26 W.), and in drill core about 2 miles north of the Empire mine, in the west-central part of sec. 7, T. 47 N., R. 26 W. In the latter area, the riebeckite is associated with aegirinaugite, with magnetite, and with porphyroblasts of potassic feldspar. Veinlets rich in coarse riebeckite cut the riebeckite-bearing iron-formation in sec. 7. Identification is based on amphibole form, strong blue color, characteristic pleochroism, and X-ray pattern. Blades of riebeckite commonly range from about 0.1 mm to 2 mm in length.

AEGIRINAUGITE

Aegirinaugite (variable composition between diopside, $CaMgSi_2O_6$, and acmite, $NaFeSi_2O_6$) is present in some of the riebeckite-bearing iron-

formation in the Empire mine and in sec. 7, T. 47 N., R. 26 W. The mineral is pale yellow green both megascopically and in thin section, is virtually nonpleochroic, has high refringence, is characterized by second-order red and green interference colors, and resembles epidote. The mineral occurs in granular aggregates. Grains commonly are a few tenths of a millimeter to about 1 mm in diameter. Identification is based on chemical and X-ray analyses, on indices of refraction, and on orientation of the optic plane relative to single sets of conspicuous cleavage. The index of refraction, N_y, of 1.78 in one sample from sec. 7 indicates that aegirinaugite there contains about 73 percent of the acmite molecule.

K-FELDSPAR

Small porphyroblasts of potassic-feldspar ($KAlSi_3O_8$), mostly microcline, occur in several layers of riebeckite-bearing iron-formation in a 13-foot run of drill core from the west-central part of sec. 7, T. 47 N., R. 26 W. Crystals of potassic feldspar are intergrown with riebeckite and minor sideritic(?) carbonate and magnetite, or with riebeckite and aegirinaugite. A riebeckite-microcline vein cuts some of the same iron-formation. Microcline has been identified by its characteristic plaid twinning and untwinned potassic feldspar by its low refringence.

MANGANITE AND OTHER MANGANESE MINERALS

Manganite ($Mn_2O_3 \cdot H_2O$) and other manganese minerals occurs in veinlets and as coatings in vugs in altered (oxidized) and leached parts of the iron-formation within 600 feet of the surface, mainly in the N½ sec. 7, T. 47 N., R. 26 W. D. F. Hewett (written commun., 1967) found only the dark-brown variety of manganite, having a brown streak, in samples of drill core from sec. 7. Identification has been made by X-ray fluorescence and X-ray precession photographs, by Richard Erd, U.S. Geological Survey. Veinlets of an unidentified soft black probable manganese mineral have been seen in some of the same drill cores of the altered iron-formation that contain manganite.

CHERT

According to long-established practice among students of Precambrian iron-formation, the term "chert" is used in the present report for microcrystalline and fine-grained quartz that is characteristically interlayered and somewhat intermixed with the iron minerals. Typically it forms colorless even-grained mosaic-textured and wormy aggregates. Layers range from about 0.1 mm to 10 cm in thickness. It probably formed by the recrystallization of true chert—chalcedonic or opaline silica—derived from primary precipitates of colloidal silica.

PRIMARY FEATURES OF THE IRON-FORMATION

DEFINITION

Iron-formation described in this report accords with the definition of James (1954, p. 239; 1966, p. W1, W11); it is a regularly and thinly layered metasedimentary rock containing more than 15 percent iron of depositional and diagenetic origin. Chert-rich laminae are common but not essential. Variations in the iron-formation that date from deposition or diagenesis are caused by different mixtures and proportions of iron minerals and chert, and by differences in layering.

COMPOSITION

Varieties of iron-formation in the Palmer quadrangle are produced by different amounts and combinations of siderite or other iron-rich carbonate, minnesotaite, stilpnomelane, magnetite, hematite, and chert. In one or two very limited areas, chlorite, aegirinaugite, and riebeckite are also important minerals in the iron-formation. These minerals may have formed during sedimentation, diagenesis, or low-grade regional metamorphism. Lenses of graywacke and ferruginous quartzite, sandy seams, and isolated clastic grains are common in the iron-formation in the Palmer basin and in the adjacent Empire-south limb sector of the Marquette synclinorium. Discrete layers of the iron-formation generally consist of the following minerals or combinations of minerals:

1. carbonate [5]
2. carbonate-chert
3. carbonate-magnetite
4. carbonate-magnetite-chert
5. carbonate-stilpnomelane
6. carbonate-stilpnomelane-magnetite
7. carbonate-stilpnomelane-magnetite-chert
8. carbonate-stilpnomelane-chert-clastic quartz-chlorite
9. carbonate-minnesotaite
10. carbonate-minnesotaite-chert
11. carbonate-minnesotaite-stilpnomelane-magnetite
12. minnesotaite
13. minnesotaite-chert
14. minnesotaite-carbonate
15. minnesotaite-magnetite
16. minnesotaite-stilpnomelane-carbonate-magnetite-chert
17. minnesotaite-carbonate-magnetite-chert
18. stilpnomelane
19. stilpnomelane-magnetite
20. stilpnomelane-chert

[5] "Carbonate" as used in discussion of Negaunee Iron-Formation in this report refers to sideritic carbonate.

21. magnetite
22. magnetite-chert
23. magnetite-carbonate-chlorite
24. magnetite-carbonate-chlorite-chert
25. magnetite-carbonate-chlorite-chert-clastic quartz
26. chert
27. chert-hematite
28. clastic quartz
29. clastic quartz-chlorite (graywacke)
30. clastic quartz-hematite (ferruginous wacke)

Layers containing carbonate, an iron silicate, magnetite, or chert, alone or in mixtures as listed above, can be associated with one another in virtually all possible combinations.

The minerals of each assemblage tend to have only slightly varying proportions in a given layer but may range widely in proportions in different layers. Colors of layers vary accordingly; for dominant carbonate they are pale yellow, gray, or gray green; for magnetite, dark gray or black; for minnesotaite, pale green; for chert, pale gray; for stilpnomelane, brown or green; for hematite, shades of red; and for chlorite, deep green. The colors are those seen on abraded surfaces of drill cores. The colors of the iron-formation on fresh fractures are generally less distinctive: gray, gray green, dark gray, black or dark red.

Clastic materials may be interlayered with iron-formation that is rich in any of the principal minerals: carbonate, magnetite, hematite, silicate.

FACIES AND INFERRED CONDITIONS OF DEPOSITION

James (1954) has recognized sulfide, carbonate, oxide, and silicate facies of iron-formation on the basis of the dominant iron mineral. The facies were correlated by James with a model of critical environmental conditions of chemical deposition, ranging from poor bottom ventilation and strong reducing conditions (negative redox potential or Eh) for the sulfide facies, through reducing conditions for the carbonate facies, to mildly reducing to well-aerated and strongly oxidizing conditions for the oxide facies. The silicate facies was related to a wide range of conditions from reducing to oxidizing. Parts of the Negaunee Iron-Formation, as indicated by the assemblages listed above, belong to the carbonate, oxide, or silicate facies. In the Palmer quadrangle, mixed facies of carbonate-oxide (magnetite)-silicate and carbonate-silicate are dominant, but virtually pure carbonate and oxide facies are also common. Interbedding and intergradations of the pure and mixed facies are the rule; commonly because of fine grain sizes, thin sections are needed to make distinctions between pure and mixed varieties. Jaspilite—nominally a variety of iron-formation consisting principally of alternating laminae of red hematitic chert (jasper) and dark-red to black specular hematite—consists generally in the Palmer quadrangle of jasper and martite and may have originated as a mixed hematite-magnetite-chert facies. Such jaspilite is dominant in the Jackson mine area near the northwest corner of the quadrangle and in the vicinity of the Isabella syncline and Old Volunteer mine in the western half of the Palmer basin.

Modal compositions (in volume percent) of diferent facies of the Negaunee Iron-Formation are listed in table 6.

THIN AND THICK BEDS

Primary layers of iron minerals and chert range greatly in thickness, from about 1/50 inch or less to 6 inches. Thin layers typically range from about 1/50–½ inch in thickness, and individual layers maintain an even thickness for many feet. Thicker layers and lenses are distributed irregularly, vary notably in thickness in short distances, and commonly are grouped in zones. Such zones generally are less than 50 feet thick, extend only short distances laterally, and are distributed irregularly through any given vertical section, except as noted below. Assemblages of the thin-layered and thicker layered iron-formation resemble typical "slaty" and "cherty" or "taconitic" members of the Ironwood and Biwabik Iron-Formations of the Gogebic (Hotchkiss, 1919; Aldrich, 1929, p. 136–143) and Mesabi (White, 1954, p. 19–32; Gunderson and Schwartz, 1962, p. 8–10, 22–24) iron ranges, respectively. Grouping of these varieties of iron-formation into persistent members is not realized in the Negaunee as it is in the Ironwood and Biwabik formations. However, Joseph J. Mancuso (oral commun., 1965) found that thick layers of iron-formation are grouped in a zone about 150–200 feet thick immediately beneath the Tracy sill in sec. 7, T. 47 N., R. 26 W. This zone has also been found during the present study, in drill core from several places in sec. 18, T. 47 N., R. 26 W. The base of the zone is rather poorly defined, and I have not recognized the zone southwest of sec. 18. The evenness of thin beds and the irregularities and common granular structure of thick beds suggest deposition of the former in comparatively deep quiet water and of the latter in shallow agitated water.

GRANULES

Granules are present in all facies of the Negaunee Iron-Formation in the Palmer quadrangle, but in

TABLE 6.—*Modes of Negaunee Iron-Formation*

Mineral	Type of iron-formation (named from iron minerals															
	Carbonate							Magnetite		Silicate			Magnetite-silicate			
	1	2	3	4	5	6	7	8	9	10	11	12	13	14	15	16
Chert	3.8	40.6	13.5	31.6	42.2	48.4	3.6	27.8	60.2	Tr	6.2	4.0	30.3	Tr	5.8	66.0
Jasper [2]	---	---	---	---	---	---	---	---	---	---	---	---	---	---	---	---
Carbonate [3]	77.8	51.2	83.6	62.5	53.6	46.8	70.2	1.0	---	1.2	.5	---	4.0	---	7.5	---
Magnetite [4]	.4	.6	---	.1	1.8	.4	10.5	61.4	36.0	---	1.0	2.5	33.2	60.2	61.0	26.2
Martite	---	---	---	---	---	---	---	---	---	---	---	---	---	---	---	---
Hematite	---	---	---	---	---	---	---	---	[6] 3.8	---	---	---	---	---	---	---
Iron silicate [7]	---	---	---	---	---	[8] 4.2	---	9.8	---	---	---	---	---	---	---	---
Stilpnomelane	18.0	7.6	---	---	---	---	13.2	---	---	---	22.0	90.0	32.6	---	25.6	---
Minnesotaite	---	---	---	---	---	---	1.5	---	---	18.4	49.5	3.5	---	39.2	---	---
Iron silicate and magnetite [11]	---	---	---	---	---	---	---	---	---	54.4	---	---	---	---	---	---
Grunerite	---	---	---	---	---	---	---	---	---	20.9	[12] 20.6	---	---	---	---	---
Chlorite	---	---	2.4	5.5	2.2	---	.7	---	Tr	---	---	---	---	---	---	7.6
Secondary hematite	---	---	---	---	---	---	---	---	---	5.1	---	---	---	.6	---	---
Clastic quartz	---	---	.2	.3	.2	.2	.2	---	---	---	---	---	---	---	---	.2

[1] Includes dusty hematite.
[2] Mixture of chert and tiny flakes of hematite in approximately equal amounts.
[3] Most is siderite.
[4] Includes small amounts of hematite.
[5] Includes a few percent of hematite that was probably derived by oxidation of iron carbonate and silicate.
[6] Oxidized iron carbonate and (or) iron silicate.
[7] Mainly chlorite; may include some minnesotaite and stilpnomelane.
[8] Chlorite and stilpnomelane.
[9] Ferrostilpnomelane.
[10] Minnesotaite and stilpnomelane.
[11] Minerals in dark mixture difficult to distinguish; most of iron silicate is stilpnomelane.
[12] Includes 7.7 percent grunerite, and 3.2 percent quartz, 5.5 percent carbonate, and 4.2 percent magnetite-martite, all derived by the pseudomorphous replacement of grunerite.
[13] Most is sprinkled with tiny plates of translucent red hematite.

Data for drill-core samples include drill-hole location (DHL) (see pl. 8 and Drill Hole Data and Locations), footage of sample in drill hole, and approximate location of collar of drill hole in feet from section corner

1. JG–96M–66; DHL 232, 1,596 ft, 2,100N–1,300E of SW. cor. sec. 7, T. 47 N., R. 26 W. (Chemical analysis of JG–132C–66 from same zone).
2. JG–132D–66; DHL 232, 1,797–1,798 ft, 2,100N–1,300E of SW. cor. sec. 7, T. 47 N., R. 26 W. (part of chemically analyzed sample).
3. JG–135–66; DHL 194, 2,380–2,382 ft, 650S–2,400E of NW. cor. sec. 7, T. 47 N., R. 26 W. (part of chemically analyzed sample).
4. JG–143E–66; DHL 371, 484 ft, 550N–900W of SE. cor. sec. 13, T. 47 N., R. 27 W.
5. JG–5F–65; DHL 697, 422 ft, 800N–800E of SW. cor. sec. 29, T. 47 N., R. 26 W.
6. JG–6–65; DHL 696, 256 ft, 1,000N–1,500E of SW. cor. sec. 29, T. 47 N., R. 26 W.
7. JG–96R–66; DHL 232, 2,050 ft, 2,100N–1,300E of SW. cor. sec. 7, T. 47 N., R. 26 W.
8. JG–134–66; DHL 266 (764), 344–346 ft, 800N–1,000W of SE. cor. sec. 7, T. 47 N., R. 26 W. (part of chemically analyzed sample).
9. JG–139–66; DHL 819, 59 ft, 800N–150W of SE. cor. sec. 27, T. 47 N., R. 26 W.
10. JG–133–66; DHL 264, 104–111 ft, 900N–2,300E of SW. cor. sec. 7, T. 47 N., R. 26 W. (part of chemically analyzed sample).
11. JG–89C–66; DHL 264, 82 ft, 900N–2,300E of SW. cor. sec. 7, T. 47 N., R. 26 W.
12. JG–79B–66; DHL 344, 144 ft, 400N–900E of SW. cor. sec. 8, T. 47 N., R. 26 W.
13. JG–9–66; DHL 430, 41–51 ft, 50N–1,050W of SE. cor. sec. 18, T. 47 N., R. 26 W. (chemical analysis of JG–137–66 from same zone).
14. JG–96C–66; DHL 232, 212 ft, 2,100N–1,300E of SW. cor. sec. 7, T. 47 N., R. 26 W.
15. JG–96H–66; DHL 232, 698 ft, 2,100N–1,300E of SW. cor. sec. 7, T. 47 N., R. 26 W.
16. JG–3DD–65; DHL 711, 342–359 ft, 150N–2,200E of SW. cor. sec. 29, T. 47 N., R. 26 W.
17. JG–96N–66; DHL 232, 1,677 ft, 2,100N–1,300E of SW. cor. sec. 7, T. 47 N., R. 26 W.
18. JG–96P–66; DHL, 232, 2,006 ft, 2,100N–1,300E of SW. cor. sec. 7, T. 47 N., R. 26 W.
19. JG–139K–66; DHL 819, 641 ft, 800N–150W of SE. cor. sec. 27, T. 47 N., R. 26 W.
20. JG–96K–66; DHL 232, 775 ft, 2,100N–1,300E of SW. cor. sec. 7, T. 47 N., R. 26 W. (chemical analysis of JG–132–66 from same zone).
21. JG–136–66; DHL 428, 314–318 ft, 100N–2,200W of SE. cor. sec. 18, T. 47 N., R. 26 W. (part of chemically analyzed sample).
22. JG–138–66; DHL 376, 166–169 ft, 50S–1,050W of NE. cor. sec. 18, T. 47 N., R. 26 W. (part of chemically analyzed sample).
23. JG–96–66; DHL 232, 128 ft, 2,100N–1,300E of SW. cor. sec. 7, T. 47 N., R. 26 W.
24. JG–96B–66; DHL 232, 182 ft, 2,100N–1,300E of SW. cor. sec. 7, T. 47 N., R. 26 W.
25. JG–140H–66; DHL 786, 594 ft, 1,350N–200W of SE. cor. sec. 27, T. 47 N., R. 26 W.
26. JG–81A–64; DHL 725, 370 ft, 700S–1,700E of NW. cor. sec. 32, T. 47 N., R. 26 W.
27. JG–6–64; Outcrop, Moore mine, 50S–2,100W of NE. cor. sec. 33, T. 47 N., R. 26 W.
28. JG–106B–64; DHL 726, 193 ft, 650S–2,200E of NW. cor. sec. 32, T. 47 N., R. 26 W.
29. JG–71E–64; DHL 725, 273 ft, 700S–1,700E of NW. cor. sec. 32, T. 47 N., R. 26 W.
30. JG–4–64; Outcrop, Moore mine, 150N–2,050W of SE. cor. sec. 28, T. 47 N., R. 26 W.
31. JG–77A–64; Outcrop, 1,250S–1,200E of NW. cor. sec. 32, T. 47 N., R. 26 W.
32. JG–71B–64; DHL 725, 176 ft, 700S–1,700E of NW. cor. sec. 32, T. 47 N., R. 26 W.

the oxide facies, granules are characteristic only of beds of jasper. They occur in discrete beds and lenses, ½- to 4-inches thick, representing a small part of the total thickness of the iron-formation. They generally have been thought to form by the aggregation of bottom muds during agitation by wave action and currents in shallow water. The granules are generally roughly ovoid but may be pear or sausage shaped; they range in maximum dimension from about 0.2 to 1.5 mm. Concentric laminations like those characteristic of oolites are rare.

Typical granules consist of minnesotaite, magnetite, minnesotaite and magnetite, carbonate, carbonate and stilpnomelane, carbonate and minnesotaite, carbonate and magnetite, chert, chert and magnetite, or chert and hematite. As in nongranular iron-formation, these minerals formed during deposition, diagenesis, or the early stages of regional metamorphism. Taylor (*in* Hallimond and others, 1951, p. 74–85) has noted the general absence of primary magnetite in ooliths in ironstones of Great Britain, and the common alternation of primary silicate (chamosite) and limonite. Mag-

(volume percent), Palmer quadrangle

that exceed 20 percent of total iron-mineral content)

Carbonate-silicate			Carbonate-magnetite				Carbonate-magnetite-silicate		Martite			Martite-magnetite	Martite-jasper		Jasper-martite-magnetite
17	18	19	20	21	22	23	24	25	26	27	28	29	30	31	32
13.0	19.5	2.0	18.6	16.8	23.1	11.4	.7	46.2	52.0	64.7	30.4	[1] 40.7	16.3	14.6	10.8
---	---	---	---	---	---	---	---	---	---	---	11.2	---	52.3	27.2	33.0
46.0	40.0	25.6	45.6	53.8	16.3	44.2	32.5	17.2	---	---	1.0	---	---	---	---
.3	.3	18.5	35.0	23.4	56.1	40.2	43.5	25.8	---	---	---	55.0	---	---	36.4
---	---	---	---	---	---	---	---	---	40.2	[5] 35.3	52.2		30.6	45.4	
---	---	---	---	---	---	---	---	---	7.8	---	---	---	---	13.3	---
---	---	---	[9] .8	[10] 6.0	[8] 4.4	---	---	---	---	---	---	---	---	---	---
37.3	40.2	50.8	---	---	---	4.2	4.0	10.8	---	---	---	---	---	---	---
---	---	.5	---	---	---	---	19.2	---	---	---	---	Tr	---	---	1.2
---	---	---	---	---	---	---	---	---	---	---	---	---	---	---	---
---	---	---	---	---	---	---	---	---	---	---	---	---	---	---	---
---	---	---	---	---	---	---	---	---	---	---	4.8	---	---	---	[13] 11.4
---	---	---	---	---	---	---	---	---	---	---	---	.7	---	---	---
3.3	---	2.5	---	---	---	---	---	---	---	---	---	3.5	.6	---	7.2

netite has been described in sedimentary pisolitic-oolitic rocks of the Ural Mountains (Krotov, 1940) but is considered to have formed by the diagenetic reduction of ferric oxides. Magnetite commonly is concentrated in the peripheral parts of magnetite-silicate granules in the Negaunee Iron-Formation, so may be derived indirectly from the silicate. Possibly shortly after deposition in shallow water, iron silicate in the outer parts of such granules was oxidized to hematite or goethite, which in turn may have been reduced to magnetite during diagenesis. In some granules of magnetite and minnesotaite from iron-formation drilled in the SE¼ sec. 7, T. 47 N., R. 26 W., the magnetite is in the form of small rods, apparently pseudomorphs of an earlier mineral. The rod shape would seem to preclude hematite as the original mineral, so it seems most likely that the magnetite replaced prisms of goethite during diagenesis. Evidence elsewhere in the Negaunee Iron-Formation is generally not as clear cut as here that magnetite in depositional structures—beds or granules—is not itself of depositional origin. In this case, however, it seems clearly to be of postdepositional origin.

Indeed, not all granules themselves may be of depositional origin or consist of primary minerals. Commonly there are different species of iron mineral in the granules than in the matrix, or between granules and matrix there are sharp differences in the proportions of iron minerals or of iron minerals and chert. Granules that differ in composition from the matrix are difficult to explain solely as a product of the agitation of bottom muds, for there appears to be no plausible mechanism inherent in agitation to separate materials without also producing a gravity stratification. Therefore, it seems likely that the present minerals in such granules formed by diagenetic replacement of earlier granules or by concretionary growth during diagenesis.

CLASTIC SEDIMENTS

Beds and lenses of clastic sedimentary rock—graywacke and impure quartzite—are conspicuous in magnetitic, hematitic, and sideritic facies of the iron-formation in the western half of the Palmer basin, near the southeast end of the basin, and in the Empire mine at the southeast end of the main belt of iron-formation in the Marquette synclinorium proper (Gair, 1967; Davis, 1965; Mengel, 1956; Tyler and Twenhofel, 1952). In these areas, detrital quartz may also be scattered in cherty and ferruginous beds of the iron-formation, mainly the latter, and constitutes a fraction of a percent to roughly 30 percent of a given bed. The clastic materials are more prevalent in the Palmer basin than in the southeastern part of the synclinorium proper. In the south-central part of the Palmer basin, clastic seams and thin beds are rather regularly spaced throughout the 400–700-foot section of iron-formation and make up 3–6 percent of the beds. Pebbles, cobbles, and boulders are also present in places in the south part of the basin. In the Empire mine, most clastic material is in a zone less than 100 feet thick just above the magnetite-chert-carbonate zone (for details, see section on Empire mine, p. 102, 104–105).

Graywacke is most commonly interlayered with varieties of magnetite-rich iron-formation composed essentially of magnetite and chert, magnetite, carbonate, and chert, or of magnetite, carbonate, silicate, and chert. Graywacke also is interbedded with jaspilite and with nearly pure siderite-chert iron-formation in places. The clastic beds range in thickness from about 0.03 inch to 50 feet. Most clastic lenses in the Palmer basin are less than 4 inches thick and many are 1/16–¼ inch thick. Irregular forms of beds or lenses in places suggest preconsolidation slumping.

EFFECTS OF DIAGENESIS AND METAMORPHISM

The primary iron-formation minerals were all

recrystallized during Penokean metamorphism but are believed to have remained essentially unchanged chemically and mineralogically since deposition or diagenesis. James (1954, p. 274) has pointed out that diagenetic changes—those "produced in a rock after deposition and prior to lithification" and, according to some authors, also during lithification—tend to bring about chemical reduction and probably had a significant effect on iron minerals. James considered hematite, magnetite, siderite, ferrous silicates, and pyrite all possible products of deposition from sea water above the sediment-water interface. He also recognized, however, that during diagenesis, magnetite might form from hematite, iron carbonate from iron oxide or silicate, and pyrite from iron carbonate. Curtis and Spears (1968, p. 259, 261), on the other hand, concluded that ferric compounds are the only stable iron minerals in normal marine waters (pH near 8), even at Eh values down to the lowest known in present-day anoxic basins. According to them, ferrous minerals (pyrite, pyrrhotite, magnetite, siderite, chamosite, and other silicates) can, except for pyrite formed under special conditions, attain equilibrium only with sediment pore waters (pH 7 or less). The environmental requirements for the stable growth of ferrous silicates differ from those for siderite only in having low carbonate activity and saturation with an active form of silica. It therefore seems likely that the facies defined by James necessarily formed both in depositional and diagenetic environments. Because of metamorphic recrystallization, distinctions based on direct textural evidence are generally difficult or impossible to make between material that may have formed by direct precipitation or by diagenesis, or at a low grade of regional metamorphism. However, granules provide some textural evidence of postdepositional changes, and in the section on the Empire mine (this report, p. 76), Tsu-Ming Han presents much evidence from textures and structures to suggest alteration and replacement of iron-formation during diagenesis.

The iron silicates, minnesotaite, stilpnomelane, and chlorite, occur in recrystallized fabrics, and are common in slightly metamorphosed iron-formation. They probably are early products of metamorphism of primary silicate material of uncertain composition. Monomineralic layers of minnesotaite and stilpnomelane must have been derived by the recrystallization of material of virtually the same composition as the existing minerals (James, 1954, p. 267).

CARBONATE FACIES

Carbonate iron-formation consists mainly of iron carbonate and chert, but almost invariably also contains minor amounts of magnetite, chlorite, and (or) stilpnomelane. Pure carbonate iron-formation is far subordinate to mixed facies containing essential carbonate and magnetite or iron silicate, or mixtures of the three minerals. Pure carbonate iron-formation is common within 500 feet of the base of the Negaunee Iron-Formation in the axial sector of the synclinorium, about 800 feet above the base in part of the New Volunteer mine in the Empire-south limb sector, and approximately 2,800–3,500 feet above the base in the boundary area between the axial and Empire-south limb sectors, near the NW. cor. sec. 19, T. 47 N., R. 26 W. Within 2,000 feet of that corner, in secs. 18, 19, and secs. 13, 24, T. 47 N., R. 27 W., carbonate iron-formation extends stratigraphically from about 800 feet below to about 200 feet above the Summit Mountain sill.

In the lower 500 feet of the iron-formation in the axial sector, essentially pure carbonate iron-formation is in several zones, each less than 20 feet thick, that are gradational with mixed facies of cherty iron carbonate and iron silicate. Near the common corner of secs. 18, 19, 13, and 24, many thin zones of nearly pure carbonate iron-formation are similarly interbedded and gradational with mixed carbonate-silicate, carbonate-magnetite, and carbonate-magnetite-silicate iron-formation, but several zones of the purer carbonate iron-formation are 35–275 feet thick.

Carbonate iron-formation very similar to that near the common corner of secs. 18, 19, 13, and 24 occurs beneath the Isabella syncline in the Palmer basin, in the SW¼ sec. 29. About 50 feet of this rock, cut in one drill hole, is between zones of hematitic and magnetitic iron-formation, and another drill hole cuts about 140 feet of dominantly carbonate iron-formation and ends in that rock approximately 500 feet above the base of the Negaunee. Near the southeast end of the Palmer basin, numerous thin beds of carbonate iron-formation, 1 to about 10 feet thick, are interbedded with graywacke in a transition zone about 100 feet thick between the Negaunee Iron-Formation and underlying Siamo-Ajibik rock.

It is likely that carbonate iron-formation has previously been more extensive, but that it has been oxidized and made indistinguishable from oxidized silicate or mixed facies, particularly between the Tracy sill and the Siamo Slate in the axial sector, west of the New Volunteer mine along the south limb, and east of the Isabella syncline in the Palmer basin.

Carbonate iron-formation typically is pale gray or pale greenish gray or yellowish gray. Figure 19

shows common varieties of carbonate iron-formation and mixed facies rich in iron carbonate, as seen in drill cores. On abraded surfaces of drill core the grayish colors may be modified to nearly white or to pale yellow shades. Surface exposures are almost always somewhat brown, owing to oxidation of iron carbonate to hematite or goethite; the darkening effect of oxidation is also shown in drill-core samples B1 and B3 in figure 19. Layers generally are 0.04–3 inches thick and may have internal laminations. Layering is caused by alternations of carbonate and chert, carbonates of fine-grained and coarser size, or of carbonate and mixed carbonate, iron silicate, magnetite, and (or) clastic quartz. In a few places internal laminations consist of strongly alined, overlapping, possibly flattened lenticles of carbonate, 0.02–0.04 inch thick, in a matrix of carbonate, chert, and mixtures of the two minerals.

The fabric of carbonate iron-formation typically is fine and even grained, but in some layers it is more coarsely crystalline, granular, or mottled, with irregular patchy carbonate and chert (fig. 20). Grain sizes generally are 0.006–0.03 mm. Granules are 0.1–0.6 mm in diameter, may be composed of carbonate or chert or mixtures of the two, and may be tightly packed together, or each type may be in a matrix of the same mineral, the other mineral, or mixtures of the two. Granules in the carbonate iron-formation are without internal concentric laminations (see fig. 20) and therefore are not oolites.

Minor amounts of chlorite or stilpnomelane commonly are scattered through layers of iron carbonate. Silicate blades typically are oriented at a large angle to bedding (fig. 20) and clearly crystallized after deposition of the rock.

Iron carbonate has recrystallized to relatively coarse grains, 0.1–0.2 mm in diameter, in some layers that contain scattered granules or quartz clasts. The clast-bearing layers probably were more porous and permeable and had a higher content of connate water than bordering layers, or served as conduits for water during metamorphism.

In two drill-core samples from the SE¼ sec. 13, T. 47 N., R. 27 W., relatively coarse grains of carbonate have the unusual characteristic of being pleochroic (deep brown to light tan). In one sample, from next to a metadiabase sill, probably recrystallized by contact metamorphism, grains of the pleochroic carbonate, 0.1–0.25 mm in diameter, are in a carbonate matrix cut by carbonate veins. Coarse sprays of grunerite lie along the boundary between layers of iron carbonate and chert. The other sample is hundreds of feet from known intrusive rock, a distance generally well beyond the range of evident contact metamorphic effects in the iron-formation, and probably was recrystallized only by regional metamorphism. The pleochroic carbonate—isolated crystals and clumps, 0.06–0.3 mm in diameter—is in finer grained chert. The pleochroism resembles that of stilpnomelane as it is commonly intergrown with carbonate, so possibly, tiny inclusions of stilpnomelane, too small to be seen at ×800 magnification, are strongly alined along cleavage surfaces of the pleochroic carbonate.

Chemical analyses of carbonate-rich iron-formation are listed in table 7. The carbonate iron-formation has a high content of FeO and CO_2, wide variations in the amount of SiO_2, low Fe_2O_3 and Al_2O_3, variable MgO, and a low ratio of MnO to FeO (table 7, Nos. 1–3—samples similar in appearance to drill core shown in B3, B1, and B2, respectively, in fig. 19). Differences in SiO_2 correspond largely to differences in the amount of chert. The analyzed SiO_2 represents possible maximum percentages of chert. However, because of the presence of small amounts of stilpnomelane or other silicate in the analyzed iron-formation, all SiO_2 cannot be attributed to chert. Analyses 1–3 in table 7 probably represent at least 10, 30, and 35 percent chert, respectively. Discrepancies between chemically analyzed samples of 1- to 2-foot length and compositions inferred from modal analyses of corresponding single thin sections of each sample are inherent in the

TABLE 7.—*Chemical analyses and densities of carbonate-chert iron-formation, Palmer quadrangle*

[Analyst: G. O. Riddle, U.S. Geol. Survey]

	1	2	3
SiO_2	12.41	34.62	39.62
Al_2O_3	1.56	1.43	1.14
Fe_2O_3	2.79	4.65	.73
FeO	39.87	30.96	32.60
MgO	7.01	4.38	2.42
CaO	2.29	.92	.66
Na_2O	.15	.17	.05
K_2O	.36	.38	.03
H_2O^+	.95	.90	.26
H_2O^-	.43	.55	.03
TiO_2	.03	.05	.03
P_2O_5	.11	.09	.10
MnO	1.22	.40	.20
CO_2	30.85	20.71	21.93
Cl	.01	.00	.00
F	.01	.01	.02
Subtotal	100.05	100.22	99.82
Less 0 (equiv. to F)	.00	.00	.01
Total	100.05	100.22	99.81
Bulk density	3.40	3.45	3.27
Powder density	3.42	3.22	3.22

1. JG–132C–66; drill-hole location 232; 1-ft composite, 1,595–1,603 ft.
2. JG–132D–66; drill-hole location 232; 1,797–1,798 ft.
3. JG–135–66; drill-hole location 194; 1-ft composite, 2,380–2,382 ft.

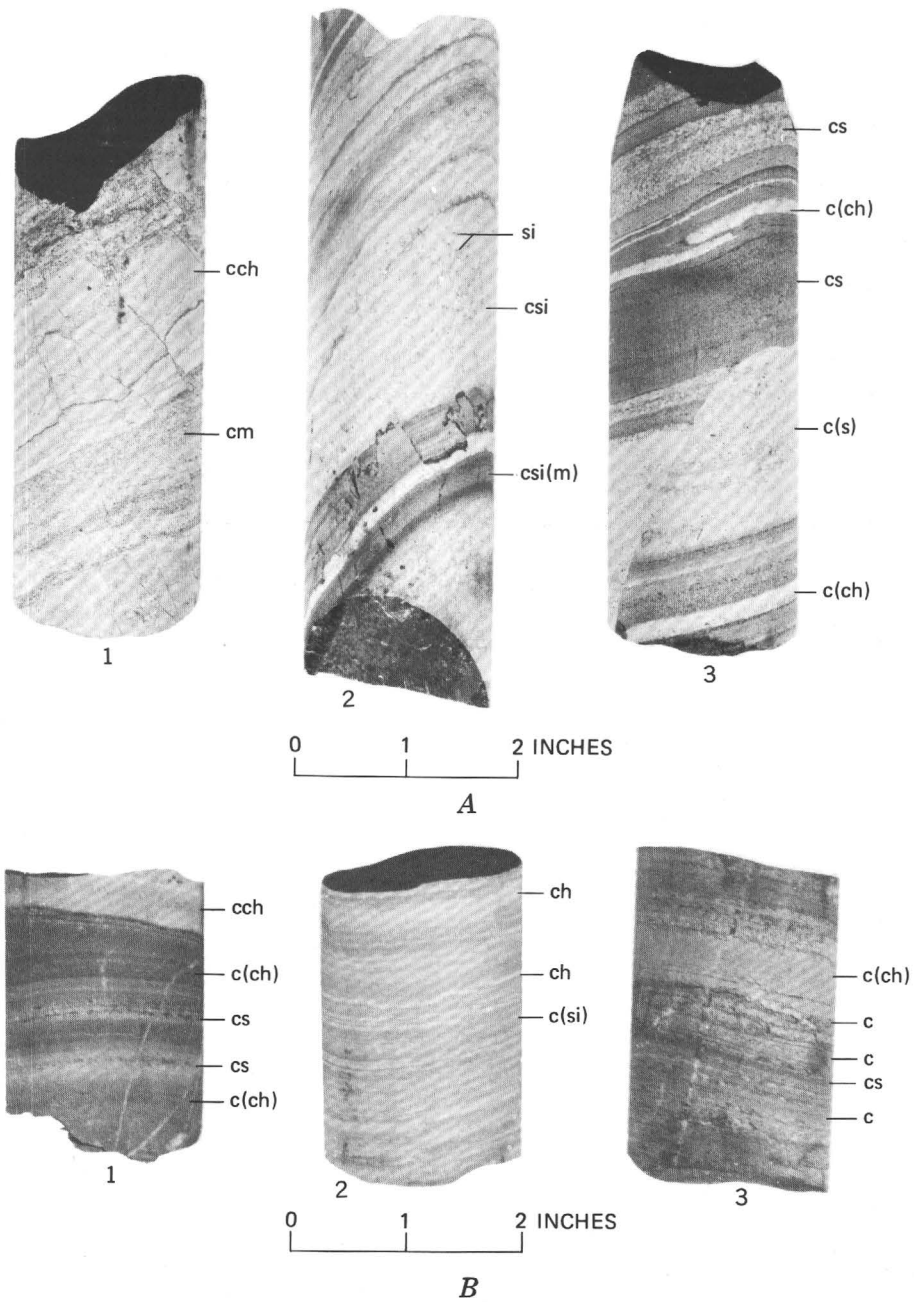

No.	Field No.	Drill-hole-location No. (see pl. 8 and p. 146) and footage	Location
A1	JG-145A-66	432, 226 ft	24-47-27
A2	JG-144E-66	365, 171 ft	13-47-27
A3	JG-144B-66	365, 68 ft	13-47-27
B1	JG-132D-66	232, 1797-1798 ft	7-47-26
B2	JG-135-66	194, 2380-2382 ft	7-47-26
B3	JG-96M-66	232, 1596 ft	7-47-26
C1	JG-141B-66	427, 678 ft	18-47-26
C2	JG-143E-66	371, 484 ft	13-47-27
C3	JG-140F-66	786, 593 ft	27-47-26

FIGURE 19.—Drill-core samples of carbonate-rich iron-formation (carbonate and mixed facies). A1, mixed carbonate-magnetite facies. A2, A3, carbonate and mixed carbonate-silicate facies. Note stylolite in A2. B1–3, carbonate facies. C1, carbonate and mixed carbonate-magnetite facies. C2, carbonate facies (plus minor silicate). C3, carbonate and mixed magnetite-silicate-chert facies. c, carbonate; ch, chert; m, magnetite; s, stilpnomelane; si, silicate; (m, si, ch), minor magnetite, silicate, chert.

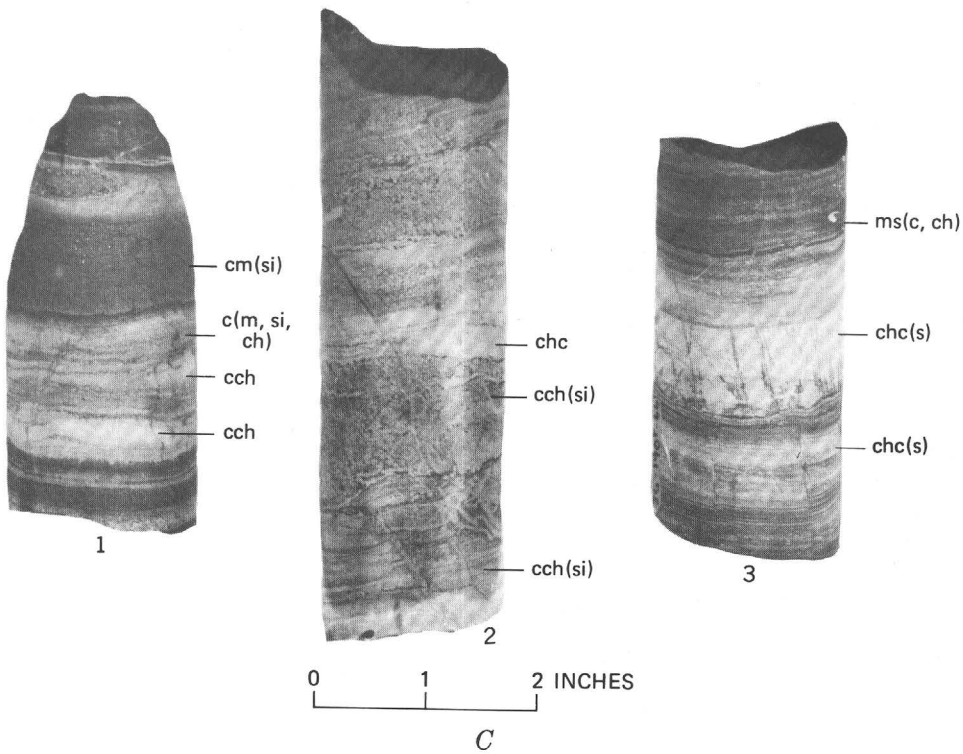

FIGURE 19.—Continued.

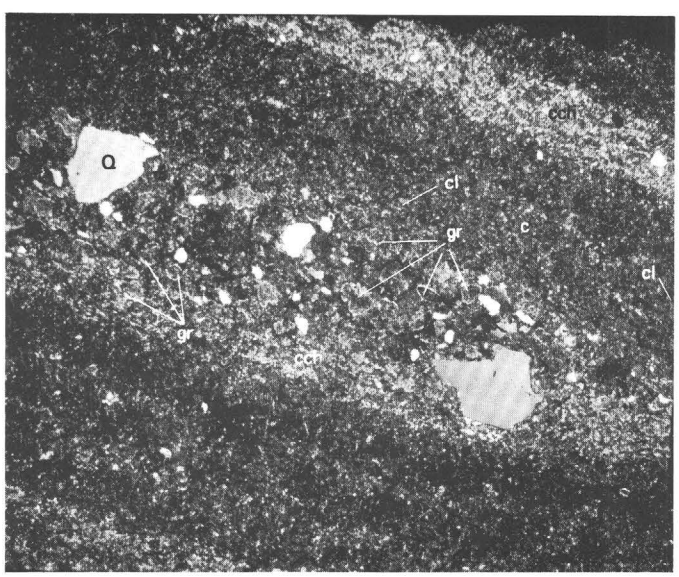

FIGURE 20.—Photomicrograph of carbonate-chert iron-formation. Layers of iron carbonate (c) alternate with layers of mixed carbonate and chert (cch). Granular layer contains carbonate granules (gr) rimmed by chert and scattered grains of detrital quartz (Q). Blades of chlorite (cl) scattered widely in carbonate layers, and oriented at large angle to bedding. Polarizers partly crossed. Drill core samples JG–6C–65, 1,050N–1,400E of SW. cor. sec. 29, T. 47 N., R. 26 W. (drill-hole location 696, 309 ft).

thinly layered iron-formation. Carbonate layers in drill-core samples B1 and B3 are darker than in sample B2 owing to slight oxidation of iron carbonate to ferric iron oxide in the former. Corresponding differences in the ratio of Fe_2O_3 to FeO are seen in the samples. Al_2O_3 is attributed to minor chlorite or other iron silicates, and MgO, both to iron silicates and possibly to a small component of $MgCO_3$ in the carbonate.

Carbonate of the iron-formation typically is sideritic.[6] The index of refraction, N_0, of carbonate is well above 1.800. Carbonate solid solutions containing a high fraction of $MnCO_3$ or $MgCO_3$ might also have N_0 above 1.800, but the low Mn in bulk chemical analyses and the universal presence of secondary iron oxide in partly oxidized grains of carbonate indicate dominance of the ferrous carbonate molecule. Minor amounts of kutnahorite [6], the manganese analogue of dolomite, are present in iron-formation in the NE¼SE¼ sec. 7, and this or other Mn-bearing carbonate may have been the source of small amounts of secondary manganese minerals occurring in druses and veinlets in leached and thoroughly oxidized iron-formation in the northern part of sec. 7 and the NW¼ sec. 8.

[6] X-ray identification by T. E. C. Keith, U.S. Geol. Survey.

OXIDE FACIES

Oxide iron-formation consists principally of one of the two iron oxides, hematite or magnetite. Chert is generally abundant, but it not an essential constituent. Hematite-banded and magnetite-banded varieties are distinguished according to the dominant iron oxide, following James (1954, p. 258–263). Primary hematite or magnetite, or oxide iron-formation, as the terms are used here, refer to low-temperature sea-bottom sediments that might have been modified compositionally at low temperature by diagenesis, but thereafter remained essentially unchanged chemically and mineralogically, despite metamorphic recrystallization. Hematitic and geothitic iron-formation that originally consisted mainly of iron carbonate, iron silicate, or magnetite —of which there is a large volume in the area— is not a primary oxide facies. Both hematite-banded and magnetite-banded iron-formation form a substantial part of the Negaunee Iron-Formation, but the presence of martite—oxidized magnetite—in most of the hematite-banded rock creates uncertainty about the primary composition of that type of rock. Much magnetite-banded or martite-banded rock containing also a substantial amount of brownish hematite probably was mixed magnetite-carbonate or magnetite-carbonate-silicate iron-formation before secondary oxidation.

Determining whether hematite and magnetite are of depositional or postdepositional origin has long been a major aspect of the study of iron-formation (for example, see James, 1954, p. 256–258, and LaBerge, 1964). Evidence from the Negaunee Iron-Formation in the Palmer quadrangle relating to this problem is considered in detail on later pages. Some workers (for example, Krotov, 1940; Alling, 1947; Lepp and Goldrich, 1964) have postulated a derivation of magnetite or hematite by diagenetic alterations of other minerals. Magnetite is rare in post-Precambrian (unmetamorphosed) iron-rich rock (James, 1954; Taylor, *in* Hallimond and others, 1951) and is also rare in the virtually unmetamorphosed Precambrian Gunflint Iron-Formation (Goodwin, 1956), in contrast to ferric oxide; so primary magnetite is a less certain possibility than primary hematite. LaBerge (1964) concluded that magnetite originated mainly by the oxidation-replacement of siderite during low-grade regional metamorphism. Both CO_2, derived from the breakdown of siderite, and water are believed by LaBerge to have been sources of oxygen.

After deposition and diagenesis of the iron minerals in the Marquette district, hematite (or goethite) may have originated before metamorphism by supergene oxidation of carbonate or silicate adjacent to the post-Negaunee, pre-Goodrich erosion surface. Distinctions between depositional and later iron oxides after they have been metamorphically recrystallized are difficult or impossible to make without the help of relict structures. In the Palmer quadrangle, diagenetic iron oxide (magnetite) is definitely recognized only at the Empire mine where extensive exposures of unweathered iron-formation reveal numerous replacement and relict structures (see p. 85, 92–96).

In advocating a metamorphic origin for magnetite, LaBerge emphasized textural differences between magnetite and siderite or greenalite, iron minerals that are more certainly primary. Nevertheless, most magnetite fits criteria given by LaBerge for primary iron minerals; namely, it has uniform fine grain size of 0.01–0.03 mm (although grains average perhaps twice the size of siderite or iron silicate grains), and it commonly defines the primary structure, bedding. My observation in the Palmer quadrangle is that discordances, such as irregular growth across bedding surfaces and coarse and variable grain sizes cited by LaBerge in support of a secondary origin for magnetite, generally are local. No doubt these are postdepositional modifications, but siderite, too, is similarly modified in places by recrystallization.

Abrupt alternations of laminae of siderite, magnetite, and iron silicate are typical of much iron-formation in the Palmer quadrangle. The derivation of magnetite laminae in such iron-formation by the selective oxidation of siderite laminae during regional metamorphism while alternate siderite laminae remained unaffected would seem to require a highly unlikely precision in the control of oxidizing potential from lamina to lamina. The indicated variation or lack of equilibration in oxidation level from lamina to lamina would seem more likely to take place near the sediment seawater interface either during deposition or shortly thereafter, rather than under pervasive metamorphism.

Features cited in the section on the Empire mine by T-M. Han indicate that some and perhaps much magnetite there is of diagenetic origin, formed by the replacement of siderite, magnetitic siderite, and magnetitic chert. Experimental data and conclusions by Garrels (1960, p. 129–143) suggest that magnetitization of siderite was accomplished either by an increase in the partial pressure of oxygen (increase in Eh) in pore fluids in which the partial pressure of CO_2 remained constant, or by an increase in pH of pore fluids with or without any change in Eh, depending on whether the partial pressure of CO_2

was constant or changing. Such chemical conditions could have been realized by a shallowing of the sea bottom and an attendant increase in the oxygen content of sea water and adjacent interstitial water in sideritic bottom sediments, or by shallowing and an attendant increase in the pH from near neutral to more than 8 because of improved circulation near the shallower sea bottom.

MAGNETITE-BANDED ROCK

Magnetite-banded oxide iron-formation consists principally of interlaminated magnetite and chert; minor amounts of iron carbonate, iron silicate, or both, however, are commonly intermixed in the magnetite-rich and cherty layers. With gradations to magnetite-banded rock that also contains abundant iron carbonate and (or) iron silicate, oxide iron-formation grades into mixed-facies iron-formation.

The distribution of primary magnetite-chert rock in the Negaunee Iron-Formation is difficult to assess megascopically because of its similarity to mixed-facies magnetite-rich iron-formation. Furthermore, the very common secondary oxidation may make it difficult, if not impossible, even microscopically, to distinguish between magnetite-martite-hematite-chert rock derived from mixed facies magnetite-rich iron-formation and some secondarily oxidized facies of primary magnetite-chert iron-formation. Nevertheless, layers of purer magnetite-chert iron-formation generally less than 30 feet thick, occur below the Tracy sill in the southeastern part of sec. 7, T. 47 N., R. 26 W., between the Tracy and Summit Mountain sills in the west-central part of sec. 7, below the Tracy sill near the S1/4 cor. sec. 18, and in outcrops below the Summit Mountain sill in the NW1/4 sec. 19, and in parts of the Empire mine. Also, in the vicinity of the Isabella syncline in the Palmer basin, and in a drill hole east of the village of Palmer near the center of sec. 29, beds of magnetite-chert iron-formation are particularly common in the lower half of the Negaunee, and typically are interbedded with jaspery (martite-hematite-chert) iron-formation and magnetic graywacke. To the southeast, magnetite-banded iron-formation is the dominant facies in the lower 200–300 feet of the Negaunee across the NE1/4 sec. 32. Farther east, at the southeast end of the Palmer basin, a "dirty" magnetite-chert iron-formation characterized by small amounts of chlorite on interfaces between chert grains, makes up a considerable part of a 500-foot section above a 100-foot transition zone of carbonate iron-formation and graywacke at the base of the Negaunee and the top of the Ajibik-Siamo formations. Much secondarily oxidized iron-formation east of the Isabella syncline may have been primary magnetite-banded rock, and much of the jaspilite in the area, discussed below under hematite-banded rocks, may originally have been magnetite-banded oxide iron-formation.

Magnetite-banded oxide iron-formation consists of even-bedded black to gray and very pale gray layers, 0.02–0.2 inch thick, representing aggregates of nearly pure magnetite, mixed magnetite and chert, and nearly pure chert. The rock commonly has a reddish-brown cast with or without blue-black specks, owing to the formation of some martite, and reddish-brown, possibly hydrated, ferric oxide by the secondary oxidation of magnetite and minor iron carbonate or iron silicate. Magnetite here is in octahedral grains, 0.005–0.25 mm in diameter, but most are less than 0.05 mm. In some layers, magnetite grains are in two size ranges, 0.025–0.04 mm and 0.1–0.25 mm, the larger grains being scattered irregularly or strung along certain laminae. Chert grains are 0.01–0.03 mm in diameter. Chert forms layers and patches of matrix between grains of magnetite. Dusty opaque magnetite or hematite forms compact clusters at the cores of many chert grains. Relatively large magnetite grains, 0.1–0.25 mm in diameter, commonly are scattered through layers of mixed chert and finer grained magnetite and overprint the finer grained fabric, straddling and truncating the edges of the smaller grains. Larger magnetite crystals may protrude into grains of clastic quartz, and combs of secondary quartz may extend out perpendicularly from the faces of larger magnetite crystals. Some thin quartz laminae between magnetite layers consist entirely of comb quartz that has grown perpendicular to the layers of magnetite. Evidently no other material than silica has occupied the spaces between the magnetite layers; so the comb quartz probably formed merely by recrystallization of original layers of chert, growth of quartz starting at chert-magnetite interfaces perhaps because such chert layers contained relatively large amounts of connate water. These relationships indicate that the large magnetite grains crystallized after the deposition of clastic grains and after recrystallization of the chert and finer grained magnetite, and that other quartz crystallized later than the magnetite. Possibly the entire sequence of crystallizations, however, occurred during Penokean metamorphism.

Somewhat pod-shaped granular layers of chert and subordinate magnetite, 0.5–3 inches thick, form a small part of the iron-formation, between much thicker zones made up of the thin evenly bedded

magnetite and chert. Granules in the thick layers are approximately 0.2 to 1.5 mm in diameter and may be composed entirely of chert, of mixtures of chert and magnetite, or almost entirely of magnetite.

Lenses of graywacke and scattered quartz clasts are common in magnetite-banded iron-formation in the Palmer basin (figs. 21–23) and in parts of the Empire-south limb sector. Magnetite and chert in clastic lenses commonly are coarser grained than magnetite or chert in adjacent nonclastic layers, probably because the clastic lenses were more porous and permeable than adjacent layers during metamorphism, or served as local "reservoirs" of connate water in the iron-formation.

A chemical analysis of magnetite-chert iron-formation is shown in table 8. The relatively high content of FeO derives from magnetite, iron silicate, and iron carbonate, and the Al_2O_3 from the substantial amount of iron silicate in the rock (see mode of part of analyzed rock, table 6, No. 7).

TABLE 8.—*Chemical analysis and density of magnetite-chert iron-formation, Palmer quadrangle*

[Rock contains subordinate iron silicate and iron carbonate. Sample JG–134–66, Drill-hole location 266, 1-foot composite, 344–346 ft, SE¼SE¼ sec. 7, T. 47 N., R. 26 W. For mode of part of analyzed sample, see table 6, No. 7. Analyst: G. O. Riddle, U.S. Geol. Survey]

SiO_2	43.49	TiO_2	.06
Al_2O_3	2.50	P_2O_5	.28
Fe_2O_3	29.48	MnO	.21
FeO	15.89	CO_2	3.12
MgO	1.87	Cl	.00
CaO	2.32	F	.03
Na_2O	.05		
K_2O	.03	Total	100.31
H_2O^+	.95	Bulk density	3.17
H_2O^-	.03	Powder density	3.43

HEMATITE-BANDED ROCK

Hematite-banded iron-formation in the Palmer quadrangle consists of alternating layers of dark red to blue-black hematite and red, orange-red, or reddish-gray hematitic chert. The variety jaspilite, characterized by layers of crystalline hematite and red chert (jasper), is by far the most common of such rock. However, much of it is not a pure hematite facies, but after deposition or diagenesis contained more magnetite than hematite. Existing hematite layers generally consist largely of martite—octahedral-shaped hematite pseudomorphs of magnetite. Hematite-banded rock, including jaspilite, that was once mixed magnetite-hematite rock is limited virtually to the Jackson mine area and the hill on the south, near the northwest corner of the quadrangle, and to the western half of the Palmer basin.

Martite grains are tightly packed in ferruginous layers or are separated by selvages of chert and platy and flat rhombohedral hematite (fig. 24). The rather uncommon jaspilite containing ferruginous

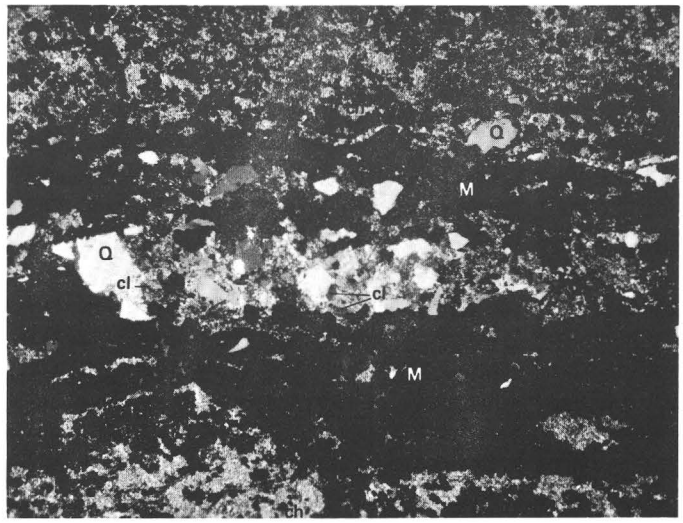

FIGURE 21.—Photomicrograph of magnetite-chert iron-formation, Palmer basin, containing lens of graywacke (gw) and scattered quartz clasts (Q). Magnetite (M) concentrated in layers and less densely distributed in layers of chert (ch). Some chlorite commonly mixed with chert. Graywacke composed of clastic quartz (Q) in matrix of chert and chlorite (cl). Postdepositional crystallization of magnetite shown by magnetite crystals attached to surfaces of clastic quartz. Crossed polarizers. JG–54–64, approximately 950S–1,800W of NE. cor. sec. 32, T. 47 N., R. 26 W.

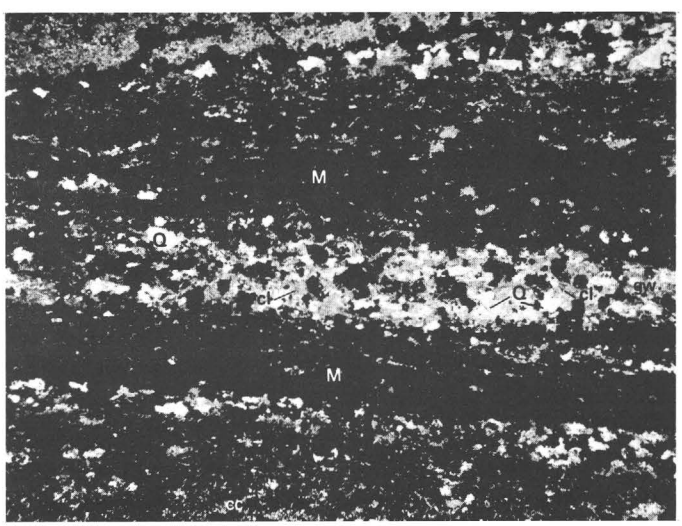

FIGURE 22.—Photomicrograph of magnetite-chlorite-chert iron-formation and interbedded graywacke, Isabella syncline, Palmer basin. Layers of coalesced magnetite (M), mixed magnetite-chlorite-chert (cc), and graywacke (gw). Graywacke composed of clastic quartz (Q) and magnetite set in matrix of chlorite (cl). Plane-polarized light. Drill-core sample JG–4L–65, approximately 200N–1,550E of SW. cor. sec. 29, T. 47 N., R. 26 W., about 260 feet beneath Negaunee-Goodrich contact. (Drill-hole location 709, 382 ft.)

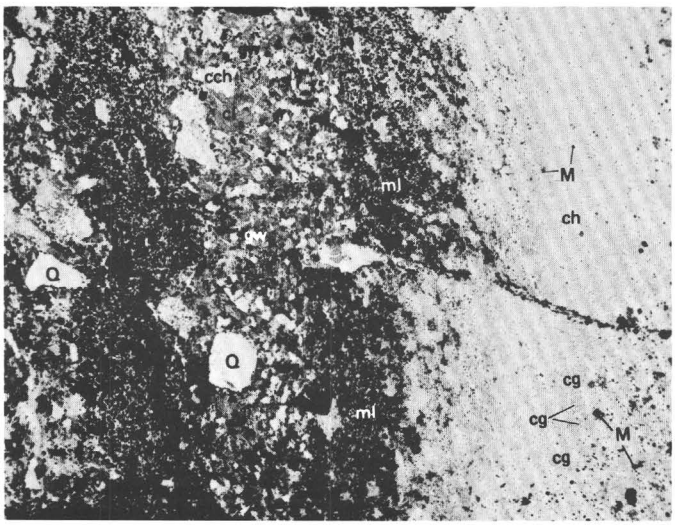

FIGURE 23.—Photomicrograph of magnetite-chert iron-formation and interbedded graywacke, Isabella syncline, Palmer basin. Chert layer on right (ch) contains granules of chert (cg) and scattered grains of magnetite (M). Chert layer grades to left into magnetite-rich layer (ml) containing some irregular chert granules. Magnetite-rich layer grades to left into graywacke (gw) consisting of clastic quartz (Q), clastic chert (cch) or fine-grained quartzite, and scattered magnetite in a matrix of chlorite (cl). Beds at right offset by small fault along which magnetite has formed. Plane-polarized light. Drill-core sample JG–3FF–65, approximately 100N–2,200E of SW. cor. sec. 29, T. 47 N., R. 26 W., about 270 feet below Negaunee-Goodrich contact and 200–300 feet above Negaunee-Ajibik contact. (Drill-hole location 711, 382 ft.)

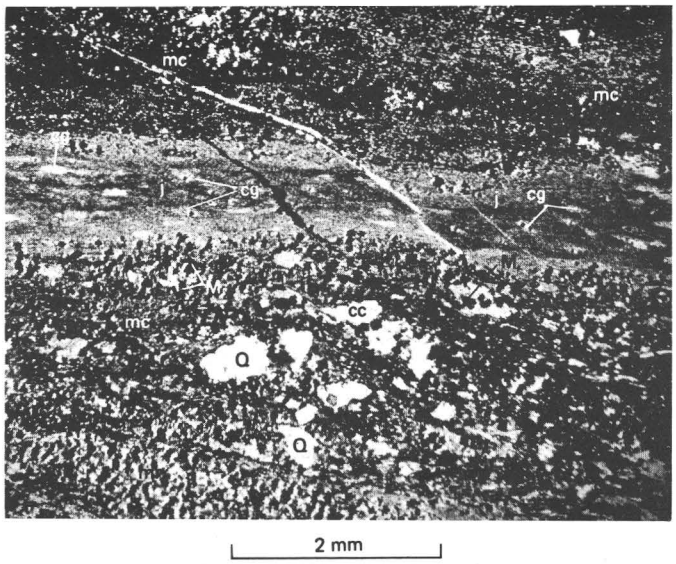

FIGURE 24.—Photomicrograph of martite jaspilite, south side of Palmer basin. Layers of martite-chert (mc) and jasper (j). Coalesced martite crystals (M) tend to be arranged in short "ribbons" (mr) alined at a large angle to bedding, suggesting that crystallization of magnetite (martite) occurred after consolidation of the rock. Martite-chert layers contain clastic quartz (Q) and clastic chert (cc). Jasper consists of clusters of red hematite particles within chert grains, scattered tiny laths of recrystallized hematite, extensively martitized octahedra of magnetite, and flattened granules of slightly hematitic chert (cg). Crossed polarizers. JG–77A–64, approximately 150N–1,200E of SW. cor. sec. 29, T. 47 N., R. 26 W.

layers mainly of hematite is found mainly within 100–200 feet stratigraphically below Goodrich Quartzite.

Layers of red hematite chert (jasper) contain scattered small flat rhombohedra of hematite and octahedra of magnetite or martite. The distinctive color of the jasper is produced by tiny red flakes and dusty particles of hematite that are clustered compactly within individual chert grains (fig. 25), or less commonly are distributed more or less indiscriminately within and between grains of chert. The clusters of hematite particles are of varied shape, but many have angular equant outlines suggestive of crystals, so may be pseudomorphs of iron carbonate. Other possible explanations of the angular clusters are (1) that desiccation and consolidation of original ferruginous silica gel caused separation into angular pieces which subsequently were surrounded by clear silica gel or quartz, or (2) that during metamorphic recrystallization, hematite that was originally distributed evenly through silica gel was forced to the centers of crystallizing chert grains and was concentrated there in clusters that somewhat mimicked the shapes of the surrounding grains. The angular shapes would seem to rule out the hematite clusters being microgranules. Chert grains are approximately 0.01–0.03 mm in diameter, and the clusters of hematite are generally 0.003–0.02 mm in size, and occupy less than half the volume of each chert grain. In some exceptionally ferruginous parts of the jasper, however, hematite clusters are nearly as large as the enclosing grains of chert. Individual hematite flakes in the clusters are approximately 0.3 micron or less in diameter. Scattered crystals of magnetite and plates of hematite generally straddle boundaries between chert grains (fig. 25*A*); crystals of magnetite may extend into chert grains and may be molded partly around clusters of hematite, but they rarely protrude into the clusters.

Most layers of jasper contain elliptical granules of hematite and (or) chert, 0.2–0.75 mm long (fig. 26). The hematite granules consist of evenly packed hematite particles or clusters of dusty hematite partly separated by thin cherty selvages. The ferru-

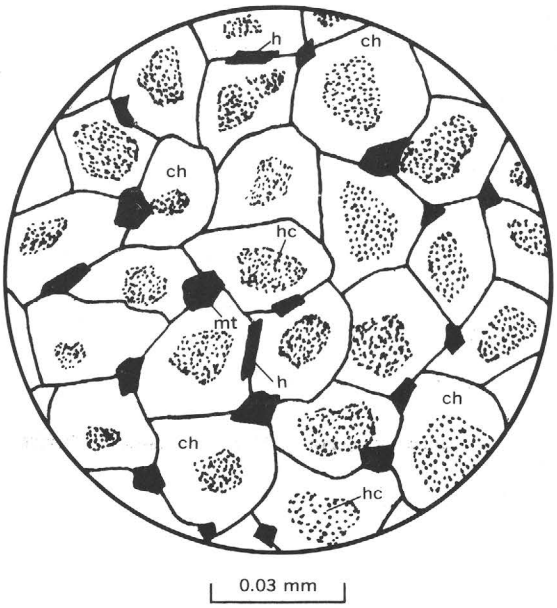

FIGURE 25.—Sketches of jasper as seen under a microscope. Hematite flakes and clusters are red in obliquely reflected light. Sutures between chert grains in *A* not visible in *B*. ch, chert; h, rhombohedral hematite; hc, hematite cluster; hf, hematite flake; mt, magnetite.

ginous granules may be surrounded by clear chert or by hematitic chert containing a lower proportion of hematite to chert than do the granules. Chert

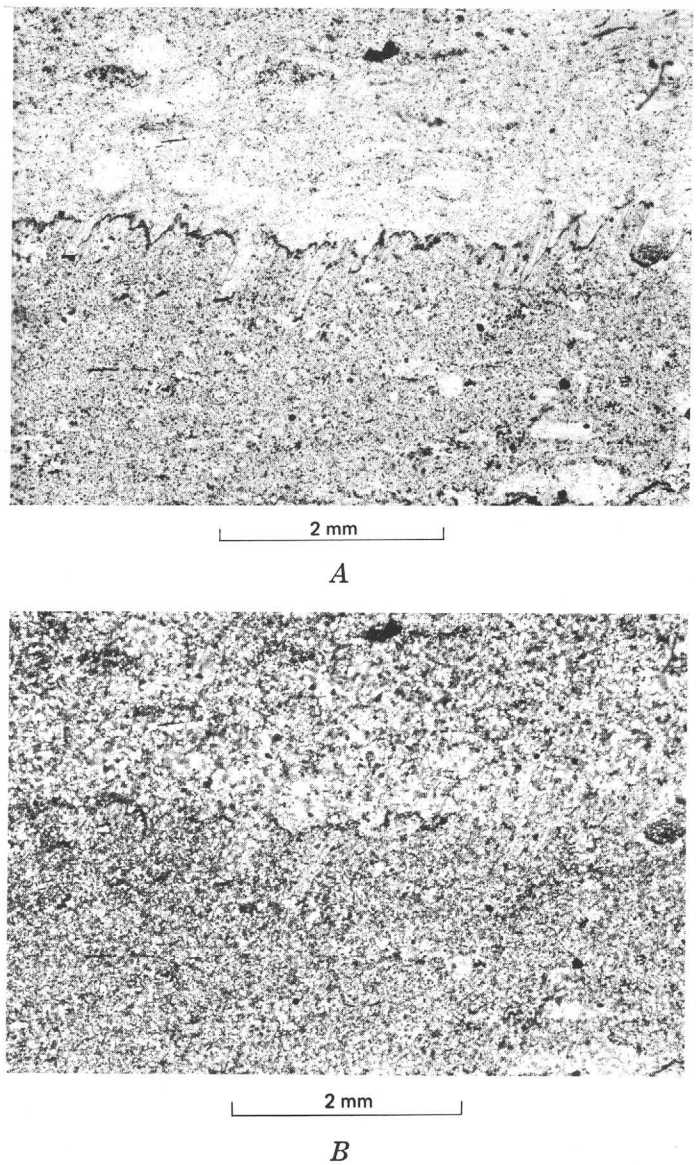

FIGURE 26.—Photomicrographs of pale-red jasper layers in jaspilite, south side of Palmer basin. Granular chert and small opaque patches of hematite and martite. *A*, Plane-polarized light. *B*, Crossed polarizers. JG–73–64, approximately 450S–860E of NW. cor. sec. 32, T. 47 N., R. 26 W.

granules generally contain very little hematite, if any, and stand out against a red-tinged background of hematitic chert (fig. 24). Stylolites are present in a few places between chert layers (fig. 26*A*).

Hematite-banded iron-formation consists very largely of SiO_2 and Fe_2O_3 (table 9, No. 2), which is to be expected from the mineralogy of the rock. Mixed hematite-magnetite rock contains significantly more FeO than the purer hematitic iron-formation, as shown by analyses from the Hammersley Range, Western Australia (Miles, 1942, table 4, p. 30), and the Ukraine, U.S.S.R. (James, 1966, table 10, p. 20).

TABLE 9.—*Chemical analyses of hematite-rich iron-formation from the Marquette and Menominee iron ranges*

	1	2
SiO_2	37.23	40.1
Al_2O_3	.20	.80
Fe_2O_3	[1]62.51	50.1
FeO		1.6
MnO		.2
MgO	.07	2.0
CaO	[2].04	1.4
Na_2O		
K_2O		
P_2O_5		.07
CO_2		2.6
S		.009
Total	100.05	98.88

[1] Specific oxides not listed; percentage given only for "soluble matter, chiefly iron oxide."
[2] Specific oxides not listed; percentage given only for "alkali oxides."

1. Jaspilite, Marquette Range; Van Hise and Bayley, 1897, p. 363.
2. Hematite iron-formation, Menominee district, Michigan; James, 1966, table 10, p. 20.

Recrystallization during regional metamorphism evidently produced the existing fabrics of intergrown magnetite or martite (magnetite at time of recrystallization), lath-shaped rhombohedral hematite, and chert. Plates and laths of hematite in ferruginous or jasper layers are derived from premetamorphic hematite that may have been primary. Generally there is no problem in distinguishing iron-formation that must have contained hematite at the time of recrystallization from that containing hematite derived after metamorphism. Iron-formation having premetamorphic hematite is characterized by beds of red jasper and deep-red or blue-black hematite and is hard and flinty. Iron-formation having postmetamorphic hematite tends to be rusty or brown and is softened and earthy or sooty. Megascopically, martite in such rock is blue-black or dark rust-coated specks, but in polished section is generally similar to martite in the hard flinty hematitic rock. Surrounding, probably hydrated, ferric oxide, derived from metamorphically recrystallized iron carbonate, iron silicate, or hematite, on the other hand, forms irregular pitted grains with strong internal reflections in polished section.

Premetamorphic hematite, recrystallized with magnetite and chert, was either primary or a product of weathering-oxidation of carbonate or silicate shortly after Negaunee deposition. Erosion at that time bared parts of the iron-formation and contributed fragments of the iron-formation to the overlying Goodrich Quartzite. The fragments typically are of jaspilite or jasper. Most iron-formation containing premetamorphic (recrystallized) hematite in the Marquette district is within a few hundred feet stratigraphically below the Negaunee-Goodrich erosion surface, as noted by Van Hise and Bayley (1897, p. 363, 403) in proposing that the hematite formed by oxidation during the Negaunee-Goodrich interval. The spatial relationship of jaspilite to the Negaunee-Goodrich contact is indeed striking, particularly because the Goodrich, in cutting into the Negaunee, appears to come into contact with different stratigraphic levels of the iron-formation, yet is underlain by jaspilite almost everywhere the contact zone has been observed. If most existing variations in the thickness of the Negaunee were attributed without doubt to the pre-Goodrich erosion, it would be difficult to make a case for primary hematite in all the jaspilite adjacent to the Negaunee-Goodrich contact. However, evidence that variations in the thickness of the Negaunee were mainly primary and affected little by pre-Goodrich erosion (see p. 118–119) implies a coming together of conditions for hematite deposition in the iron-formation, and Goodrich deposition just afterwards. Uplift and exposure of the Negaunee to erosion would necessarily be preceded by shallowing of the margins of the Negaunee depositional basin. Oxidizing conditions favorable to the development of primary hematite could therefore be a precursor to pre-Goodrich erosion and to deposition of the Goodrich everywhere in the area.

Jaspilitic parts of the iron-formation in places contain unoxidized lenses of graywacke. As with magnetite-layered jaspilite, the unoxidized condition of the interbedded material—the chlorite matrix of the graywacke—tends to preclude derivation of the hematite by secondary oxidation.

Hematite in a few granular and nongranular layers or lenses as much as 2 inches thick in drill core from 100–200 feet below the surface in the NW¼ sec. 7, T. 47 N., R. 26 W., also appears to be primary. The hematitic lenses are sharply bounded by gray-green layers of mixed magnetite, sideritic carbonate, and iron silicate. Most magnetite grains are not even marginally altered to martite. If the hematitic layers were a product of postmetamorphic oxidation, presumably the oxidation would also have encroached on the adjacent layers. The characteristic granules in such layers denote shallow-water deposition and also suggest depositional origin of the hematite (James, 1954, p. 259–260, 261).

A subordinate part of the jaspilite in the Palmer basin is similar to that just described except that martite-magnetite layers also contain many rhombohedral laths of hematite that must have formed during metamorphic recrystallization. The hematite existed prior to recrystallization and could have been primary or a product of the partial oxidation of magnetite or other iron minerals during the Negaunee-Goodrich interval.

As noted earlier, beds of jasper commonly con-

tain granules of chert and hematite. Typically, granular jasper occurs as relatively thick lenses (½–2 in.) and in this respect is similar to granular magnetitic and silicate iron-formation. The association of granules and thick lenticular beds is probably a result of deposition in a shallow-water environment, subject to wave and current action. Hematite, magnetite, and iron silicate would be compatible with the oxidizing conditions postulated for such an environment (James, 1954). Granular hematitic beds might conceivably have formed by the premetamorphic oxidation of granular magnetite or silicate. However, a high chert content is not characteristic of lenses of granular silicate iron-formation in the area, as it is of much of the granular magnetitic and hematitic rock; therefore, hematite granules in jasper are probably either primary or derived by the oxidation of magnetite granules. The presence of magnetite-rich beds in places adjacent to lenses of granular jasper tends to rule out the development of hematite by oxidation of the rock after the deposition of the magnetite; so most hematite granules are considered to be primary. In one sample of drill core from near the NE. cor. of sec. 24, T. 47 N., R. 27 W. (see pl. 8, "Drill-Hole Data and Locations," drill-hole location 431A, sample from 301½ ft), hematite that is almost certainly primary is associated with granular structure. Granular hematitic chert surrounds nongranular patches or lenses of carbonate-magnetite-chert iron-formation. The unoxidized condition of the latter rock probably precludes development of the associated hematitic chert by secondary oxidation after deposition.

Platy and rhombohedral hematite in nonmartitic and nonmagnetitic ferruginous layers that alternate with lenses of jasper may be either recrystallized primary hematite or recrystallized hematite derived from the premetamorphic oxidation of iron carbonate or iron silicate. A common well-alined lenticle structure in such layers probably represents flattened granules (James, 1954, p. 259), and if so, indicates shallow water favorable for oxidation. James believes that granules were abundant in hematitic layers as well as in cherty layers, but that they are less well preserved in the former.

An alternate explanation of the lenticle structure is that it is of organic origin. The regular distribution, consistent sizes, and slightly arched form of the lenticles is similar to probable algal structures in parts of the Kona Dolomite and therefore might be a vestige of algal colonies. The presence of algal structures in the older Kona Dolomite in probably the same depositional basin indicates that algae were probably present during Negaunee deposition. Wygant and Mancuso (1969) have described possible organic structures in the Negaunee Iron-Formation. The well-known studies of Tyler and Barghoorn (1954) and Barghoorn and Tyler (1965) on the Gunflint Iron-Formation of northeastern Minnesota have shown the presence of algal remains in rock of roughly similar type and approximately the same age as the Negaunee (James, 1958). LaBerge (1967) also found undoubted organic remains in middle Precambrian iron-formation. The shallow water implicit for algal growth would probably have provided conditions more suitable for the development of primary hematite than magnetite. Metamorphic recrystallization of the Negaunee probably prevents proving the presence of algal remains.

Before the development of martite, the martitic jaspilite evidently consisted of magnetite, lath-shaped rhombohedral hematite, and chert that had recrystallized together during regional metamorphism. However, the premetamorphic crystallization of magnetite octahedra, perhaps during diagenesis, and their conversion to martite during metamorphism cannot be ruled out entirely. Octahedra of magnetite that protrude into quartz clasts are clearly of postdepositional origin and could be diagenetic. However, the regular distribution and generally consistent size of existing magnetite octahedra and grains of recrystallized chert and carbonate suggest similar and pervasive conditions of crystallization for all the grains, which would seem best related to regional metamorphism. Martite is entirely similar in size and distribution to the magnetite in magnetite-banded and mixed facies iron-formation, so present martite octahedra probably formed under the same influences as the existing magnetite. Therefore, martite grains, too, probably first formed as magnetite during regional metamorphism and subsequently were converted to hematite pseudomorphs. The similarity of martite in jaspilite and in iron-formation oxidized after regional metamorphism is evidence that martite in the jaspilite could have formed after metamorphism. The association, in the premetamorphic form of the present martitic jaspilite, of primary magnetite and hematite suggests mildly to strongly oxidizing depositional conditions.

SILICATE FACIES

In the Palmer quadrangle, pure silicate iron-formation is not abundant—that is, varieties containing mainly minnesotaite, stilpnomelane, grunerite, or mixtures of silicates and chert. Individual layers commonly consist mainly of one or more of the iron silicates, but such beds are generally less

than 6 inches thick and alternate with beds of mixed silicate and carbonate, silicate and magnetite, or all three minerals, or with beds of nearly pure carbonate or magnetite. Mixed-facies rock containing iron silicate is common in much of the iron-formation.

Relatively pure silicate iron-formation, although not abundant, is widely distributed laterally and perpendicular to the strike of iron-formation in the eastern part of the Marquette synclinorium proper. For example, in the axial sector it has been found in drill holes at points about 80, 450, 510, and 1,000 feet below the Tracy sill in the SE¼ sec. 7, and the SW¼ sec. 8, and between the Tracy and Summit Mountain sills in the NW¼NE¼ and the SE¼ sec. 18, T. 47 N., R. 26 W. Also, silicate iron-formation has been found in outcrops between the Tracy and Summit Mountain sills in the east-central part of sec. 12, and between the Partridge Creek and Suicide sills in the NE¼NE¼ sec. 13, T. 47 N., R. 27 W. Undoubtedly, more extensive sampling and thin sectioning of the iron-formation would reveal much more about the distribution of purer beds of iron silicate. Relatively pure silicate iron-formation has not been seen in the Palmer basin.

Minnesotaite is the most common iron silicate in the iron-formation of the Palmer quadrangle. Colorless to very pale green or pale-olive-green flakes, tufts, and blades typically form felted matted aggregates in the purer layers. Grains are commonly less than 0.02 mm in maximum dimension. In thin section they have characteristic yellow and orange-yellow interference colors similar to those of sericite. Megascopically, layers of minnesotaite are pale green, very fine grained and dense, with almost a chertlike appearance. Granules of minnesotaite occur in some layers, are 0.3–0.8 mm in maximum diameter, and commonly are internally coarser grained than the minnesotaite of the matrix surrounding the granules. In some layers, granules consisting only of minnesotaite are surrounded by a matrix of minnesotaite and magnetite, minnesotaite and stilpnomelane, or stilpnomelane alone. Such granules could not have formed simply by the agitation of materials on the sea bottom, a commonly accepted mechanism, but must be largely a result of some kind of selective replacement or concretionary growth, probably during diagenesis.

Stilpnomelane occurs widely in the iron-formation, but rarely as monomineralic layers; typically it is mixed with carbonate, magnetite, or minnesotaite, and probably is considerably subordinate to minnesotaite in total amount. It occurs in scattered flakes and needles and in aggregates. Needles may be as much as 0.1 mm long, but most flakes are shorter than 0.05 mm. Most of the stilpnomelane is the variety ferristilpnomelane, on the basis of strong pleochroism from pale straw yellow, pale brown, or pale greenish brown to deep brown or black. Some stilpnomelane that is pleochroic from pale straw yellow or pale green to bright grass green or dark green evidently is the variety ferrostilpnomelane. Some of the iron-formation contains intergrown brown and green stilpnomelane, which may be a product of equilibration between ferric and ferrous iron during deposition, or of incomplete diagenetic oxidation of the ferrous variety or reduction of the ferric variety, depending on depth below the sediment-water interface. James (1954, p. 269) concluded that variations in the ferric-ferrous ratio from layer to layer of stilpnomelane within thicknesses of a few millimeters are primary differences, on the assumption that if ferric-ferrous ratios had been established by metamorphic equilibrium, they would be consistent through much thicker layers.

Chlorite is a minor silicate in the iron-formation and is absent from a large proportion of the rock. It is virtually nowhere the sole iron mineral present. It is most common in the Palmer basin in parts of the iron-formation containing beds of graywacke (figs. 21–23), and in the lower part of the Negaunee in the axial sector of the synclinorium, particularly in the transition zone with the Siamo Slate. Most of the chert through some 500 feet of magnetite-chert iron-formation at the southeast end of the Palmer basin is "dirtied" by shreds of chlorite on interfaces between chert grains. Most aggregates of clastic quartz in the iron-formation, even where they are clusters of only a few grains, contain intermixed chlorite, which suggests that the chlorite was a clastic sediment or derived from one, rather than from a chemical precipitate.

ANOMALOUS GRUNERITE

Grunerite is a common but anomalous silicate in iron-formation in the axial sector of the synclinorium in the zones between the Tracy and Summit Mountain sills and between the Summit Mountain and Partridge Creek sills. Mineral assemblages in metadiabase indicate the chlorite zone of regional metamorphism in this area; grunerite is characteristic of higher metamorphic grades; so in the Palmer quadrangle it is not related to regional metamorphism. The grunerite appears to be most abundant just above the Tracy sill. Laminae, approximately 1–10 mm thick, may be virtually entirely grunerite and alternate with laminae rich in iron carbonate or minnesotaite plus chert, or with layers containing mixtures of iron carbonate, minnesotaite, and gru-

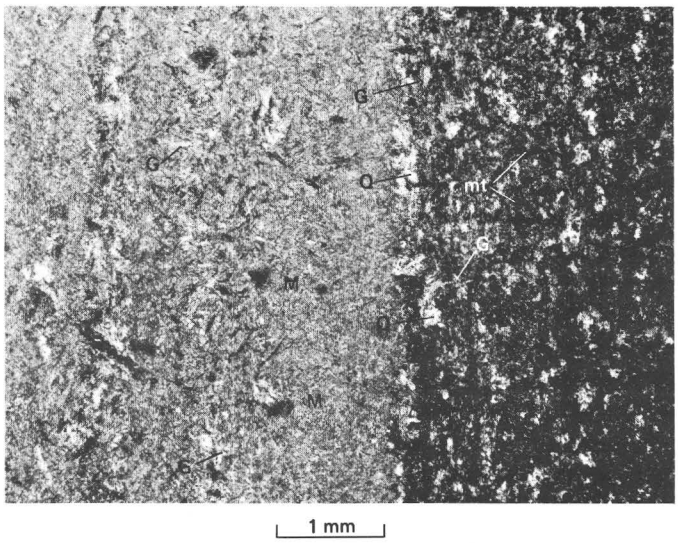

A

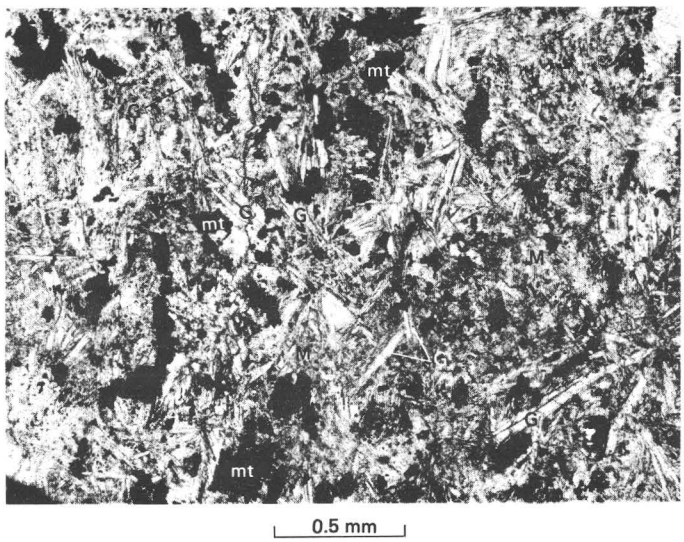

C

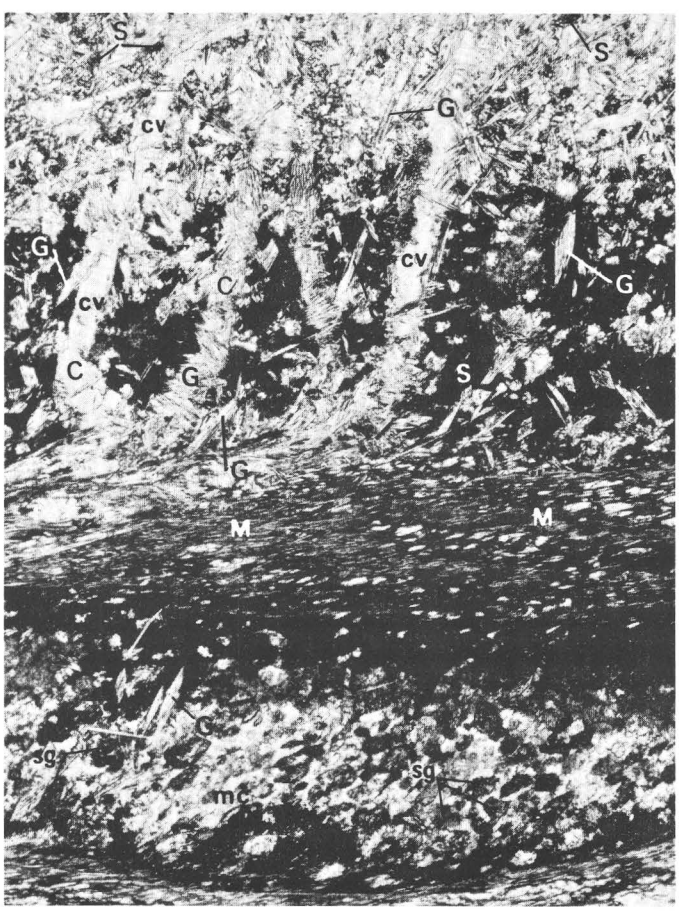

B

FIGURE 27.—Photomicrographs of grunerite-bearing iron-formation. *A*, Minnesotaite-grunerite iron-formation lens in Partridge Creek sill. Light-colored layer, mainly minnesotaite (M), contains scattered porphyroblasts of grunerite (G). Dark layer contains abundant porphyroblasts of grunerite and small grains of magnetite (mt). Quartz (Q) is a minor constituent in both layers. Crossed polarizers. JG–32–65, approximately 2,950N–2,950W of SE. cor. sec. 12, T. 47 N., R. 27 W. *B*, Grunerite (G) in minnesotaite (M)-stilpnomelane (S)-carbonate (C) iron-formation from zone between Tracy and Summit Mountain sills. Minor chert intergrown with minnesotaite in one layer (mc), in which are scattered granules of stilpnomelane (sg). Light-colored layer at top of photomicrograph is mainly grunerite through which are scattered carbonate and small clots of stilpnomelane. Carbonate veins (cv) and many blades of grunerite lie at large angles to bedding. Plane polarized light. Drill-core sample JG–11E–66, approximately 900N–2,200E of SW. cor. sec. 18, T. 47 N., R. 26 W. (Drill-hole location 424, sample from 550 ft.) *C*, Minnesotaite-grunerite-magnetite iron-formation from base of Suicide sill. Sprays of grunerite (G) and small aggregates of magnetite (mt) set in matrix of minnesotaite (M). Plane-polarized light. JG–51–65, approximately 1,700N–2,100W of SE. cor. sec. 13, T. 47 N., R. 27 W.

nerite, with or without magnetite or stilpnomelane (fig. 27). Typically, grunerite forms isolated silvery to brownish bladelike porphyroblasts in layers of minnesotaite or minnesotaite and siderite in which stilpnomelane may be present. In some layers it replaces virtually all the other iron minerals. Grunerite also occurs along some contacts between layers

of minnesotaite, stilpnomelane, or carbonate and chert.

Grunerite porphyroblasts commonly range from 0.06–0.4 mm in maximum dimension. Locally, veinlets of grunerite cut adjacent gruneritic beds. Carbonate is scarce in a grunerite-rich zone within about 50 feet above the Summit Mountain sill in the axial part of the synclinorium; apparently carbonate and grunerite are antipathetic. Carbonate grains may have been growth centers for grunerite and provided some of the necessary iron. Some iron, though, was derived from earlier iron silicate, as shown by the extension of many blades of grunerite into aggregates of pure minnesotaite.

Grunerite is a metamorphic mineral, and in various layers of porphyroblasts it is clearly derived from iron carbonate and chert, or from minnesotaite or stilpnomelane. The anomalous occurrence of grunerite is attributed to contact metamorphism during emplacement of the present metadiabase, before regional metamorphism. The confinement of a thin belt of iron-formation between the comparatively thick magma bodies of the Tracy and Summit Mountain sills evidently raised temperature enough in that belt to produce grunerite. Conversion of the sills to metadiabase occurred subsequently, during regional metamorphism. Modifications of the grunerite seen in thin and polished sections tend to confirm that it predated the regional metamorphism. Although grains of magnetite, sideritic carbonate, minnesotaite, and stilpnomelane have not been altered since they crystallized during regional metamorphism (aside from small amounts of near-surface oxidation), intergrown blades of grunerite typically have been partly or entirely replaced pseudomorphously by quartz, magnetite, and minor carbonate (fig. 28). Wide variations in the proportions of quartz, magnetite, and carbonate are seen in thin sections and suggest exchanges of material between grunerite and the matrix during the replacement. The retrograde growth of carbonate certainly must have involved an introduction of CO_2 into the grunerite. Magnetite replacements of grunerite have been extensively martitized in places and are reprsented now only by small remnant inclusions in hematite pseudomorphs of grunerite. It seems certain that these changes in the grunerite could not have taken place after regional metamorphism without related changes affecting the surrounding minerals of the iron-formation. Except for the unaltered conditions of surrounding minerals of the iron-formation, particularly magnetite, the martitization of the magnetite pseudomorphs of grunerite might be considered a postregional metamorphic change, analogous to surface-related or hydrothermal martitization of "normal" magnetite in other parts of the iron-formation. All the modifications of grunerite, however, must have taken place either during the low-grade regional metamorphism that recrystallized the other minerals of the iron-formation, or earlier by retrograde action shortly after the grunerite formed, or by a combination of both. In any case, the grunerite predated regional metamorphism and must be related to the only earlier thermal event known to have affected the iron-formation, namely, the intrusion of the present metadiabase sills.

Six of eight chemical analyses of Precambrian silicate iron-formation listed by James (1954, table 8), reporting both FeO and Fe_2O_3, contain between 20 and 34 percent FeO, and five contain less than 10 percent Fe_2O_3. Silica varies from 34 to about 53 percent, except in a sample of pure minnesotaite-chert rock in which it is 65.42 percent. The other samples evidently contain substantial amounts of other iron minerals besides silicate. Results of chemical analysis of silicate-rich iron-formation from the Palmer quadrangle are listed in table 10. The analyzed rock contains layers of minnesotaite, grunerite, and stilpnomelane-magnetite-grunerite (see table 6, No. 9). Carbonate is a minor constituent in the stilpnomelane-rich layers. The rock chemically is well within the compositional range of typical silicate iron-formation, except for its relatively high content of Fe_2O_3. The Fe_2O_3 is present mainly in hematite derived from the secondary oxidation of some of the minnesotaite, grunerite, magnetite, and possibly also stilpnomelane. Some brown secondary hematite is not readily distinguished from stilpnomelane-magnetite under the microscope; so the measured percentages of these minerals in the mode (table 6, No. 9) are somewhat questionable.

TABLE 10.—*Chemical analysis and density of silicate iron-formation, Palmer quadrangle*

[JG–133–66, drill-core sample from between Tracy and Summit Mountain sills, 980N–2,300E of SW. cor. sec. 7, T. 47 N., R. 26 W. (Drill-hole location 264, 1-ft composite from 104–111 ft). Analyst: George O. Riddle, U.S. Geol. Survey]

SiO_2	45.12	TiO_2	.05
Al_2O_3	2.13	P_2O_5	.11
Fe_2O_3	17.32	MnO	2.40
FeO	24.03	CO_2	1.40
MgO	2.47	Cl	.01
CaO	1.16	F	.02
Na_2O	.36		
K_2O	.53	Total	100.58
H_2O^+	2.62	Bulk density	3.32
H_2O^-	.85	Powder density	3.27

MIXED FACIES

A large part of the Negaunee Iron-Formation consists of mixtures of iron carbonate, iron silicate, and iron oxide, incorporated in assemblages of car-

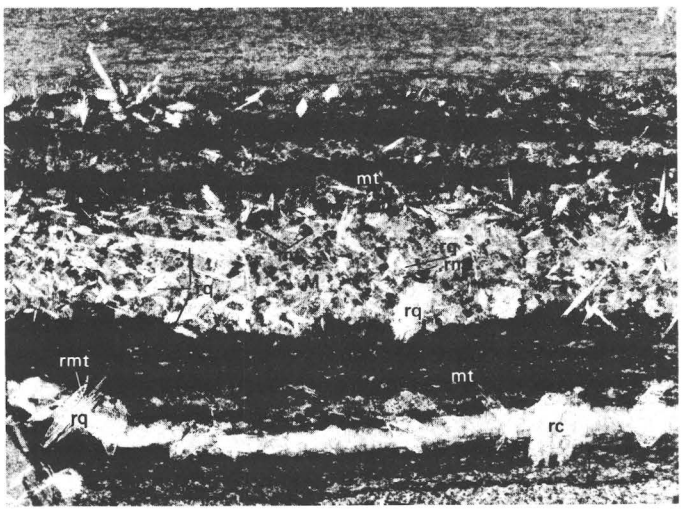

A

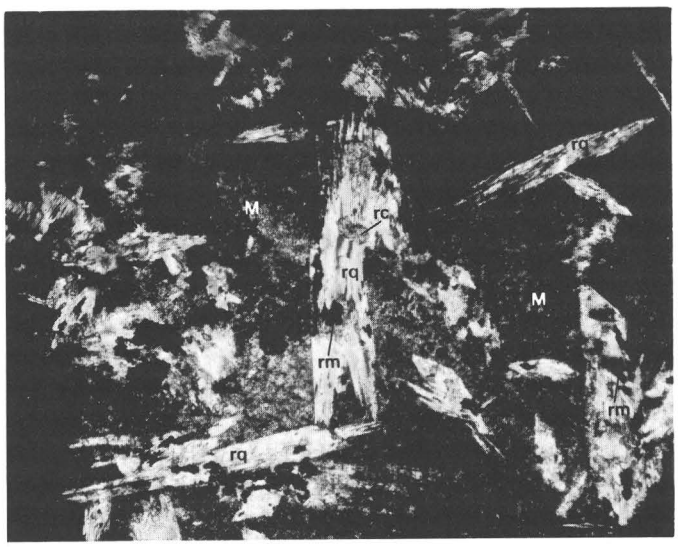

B

FIGURE 28.—Photomicrographs of iron-formation showing replacement of grunerite. Zone between Tracy and Summit Mountain sills, approximately 1,200N–900W of SE. cor. sec. 18, T. 47 N., R. 26 W. (Drill-hole location 423.) *A*, Minnesotaite-magnetite-carbonate-grunerite iron-formation. Layers are rich in minnesotaite (M), magnetite (mt), and carbonate. Layers containing mixtures of minnesotaite and magnetite or carbonate and minnesotaite have been "overprinted" by porphyroblasts of grunerite. Porphyroblasts completely replaced by quartz (rq), quartz and carbonate (rc), or quartz and magnetite (rmt). Vein of carbonate and minnesotaite cuts bedding in lower left part of photomicrograph. Plane-polarized light. Drill-core sample JG–6C–66; sample from 400 feet. *B*, Pseudomorphs of grunerite porphyroblasts in layer of minnesotaite (M). Porphyroblasts have been replaced by quartz (rq), carbonate (rc), and magnetite (rm). Crossed polarizers. Drill-core sample JG–6B–66; sample from 384 feet. *C*, Stilpnomelane-carbonate-grunerite-quartz iron-formation. Porphyroblasts of grunerite (G) located mainly in layers of dark-brown stilpnomelane (S). Some grunerite also in carbonate part of carbonate (C)-quartz (Q) layer. Some grunerite partly replaced pseudomorphously by quartz (rq). Plane-polarized light. Drill-core sample JG–6F–66; sample from 491 feet.

C

bonate-magnetite, magnetite-silicate, carbonate-silicate, and carbonate-magnetite-silicate. The three-mineral mixed facies is much more abundant than any of the two-mineral facies. The latter, in a sense, are purer and generally persist only through short stratigraphic intervals. Individual laminae may be virtually monomineralic or may contain mixtures of the iron minerals with more or less chert, varying in practically all proportions. Laminations typically have resulted from small changes in the proportions of individual minerals. Minerals associated within individual laminae are listed on p. 44–45, in

assemblages 3–11, 14–17, 19, and 23–25. With assumed reducing conditions for the precipitation of iron carbonate, mildly oxidizing conditions for magnetite, and a range of these conditions for iron silicate (James, 1954, p. 272–273), it is clear that during much of Negaunee time, borderline conditions and numerous fluctuations from mildly reducing to mildly oxidizing occurred on the sea bottom.

CARBONATE-MAGNETITE ROCK

Carbonate-magnetite rock is common in the Negaunee Iron-Formation. It occurs beneath the Tracy sill in the axial sector in secs. 7 and 18, T. 47 N., R. 26 W., mainly between 500 and 1,000 feet above the base of the formation. Much secondarily oxidized iron-formation in that area and farther north was derived from similar mixed-facies iron-formation. Such rock also occurs in the axial sector between the Summit Mountain and Partridge Creek sills in the SW¼ sec. 18, and near the common corner of secs. 18, 19, T. 47 N., R. 26 W., and 13, 24, T. 47 N., R. 27 W., within a few hundred feet above and below the Summit Mountain sill. One of the two main ore zones in the Empire mine is in carbonate-magnetite-chert iron-formation, about 700–900 feet above the base of the Negaunee. Southwestward from there to the New Volunteer mine, similar rock forms a considerable part of the section, 300–800 feet above the base. At the southeast end of the Palmer basin, the abundant "dirty" magnetite-chert iron-formation described earlier is interbedded with carbonate-magnetite-chert rock throughout the section. In the vicinity of the Isabella syncline, small amounts of carbonate-magnetite rock are interbedded with the dominant martite-jasper and martite-hydrated(?) hematite-jasper rock, some of which is probably secondarily oxidized carbonate-magnetite rock.

Carbonate-magnetite iron-formation contains monomineralic and mixed laminae of the iron minerals and chert (fig. 29). Beds vary from thin and regular to thick (½–3 in.) and highly irregular. Chert-rich pods are common (fig. 29, B4, C2, C3). Imbrication and overfolding of pods and irregular beds (fig. 29, A3, B2, B3, B4, C2) were probably caused by preconsolidation slumping and suggest that pods were either primary deposits or formed during diagenesis.

The principal chemical components of carbonate-magnetite iron-formation, SiO_2, Fe_2O_3, FeO, and CO_2, vary widely with different proportions of chert, carbonate, and magnetite (table 11). Modes of a single thin section from each chemically analyzed sample are listed in table 6, Nos. 6–8.

TABLE 11.—*Chemical analyses and densities of carbonate-magnetite-chert iron-formation, Palmer quadrangle*

[Analyst: George O. Riddle, U.S. Geol. Survey]

	1	2	3
SiO_2	44.40	34.01	40.83
Al_2O_3	1.96	1.38	1.23
Fe_2O_3	25.44	20.07	30.61
FeO	17.42	24.37	18.86
MgO	2.68	2.39	2.20
CaO	.44	2.03	.49
Na_2O	.10	.14	.06
K_2O	.44	.26	.03
H_2O^+	.52	.77	.42
H_2O^-	.06	.32	.00
TiO_2	.06	.03	.03
P_2O_5	.07	.09	.16
MnO	.56	2.16	.54
CO_2	6.01	12.22	4.92
Cl	.00	.00	.00
F	.02	.01	.02
Subtotal	100.18	100.25	100.40
Less O	.01	.00	.01
Total	100.17	100.25	100.39
Bulk density	3.39	3.53	3.58
Powder density	3.40	3.41	3.54

1. JG–132–66; drill-hole location 232; from 775–776 ft.
2. JG–136–66; drill-hole location 428; 2-ft composite, from 314 to 318 ft.
3. JG–138–66; drill-hole location 376; 1-ft composite, from 166 to 169 ft.

CARBONATE-SILICATE ROCK

Carbonate-silicate rock is common beneath the Tracy sill in the axial sector of the Marquette synclinorium, particularly in the lower 500 feet of the iron-formation. Such rock is also present in the lower (southeast) part of the section in the Empire mine. Iron-formation composed of carbonate, chlorite, and stilpnomelane occurs within 50 to 100 feet of the bottom of the Negaunee in the eastern half of the Palmer basin; at the southeast end of the basin such rock is interbedded with coarse-grained graywacke (fig. 30). In the axial and Empire-south limb sectors, carbonate-silicate iron-formation is comparatively thin bedded. Layers contain combinations of stilpnomelane, minnesotaite, carbonate, and chert. Stilpnomelane is considerably in excess of minnesotaite in most places. Flakes, small clumps, and blades of stilpnomelane typically are dispersed through layers of carbonate. Stilpnomelane blades generally are oriented at a large angle to bedding; so in their present form they must be products of crystallization after deposition of the rock. Clastic quartz is present in the Palmer basin, as shown in figure 30, and in some carbonate-silicate rock in the south part of sec. 7, T. 47 N., R. 26 W., and south and southwest from there to the Empire and New Volunteer mines.

Granules in some carbonate-silicate iron-formation are of stilpnomelane, carbonate, or mixtures of the two. The granules may be surrounded by either mineral or by mixtures of the two. The proportions

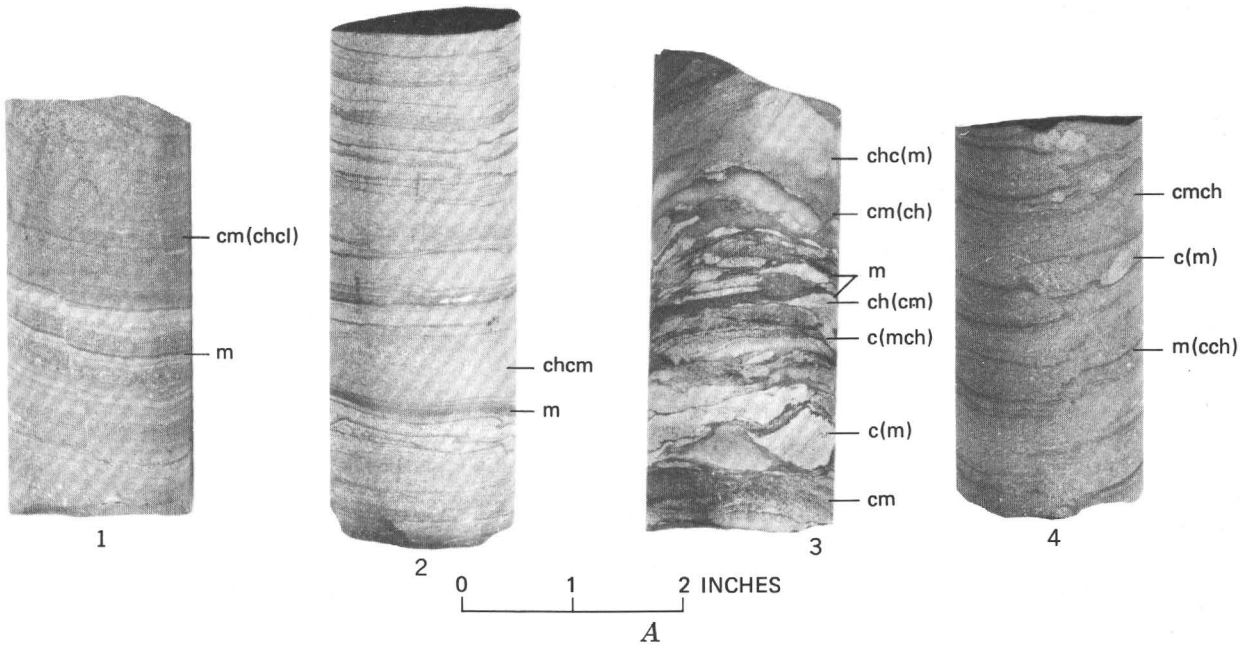

A

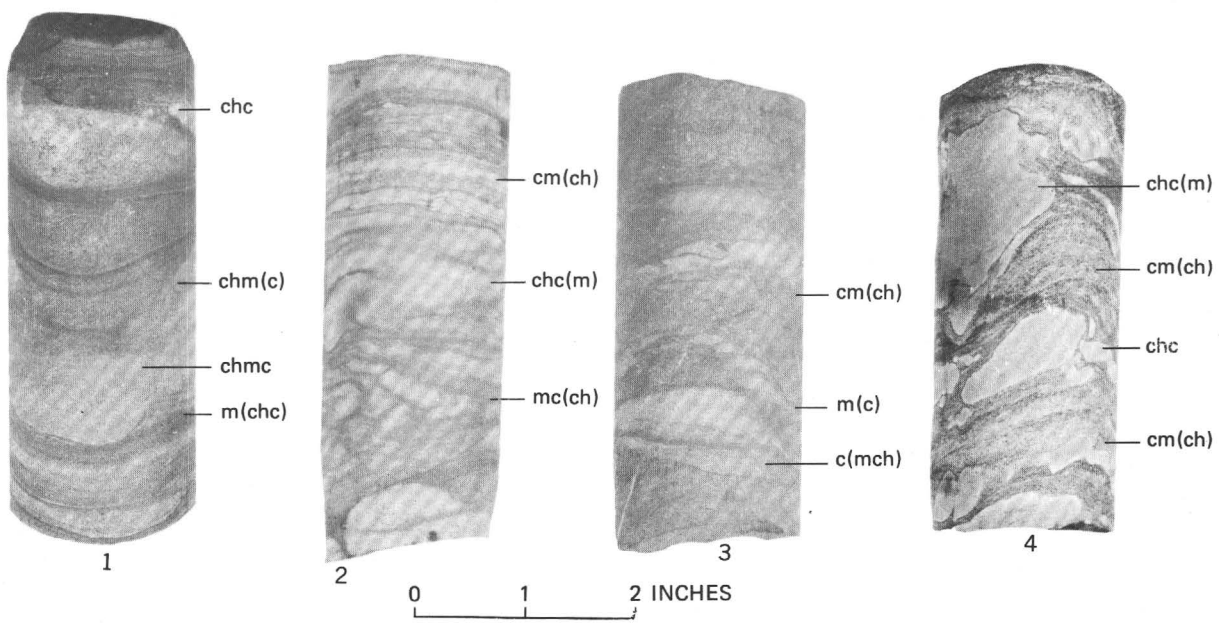

B

No.	Field No.	Drill-hole location (see pl. 8 and p. 146) and footage	Location
A1	JG–141E–66	427, 844 ft	18–47–26
A2	JG–145–66	432, 110 ft	24–47–27
A3	JG–143F–66	431, 534 ft	13–47–27
A4	JG–143H–66	431, 825 ft	13–47–27
B1	JG–143D–66	431, 458 ft	13–47–27
B2	JG–143G–66	431, 534 ft	13–47–27
B3	JG–142–66	431A, 296 ft	24–47–27
B4	JG–144L–66	365, 336 ft	13–47–27
C1	JG–143B–66	371, 299 ft	13–47–27
C2	JG–143C–66	371, 332 ft	13–47–27
C3	JG–143A–66	371, 271 ft	13–47–27
C4	JG–144G–66	365, 258 ft	13–47–27

FIGURE 29.—Drill-core samples of carbonate-magnetite iron-formation. c, carbonate; ch, chert; cl, chlorite; m, magnetite; s, stilpnomelane; (c, ch, cl, m), minor carbonate, chert, chlorite, magnetite.

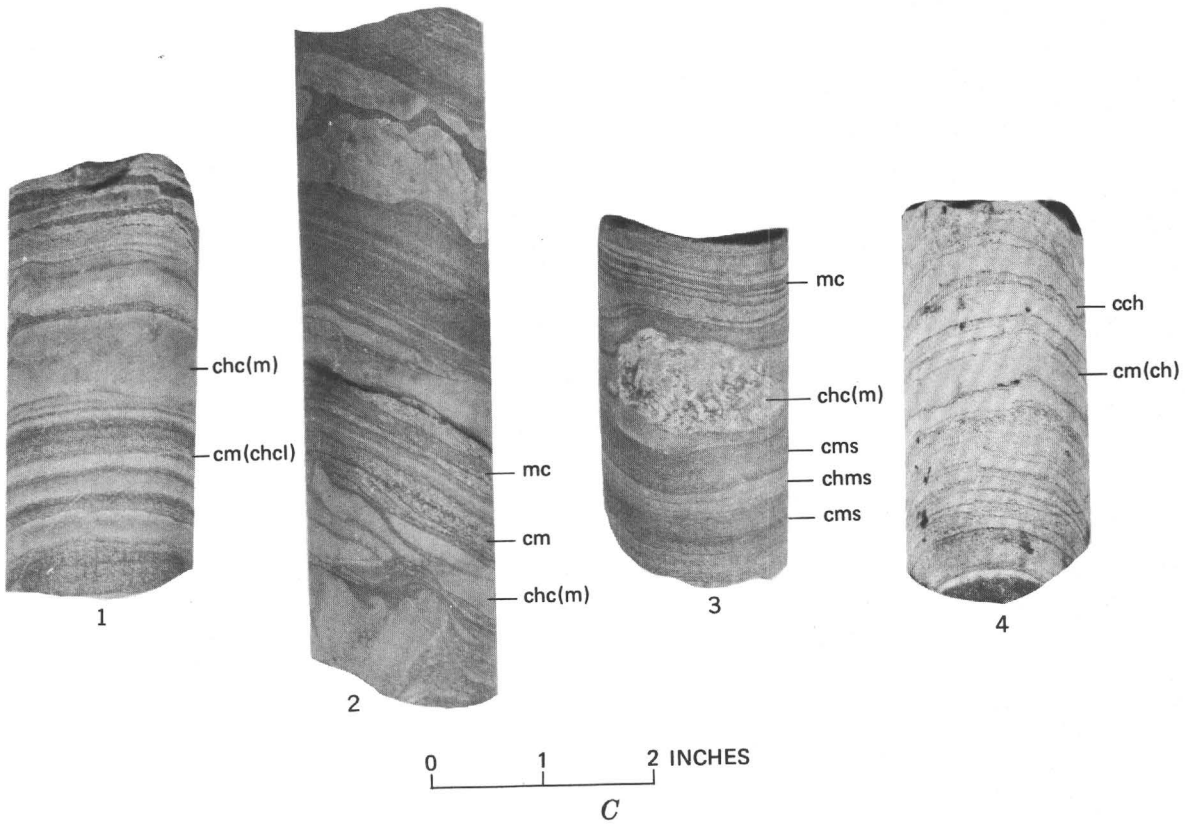

FIGURE 29.—Continued.

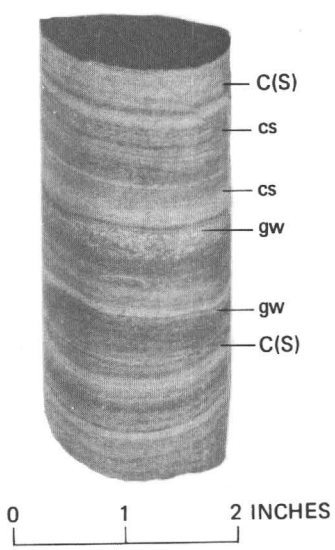

FIGURE 30.—Drill-core sample of carbonate-silicate iron-formation and interbedded graywacke (gw). Iron-formation consists of layers containing mainly carbonate (C) and carbonate-stilpnomelane (cs). Traces of chlorite and minor stilpnomelane (S) are present in most layers of carbonate. Graywacke layers composed of clastic quartz and a matrix of carbonate, chlorite, and stilpnomelane. Minor mineral shown in parentheses. Drill-core sample JG–140K–66. Drill-hole location approximately 1,350N–250W of SE. cor. sec. 27, T. 47 N., R. 26 W. (Drill-hole location 786; sample from 698 ft).

of mixed carbonate and silicate are generally different in granules and matrix.

Near intrusions of diabase in the SE¼ sec. 18, T. 47 N., R. 26 W. (known only in drill core), carbonate-silicate rock has been recrystallized more coarsely in the purer layers of carbonate and silicate than in layers containing mixtures of the iron minerals (figs. 31–33). Mobilization of carbonate is evident from beadlike clustering of carbonate grains along cracks. The mixed layers apparently are composed mainly of stilpnomelane and carbonate but may also contain considerable brownish secondary hematite. Coarse carbonate crystals superimposed on a layer of minnesotaite are bordered by brownish rims of secondarily oxidized minnesotaite (fig. 31*B*). The absence of grunerite suggests that recrystallization was due mainly to water and CO_2 issuing from the diabase rather than to the rise in temperature, which was insufficient to cause dehydration.

MAGNETITE-SILICATE ROCK

Beds of magnetite-silicate rock in the Palmer quadrangle are rarely more than a few feet thick. The thicker of such beds apparently occur mainly between the upper and lower layers of the Partridge Creek sill and between that sill and the Suicide sill

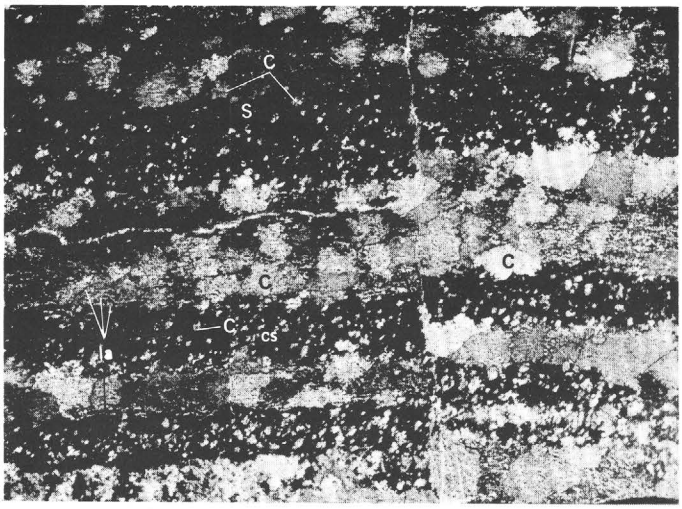

A

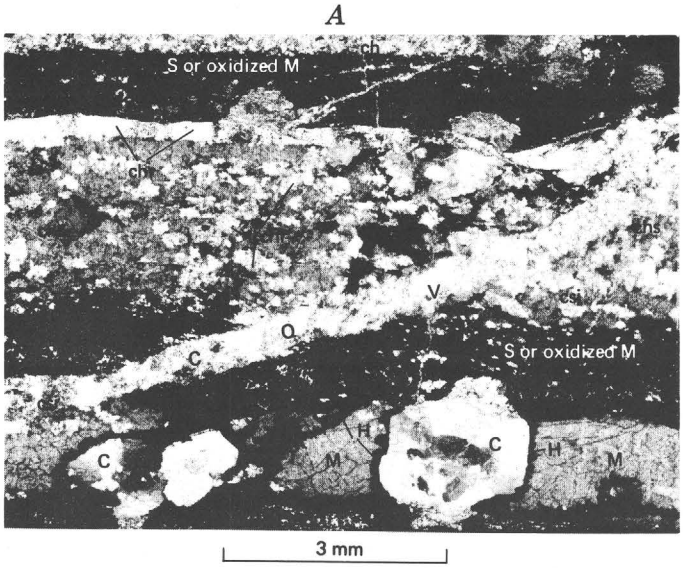

B

FIGURE 31.—Photomicrographs of carbonate-silicate iron-formation. Zone beneath Tracy sill. *A*, Layers of carbonate (C) and carbonate-stilpnomelane (cs). Latter beds also contain minor magnetite (not marked). Thinly spaced primary laminations (la) retained faintly in coarsely recrystallized carbonate-rich layers. Recrystallization probably caused by aqueous solutions from nearby diabase intrusion. *B*, Different area in same thin section as *A*. Layers of carbonate-silicate (csi), chert-silicate (chs), and chert (ch). Silicate mainly or entirely minnesotaite (M). Most carbonate (C) and some chert (chr) has been coarsely recrystallized. Quartz (Q), carbonate, and silicate in vein (V) probably derived from adjacent beds. Stilpnomelane (S) associated with carbonate in some layers. Minnesotaite is secondarily oxidized to brown (opaque) hematite (H) adjacent to contacts of the silicate with carbonate crystals. Opaque layers consist of similar brown material and may be of similar derivation, or may be mainly stilpnomelane. Crossed polarizers. Drill-core sample JG–7C–66, drill-hole location approximately 800N–880W of SE. cor. sec. 18, T. 47 N., R. 26 W. (Drill-hole location 426, sample from 429 ft.)

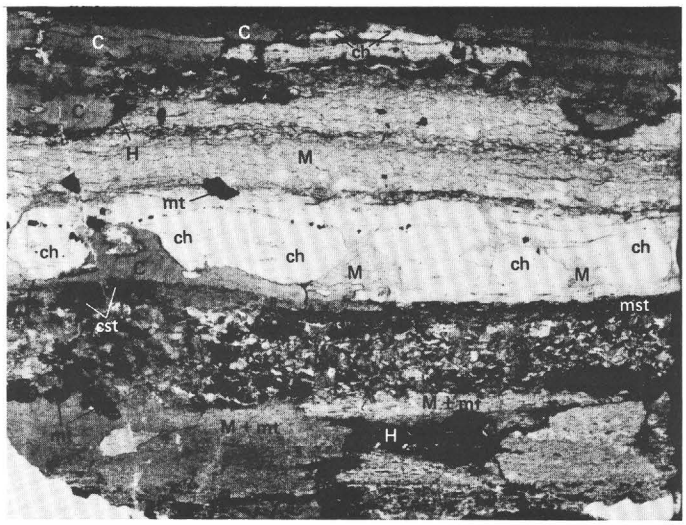

A

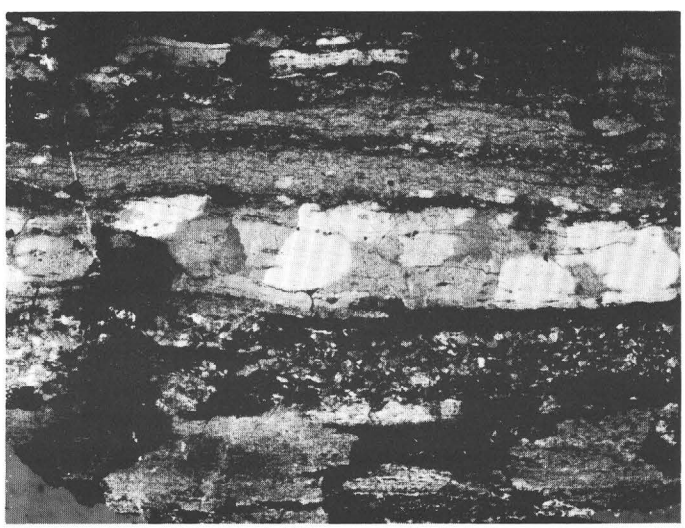

B

FIGURE 32.—Photomicrographs of carbonate-silicate-chert iron-formation. Rock also contains small amounts of magnetite. Zone beneath Tracy sill. *A*, Layers of carbonate (C)–chert (ch)-minnesotaite (M), minnesotaite alone, granular minnesotaite (mg), and magnetite-stilpnomelane (mst). Local patches of carbonate-stilpnomelane (cst), and scattered magnetite (mt). Some carbonate and minnesotaite secondarily oxidized to brown (opaque) hematite (H). Ragged boundaries between carbonate and chert may be stylolites. Plane-polarized light. *B*, Same as *A*. Crossed polarizers. Showing coarsely recrystallized areas having unit extinction in cherty layers. Drill-core sample JG–7D–66, drill hole location approximately 800N–880W of SE. cor. sec. 18, T. 47 N., R. 26 W. (Drill-hole location 426, sample from 500 feet.)

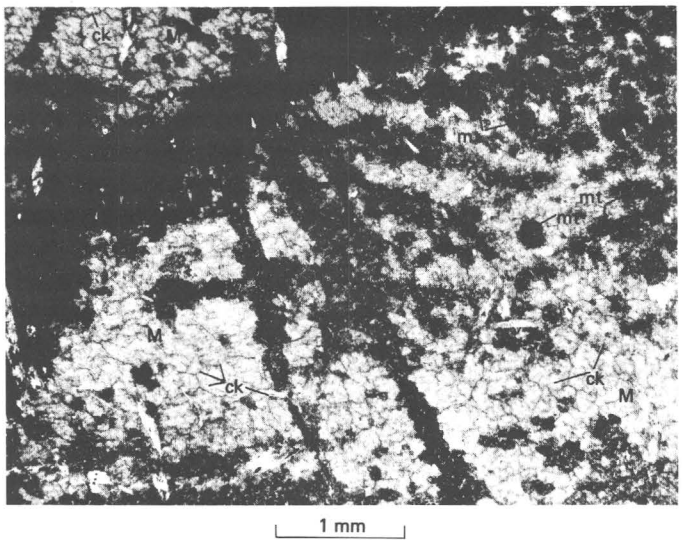

FIGURE 33.—Photomicrograph of minnesotaite-carbonate-magnetite iron-formation, next to contact with metadiabase. Dark lenses, veins, and clumps consist principally of carbonate and are largely or entirely secondary to minnesotaite (M). Crystals of magnetite (mt) associated with some clumps of carbonate. Stilpnomelane needles present in most areas of carbonate. Stilpnomelane, slightly altered to brownish iron oxide, is present along faint irregular cracks (ck) in areas of minnesotaite. Bedding of iron-formation roughly parallel to top of photograph. Veins of carbonate-stilpnomelane branch from primary or secondary lenses lying parallel to bedding. Secondary carbonate, stilpnomelane, and magnetite are probably contact metamorphic effects of adjacent intrusive rock. Secondarily oxidized crack (dark zone) crosses left side of photograph diagonally from near middle of left edge. Plane-polarized light. Drill-core sample JG–6–66, drill-hole location approximately 1,200N–900W of SE. cor. sec. 18, T. 47 N., R. 26 W. (Drill-hole location 423, sample from 214 ft.)

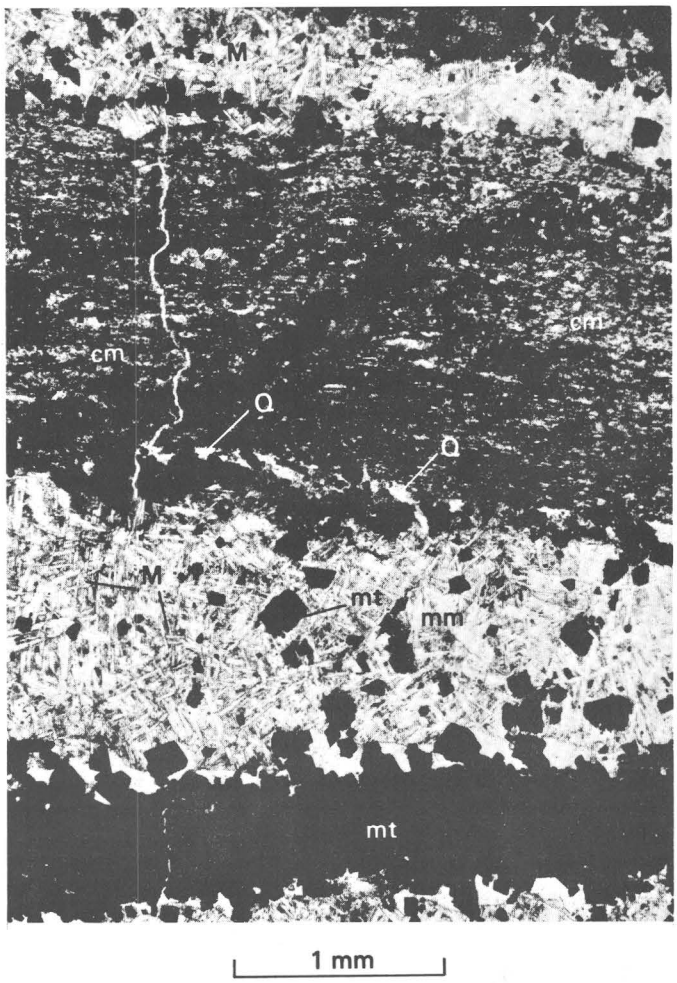

FIGURE 34.—Photomicrograph of magnetite-silicate iron-formation from zone between Summit Mountain and Suicide sills (horizon of Partridge Creek sill). Layers of magnetite (mt), minnesotaite-magnetite (mm), and chert-magnetite (cm). Blades of minnesotaite (M) arranged in characteristic criss-cross pattern. Chert-magnetite layer darkened by opaque dust and tiny shreds of silicate. Recrystallized quartz (Q) is molded around magnetite crystals. Crossed polarizers. Surface sample JG–44–65, approximately 2,100S–1,500E of NW. cor. sec. 18, T. 47 N., R. 26 W.

in the axial part of the synclinorium, but laminae less than one-half inch thick are present in many other parts of the iron-formation. Magnetite-silicate rock consists of monomineralic laminae of magnetite alternating with laminae of nearly pure silicate, and of magnetite crystals sprinkled through silicate aggregates (fig. 34). Minnesotaite and stilpnomelane are the silicates generally associated with magnetite. Chlorite and magnetite characteristically occur together in clastic beds and in some adjacent layers of iron-formation in the Palmer basin and Empire mine.

Granules are common in magnetite-silicate rock; the magnetite in granular layers is virtually restricted to the granules. Granules may be composed of minnesotaite and be rimmed by magnetite, may be intergrowths of magnetite and minnesotaite or magnetite and chert, surrounded by a matrix of minnesotaite, or may be intergrowths of magnetite, stilpnomelane, and chert, surrounded by chert. In a few places, granules are mixtures of minnesotaite and a chlorite, possibly greenalite. Carbonate may be a minor constituent of granules or matrix.

A chemical analysis of magnetite-stilpnomelane-chert iron-formation is listed in table 12, showing about twice as much Fe_2O_3 as FeO, and less than 2 percent Al_2O_3 and CO_2. The rock is rather similar chemically to silicate-bearing magnetite-banded iron-formation in table 8.

CARBONATE-MAGNETITE-SILICATE ROCK

The two-mineral mixed facies of iron-formation already discussed are generally interlayered and gradational with dominant carbonate-magnetite-silicate rock, which forms much of the Negaunee in the axial and Empire-south limb sectors, and in the east half of the Palmer basin. The three-mineral mixed facies may consist of laminae that are virtually monomineralic, containing any of the three minerals or chert, and of laminae containing mixtures of two or all three iron minerals with or without chert (figs. 35–38). Laminae of iron silicate alone

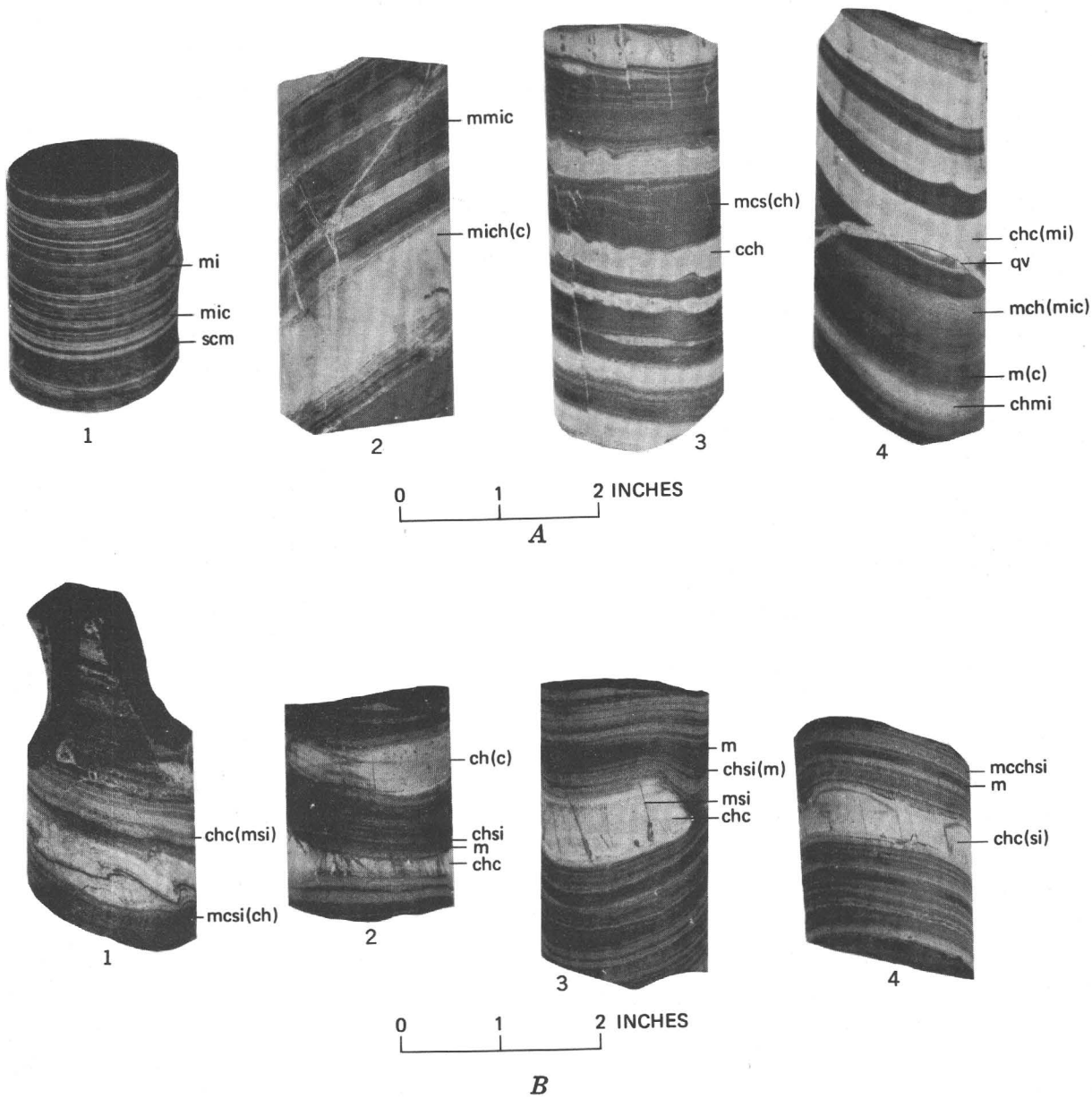

No.	Field No.	Drill-hole location (see pl. 8 and p. 146) and footage	Location
A1	JG–80–66	343, 351 ft	8–47–26
A2	JG–87–66	266(J770), 90 ft	7–47–26
A3	JG–140C–66	786, 537 ft	27–47–26
A4	JG–83A–66	268, 43 ft	7–47–26

No.	Field No.	Drill-hole location (see pl. 8 and p. 146) and footage	Location
B1	JG–140I–66	786, 666 ft	27–47–26
B2	JG–140H–66	786, 594½ ft	27–47–26
B3	JG–140G–66	786, 594 ft	27–47–26
B4	JG–140J–66	786, 666 ft	27–47–26

FIGURE 35.—Drill-core samples of carbonate-magnetite-silicate iron-formation. Comparatively thick, wavy, and podded chert-rich layers are common. c, carbonate; ch, chert; m, magnetite; mi, minnesotaite; qv, quartz vein; s, stilpnomelane; si, silicate; parentheses indicate minor mineral.

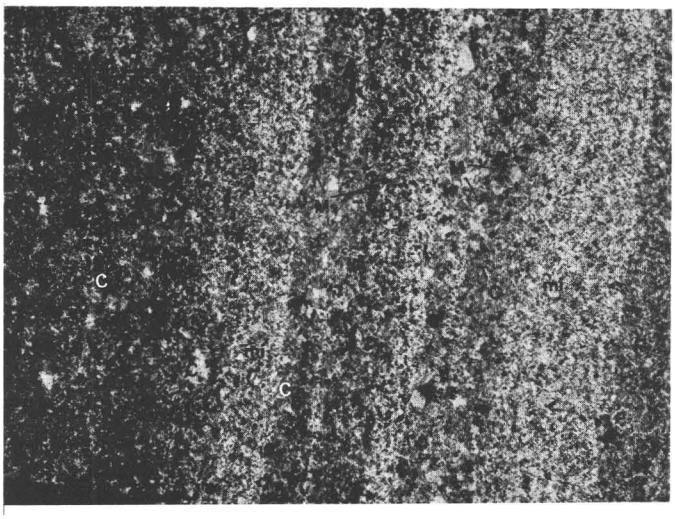

FIGURE 36.—Photomicrograph of carbonate (C)-minnesotaite (mi)-magnetite (M) iron-formation. Note tiny "needles" of minnesotaite and relative concentration of magnetite grains in carbonate layers. Crossed polarizers. Drill-core sample JG–13A–66; drill-hole location approximately 100S–1,280E of NE. cor. sec. 18, T. 47 N., R. 26 W. (Drill-hole location 375, sample from 749 ft.)

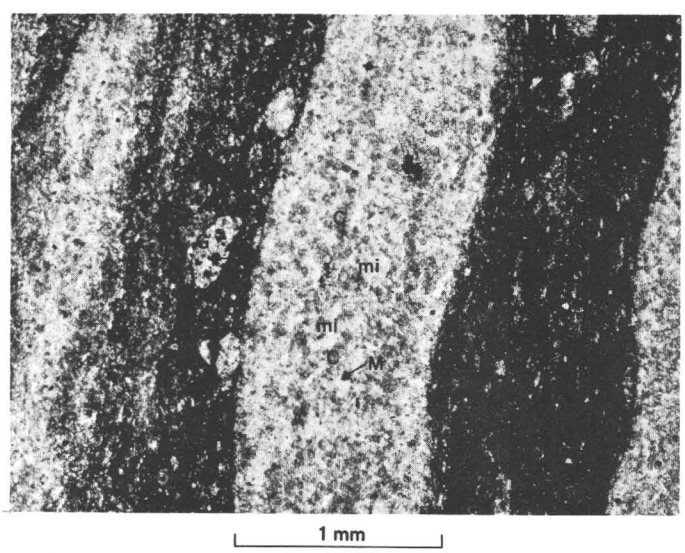

FIGURE 37.—Photomicrograph of carbonate (C)-minnesotaite (mi)-stilpnomelane (S)-magnetite (M) iron-formation. Layers of minnesotaite-carbonate alternate with granule-bearing layers of stilpnomelane-carbonate-magnetite (SCM). Granules (G) consist of carbonate and minnesotaite with or without magnetite. Plane-polarized light. Drill-core sample JG–14G–66; drill-hole location approximately 800S–1,450W of NE. cor. sec. 18, T. 47 N., R. 26 W. (Drill-hole location 382, sample from 766 ft.)

are comparatively rare, and silicate is generally subordinate in amount to carbonate and magnetite.

Granules of minnesotaite, carbonate, carbonate-silicate, magnetite, or magnetite-silicate are present in some layers (for example, figs. 37, 38). Layers may be composed almost entirely of silicate granules, or granules and matrix may be of the same silicate. Commonly, however, granules and matrix are different minerals or mixtures (fig. 37).

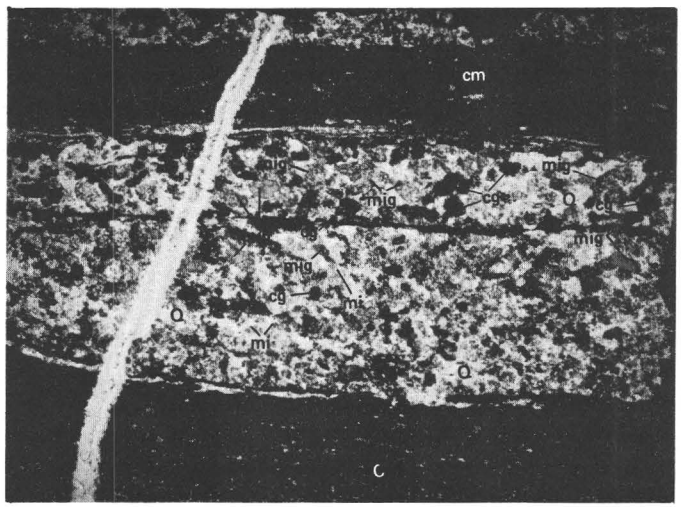

FIGURE 38.—Photomicrograph of carbonate-minnesotaite-magnetite-quartz iron-formation. Granular layers alternate with layers of carbonate (C) and carbonate-magnetite (cm). Granules of minnesotaite (mig) or carbonate (cg) are set in matrix of quartz (recrystallized chert) (Q) and scattered minnesotaite (mi). Vein composed mainly of quartz. Plane-polarized light. Drill-core sample JG–4B–66; drill-hole location approximately 2,430N–850W of SE. cor. sec. 18, T. 47 N., R. 26 W. (Drill-hole location 411, sample from 486 ft.)

Different samples of carbonate-magnetite-silicate iron-formation may differ from one another considerably in chemical composition with variations in the proportions of the iron minerals and chert. Average carbonate-magnetite-silicate iron-formation should have a composition about intermediate between that of carbonate-magnetite iron-formation (table 11, No. 2) and magnetite-silicate iron-formation (table 12).

TABLE 12.—*Chemical analysis and density of magnetite-stilpnomelane-chert iron-formation, Palmer quadrangle*

[Drill-core sample JG–137–66; drill-hole location 430; 1-ft composite sample from 41–51 ft. Standard rock analysis by G. O. Riddle, U.S. Geol. Survey]

SiO_2	37.61	TiO_2	.04
Al_2O_3	1.77	P_2O_5	.05
Fe_2O_3	34.43	MnO	.50
FeO	19.27	CO_2	1.93
MgO	2.21	Cl	.00
CaO	.76	F	.01
Na_2O	.18		
K_2O	.28	Total	100.57
H_2O^+	1.34	Bulk density	3.63
H_2O^-	.19	Powder density	3.54

RIEBECKITE-BEARING ROCK

Riebeckite-bearing iron-formation has been found in two areas in the Palmer quadrangle. Some of the riebeckite-bearing rock also contains aegirinaugite. The principal occurrence is in a stratigraphic zone in the Empire mine, first recognized by Mr. Tsu-Ming Han of the Cleveland Cliffs Iron Co., and described by him in a later section of this report (p. 99–102). The zone is about 20 feet thick three-fourths mile or more long, extends downdip nearly one-half mile, and is associated with a zone of clastic sediment in the iron-formation.

The other occurrence is in the NW¼ sec. 7, T. 47 N., R. 26 W., in a vertical drill hole approximately 2,850 feet north and 1,870 feet west of SW. cor. sec. 7 (drill-hole location 224). The drill hole enters the thick-layered zone of iron-formation about 75 feet stratigraphically below the Tracy sill, and between depths of 340 and 384 feet—nominally about 375–410 feet below the Tracy sill and below the thick-layered zone—cuts iron-formation containing riebeckite in beds and veinlets. Immediately above 340 feet, the drill hole cuts 25 feet of chloritic mafic intrusive rock and also cuts several thinner layers or dikes of similar rock at shallower depths. The intrusive rocks may lie along small faults, as the drill hole is only a short distance south of a major east-trending fault, so the stratigraphic position of the riebeckite-bearing iron-formation is uncertain. It may belong near the bottom of or a little beneath the thick-layered zone described below from immediately beneath the Tracy sill, or it may have been above the Tracy sill and have been faulted into the drilled section. If it is the same zone as in the Empire mine, the inferred position beneath the Tracy sill would be correct.

Mineral assemblages in separate laminae of the riebeckite-bearing iron-formation in the drill hole in the NW¼ sec. 7 consist of:

riebeckite-carbonate-magnetite (includes martite)
riebeckite-chert (quartz)-magnetite (martite) plus minor carbonate
riebeckite-chert-minnesotaite-magnetite (martite)
minnesotaite-chert-magnetite (martite)-plus minor riebeckite, sphene, and carbonate
stilpnomelane-chert-magnetite (martite)-riebeckite
aegirinaugite-riebeckite-carbonate-magnetite (martite)
aegirinaugite-riebeckite plus minor potassic feldspar and brown semi-opaque material, possibly oxidized aegirinaugite
magnetite (martite)-aegirinaugite plus minor riebeckite
magnetite-carbonate plus minor riebeckite

Laminae in the riebeckite-bearing iron-formation are approximately 0.02–8 inches thick. They are alternatively reddish brown, bluish black, or tan-yellow-green, depending on whether the dominant mineral respectively is martitic magnetite, riebeckite, or aegirinaugite. Modes of three samples of riebeckite iron-formation are listed in table 13.

TABLE 13.—*Modes (volume percent) of riebeckite-bearing iron-formation, sec. 7, T. 47 N., R. 26 W., Palmer quadrangle*

	1	2	3
Magnetite (including martite)	22.8	28.6	20.8
Riebeckite	46.0	31.2	19.4
Aegirinaugite		31.3	53.4
Quartz	12.4	Minor [1]	Trace
K-feldspar [2]	11.4	3.5	1.4
Carbonate	5.0	Minor	3.2
Brown iron oxide		4.4	1.8
Minnesotaite-chlorite	2.2	—	—
Sphene	Tr	--	--
Biotite	Tr	--	--

[1] Less than 3 percent.
[2] Mainly microcline, but some is untwinned and has indices of refraction much less than index of balsam and similar to indices of plaid-twinned microcline.

1. JG–102C–66; drill-hole location 224, sample from 363 ft; approx. 2,900N–1,540E of SW. cor. sec. 7, T. 47 N., R. 26 W.
2. JG–102E–66; drill-hole location same as 1, from 371 ft.
3. JG–102F–66; drill-hole location same as 1, from 371 ft.

Martitic magnetite forms 20–30 percent of the material in several samples of drill core, riebeckite forms 19–46 percent, and aegirinaugite is 0 to about 53 percent. Riebeckite has been identified optically, particularly by its characteristic blue color and pleochroism; aegirinaugite has been identified optically and by X-ray.[7] The intermediate index of refraction, N_Y, of the aegirinaugite is 1.78, indicating about 73 percent of the acmite molecule. Layers having dominant riebeckite are well foliated, owing to a strong alinement of riebeckite blades. Layers rich in aegirinaugite, in contrast, have an equigranular fabric, and in these layers, riebeckite is scattered and randomly oriented. Small magnetite octahedra are spread loosely through some layers or may be clustered in lenses. At a depth of 371 feet in the above-mentioned drill hole, several laminae contain rodlike aggregates of martitized magnetite which form open frameworks similar to coarse skeletal octahedral crystals. The areas enclosed by the open frameworks are 0.5–1.5 mm in diameter and are filled with a mixture of riebeckite, carbonate, and aegirinaugite.

Potassium feldspar is minor but deserves mention

[7] X-ray identification by T. E. C. Keith, U.S. Geological Survey.

because it is rare in iron-formation. It is irregularly distributed in single ragged grains of varying size and generally appears to be interstitial to riebeckite, aegirinaugite, or magnetite. Some grains contain inclusions of riebeckite, and some are straddled by separate grains of riebeckite. Most of the feldspar is microcline, identified by characteristic plaid twinning and low indices of refraction relative to balsam; some that is untwinned and has similar low indices of refraction is probably orthoclase.

A few veins of riebeckite or riebeckite and microcline cut the iron-formation in this zone. They appear to represent a selective leaching and redeposition from the wall rock.

Chemical analyses of the iron-formation from sec. 7 containing riebeckite or aegirinaugite are listed in table 14.

TABLE 14.—*Chemical analyses and densities of riebeckite- and aegirinaugite-bearing iron-formation, SW¼ sec. 7, T. 47 N., R. 26 W.*

[Standard rock analysis by C. L. Parker, U.S. Geol. Survey]

	1	2
SiO_2	47.82	47.09
Al_2O_3	5.19	.98
Fe_2O_3	24.29	33.03
FeO	5.40	4.16
MgO	4.40	3.02
CaO	3.49	2.54
Na_2O	2.86	5.96
K_2O	.87	.11
H_2O^+	.68	.56
H_2O^-	.11	.11
TiO_2	.52	.05
P_2O_5	.50	.16
MnO	.82	.70
CO_2	3.40	1.96
Cl	.01	.01
F	.07	.04
S	.02	.02
Subtotal	100.45	100.50
Less O	.04	.03
Total	100.41	100.47
Powder density	3.20	3.46
Bulk density	3.06	3.46

1. JG–1A–68; drill-core composite, riebeckite-bearing iron-formation, from 373 to 390 ft, drill-hole location 224, 2,900N–1,540E of SW. cor. sec. 7, T. 47 N., R. 26 W.
2. JG–1–68; drill-core composite, aegirinaugite-bearing iron-formation, from 363 to 372 ft, drill-hole location 224, 2,900N–1,540E of SW. cor. sec. 7, T. 47 N., R. 26 W.

Iron-formation containing crocidolite or other riebeckite is known from several places in the world, most notably South Africa (Peacock, 1928; Hall, 1930), Western Australia (Miles, 1942; Trendall and Blockley, 1970), and Labrador (Klein, 1966). White (1954, p. 64–66) reported one occurrence from the Mesabi Range, Minn. Peacock and Miles have pointed out that except for sodium content, riebeckite or crocidolite differ little in composition from the host iron-formation, although crocidolite generally has slightly more MgO than the iron-formation. In the Palmer quadrangle also, iron-formation carrying sodium amphibole and sodium pyroxene differs chemically from surrounding iron-formation mainly in its sodium content. The presence of riebeckite and aegerinaugite in the iron-formation therefore poses the problem of accounting for the sodium. The occurrences of sodium amphibole in South Africa and Australia are strikingly similar: sodium amphibole is widespread, is found strictly in beds or lenses in ferruginous or sideritic cherty iron-formation, or is interbedded with thin layers of dolomite, appears to be unrelated to igneous intrusions, and occurs in rocks of very low metamorphic grade that have not been buried at depths greater than a few thousand feet. Trendall and Blockley (1970, p. 271) consider it likely that the sodium of riebeckite in the Brockman Iron-Formation of Western Australia was of sedimentary origin. Milton and Eugster (1959, p. 141) found that sodium amphibole and sodium pyroxene can form at near-surface conditions. Both Peacock and Miles concluded that the crocidolite had formed in primary sodium-rich sedimentary rock by load metamorphism, but neither ventured an explanation for the sodium-rich beds. Klein (1966, p. 295) found a sympathetic distribution of Na, Fe^{+3}, and Mn in the Wabush Iron-Formation, Labrador; all three increased with increases in the oxidation state of the rock. The distribution of the sodium, therefore, is clearly related to sedimentation. Crocidolite on the Mesabi Range, on the other hand, was considered by White to be a contact metasomatic effect of the intrusion of the Aurora diabase sills into the Biwabik Iron-Formation.

The riebeckite and sodium pyroxene in the Negaunee Iron-Formation occur principally in beds, so appear to be related to sedimentation. The cross-cutting veinlets of riebeckite in sec. 7 cut, and appear to be derived from, the bedded riebeckite. Mafic dikes in the iron-formation are not next to, or in any known symmetrical spatial relation with the riebeckite-bearing beds. Metadiabase is present a short distance above the riebeckite-bearing rock in sec. 7, but the spatial relation of the two rocks laterally away from the drill hole is unknown. The apparent lack of a symmetrical relation to intrusive contacts, and the lack of evidence of sodium metasomatism along the innumerable known contacts of mafic igneous rock and iron-formation in the area tend to rule out a metasomatic origin for the riebeckite and aegirinaugite. As in Australia and South Africa, it seems likely that the minerals formed in primary sodium-rich beds.

The riebeckite-bearing beds in the Empire mine are overlain by iron-formation containing many coarse-grained poorly sorted ungraded clastic lenses. If ungraded lenses of wacke or graywacke reflect shallow-water deposition in contrast to graded beds (see p. 40), the sodium-rich iron-formation probably was deposited in fairly shallow water. The nonclastic potassium feldspar associated with the sodium-bearing minerals indicates at least small local concentrations of potassium. The bedded nature of these deposits, the probable shallow-water deposition, the association of sodium and potassium in one place, and, in Australia and South Africa, the association of riebeckite-crocidolite rock with beds of dolomite suggest the deposition of evaporites. Klein (1966, p. 269, 295, 297) stated that the sodium-bearing parts of the Wabush Iron-Formation formed in an environment of high Eh (oxidation-reduction potential) and of high salinity. The restricted occurrences in the Palmer quadrangle indicate that only very local parts of the Negaunee depositional basin became sufficiently isolated to produce evaporites, and only for relatively brief periods.

LITHOLOGY AND STRATIGRAPHY OF IRON-FORMATION IN AXIAL SECTOR OF MARQUETTE SYNCLINORIUM

ZONE BETWEEN TOP OF SIAMO SLATE AND BASE OF TRACY SILL

The 1,100–1,200 feet of iron-formation between the top of the Siamo Slate and the base of the Tracy sill in the axial part of the synclinorium is best studied in the eastern part of secs. 7 and 18, and in the SE¼ sec. 6, T. 47 N., R. 26 W., in workings of the Tracy mine (closed January 1971) and abandoned pits south of Negaunee, and in drill cores. Drill cores are the most satisfactory source of information.

The iron-formation is dominantly a thinly laminated yellow-green, yellow-gray, dark green, and dark-gray rock in the lower 900–1,000 feet of the zone and is dominantly thickly layered and alternating pale green or gray and dark gray in the upper 150–200 feet. The distribution of thickly and thinly laminated iron-formation beneath the Tracy sill is shown in figure 39. Layers are 1/50–½ inch thick (or less) in the thinly laminated rock and ½–4 inches (or more) in the thickly laminated rock. The two varieties correspond in general appearance respectively to the well-known "slaty" and "cherty" varieties of iron-formation of the Gogebic and Mesabi Ranges. Much of the thinly and evenly laminated iron-formation, within about 200 feet above the top of the Siamo, tends to split along bedding into thin plates, and because of its resulting appearance in drill cores has been termed "poker-chip iron-formation" by local geologists. The zone of poker-chip iron-formation occurs in the north half of the axial sector and extends into the north limb of the synclinorium. Beds of poker-chip iron-formation are present on the north limb as much as 8 miles west of the northwest corner of the quadrangle, in drill core near the old Blueberry mine. Some thin laminae in thin section have a regular slight wavy or cusp-like internal structure, with wavelengths of 0.5–2.0 mm and amplitudes of 0.03–0.06 mm, suggestive of local algal growth during deposition.

A distinctive striped variety of the thinly laminated iron-formation is produced by groups of abruptly alternating light and dark layers, 1/10–7/10 inch thick. Zones characterized by striped banding alternate irregularly with zones of thinner bedded iron-formation, particularly from the lower part of the zone of thickly laminated iron-formation down to about the top of the zone of poker-chip iron-formation, about 200 feet above the top of the Siamo Slate. No continuity has been established for zones of striped-banded iron-formation.

Sideritic carbonate is probably the dominant iron mineral, but magnetite and iron silicates are also abundant in the thinly laminated iron-formation.

Beds of green chloritic slate range from a few inches to about 10 feet in thickness in the lower part of the iron-formation, within about 100 feet above the Siamo Slate. Small amounts of clastic quartz are present in the same zone. The contact between the two formations is placed at the base of the transitional zone of iron-formation and slate. Below that, slate and interbedded graywacke extend downward for many hundreds of feet. Clusters of thin laminae of white chert are common in the green slate a few feet below the contact (fig. 15) and are evidence that conditions favoring the deposition of chert alone briefly preceded conditions favoring the combined deposition of chert and iron minerals.

Zone of thick granular and nongranular layers.—The upper 150–200 feet, approximately, of the zone of iron-formation between the Siamo Slate and the Tracy sill is characterized by pale-gray and pale-green layers, ½–4 inches thick. The zone of thick layers extends across secs. 7 and 18, T. 47 N., R. 26 W. The continuity of the zone was first recognized by Joseph J. Mancuso (consultant, Jones & Laughlin Steel Corp., oral commun., 1965). The thick layers commonly are granular and alternate with dark-

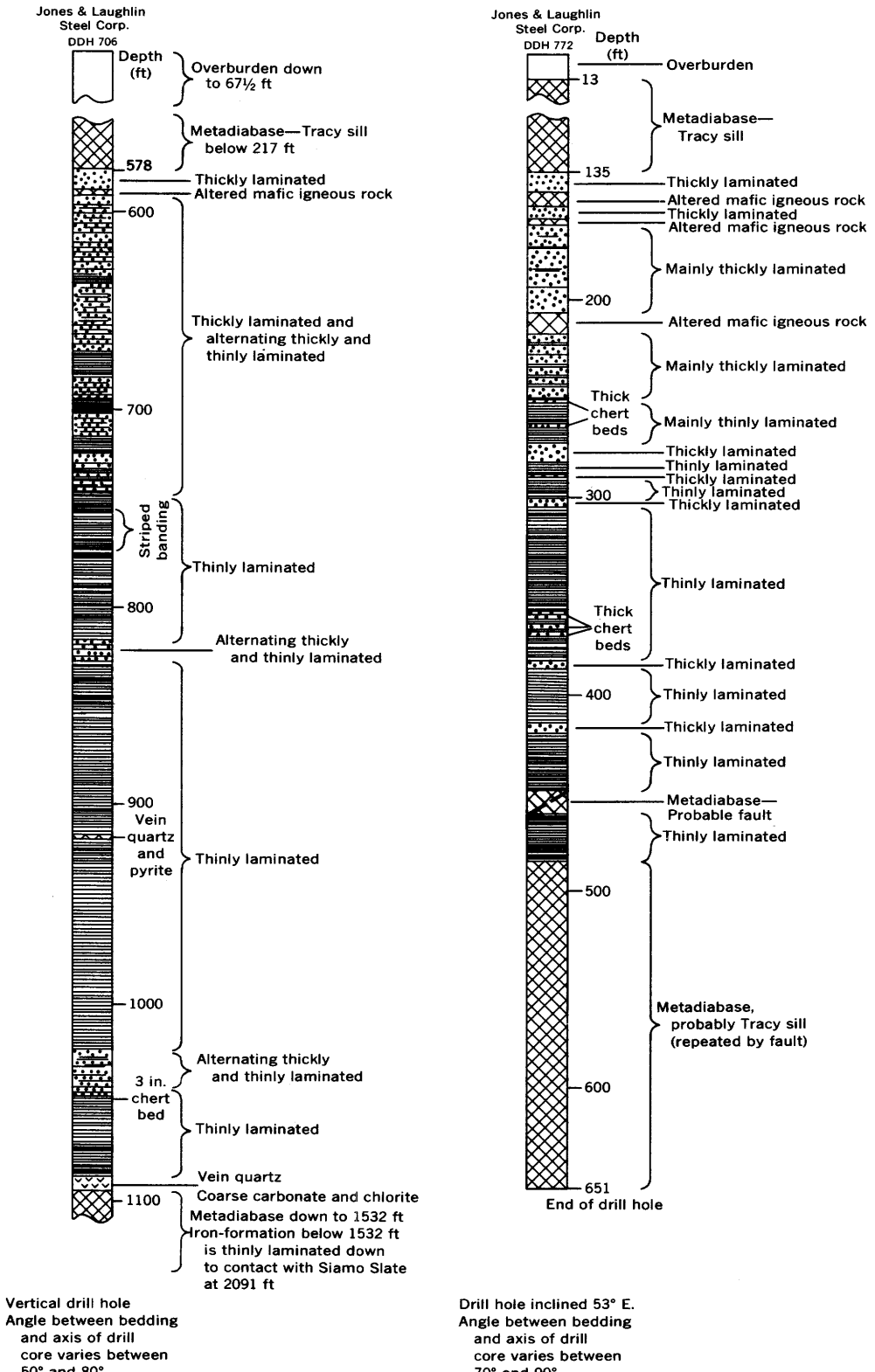

FIGURE 39.—Stratigraphic sections cut by two drill holes showing distribution of thickly and thinly laminated parts of Negaunee Iron-Formation in zone below Tracy sill.

gray or gray-green silicate-magnetite layers of comparable thickness that are internally laminated. The granular iron-formation of this zone has been called "taconitic" by local geologists, after somewhat similar iron-formation in the Mesabi Range, which in that area is a common source of "taconite ore" for pellets (see p. 132, this report). The granular layers are pale green, and their principal mineral is minnesotaite. Thick nongranular layers also are pale green and consist almost entirely of minnesotaite or are gray and contain mainly chert or mixtures of chert and minnesotaite and subordinate carbonate and magnetite. In many thick layers, scattered coarse crystals of carbonate are imprinted on granoblastic mosaics or felted fabrics, and granules of minnesotaite, magnetite, or carbonate may be surrounded by overgrowths of carbonate.

ZONE BETWEEN TRACY AND SUMMIT MOUNTAIN SILLS

The zone between the Tracy and Summit Mountain sills in the axial part of the synclinorium is in the SW¼ sec. 7, and the E½ and SW¼ sec. 18, T. 47 N., R. 26 W.—encompassing the local Belleview and Cliffs Drive areas. A short extension of the zone extends northeast of a faulted segment of the Summit Mountain sill in the NW¼ sec. 7.

The varying thicknesses of iron-formation in the SW¼ of sec. 7 and the N½ of sec. 18—from about 120 to 340 feet—are probably caused by local steplike and low-angle crosscutting by the sills to different levels in the iron-formation. The Tracy sill thins southward across sec. 18. Trends swing from south-southeast to west-southwest across the south-central part of the section, and the thickness of the iron-formation increases to about 600 feet on the bend of the fold in that area. The increased thickness may be a result either of the sills being injected farther apart during syntectonic emplacement or being forced apart by imbrication of the iron-formation during folding.

Data about the zone of iron-formation between the sills have been obtained from numerous exposures in sec. 18, from a few in sec. 7, and from four drill holes in each section.

The iron-formation between the Tracy and Summit Mountain sills is mainly rather uniformly gray-green and thinly laminated, with beds 1/20–½ inch thick. Separate layers, 1–2 inches thick, and narrow zones with thinly striped layers are interbedded irregularly. Most of the thinly laminated iron-formation consists of varying mixtures of sideritic carbonate, minnesotaite, stilpnomelane, magnetite, chert, and grunerite. Chert generally is much subordinate to the iron minerals, and chert-rich laminae are generally few and far between. The thicker beds contain mostly minnesotaite or minnesotaite and magnetite, but some consist of chert or mixed chert and magnetite, and many are granular. Granules typically are aggregates of coarse minnesotaite, fine-grained magnetite, or magnetite and chert, as they are in the thick-layered zone beneath the Tracy sill. Minnesotaite granules generally are set in a mesh of fine-grained minnesotaite; magnetite granules are in a matrix of minnesotaite or chert. Grunerite is most abundant just above the Tracy sill and is attributed to contact metamorphism during emplacement of the sill, as noted above. The iron-formation in the zone overlying the Tracy sill thus is much like the thinly laminated iron-formation in the zone below the sill, except for the presence of grunerite, somewhat thicker layers, and the virtual absence of poker-chip iron-formation.

In the axial part of the synclinorium, the iron-formation between the Tracy and Summit Mountain sills has been only slightly altered by weathering and the postmetamorphic oxidation of iron minerals. Exposed iron-formation generally is covered with a brownish oxidation rind less than an inch thick, in contrast to the throughgoing oxidation of similar near-surface iron-formation between the Tracy sill and the top of the Siamo. Beneath the rind, within about 6 inches to 1 foot of outcrop surfaces, thin brownish seams of oxidized material are common between unoxidized greenish-gray layers. In drill cores, such alterations are seen to reach only a few feet down from the bedrock surface, except along a few relatively permeable granular beds and adjacent beds in the NW¼ sec. 7, where secondary oxidation is deeper.

ZONE BETWEEN SUMMIT MOUNTAIN AND PARTRIDGE CREEK SILLS

The iron-formation between the Summit Mountain and Partridge Creek sills passes across the axial part of the synclinorium in the SW¼ SW¼ sec. 7, and the W½ sec. 18, T. 47 N., R. 26 W. The Partridge Creek sill is separated into two layers southeast of the main body of the sill in sec. 12, T. 47 N., R. 27 W. The stratigraphic interval occupied by the iron-formation and the layers of the Partridge Creek sill near the SW. cor. sec. 7 is about 1,000 feet, of which 70–140 feet is iron-formation beneath the sill (and above the Summit Mountain sill), and about 100 feet is iron-formation between the layers. Because of pinching out of the lower layer and thinning of the upper layer south of the NW¼NW¼ sec. 18, the iron-formation there occupies about 850 feet of the 1,000-foot interval. The upper layer of the sill

is extended from the NW¼NW¼ to the SW¼ sec. 18 by drill data. South of the pinchout of the Partridge Creek sill, structural trends turn southwestward, and the thickness of iron-formation between the Summit Mountain and Suicide sills is drastically reduced, probably by the sills converging across the iron-formation. Data have been obtained from numerous outcrops and six drill holes.

The iron-formation between the Summit Mountain and Partridge Creek sills is rather uniformly dark. Dark-gray to nearly black layers of iron silicate-magnetite, 2–10 inches thick, containing faint internal laminations are separated by light-green gruneritic lenses, one half inch or less thick. The iron minerals in the dark layers in addition to magnetite are mainly minnesotaite and stilpnomelane. Typical assemblages in separate laminae are: minnesotaite - magnetite, magnetite - stilpnomelane, minnesotaite-stilpnomelane-magnetite, minnesotaite or stilpnomelane with carbonate, and nearly monomineralic layers of magnetite or minnesotaite. Much stilpnomelane is of the green ferro variety. Small granules of minnesotaite, carbonate, and mixtures of the two minerals are common, and most carbonate in this zone is in granules. Stilpnomelane, minnesotaite, and magnetite are commonly between granules. Granular layers generally alternate with thinner "slaty" layers, which are of the same material as the granular layers but have abundant anastomosing seams of magnetite subparallel to bedding. Slight flattening of granules parallel to bedding is common; in places, flattening is extreme and produces a strong bedding fissility. Laminae of carbonate and chert are much less common than in underlying parts of the iron-formation. Almost the only carbonate in parts of the Summit Mountain-Partridge Creek belt is found as coarse porphyroblasts in layers of iron silicate; the porphyroblasts are possibly related to mafic intrusions. Quartz (chert) is a minor component; in some lenses, though, it is in coarse aggregates having unit extinction under crossed polarizers, similar to that in figure 32*B*.

Grunerite is more abundant within 50 feet stratigraphically above the Summit Mountain sill. Iron-formation drilled near the east-west centerline of sec. 18, south of the main pinchout of the Partridge Creek sill, consists of roughly 40–50 percent of thin grunerite-rich laminae to about 200 feet above the Summit Mountain sill. Higher in that zone, grunerite occurs sporadically to about 600 feet above the sill.

ZONE BETWEEN PARTRIDGE CREEK AND SUICIDE SILLS

The iron-formation between the Partridge Creek and Suicide sills is near the west edge of sec. 18, T. 47 N., R. 26 W., and in the SE¼ sec. 12 and the E½ sec. 13, T. 47 N., R. 27 W. In the Palmer quadrangle this zone is almost entirely in the axial part of the synclinorium. The maximum thickness of iron-formation in the zone is about 900 feet, in sec. 12. Variations in thickness probably result from crosscutting of the iron-formation by the sills. Southwest of the pinchout of the Partridge Creek sill, the Summit Mountain and Suicide sills converge in the NE¼SE¼ sec. 13 and in the west-central part of sec. 24, probably by cutting across the iron-formation at a low angle. The intervening iron-formation in that area is about 200 feet thick and cannot be correlated specifically with zones above or below the Partridge Creek sill to the northeast.

The iron-formation in the zone between the Partridge Creek and Suicide sills is greenish gray, thinly laminated, and consists largely of layers of felted minnesotaite and minnesotaite plus disseminated magnetite. Carbonate, stilpnomelane, and chert are important constituents of some layers. Other common combinations of minerals consist of chert-magnetite-stilpnomelane, minnesotaite-stilpnomelane-carbonate, and minnesotaite-stilpnomelane-magnetite-carbonate. Granules, 0.1–0.5 mm in diameter, are common in layers of minnesotaite. Near the NE. cor. sec. 13, irregular bulges of the Partridge Creek and Suicide sills cut the iron-formation and approach within 100–150 feet of one another. The intervening thinly laminated iron-formation is composed mainly of coarse elongate carbonate, clumps of stilpnomelane, and scattered blades of minnesotaite. Carbonate forms about 50 percent of the rock. Optically uniform grains and lenses of carbonate are as much as 3.5 mm long and poikiloblastically enclose blades of minnesotaite and stilpnomelane. The carbonate was probably coarsely recrystallized during intrusion of the crosscutting parts of the sills so close to one another, and some of the carbonate may have been introduced, inasmuch as it is considerably more abundant here than elsewhere in the same zone of iron-formation.

"UPPER" ZONE IN JACKSON MINE AREA

Jaspilite is extensively exposed in the north part of the axial sector, in workings of the old Jackson mine near the northwest corner of the quadrangle and in the adjacent hill to the south in the SE¼ sec. 1, T. 47 N., R. 27 W. Goodrich conglomerate overlies jaspilite in three exposures along the north side of the area. The exposures of jaspilite are somewhat isolated from other outcrop areas of the

iron-formation and separated from them by faults; so the stratigraphic position of the jaspilite cannot be determined directly. Iron-formation immediately beneath Goodrich conglomerate nominally would be stratigraphically the highest in the Negaunee, but a considerable thickness of iron-formation may have been removed along the post-Negaunee, pre-Goodrich erosion surface. In the Palmer basin, for example, the stratigraphic distance of Goodrich Quartzite from the base of the iron-formation varies between about 200 and 1,500 feet, and an undetermined part of the variation was caused by erosion. The jaspilite near the northwest corner of the quadrangle is continuous westward into the Ishpeming quadrangle, where mapping by G. C. Simmons (oral commun., 1968), of the U.S. Geological Survey places it at least above the Summit Mountain sill and possibly above the Suicide sill.

The jaspilite is in large open folds, but locally is crumpled, brecciated, and probably displaced along faults now marked by dikes of highly altered metadiabase(?); so its thickness cannot be determined. Continuous exposures on pit walls of the old Jackson mine suggest a minimum thickness of about 100 feet, but this figure may be as much as several hundred feet less than the true thickness.

LITHOLOGY, STRATIGRAPHY, AND PETROLOGY OF IRON-FORMATION AT THE EMPIRE MINE

By Tsu-Ming Han[8]

INTRODUCTION

The Negaunee Iron-Formation in the Empire-south limb sector of the Marquette synclinorium in the Palmer quadrangle is exposed and has been drilled principally at the Empire and New Volunteer mines and immediate vicinity, where it is probably the least metamorphosed part of the formation in the district. Mainly unoxidized iron-formation at the Empire mine in sec. 19, T. 47 N., R. 26 W., strikes into partly oxidized iron-formation at the New Volunteer mine, about one-four mile to the south in sec. 30, T. 47 N., R. 26 W., and southwest in sec. 25, T. 47 N., R. 27 W. Most that is known about unoxidized iron-formation in the sector is obtained from the Empire mine, the largest iron mine in Michigan. There, many small-scale features of the iron-formation can be seen that are not known elsewhere, and evidence has been found of postdepositional changes that added significantly to the magnetite content of the rock. The open pit, which is about three-fourths mile long and as much as one-half mile wide, the freshness of the rock, and thousands of feet of drill core provide a "view" of the iron-formation unparalleled in the eastern half of the Marquette iron district.

The increase in magnetite content of the iron-formation after deposition, by the replacement of sideritic carbonate, involved decarbonation and oxidation. It is arguable whether these changes took place during diagenesis—that is, soon after deposition, prior to or during lithification of the iron-formation, at near-surface temperatures and pressures—or much later during regional metamorphism. Evidence cited below suggests that most of the replacement magnetite is diagenetic.

At the mine, the strike of the iron-formation changes from north-south at the north side of sec. 19 to nearly east-west at the south edge of the section, and the dip varies from about 30° to 40° W. to NNW. (pl. 2). The iron-formation in the mine has been offset by several faults and intruded by 12 or more mafic dikes. Secondary oxidation occurs locally in zones of structural weakness and in places has converted magnetite to martite and caused some enrichment in iron content, particularly near the south edge of the existing pit.

The iron-formation at the mine is of three main lithologic types, as follows (minerals listed in order of relative abundance):

1. Magnetite-chert-carbonate—alternating layers of of magnetite-chert plus some carbonate, and chert plus some carbonate and (or) magnetite (fig. 40*A*). At least some of the magnetite is believed to have formed by the replacement of carbonate.
2. Magnetite-carbonate-silicate-chert — laminae of concentrated magnetite and alternating layers of silicate-chert, carbonate-chert plus some silicate, and carbonate-silicate-chert (fig. 40*B*).
3. Carbonate-chert—laminae of carbonate-chert and chert plus subordinate carbonate, locally containing appreciable magnetite that apparently formed by the replacement of carbonate (fig. 40*C*).

Average chemical analyses of the three main lithologic varieties are listed in table 15. Minor rock types include assemblages of magnetite-hematitic chert plus some clastic layers, riebeckite-magnetite-chert-carbonate plus some clastic layers, aegirinaugite-riebeckite-magnetite-chert-carbonate, magnetite-chert-carbonate-chlorite, and magnetite-chlorite-chert.

The mapped units of iron-formation (pl. 2), are as follows, in upward sequence above the transition zone from Siamo Slate into Negaunee Iron-formation:

[8] Cleveland Cliffs Iron Co., Ishpeming, Mich.

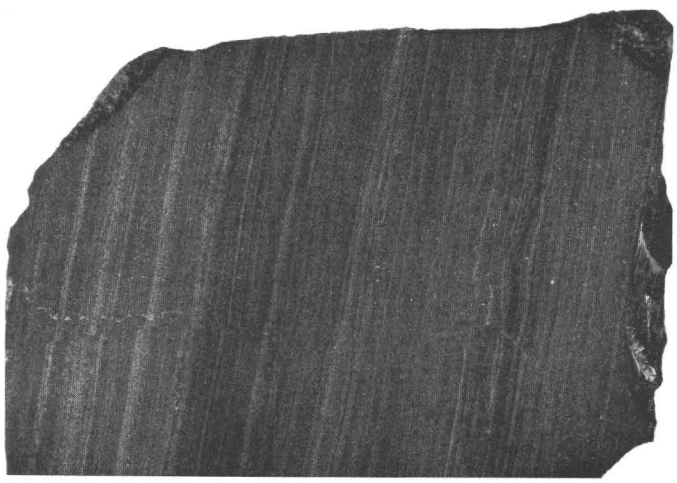

2 cm

A

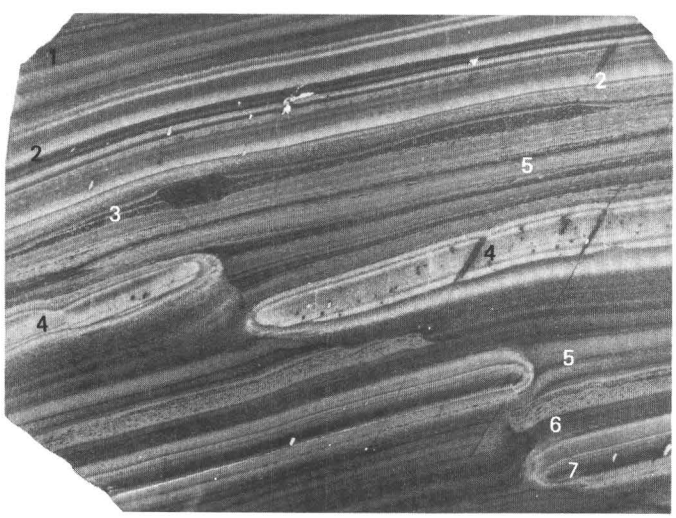

2 cm

B

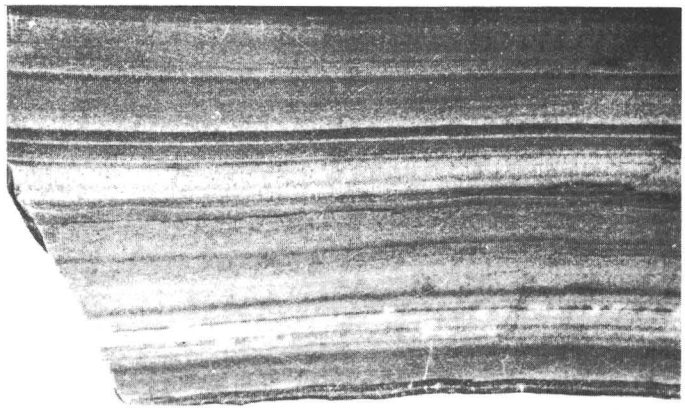

2 cm

C

FIGURE 40.—The three main lithologic types of iron-formation at the Empire mine. Finely ground surfaces. *A*, Massive-looking laminated magnetite-chert-carbonate iron-formation. Laminae mainly magnetite and chert-carbonate. *B*, Thinly layered magnetite-carbonate-silicate-chert iron-formation. 1, alternating laminae of magnetite and silicate-chert; 2, green silicate-chert; 3, clastic lens; 4, chert-carbonate layer (broken) with rim of secondary carbonate; 5, laminated magnetite-rich zone; 6, granular magnetite; 7, brown silicate-chert with rim of carbonate-silicate. Note selective replacement of layers by stilpnomelane along fractures. The veins are stilpnomelane and are noticeably wider in gangue layers than in magnetite-rich layers. *C*, Carbonate-chert iron-formation.

TABLE 15.—*Average chemical analyses of three main iron-formation rock types at Empire mine*

[Analyses by Chemical Laboratory, Cleveland Cliffs Iron Co., listed in separate tables in this section of report L.O.I., loss on ignition]

	Magnetite-chert-carbonate iron-formation		Magnetite-carbonate-silicate-chert iron-formation		Carbonate-chert iron-formation		
	Average of 13 analyses	Standard deviation	Average of 11 analyses	Standard deviation	Composite, 245 feet of drill core	Average of 3 analyses	Standard deviation
SiO_2	46.23	4.35	41.63	11.38	33.63	35.31	15.2
Al_2O_3	1.10	.37	1.18	.93	.50	1.87	1.09
Fe_2O_3	27.84	2.59	23.54	9.51	6.72	2.91	1.03
FeO	17.34	1.68	20.88	4.15	32.81	30.61	6.43
MnO	.44	.13	.52	.40	1.12	1.02	1.13
MgO	1.19	.19	1.68	.62	2.22	3.90	1.81
CaO	.74	.25	1.18	.62	.30	1.70	1.84
TiO_2	[1].11	.04	[2].09	.05	.11	.14	.06
P_2O_5	.09	.04	[3].25	.21	.04	.09	.04
FeS_2	----	----	[4].05	.02	----	----	----
L.O.I.	2.41	1.65	6.27	3.23	18.32	19.59	5.53

[1] Average of 6 analyses.
[2] Average of 8 analyses.
[3] Average of 10 analyses.
[4] Average of 4 analyses.

1. Lower unit of undifferentiated iron-formation (contains some clastic beds). Corresponds to recovery-data zones D and E in figure 41.
2. Unit of magnetite-carbonate-silicate-chert iron-formation (contains some clastic pods and beds). Corresponds to recovery-data zone C in figure 41.
3. Unit of magnetite-chert-carbonate iron-formation. Corresponds to recovery-data zone B in figure 41.
4. Upper unit of iron-formation and interbedded clastic rock. Corresponds to lower part of recovery-data zone A in figure 41.
5. Upper undifferentiated iron-formation. Corresponds to upper part of recovery-data zone A in figure 41.

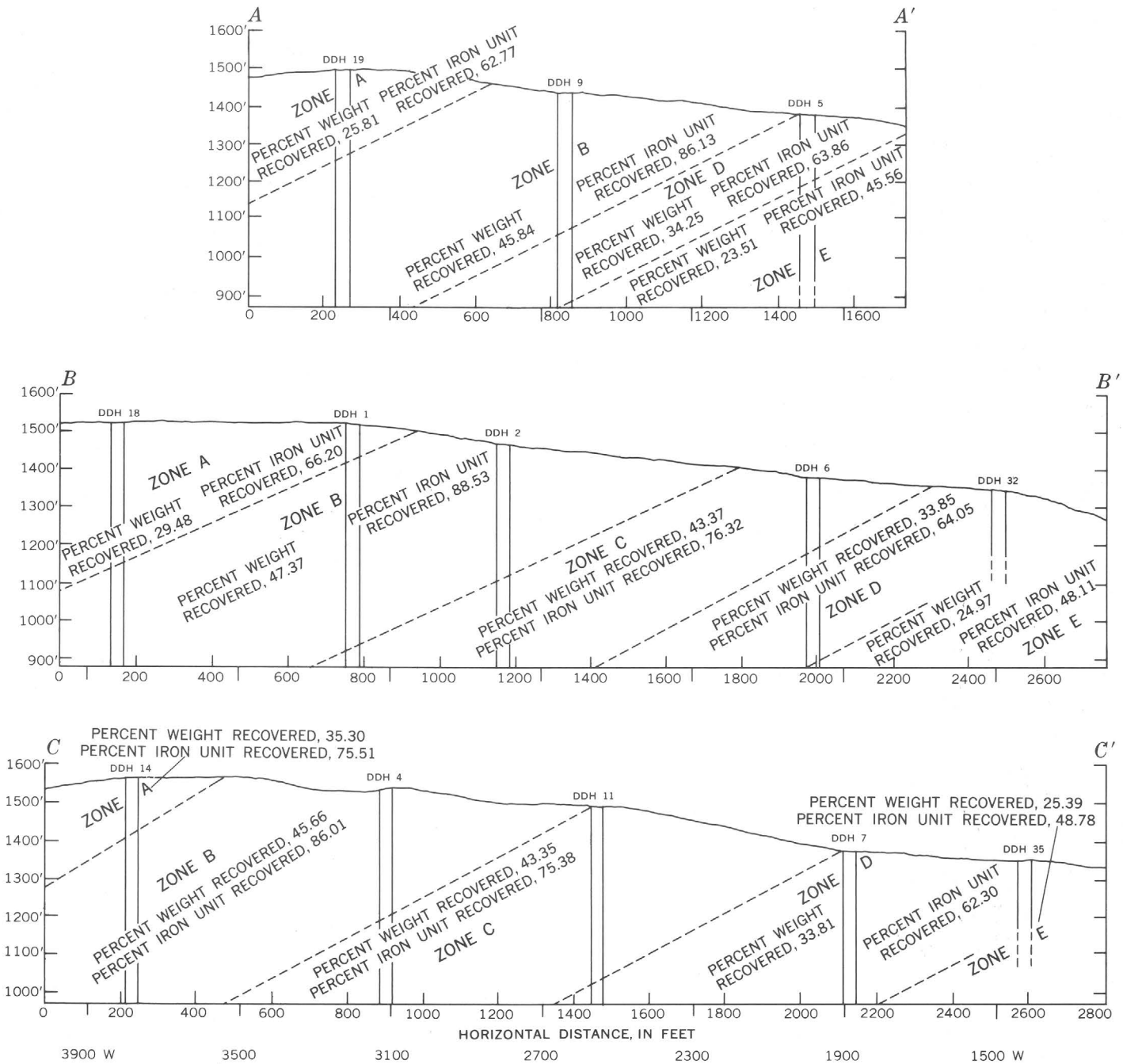

FIGURE 41.—Geologic sections showing recovery data during laboratory beneficiation of ore from various zones of the iron-formation at the Empire mine. Zones are defined in text. Lines of section shown on plate 2; dikes and faults shown on plate 2 are not shown here.

In the following pages a detailed account is given only of units 2, 3, and 4, from which virtually all the taconite ore at the mine is derived. The undifferentiated iron-formation, units 1 and 5, contains substantial amounts of the carbonate-chert variety.

The varieties of iron-formation have characteristic colors, textures, and mineral compositions and can be distinguished by naked eye without much difficulty. They change laterally in thickness and lithology, which makes close stratigraphic correlation almost impossible. Probable primary lateral variations are complicated by secondary changes—magnetitization, carbonatization, silicification, silication,[9] recrystallization, and postmetamorphic oxida-

[9] Silication is the diagenetic or metamorphic growth of a silicate mineral by the combination of silica and suitable cations.

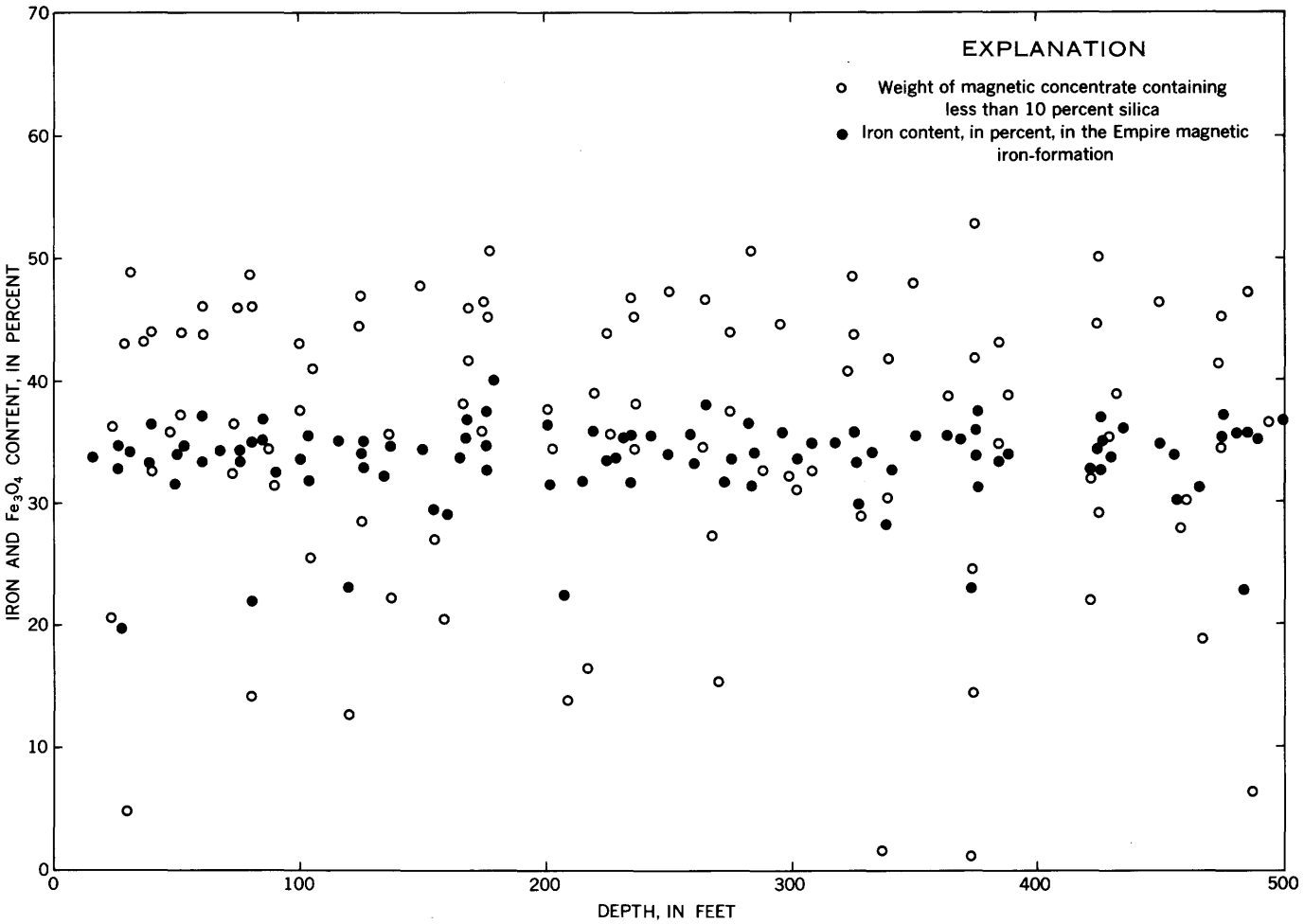

FIGURE 42.—Relationship of iron and magnetite to drill-hole depths, Empire mine.

tion. Changes in thickness and lithology are well shown in three cross sections (fig. 41).

The iron content of the iron-formation at the mine is rather uniform, generally 32–35 percent, whereas concentratable magnetite ranges from less than 1 percent to about 50 percent (fig. 42). The amount of magnetite seems to decrease toward the footwall (fig. 43). In general, magnetite-chert-carbonate iron-formation contains more Fe_2O_3, SiO_2 and less FeO, Al_2O_3, CaO, MnO, CO_2, P_2O_5, and S than does magnetite-carbonate-silicate-chert iron-formation. Both types appear to contain less FeO, Al_2O_3, MgO, and S and more MnO than does the magnetite-silicate-carbonate-chert iron-formation that contains clastic beds.

Magnetite-carbonate-silicate-chert iron-formation (unit 2—recovery-data zone C) and magnetite-chert-carbonate iron-formation (unit 3—recovery-data zone B) are the two principal types of taconite ore at the mine. The size, quantity, distribution, crystallinity, and mineral associations of magnetite all have direct bearings on the grade of concentrates, grindability, weight recovery, and iron-unit recovery. Magnetite grains commonly are 5–30 microns in size and constitute about 40 percent of the iron-formation by weight. Magnetite is liberated from gangue by

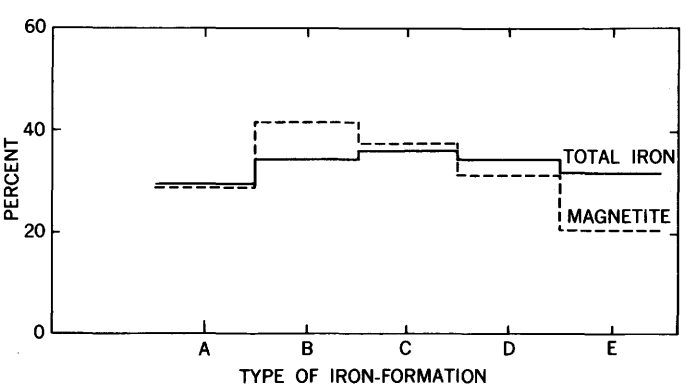

FIGURE 43.—Iron and magnetite content of the various types of iron-formation at the Empire mine. Zones A–E are described in text.

autogenous grinding and pebble milling, concentrated by magnetic separation, and upgraded by siphonizing and flotation. Concentrates contain approximately 67 percent metallic iron. Concentrates are mixed with 0.8 percent bentonite and balled in drums. The "green" balls are processed through a grate-kiln-cooler system. Production is approximately 3,400,000 long tons of hematite pellets per year. Pellets are ½–⅜ inch in diameter but most are not less than seven-sixteenths of an inch; they contain about 65 percent iron and have been the most suitable blast-furnace feed on the current market.

The deposit was explored by the Cleveland Cliffs Iron Company and developed, production beginning late in 1963, by the Empire Mining Company. Cleveland Cliffs is a partner in the Empire Mining Company and operates the mine and pellet plant.

MAGNETITE-CARBONATE-SILICATE-CHERT IRON-FORMATION

Distribution, Thickness, and Composition

The unit of magnetite-carbonate-silicate-chert iron-formation forms a major part of the Empire ore body (pl. 2). It has been wholly or partly cut by diamond-drill holes 1, 2, 4–8, 11, 12, 23, 30, and 72. The contact with the underlying unit of lower undifferentiated iron-formation is poorly defined, but the thickness of magnetite-carbonate-silicate-chert iron-formation may be as much as 850 feet. Toward the southwest and northeast ends of the pit, it seems to grade into magnetite-bearing chert-carbonate iron-formation, which is secondarily oxidized to a martite-earthy hematite-chert rock. The unit is divided into lower and upper zones on the basis of the oxidation ratio computed from chemical analyses of the iron-formation [10] and the ratio of iron-formation to clastic sediments. The lower zone is 400 feet thick or less and contains more carbonate and clastic sediment and less magnetite than the upper zone, which is about 450 feet thick. The lower zone has oxidation ratios of about 58–68, whereas ratios in the upper zone are 69–71.

The unit is characterized by extremely well segregated, homogeneous thin uniform alternating layers of ore and gangue (fig. 40*B*). Ore layers consist, 50–100 percent, of massive, laminated, or granular magnetite. Iron silicate, carbonate, chert, and clastic grains are additional common, but minor, constituents of ore layers. Gangue layers are dominantly green, brownish-gray, or gray-white mixtures of iron silicate, carbonate, chert, magnetite, and clastic sediment. Magnetite generally forms less than 20 percent of such material. Greenish layers are mainly mixtures of minnesotaite and chert, brownish layers are stilpnomelane and chert, gray layers are mainly chert, and gray-white layers are mainly siderite. Layers typically are not more than 2 mm thick. Ankerite in porphyroblastlike crystals is commonly scattered in gangue layers or may be concentrated at the top and bottom of such layers, or as rims on lenses of minnesotaite-chert.

About 95 percent of the magnetite in the unit is in anhedral to euhedral grains ranging in size from 5 to 20 microns (fig. 44*A*). Magnetite, in addition, occurs in euhedral grains embedded in mixtures of silicate-chert, carbonate-silicate-chert, and in quartz veinlets. Scattered coarse grains, granules, and clusters of magnetite contain rounded lamellar grains of magnetite-ilmenite at their centers in many clastic layers and are interpreted as products of the authigenic growth of magnetite around detrital ilmenite-magnetite grains that probably were derived from the erosion of mafic dikes in the lower Precambrian basement.

Microprobe analyses and microscopic examination reveal sideritic and ankeritic carbonate in the iron-formation. The bulk of the carbonate is sideritic. The sideritic carbonate contains minor magnesium, manganese, and very little calcium. Siderite grains range in size from about 0.01 mm to coarse, but most are less than 0.04 mm. Relatively coarse-grained siderite is intergrown with iron silicate in places, forms some discrete layers (veins?), or is a constituent of quartzose veinlets. The ankeritic carbonate contains principally iron and calcium, but also has noticeable magnesium and some manganese. Medium-grained ankerite is uniformly distributed in some chert-silicate layers, and euhedral crystals, 0.1 mm to 1.0 mm in diameter, are scattered through layers of chert-siderite, silicate-chert, chert-siderite-silicate, and magnetite-silicate-chert, in lenses or chain clusters and at interfaces between silicate-chert and magnetite-rich layers. Such crystals commonly have inclusions of chert, and some also contain magnetite, siderite, and iron silicate.

Minnesotaite and stilpnomelane are the principal iron silicates in the unit. Tiny silicate plates or blades commonly transect grains of chert and carbonate (fig. 44*B*). Layers of iron silicate appear to replace chert along boundaries between layers rich in chert and magnetite. In clastic layers, iron silicate may replace parts of quartz grains.

Fibrous hematite is a minor mineral in some jasperlike layers and probably formed by premetamorphic oxidation (weathering?) of iron silicate. Several other occurrences of hematite are known in the unit, associated with quartz veins, or of uncertain origin.

[10] Oxidation ratio is $(2\ Fe_2O_3 \times 100)/(2\ Fe_2O_3 + FeO)$.

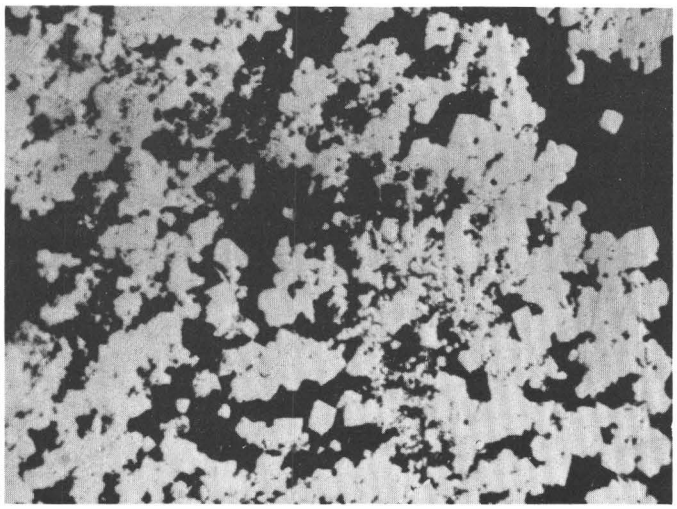

0.04 mm

A

0.04 mm

B

FIGURE 44.—Photomicrographs of polished sections of magnetite-carbonate-silicate-chert iron-formation from the Empire mine. *A*, Magnetite in chert. Note two sizes of magnetite grains. *B*, Parts of layers of silicate-chert (sch) to left and carbonate (C) to right. Carbonate near contact of layers (dashed line) is generally free of chert (ch) inclusions, but contains silicate (si) blades. Magnetite (M) scattered in both layers.

Pyrite, arsenopyrite, pyrrhotite, and chalcopyrite are minor minerals in the unit. Pyrite, the most abundant of the sulfides, is associated with magnetite in places, scattered through some layers of the iron-formation, or rims grains of arsenopyrite. The origin of the sulfides is uncertain.

Chemical analyses of drill core cutting the entire unit of magnetite-carbonate-silicate-chert iron-formation show that the upper zone of the unit contains more silica, Fe_2O_3, MnO, P_2O_5, and FeS_2 than the lower zone and less Al_2O_3, FeO, and MgO, and a lower loss on ignition (L.O.I.) than the lower zone (table 16). Chemical analyses of selected samples of iron-formation (table 17, Nos. 1–6) agree rather closely with the analyses of the upper and lower zones of the iron-formation unit as a whole. Analyses of clastic rock in the iron-formation (table 18), on the other hand, differ markedly from those of the iron-formation, mainly in having much more SiO_2 and Al_2O_3 and much less Fe_2O_3.

CLASTIC SEDIMENT

Silty, sandy, and fragmental clastic material—mainly quartz and pieces of iron-formation—occur in discrete layers or lenses (figs. 40*B*, 45*A*), as small ridges (fig. 45*B*), and as various ball-shaped, disc-shaped, and spiral bodies (figs. 45*C*, *D*), as bead-shaped bodies, and as scattered grains between or within layers of the iron-formation. Balls or discs may terminate stratigraphically downward in spirals (figs. 45*C*, *D*), like the "whirl balls" described by Dzulynski and Walton (1965), which were attributed to the concentration of coarser clastic sediment in vortices of mudflows and preservation by the almost instantaneous stoppage of the flow.

Chemical analyses of the iron-formation and clastic material shown in figure 45*C* are listed in tables 17 and 18, respectively. Some clastic beds are graded. Many are not graded and contain randomly scattered grains of two widely different ranges in size. Detrital magnetite sand is present in most clastic lenses, and grains may have ilmenite-magnetite intergrowths at their cores surrounded by secondary overgrowths of magnetite as noted above. Magnetite clasts are 0.08–0.2 mm in size, in contrast to neighboring sand grains, which typically are larger than 0.15 mm. Granules of iron minerals and chert are common in and largely confined to clastic or partly clastic lenses (fig. 45*E*). Granules commonly are mainly chert, iron carbonate, stilpnomelane, or mixtures of carbonate and silicate. Magnetite granules are less common. Cherty granules may have marginal concentrations of iron silicate.

SHALLOW-WATER FEATURES AND PRECONSOLIDATION SLUMP STRUCTURES

The iron-formation unit contains many features that are attributed to shallow-water deposition, preconsolidation slumping, and differential compaction.

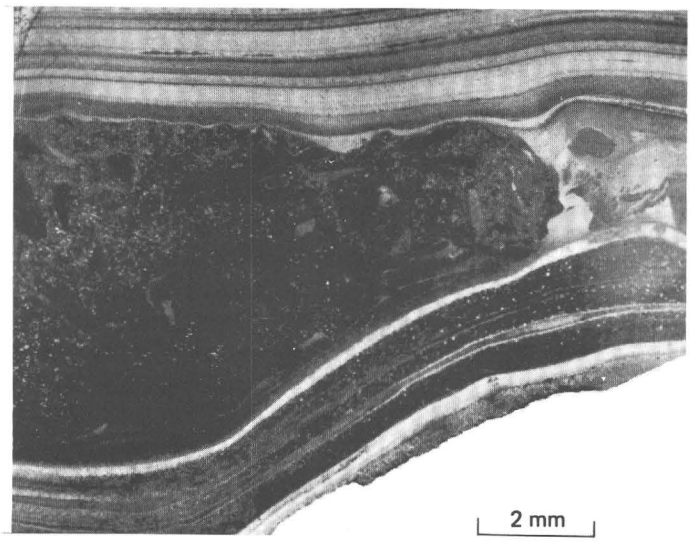

A

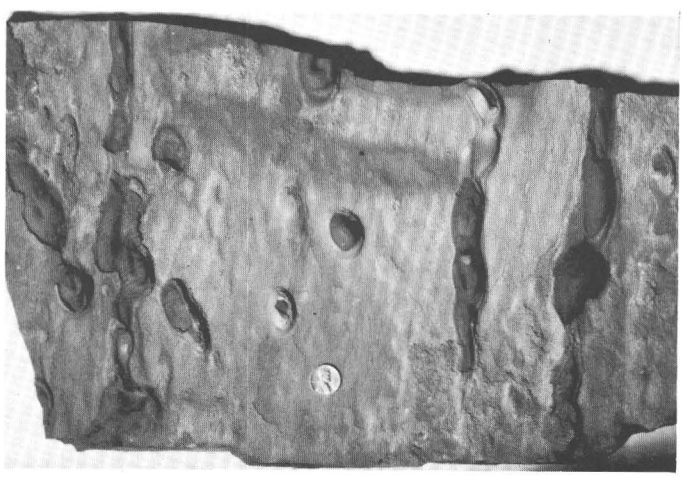

B

C

D

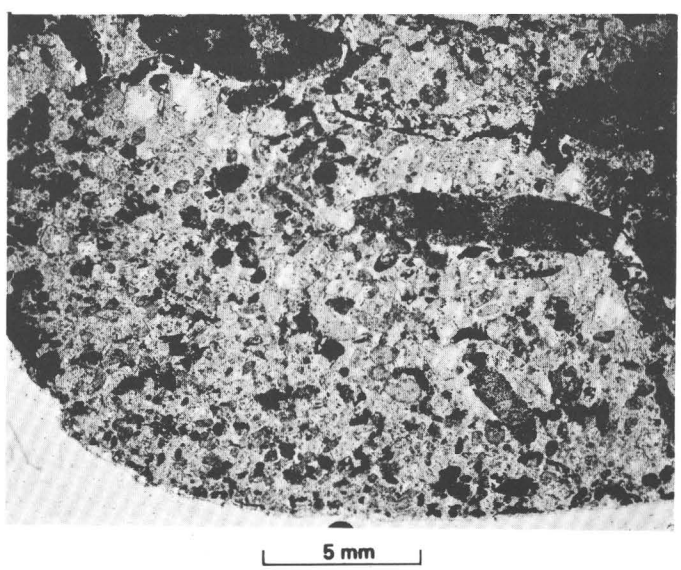

E

FIGURE 45.—Clastic sedimentary features in iron-formation at the Empire mine. *A*, Finely ground surface showing clastic lens within thinly laminated iron-formation. Note platy fragments of iron-formation within the lens. *B*, Bedding surface of silicate-chert iron-formation showing small ridges and pods of clastic material embedded in iron-formation. *C*, Walnut-shaped clastic pod (left) in iron-formation and mold on right made in underlying layer by the pod. Bottom of pod now turned upward. Note spiral, whirl-ball form on near side of pod, originally directed downward into bottom of mold. *D*, Molds of clastic pods in bedding surface of carbonate-chert-silicate layer of iron-formation. Note apparent dragging effect in hook-shaped

F

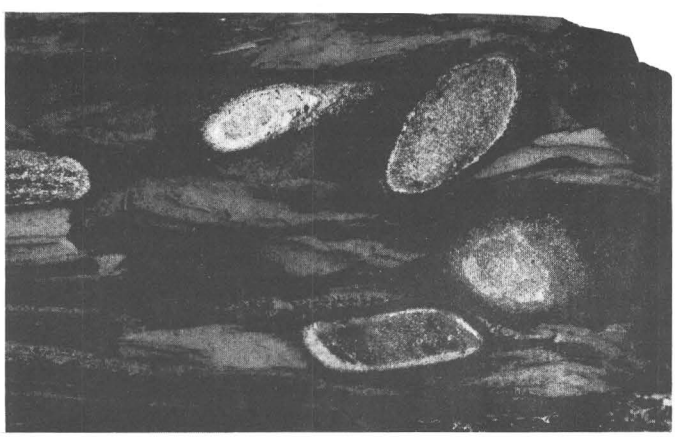

G

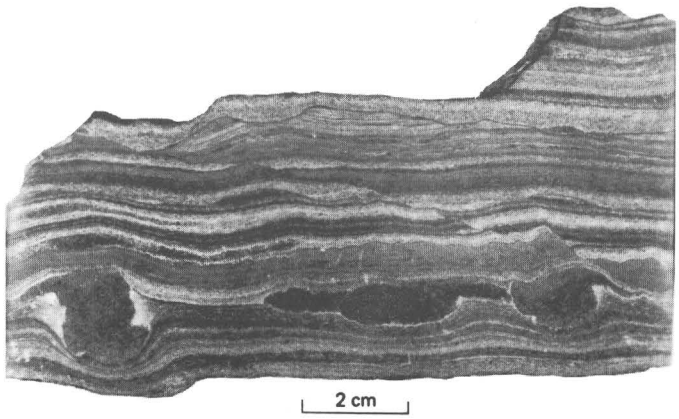

H

I

depression, and spiral-shaped bottom of rightmost depression. *E*, Photomicrograph of thin section showing lens of mixed clastic grains and granules. Plane-polarized light. *F*, Ripple marks or preconsolidation flow ridges in iron-formation. *G*, Finely ground surface showing pebblelike fragments of iron-formation in laminated disrupted magnetite-carbonate-chert-silicate iron-formation. *H*, Finely ground surface showing iron-formation layers arched around clastic pods by differential compaction. Note cut-and-fill structure along some layers. *I*, Finely ground surface showing pull-apart of gangue layer caused by preconsolidation slumping in iron-formation.

The most common are: ripple or mudflow marks (fig. 45*F*); load casts; pebbles of chert-carbonate embedded in disrupted magnetite-rich layers (fig. 45*G*); fragments of iron-formation having a wide range in size, low sphericity, and high roundness; granules of iron-formation minerals in clastic lenses; gentle folds produced by differential compaction of iron-formation over clastic pods or disrupted gangue layers (figs. 45*A*, *H*); ptygmatic veinlets of carbonate-quartz cutting magnetite-carbonate iron-formation; and a host of intraformational slump structures (for example fig. 45*I*). Within the unit, local erosion surfaces are overlain by lenses of granular detrital magnetite. Chemical analyses of a magnetite-rich layer and an enclosed fragment of a chert-carbonate gangue layer are listed in table 19.

TABLE 16.—*Chemical analyses of magnetite-carbonate-silicate-chert iron-formation from diamond-drill holes (DDH), Empire mine*

[Standard wet analyses by Chemical Laboratory, Cleveland Cliffs Iron Co. All samples from drill core. Failure of totals to approximate 100 percent attributed to incomplete measurement of CO_2 by loss on ignition (L.O.I.) and to lack of analyses of alkalies]

	Upper zone							Lower zone				
	DDH 1				DDH 2			DDH 2				
	596–702 ft	702–805 ft	805–898 ft	898–996 ft	310–460 ft	460–600 ft	600–713 ft	713–800 ft	800–902 ft	902–1,006 ft	1,006–1,108 ft	1,108–1201 ft
SiO_2	38.46	36.80	36.56	34.40	37.27	36.46	35.41	34.88	32.45	34.52	38.13	35.53
Al_2O_3	.87	1.11	1.02	1.17	.94	1.10	1.12	1.84	1.68	1.73	2.33	2.41
Fe_2O_3	25.78	27.17	27.68	27.27	25.59	26.88	26.79	24.64	23.62	25.51	23.01	17.59
FeO	22.93	23.03	22.57	23.56	22.64	23.03	23.04	24.66	24.74	23.43	23.04	26.24
MnO	.61	.57	.57	.05	.52	.61	.49	.28	.23	.21	.19	.15
MgO	1.44	1.48	1.67	1.86	1.64	1.70	1.85	1.89	2.38	1.91	2.18	2.20
CaO	.67	1.48	1.90	2.44	1.96	1.91	2.05	2.11	2.64	1.53	1.41	1.24
P_2O_5	.12	.17	.20	.15	.13	.19	.16	.14	.14	.11	.12	.16
FeS_2	.05	.07	.07	.08	.04	.08	.12	.05	.05	.05	.05	.08
L.O.I.	5.26	4.51	5.11	6.23	6.08	5.44	6.62	6.46	8.64	6.50	6.15	7.68
Total	96.19	96.39	97.35	97.66	96.81	97.40	97.65	96.67	96.58	95.50	96.56	93.28
Magnetite	37.36	39.37	40.12	39.52	37.09	38.96	38.83	35.71	34.23	36.97	33.34	25.49
Oxidation ratio	69.22	70.23	71.04	70.18	69.33	70.01	69.93	66.65	65.63	68.53	66.64	57.28
CaO/MgO	.47	1.00	1.14	1.31	1.20	1.12	1.11	1.12	1.10	.80	.65	.56

TABLE 17.—*Chemical analyses of selected specimens from magnetite-carbonate-silicate-chert iron-formation, Empire mine*

[Standard wet analyses by Chemical Laboratory, Cleveland Cliffs Iron Co. Failure of totals to approximate 100 percent attributed to incomplete measurement of CO_2 by loss on ignition (L.O.I.) and to lack of analyses for alkalies]

	1	2	3	4	5	6	7	8	9	10	11
SiO_2	37.70	31.00	35.92	36.22	41.37	34.10	62.38	37.66	43.41	66.64	31.54
Al_2O_3	.50	.88	1.33	2.22	3.56	1.39	.22	.74	1.29	.31	.59
Fe_2O_3	19.73	26.74	25.63	24.44	17.47	24.88	1.14	32.31	33.46	15.87	37.32
FeO	23.29	24.96	23.58	21.58	22.94	24.44	18.27	21.87	15.82	10.55	22.39
MnO	.65	.57	.45	.25	.18	.49	1.68	.49	.09	.39	.39
MgO	2.20	2.40	1.80	2.28	2.21	2.15	1.90	.95	1.00	.81	.81
CaO	.97	1.53	1.92	2.47	1.46	1.14	.90	.43	.62	.30	1.21
TiO_2	.12	.14	---	---	---	.14	.04	.06	.17	.01	.05
P_2O_5	.33	.25	.15	.12	.16	.14	---	.26	.08	.14	.84
FeS_2	---	---	.06	.04	.08	---	.03	---	Trace	---	---
L.O.I.	9.20	8.20	5.97	9.29	5.83	7.57	12.36	2.66	1.99	3.80	2.18
Total	94.69	96.67	96.85	98.91	95.26	96.44	98.92	97.43	97.93	98.82	97.32
Magnetite	28.59	38.75	37.14	35.42	25.31	36.05					
Oxidation ratio	62.88	68.18	68.49	69.37	60.37	67.06	11.09	74.71	80.88	75.05	76.92
CaO/MgO	.44	.64	1.07	1.05	.66	.53	.47	.45	.62	.37	1.49

1. Interlaminated green minnesotaite-chert and gray chert-carbonate iron-formation.
2. Green minnesotaite-chert iron-formation with some clastic lenses.
3. Interlaminated magnetite-rich and silicate-chert iron-formation.
4. Whitish-gray carbonate-rich iron-formation (drill core).
5. Magnetite-carbonate-silicate-chert iron-formation with clastic lenses.
6. Pit sample of magnetite-carbonate-silicate-chert iron-formation.
7. Layer of silicate-carbonate iron-formation (contains molds made by clastic pods). Sample shown in fig. 45*D*.
8. Layer of magnetite-silicate iron-formation underlying silicate-carbonate layer of analysis 7.
9. Iron-formation host for ball-shaped clastic body shown in fig. 45*C*.
10. Layer of chert-fibrous hematite-carbonate iron-formation underlies clastic lens shown in fig. 45*A*.
11. Layer of magnetite-silicate-chert-carbonate iron-formation overlying clastic lens shown in fig. 45*A*.

TABLE 18.—*Chemical analyses of clastic sediment in magnetite-carbonate-silicate-chert iron-formation, Empire mine.*

[Standard wet analyses by Chemical Laboratory, Cleveland Cliffs Iron Co. Failure of some totals to approximate 100 percent attributed to incomplete measurement of CO_2 by loss on ignition (L.O.I.) and to lack of analyses for alkalies]

	1	2	3	4	5	6
SiO_2	43.78	56.54	49.16	46.27	79.21	69.54
Al_2O_3	5.53	6.76	6.99	8.44	1.46	1.28
Fe_2O_3	9.72	4.15	7.58	5.00	2.43	5.53
FeO	25.60	23.54	23.54	24.44	8.88	12.87
MnO	.15	.09	.72	.09	.09	.39
MgO	2.50	2.25	2.01	3.40	1.65	1.60
CaO	1.20	.56	.38	.17	1.30	.44
TiO_2	.18	.31	.28	.45	.24	.19
P_2O_5	.04	.02	.04	.04	.05	.02
FeS_2	.03	.05	.33	.01	Trace	---
L.O.I.	6.28	5.05	4.87	6.40	3.86	6.57
Total	95.01	99.32	95.90	94.71	98.97	98.43
Magnetite	14.08	6.01	10.98	7.25		
Oxidation ratio	43.16	26.07	39.17	29.04	35.37	46.22
CaO/MgO	0.48	.25	.19	.05	.79	.27

1. Pit sample from large graded lens.
2. Same lens as analysis 1, bottom of lens.
3. Clastic lens containing tourmaline and iron silicate, from 1,050 ft in diamond-drill hole 1.
4. Clastic lens containing iron silicate, from 900 feet in diamond-drill hole 4.
5. Ball-shaped clastic body shown in fig. 45*C*.
6. Clastic lens shown in fig. 45*A*.

TABLE 19.—*Chemical analyses of magnetite-rich layer and enclosed fragment of chert-carbonate gangue layer, Empire mine*

[Standard wet analysis by Chemical Laboratory, Cleveland Cliffs Iron Co. L.O.I., loss on ignition. Reason unknown for total of 1 not approximating 100 percent]

	1 Magnetite-rich layer	2 Chert-carbonate fragment
SiO_2	31.94	74.42
Al_2O_3	.75	.50
Fe_2O_3	38.89	.98
FeO	22.77	12.74
MnO	.28	.73
MgO	.85	1.45
CaO	.07	.23
TiO_2	.05	.04
P_2O_5	.01	.02
L.O.I.	1.31	8.12
Total	96.92	99.23

Peculiar rodlike bodies of iron silicate-chert, carbonate-chert, or magnetite-chert-silicate, generally similar in composition and texture to host layers, may be of organic origin but could be merely inorganic growths along cracks. These bodies were discovered by Wygant and Mancuso (1969), who kindly lent me their material for examination. The rodlike features generally are confined to gangue layers, across which they may be inclined at large angles.

Recrystallization and Replacement

The magnetite-carbonate-silicate-chert iron-formation has been thoroughly recrystallized since deposition and contains many small-scale replacement features that I interpret to be results of diagenesis or low-grade regional metamorphism. The replacements constitute evidence for a wide range of postdepositional chemical reactions within the iron-formation. Chemically deposited silica has recrystallized to quartz grains that are mainly in the size range 10–40 microns. Magnetite grains are as small as 2 microns, but most are 15–25 microns and are believed to have recrystallized from grains comparable to the smaller grains. The dominant fine-grained siderite is probably primary or diagenetic; coarser siderite is clearly recrystallized from such fine-grained carbonate. Aggregates of relatively coarse siderite may surround "islands" of fine-grained siderite, and individual relatively coarse siderite crystals may contain abundant chert inclusions, presumably remnants of primary chert. Some coarser siderite grains or aggregates appear to have replaced chert, iron silicate, or magnetite (fig. 46*A*).

The iron-formation unit contains much evidence of the growth of iron silicate at the expense of earlier minerals. Minnesotaite or stilpnomelane commonly is in rims or borders on chert-rich lenses or layers; "islands" of magnetite-carbonate-chert may be enveloped by silicate-carbonate-chert, and plates or blades of iron silicate grow into and across carbonate, chert, and clastic quartz (figs. 44*B*, 46*B*). Chert granules and quartz clasts may be replaced by iron silicate (figs. 46*C*, *D*). I interpret the silicate rings within the quartz grains (fig. 46*D*), as having formed by reactions between the quartz and iron hydroxide coatings on original quartz clasts, after the enlargement of the iron hydroxide-coated clasts by overgrowths of secondary quartz. Some granules that consist entirely of silicate may be replaced chert granules or may be completely replaced grains of clastic quartz (figs. 46*C–F*). Iron silicate blades commonly have grown across chert or carbonate with a decussate or latticelike pattern (figs. 46*G*, *H*) that clearly is secondary to the chert and carbonate.

Carbonate is present as relatively coarse euhedral grains of ankerite. These grew during diagenesis or regional metamorphism by replacement of siderite and by carbonatization of chert, iron silicate, or magnetite, all of which had recrystallized earlier and are commonly found as relicts within the ankerite grains. Such ankerite is irregularly distributed in grains, clusters, and layers. Ankerite layers probably were derived from layers of siderite. Coarse ankerite grains are more susceptible to secondary oxidation than coexisting siderite and may be completely replaced by hematite in the midst of fresh siderite. Another result of carbonatization is siderite-rich shells around fragments and the broken ends of cherty layers (fig. 40*B*).

Most magnetite in the unit probably formed by recrystallization and consolidation of earlier finer grained magnetite. Remobilization of magnetite is shown by the presence of magnetite porphyroblasts, and in some clastic layers, by magnetite overgrowths on magnetite-ilmenite grains. In places, magnetite clearly has replaced layers rich in iron silicate, leaving "islands" of the silicate-rich material. Such evidence for the conversion of other iron minerals into magnetite is sparse in this unit, and perhaps only a small amount of magnetite in the unit was thus derived. However, in the overlying unit, as detailed below, similar magnetitization was an important process.

Magnetite-Chert-Carbonate Iron-Formation

Distribution, Thickness, and Composition

The unit of magnetite-chert-carbonate iron-formation overlies the magnetite-carbonate-silicate-chert unit, is about 350–400 feet thick, and extends across the mine from the southwest to the northeast part of sec. 19 (pl. 2). Iron-formation from this zone is the most favorable material for beneficiation and a major source of taconite ore in the mine. The rock is generally gray and fine grained and is made up of magnetite-rich and chert-rich layers. Locally in about the upper 150 feet of the unit a few lenses of magnetite-hematitic chert-carbonate iron-formation contain riebeckite and aegirinaugite. Such material also is common in the lower part of the overlying unit of interbedded iron-formation and clastic rock. Contacts between layers in the magnetite-chert-carbonate unit tend to be somewhat indistinct, the distinctness being influenced largely by the distribution and concentration of magnetite. Clastic seams occur between the magnetite-rich and chert layers in places. Layers vary widely in thickness from about 5 to 35 mm. Intraformational deformation is a

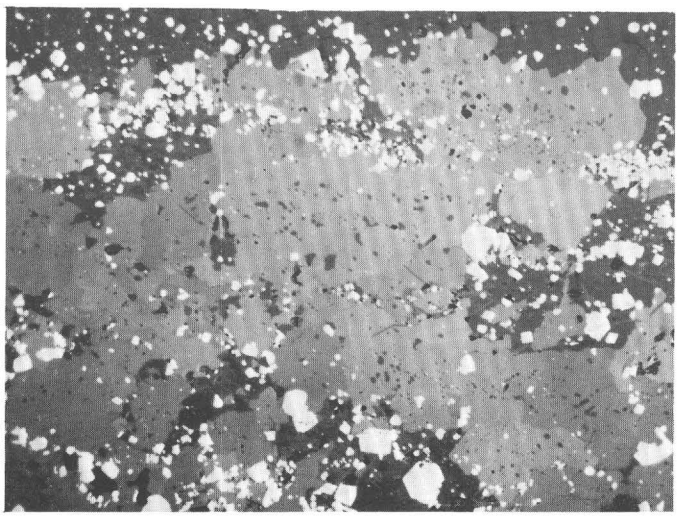

A

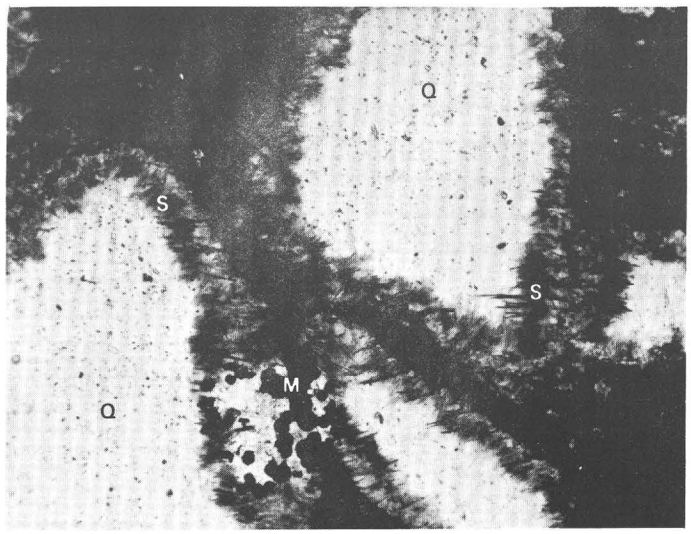

C

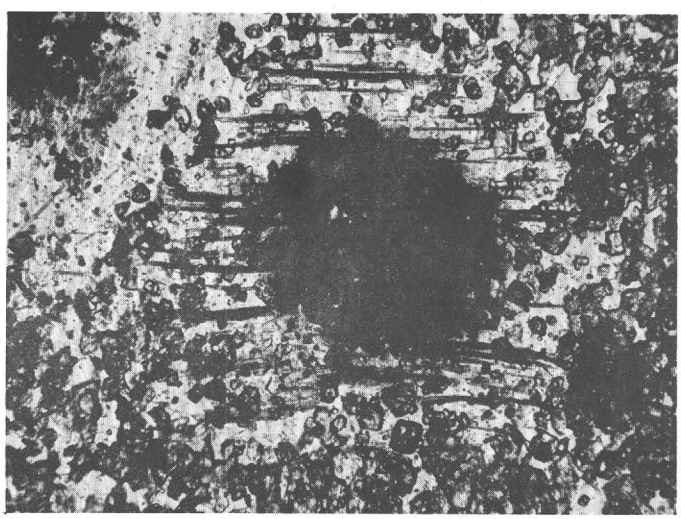

B

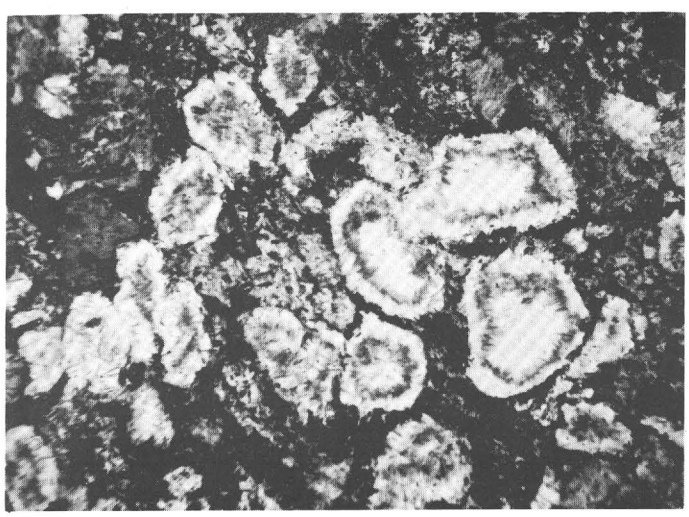

D

FIGURE 46.—Photomicrographs showing replacement features in magnetite-carbonate-silicate-chert iron-formation and associated rocks at the Empire mine. *A*, Polished section showing partial replacement of magnetite layer by siderite. Magnetite (white) is heavily concentrated in areas of silicate-chert (dark gray) and is sparse in areas of siderite (light gray). *B*, Thin section showing parallel blades of stilpnomelane overprinting siderite-chert assemblage and projecting into granules of siderite-stilpnomelane (dark), possibly along incipient fractures. Plane-polarized light. *C*, Thin section showing peripheral replacement of quartz (Q) clasts by stilpnomelane (S) in graywacke. Matrix of graywacke consists of fine-grained stilpnomelane plus carbonate and magnetite (M). Plane-polarized light. *D*, Thin section showing silicate rings replacing parts of clastic quartz grains in a clastic lens. Plane-polarized light. *E*, Thin section of graywacke showing

characteristic feature. Clastic dikes and ptygmatic-like quartz veinlets occur in places. Replacements and alterations of diagenetic and metamorphic origin are common in the iron-formation throughout the mine. Diagenetic replacements in particular had a significant effect in enriching the iron-formation in magnetite.

In the lower part of the zone of magnetite-chert-carbonate iron-formation, the rock is dark gray, straight-banded, compact, and massive looking (fig.

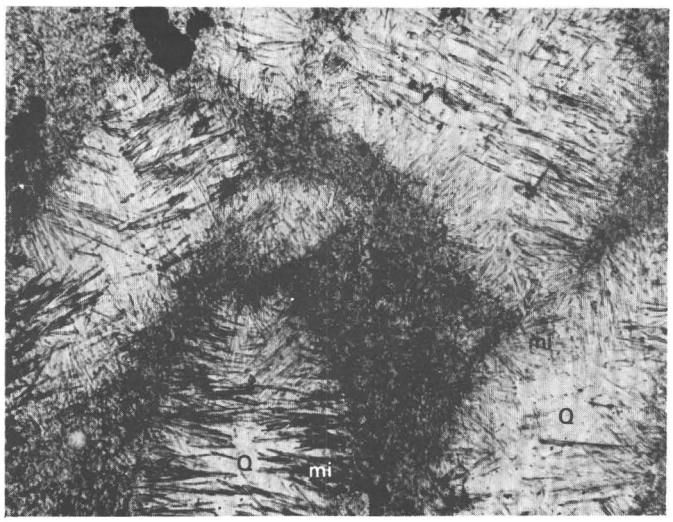

E

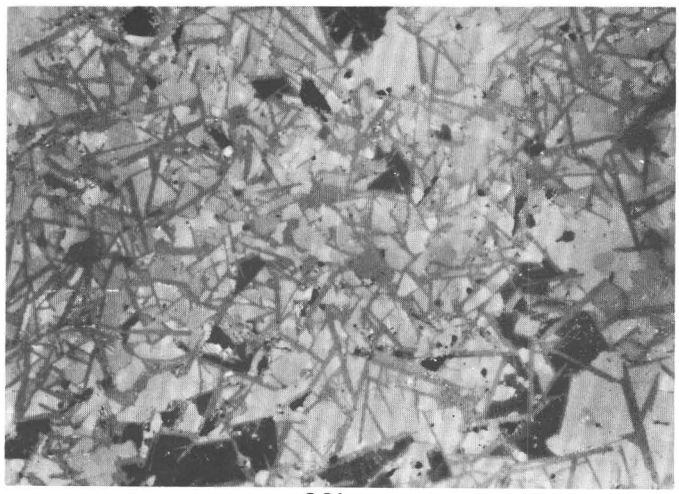

G

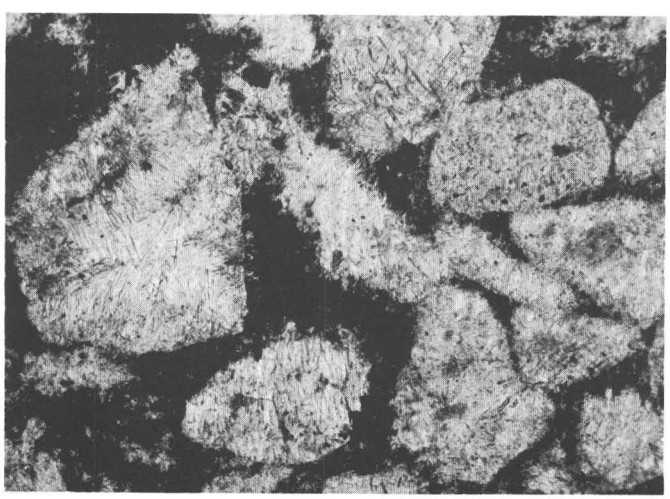

F

H

partial replacement of clastic quartz grains (Q) by coarse blades of minnesotaite (mi), alined at large angles to surfaces of clasts. Interstices filled by fine-grained minnesotaite. Plane-polarized light. *F*, Thin section showing minnesotaite granules. Form of granules and similarity of growth pattern of minnesotaite to that in partly silicated quartz clasts suggests that granules may be completely replaced quartz clasts. Plane-polarized light. *G*, Polished section showing intergrowth of carbonate (light gray), chert (dark gray), and silicate (medium-gray blades) in rim on fragment of iron-formation in clastic lens. Note decussate pattern of silicate blades. *H*, Thin section showing latticelike pattern of iron silicate needles in spherical body of silicate-carbonate-chert embedded in a layer of carbonate-chert iron-formation (not shown). Plane-polarized light.

40*A*). The magnetite-rich layers are finely laminated and usually thicker than the chert-rich layers. Cherty layers may be homogeneous or internally laminated and commonly grade into and are replaced by magnetite-rich layers. In the upper part of the magnetite-chert-carbonate unit, the iron-formation is thinly banded and layering is irregular. Dull dark-gray to slightly reddish-gray cherty layers commonly are lumpy, nodular, and podded. Cherty pods generally are rimmed by light-colored mixtures of secondary carbonate and chert.

Magnetite and chert are the two principal miner-

als; carbonate is subordinate but commonly is present throughout the rock. Noticeable quantities of chlorite are present locally.

The magnetite-chert-carbonate iron-formation is texturally similar to the carbonate-chert iron-formation. Both types are coarser grained than other types of iron-formation in the mine. The magnetite-chert-carbonate iron-formation can be distinguished from the other types by its gray to dark-gray color, relatively coarse-grained texture, thick relatively indistinct layers, extensive replacement features, simple mineralogical composition, by the uniform amount, crystal size, and distribution of its magnetite, and by its high oxidation ratio.

The iron-formation in the mine was intruded by several mafic, now chloritic dikes, adjacent to which the magnetite in the iron-formation generally is extremely fine grained. The iron-formation has been oxidized locally, generally along structural weaknesses. Most of the oxidation is of postmetamorphic age and presumably is supergene.

The chemical composition of the iron-formation is unusually uniform because of the simple compositions of the dominant chert and magnetite. Drill-core composites, pit samples, and selected rock specimens were chemically analyzed.

Drill-core composites.—The entire section of magnetite-chert-carbonate iron-formation was cut by drill hole 1, and part of the section by drill hole 2. Cores obtained from drill hole 1 were divided into 100-foot sections, and those from drill hole 2 were divided into 150-foot sections and analyzed (table 20). Locations of the drill holes are shown on plate 2.

TABLE 20.—*Chemical analyses of drill-core composites, magnetite-chert-carbonate iron-formation, Empire mine*

[Analyses by Chemical Laboratory, Cleveland Cliffs Iron Co. Failure of totals to approximate 100 percent attributed to incomplete measurement of CO_2 by loss on ignition (L.O.I.) and to lack of analyses for alkalies]

	Drill hole 1					Drill hole 2	
	100–200 ft	200–300 ft	300–400 ft	400–500 ft	500–600 ft	8–160 ft	160–310 ft
SiO_2	44.86	46.78	42.90	42.74	43.10	44.10	41.41
Al_2O_3	.87	1.01	1.18	1.49	1.42	1.23	1.61
Fe_2O_3	29.10	29.24	29.73	29.17	29.63	29.73	29.23
FeO	16.93	17.17	17.77	18.41	18.37	18.27	18.91
MnO	.44	.40	.44	.40	.32	.44	.46
MgO	1.23	.89	1.33	1.39	1.14	1.34	1.44
CaO	1.23	.58	.82	.85	.89	.76	.95
P_2O_5	.08	.13	.08	.13	.11	.12	.12
FeS_2	.03	.02	.02	.04	.04	.02	.04
L.O.I.	1.81	2.46	2.22	2.56	1.15	2.30	2.90
Total	96.58	98.68	96.49	97.18	96.17	98.31	97.07
Magnetite	42.19	42.39	43.09	42.29	42.98	43.09	42.36
Oxidation ratio	77.47	77.30	76.99	76.11	76.18	76.50	76.55
CaO/MgO	1.00	.65	.62	.61	.78	.57	.66

Pit samples.—Two pit samples were collected and analyzed about 4 years apart. Their chemical compositions are very much alike, except that amounts of CaO and P_2O_5 vary in each sample (table 21).

TABLE 21.—*Chemical analyses of pit samples of magnetite-chert-carbonate iron-formation, Empire mine*

[Analyses by Chemical Laboratory, Cleveland Cliffs Iron Co. Failure of totals to approximate 100 percent attributed to incomplete measurement of CO_2 by loss on ignition (L.O.I.) and to lack of analyses for alkalies]

	1964 sample	1968 sample	Average
SiO_2	43.42	43.58	43.50
Al_2O_3	1.31	1.35	1.33
Fe_2O_3	29.20	29.60	29.40
FeO	18.85	18.00	18.43
MnO	.42	.35	.39
MgO	1.30	1.15	1.23
CaO	.86	.42	.64
TiO_2	--	.16	.16
P_2O_5	.11	.02	.06
L.O.I.	2.56	2.69	2.63
Total	98.03	97.32	97.77
Magnetite	42.32	42.90	42.61
Oxidation ratio	75.86	76.67	76.27
CaO/MgO	.66	.37	.52

Individual specimens.—Four partial analyses were made of four individual specimens of the magnetite-chert-carbonate iron-formation from the Empire mine (table 22). Because the four individual specimens were collected mainly to study brecciation, replacement, and podding of chert-rich layers, their iron content is generally lower and silica content higher than normal for the magnetite-chert-carbonate unit.

TABLE 22.—*Chemical analyses of individual specimens of magnetite-chert-carbonate iron-formation, Empire mine*

[Analyses by Chemical Laboratory, Cleveland Cliffs Iron Co. Failure of totals to approximate 100 percent attributed to incomplete measurement of CO_2 by loss on ignition (L.O.I.) and to lack of analyses for alkalies]

	1	2	3	4	Average
SiO_2	51.62	55.08	47.44	53.90	52.01
Al_2O_3	1.21	.64	.85	.19	.72
Fe_2O_3	26.74	23.45	21.59	25.59	24.34
FeO	14.41	14.54	19.30	14.54	15.70
MnO	.43	.31	.85	.43	.51
MgO	1.15	1.10	1.25	.75	1.06
CaO	.42	.81	.23	.77	.56
TiO_2	.13	.13	.14	.13	.13
P_2O_5	.03	.17	.03	.10	.08
L.O.I.	1.33	2.43	5.54	1.43	2.68
Total	97.47	98.66	97.22	97.83	97.79
Magnetite	38.46	33.18	31.98	38.26	35.47
Oxidation ratio	78.77	76.33	69.11	77.88	75.52
CaO/MgO	.37	.74	.18	1.03	.58

1. Straight banded, massive, from lower part of zone.
2. Straight banded, from middle part of zone; partially replaced.
3. Brecciated, straight banded, from middle part of zone.
4. Podded (pinch and swell type), from upper part of zone.

COMPOSITION OF CARBONATES

From chemical analyses, using all of the MgO, MnO, CaO, and CO_2, and the required balance of FeO applied to carbonate, the following carbonate compositions have been determined:

Carbonate molecule	Proportions of carbonate molecules in carbonate			
	On fragments	On nodules	In chert lenses[1]	In chert-carbonate-layers
$FeCO_3$	82.02	76.69	57.18	71.81
$MnCO_3$	5.83	13.57	16.05	15.95
$CaCO_3$	1.44	.61	15.02	5.12
$MgCO_3$	10.71	9.13	11.75	5.94

[1] Carbonate in chert lenses consists of mixtures of ankeritic porphyroblasts and sideritic inclusions.

Modification of Primary Layers

The magnetite-chert-carbonate iron-formation was deposited as alternating iron-rich (carbonate and perhaps also magnetite) and silica-rich layers which subsequently were complicated by slumping, compaction, and diagenetic-metamorphic changes. Primary layers have been disrupted by small-scale faulting, and have been replaced, partly replaced, and corroded, especially during diagenesis, and as a result have acquired lenticular, nodular, and stylolitic structures. Normally, minerals are more or less evenly mixed within a given layer or are segregated into laminae. Primary chert-rich layers are more likely to have little or no internal lamination than are magnetite-rich layers, which almost universally are laminate. Original cherty layers in particular tend to be brecciated and corroded. Fragments commonly are angular chips, but ends may be rounded, or layering may be cut into on a zigzag front by corrosion. Magnetite-rich layers, on the other hand, are rarely brecciated or displaced by clusters of small-scale faults, but may be contorted or arched around cherty fragments or nodules by differential compaction as already noted in the underlying unit of iron-formation.

Corrosion features.—Corrosion of primary layers produces a variety of secondary features such as chains of "islands" (figs. 47*A*, *B*), gradual thinouts and pinch-and-swell structure, zigzag contacts between layers, and oriented pod-shaped lenses (fig. 47*C*). Discontinuous remnants of chert and chert-carbonate layers are separated by zones of magnetite-chert. The magnetite of such intervening zones either is disseminated or in laminae, in accordance with the internal structure of the discontinuous layers. Evidently, replacement of the cherty layers occurred without much damage to the original layered structure, although the thickness of layers generally has been noticeably reduced in the mag-

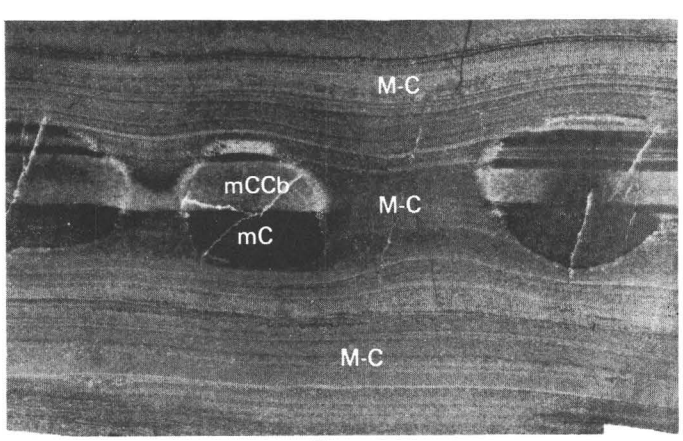

A

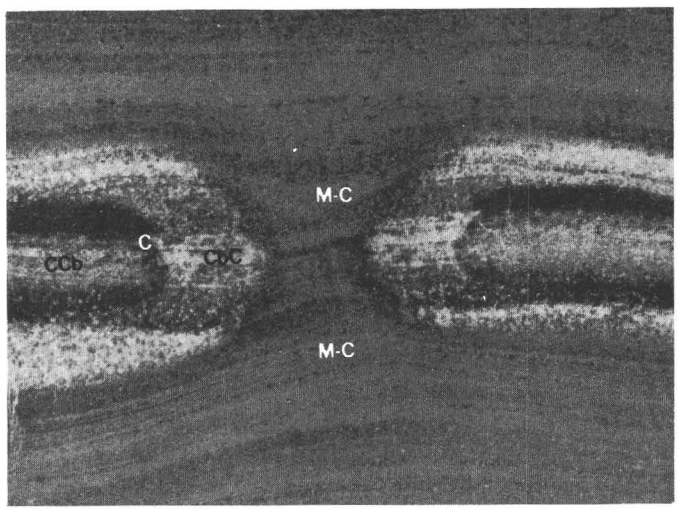

B

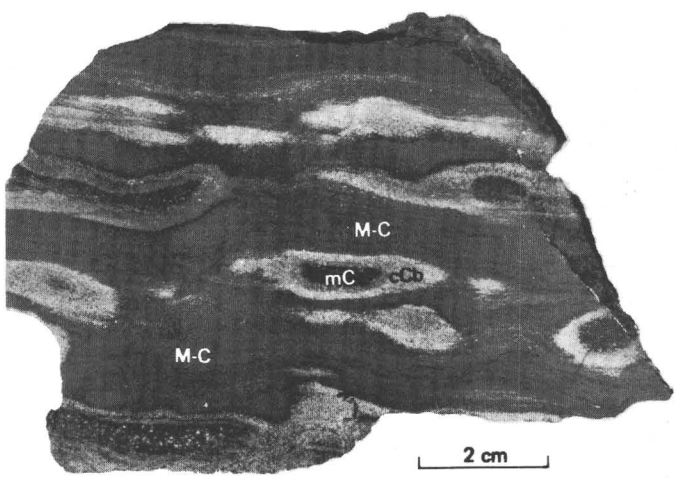

C

FIGURE 47.—Corrosion features in iron-formation at the Empire mine. *A*, Finely ground surface showing chain of "islands" composed of interlayered magnetic chert-carbonate (mCCb) and magnetic chert (mC), sandwiched between and separated by layers of laminated magnetite-chert (M-C). *B*, Finely ground surface showing "islands" of chert-carbonate (CCb) with rims of carbonate-chert (CbC), the first-named mineral in each area being the more abundant. Thin zone of chert (C) separates core of "islands" from carbonatized rims. "Islands" surrounded by laminated magnetite-chert (M-C). *C*, Finely ground surface showing partly carbonatized pods of magnetic chert (mC) between layers of magnetite-chert (M-C). Areas of secondary cherty carbonate (cCb) at ends of pods are noticeably thicker than on flanks of pods.

netite-rich areas between the discontinuous cherty segments.

Disruption features.—Asymmetrical folds, small-scale thrust faults (fig. 48), step faults, brecciation,

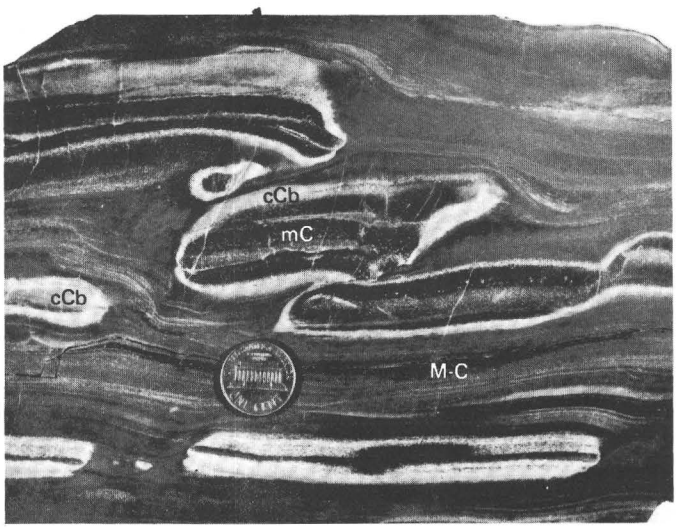

FIGURE 48.—Finely ground surface showing en echelon arrangement of broken thrust-faulted layers of magnetic chert (mC) between layers of magnetite-chert (M-C). Cherty layers peripherally replaced by (cherty) carbonate (cCb).

and probable preconsolidation folds are common intraformational structures in the magnetite-chert-carbonate iron-formation. Broken layers are angular although generally partly replaced by carbonate. There has been relatively little replacement of such segmented layers by magnetite, which, with the angularity of the segments, might mean that the fracturing and carbonatization of the layers occurred after consolidation and later than diagenetic replacements of other chert-carbonate layers by magnetite.

Lenticular and nodular structures.—Isolated and interconnected lenses of chert and chert-carbonate, with or without interlaminated magnetic chert, are sandwiched between internally laminated magnetite-rich layers (fig. 49). Lenses accordingly may be internally homogeneous or laminated. The laminated magnetite-rich layers typically are curved to conform with the enclosed lenses.

Nodules are subrounded to well-rounded grayish-white cherty aggregates which range in size from 2 to 130 mm and have a very low sphericity. They tend to be elongated parallel to bedding and to occur in the upper part of the magnetite-chert-carbonate unit, associated with clastic sediment and chlorite. They consist mainly of granular chert and minor

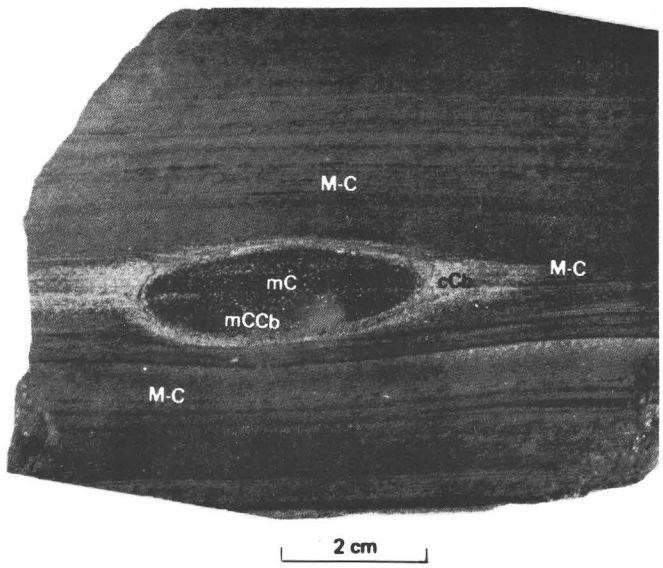

FIGURE 49.—Finely ground surface showing lens of magnetic chert (mC) and magnetic chert-carbonate (mCCb) sandwiched between laminae of magnetite-chert (M-C). Rim of cherty carbonate (cCb) envelops the lens and grades into magnetite-chert.

amounts of disseminated magnetite and carbonate. Most nodules have a siderite-rich shell. The shell also generally contains some chert but is free of magnetite. Tiny cracks in the peripheral part of the nodules are filled with mixtures of magnetite, clastic quartz, carbonate, chert, and chlorite from the enclosing layer. Bent clast-bearing layers commonly are molded around nodules, suggesting that the rounding of the nodules took place prior to deposition of the surrounding sediment. Carbonate rims probably formed after deposition.

Chemical analyses of lenses and nodules and enclosing rock are given in table 23. The comparatively low oxidation ratio of the cherty lenses and

TABLE 23.—*Chemical analyses of cherty lenses and nodules and enclosing magnetite-rich layers, magnetite-chert-carbonate iron-formation, Empire mine*

[Analyses by Chemical Laboratory, Cleveland Cliffs Iron Co. Failure of totals for columns 1 and 3 to approximate 100 percent attributed to incomplete measurement of CO_2 by loss on ignition (L.O.I.) and to lack of analyses for alkalies]

	1 Magnetite-rich host	2 Lenses	3 Magnetite-rich host	4 Nodules
SiO_2	46.06	85.07	28.98	83.60
Al_2O_3	.44	.27	2.01	.37
Fe_2O_3	25.45	4.29	36.75	3.57
FeO	17.88	5.79	22.51	7.08
MnO	.80	.31	1.16	.96
MgO	1.75	.87	1.23	.50
CaO	.08	.06	.14	.04
TiO_2	.05	.02	.09	.03
P_2O_5	.02	.02	.09	.02
L.O.I.	4.93	3.02	4.81	3.35
Total	97.46	99.72	97.77	99.52
Magnetite	36.88	6.22	53.26	5.17
Oxidation ratio	74.00	59.71	76.55	50.21
CaO/MgO	.046	.069	.11	.06

nodules reflects their low content of magnetite or other iron oxide minerals.

Concretions.—Elongated nodules having internal concentric structure have been found in one place in the upper part of the magnetite-chert-carbonate zone. They are probably concretions formed after sedimentation. The concretions each contain two or three concentric layers consisting of (1) apatite-bearing chert with some magnetite, (2) magnetite-chert with some apatite, and (3) magnetite-chert. They occur in a whitish-gray chert-rich layer that has been extensively corroded by dark-gray cherty layers on both sides. Both sets of cherty layers contain disseminated magnetite, and the dark-gray chert also has abundant tiny needles of soft hematite. The corrosion border separating the light and dark chert layers is marked by a thin seam of carbonate. These features attest to the mobilization of iron, silica, carbon dioxide, and phosphorus after sedimentation.

Stylolites.—Zigzag and suturelike contacts between cherty layers are marked by thin seams of tiny magnetite crystals and also contain carbonate and chlorite. They are common within cherty layers, "islands," lenses, and fragments but have not been found at contacts between magnetite-rich and cherty layers. Single-suture contacts are much more common than multisuture contacts. Some end at boundaries between cherty zones and magnetite-rich zones that have replaced the cherty zones, whereas others continue across such boundaries. The irregular sutures apparently are stylolites; they probably were formed by the almost simultaneous dissolving and compaction of adjacent layers and subsequently were partly obliterated by the replacement of cherty layers by magnetite.

Clastic dikes.—Rare clastic dikes, which are composed mainly of detrital quartz, chlorite, carbonate, chert, and magnetite, crosscut the upper part of the magnetite-chert-carbonate unit (figs. 50*A*, *B*). Quartz grains are sutured, have wavy extinction, and generally have been either partly replaced by chlorite and carbonate or partly disaggregated into fine-grained mosaics. A chemical analysis of the dike shown in figure 50 is given in table 24.

TABLE 24.—*Chemical analysis of clastic dike, upper part of magnetite-chert-carbonate unit, Empire mine*

[Analysis by Chemical Laboratory, Cleveland Cliffs Iron Co. L.O.I., loss on ignition]

SiO_2	57.44	CaO	6.32
Al_2O_3	6.81	TiO_2	.23
Fe_2O_3	3.88	P_2O_5	1.51
FeO	9.65	L.O.I.	9.95
MnO	.36		
MgO	3.70	Total	99.85

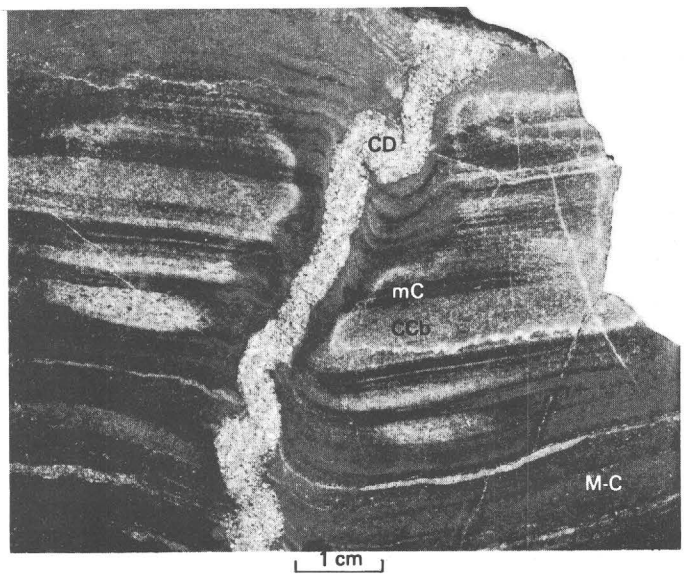

A

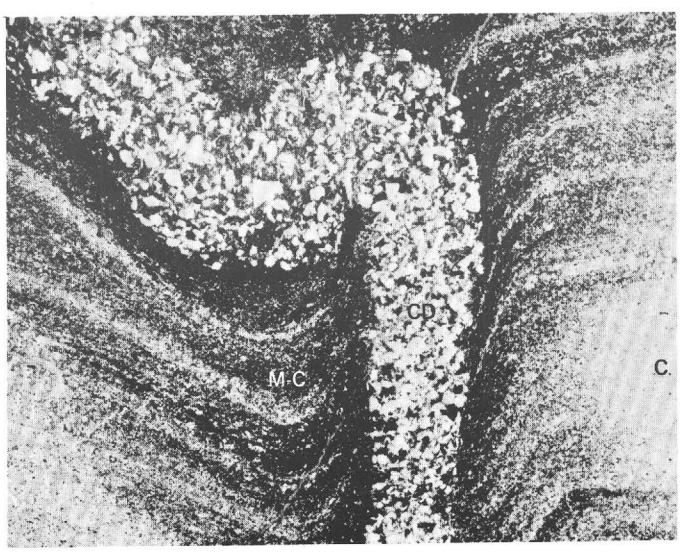

B

FIGURE 50.—Clastic dike cutting magnetite-chert-carbonate iron-formation. *A*, Polished surface. Cherty layers replaced by magnetite along sides of dike. *B*, Photomicrograph of thin section from part of area in *A* showing progressive increase in amount of magnetite toward clastic dike, and drag along dike walls. C, Chert; CCb, chert-carbonate; CD, clastic dike; mC, magnetic chert; M-C, magnetite-chert.

Magnetite enrichment both of cherty and magnetite-bearing layers has occurred along the margins of at least one such clastic dike (fig. 50). The magnetite content increases progressively toward

the dike; so the enrichment in magnetite clearly took place after deposition of the layers.

Alteration and Replacement

Numerous small-scale features in the magnetite-chert-carbonate iron-formation at the Empire mine are attributed to alteration and the replacement of the original sediments during diagenesis or during contact or regional metamorphism. The most significant of these changes resulted in enrichment in iron oxide by the magnetitization of carbonate-chert laminae, chert layers, and other layers that previously carried only small amounts of magnetite. Secondary magnetite has also formed along quartz veinlets, clastic dikes, stylolites, and fractures. Other changes include carbonatization, silicification, pyritization, and oxidation. Carbonatization commonly accompanies magnetitization. Carbonate has had a complex history in the iron-formation. Undoubtedly much of the carbonate in the Negaunee Iron-Formation considered as a whole is recrystallized primary siderite. Concentrations of secondary carbonate adjacent to magnetitized zones and carbonate replacements of nodules and fragmented layers of chert formed during diagenesis or regional metamorphism.

The replacement of layers of carbonate-chert or magnetic chert by magnetite generally results in a reduction in the thickness of laminae and considerable changes in mineral ratios, textures, and possibly in mineral assemblages, but commonly does not destroy original layering. Molecule-by-molecule conversion of siderite to magnetite should result roughly in a halving of volume and can explain the reduction in the thickness of layers of magnetitized siderite. The reduction in thickness of layers of magnetic chert upon conversion to magnetite is attributed to dehydration and volume loss as water-laden chert is replaced by magnetite. The secondary magnetite may form laminae that alternate with layers of chert or may occur in grains disseminated throughout the chert, depending, apparently, on the original arrangement of carbonate and chert in the rock before replacement occurred. Carbonatization commonly is associated with the magnetitization. Examples are discussed and illustrated in the following paragraphs.

Magnetitization of laminated carbonate-chert iron-formation and development of secondary carbonate in the transitional zone.—In places in the middle and upper parts of the magnetite-chert-carbonate unit, extensive magnetitization has left only "islands" of original chert-carbonate rock (fig. 51*A–C*). Such "islands" commonly are rimmed by a narrow zone of secondary carbonate and chert. The unreplaced rock is interlaminated carbonate and chert or laminae containing intermixed grains of carbonate and chert. The secondary carbonate of the transitional zone commonly consists of relatively large euhedra of ankerite (fig. 51*D*), which may be partly to completely oxidized to hematite. The replaced rock contains magnetite in addition to chert or chert and carbonate. Single laminae of carbonate or chert can be traced from the unreplaced rock into magnetite-bearing layers (fig. 51*E–J*). Typically, the amount of magnetite in the unreplaced rock and in much of the transitional zone is negligible. The size and distribution of isolated magnetite grains in the replaced parts of original sideritic layers somewhat resemble those of the carbonate in the unreplaced parts of the layers, suggesting that magnetite has replaced carbonate grains. It is not likely, however, that the magnetite was derived solely by in place replacement of siderite, because the amount of magnetite replacing original chert laminae is about as much as that replacing original carbonate laminae. Much of the magnetite that replaces cherty siderite-poor layers apparently was derived from initially more ferruginous layers adjacent to the cherty layers. Inclusions in the large ankerite crystals vary in quantity and type across the transitional zone. Ankerite adjacent to the unreplaced rock contains abundant chert and also contains some granular carbonate inclusions, whereas that adjacent to the enriched zone includes many euhedral magnetite crystals and contains little chert. The granular carbonate inclusions in the ankerite apparently are of the same generation as carbonate in the unreplaced layers. Microprobe analyses show that the large carbonate euhedra are ankeritic and that the granular carbonate inclusions are sideritic as shown here:

Component	*Large carbonate euhedra*	*Granular carbonate*
$CaCO_3$	66.27	0.97
$MgCO_3$	10.82	17.22
$FeCO_3$	21.57	76.94
$MnCO_3$	4.87	1.34

Along some carbonate-rich layers the size and quantity of carbonate grains increase toward areas where magnetite has replaced the original carbonate-bearing layers. The increase in grain size and quantity of carbonate may be accompanied by a decrease in the amount of chert and fine-grained magnetite. Replacement magnetite tends to be of uniform size and coarser than magnetite of

the unreplaced rock. In some transitional zones, carbonatization occurs at the expense of primary carbonate, which in a given layer is depleted adjacent to the zone of coarser secondary carbonate (fig. 51*F*). In the magnetitization of alternating layers of chert-carbonate and magnetic chert, secondary carbonate is concentrated at the interface between replaced and unreplaced rock only in layers that originally contained carbonate (fig. 51*E*).

The replacements shown in figure 51*B*, *C* were attended by appreciable additions of Fe_2O_3, FeO, and CaO, and subtractions of MgO, MnO, SiO_2, and CO_2 (loss of the last inferred from loss of carbonate) (table 25). Hence, it is concluded that the replacement involved oxidation of magnesian iron carbonate to magnetite, the growth of small grains of magnetite to larger grains, and extensive ionic diffusion.

TABLE 25.—*Partial chemical analyses from replaced and unreplaced zones in magnetitized layers of chert-carbonate and magnetic chert, Empire mine*

[Analyses by Chemical Laboratory, Cleveland Cliffs Iron Co. L.O.I. is loss on ignition]

	Sample 1 (same as shown in fig. 51B)		Sample 2 (same as shown in fig. 51C)	
	Unreplaced	Replaced	Unreplaced	Replaced
SiO_2	76.00	55.03	81.90	57.40
Al_2O_3	.44	.47	.52	.23
Fe_2O_3	3.97	24.21	7.86	27.74
FeO	7.78	12.45	5.40	12.87
MnO	.53	.28	.28	.17
MgO	1.80	.98	.48	.30
CaO	.90	1.60	.18	.40
L.O.I.	3.60	5.92	1.33	.44 (gain)
Total	95.02	100.94	97.95	99.55
Magnetite	5.75	35.09	11.39	40.20
Oxidation ratio	50.51	79.55	74.43	81.17

Magnetitization of laminated carbonate-chert iron-formation with small increase in chert and magnetite in transitional zone.—Unreplaced cherty or carbonate-rich laminae can be followed in places through a transitional zone of weakly magnetic chert into laminated magnetite-chert (fig. 51*J*). Unreplaced cherty laminae usually contain some carbonate and (or) fine-grained magnetite, and unreplaced carbonate-rich laminae generally contain a noticeable amount of chert and some magnetite. The transitional zone is weakly magnetic chert in which the magnetite is extremely fine grained. Carbonate tends to disappear across the transitional zone toward the magnetite-rich parts of the rock. In the secondary magnetite-rich rock the magnetite grains are euhedral, and most are in the size range, 15–35 microns.

Magnetitization-carbonatization of cherty layers.—Cherty layers are very commonly replaced by magnetite and carbonate, particularly in the upper part of the magnetite-chert-carbonate unit. Carbonate-chert assemblages occupy a transitional zone between unreplaced parts of original cherty layers and magnetitized parts. Secondary ankeritic carbonate typically is distributed along the peripheries of oval-shaped remnant cherty "islands" in the magnetitized layers (figs. 47*A*, *C*; 49). The secondary ankeritic carbonate may form skeletal crystals, rhombohedral aggregates, and large euhedral grains (fig. 51*D*) that contain remnants of chert and may also contain remnants of magnetite and siderite. Chert is practically the entire host. Ankeritic zones are usually thicker at the rounded ends of cherty "islands" than along bedding planes (for example, fig. 47*C*). Carbonate replacements also form irregular zigzag reentrants along bedding surfaces. These features suggest that chert-rich sideritic layers were replaced by magnetite and that ankerite represents mainly material rejected from siderite during magnetitization.

Carbonatization of magnetic chert.—Layering passes from dark magnetic chert into lighter colored pods of carbonate-chert enclosed in laminated magnetite-chert. Some such pods have cores of magnetic chert that appear to be uncarbonatized remnants (fig. 51*B*). Magnetite is fine grained and makes up about 15 percent of the magnetic chert. Much of the replacing carbonate is coarse skeletal rhombs that include abundant remnants of chert.

Replacement of chert by carbonate.—Peripheral parts of angular cherty fragments may be replaced by carbonate to form rims that range in thickness from less than 1 mm to 8 mm. In general, the parts of the rims perpendicular to layers are thicker and more irregular than the parts parallel to layers (fig. 52).

Cherty nodules are common in some zones of the iron-formation, as noted above, and generally have been centripetally replaced from outer margins by fine-grained carbonate, and are also common along fractures. Carbonate rims are usually less than 2 mm thick. The ratio of chert to carbonate on the rims is about 1:5, whereas the centers of nodules are practically free of carbonate.

Replacement of magnetite along fractures.—Near some chloritic dikes, sideritic carbonate has replaced magnetite-chert iron-formation along cracks that cut the beds at a large angle. Bedding is obliterated by the carbonate. This type of carbonatization is extremely limited in extent and is considered to be a contact metasomatic effect of the intrusion of mafic rock into the iron-formation.

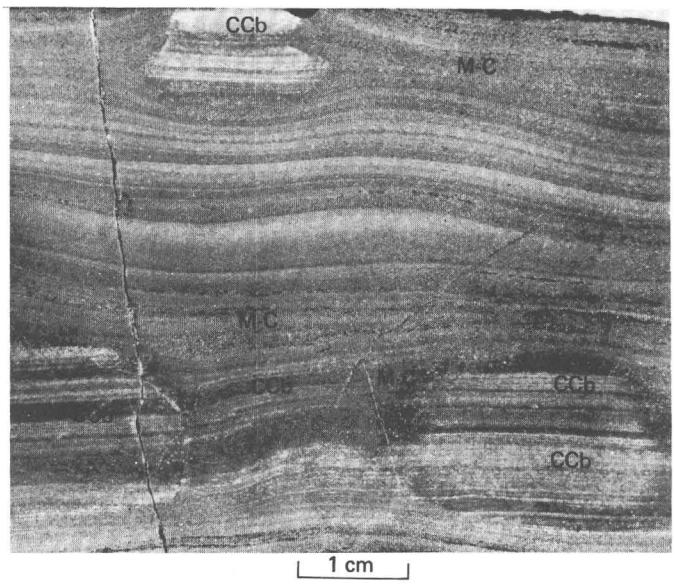

A

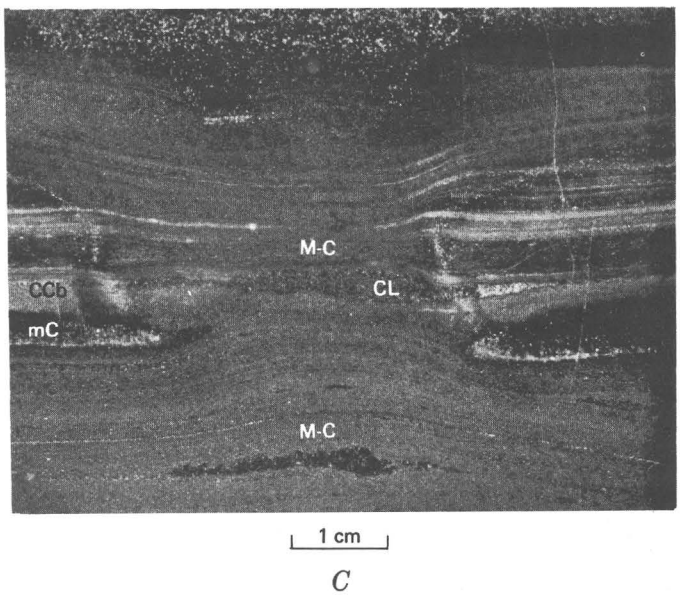

C

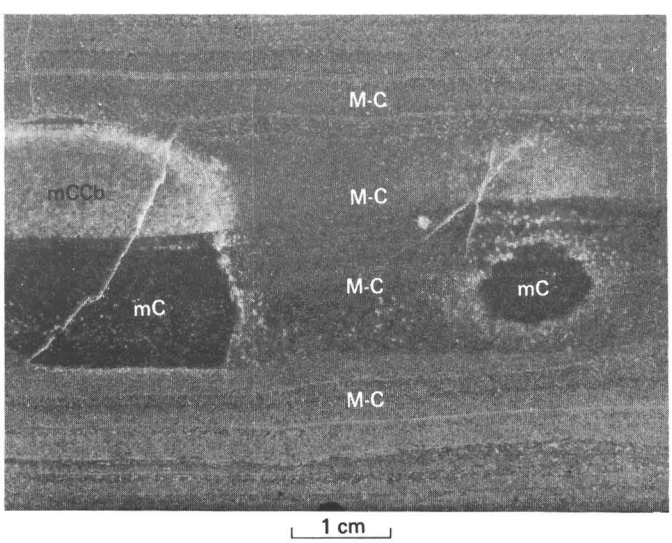

B

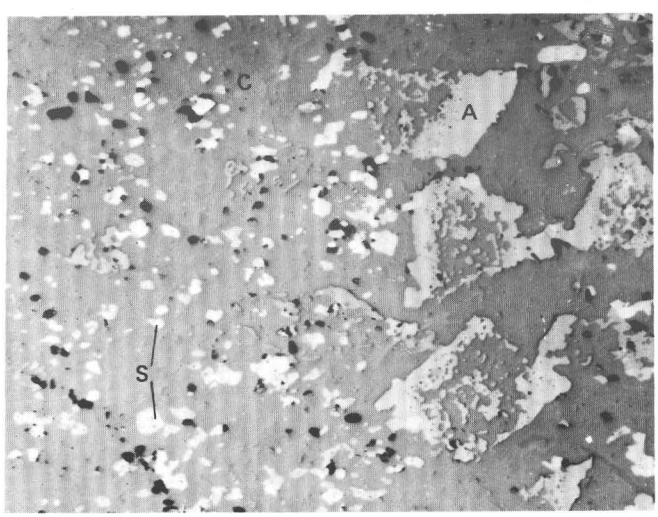

D

FIGURE 51.—Magnetitization of laminated carbonate-chert iron-formation, Empire mine. *A*, Finely ground surface showing laminated chert-carbonate (CCb) passing into magnetite-chert (M-C). Note continuation of layers from chert-carbonate to magnetite-chert. *B*, Finely ground surface showing layers of magnetic chert (mC) and magnetic chert-carbonate (mCCb) extending into laminated and disseminated magnetite-chert (M-C) in which magnetite grains are about six times as large as those in the magnetic chert. *C*, Finely ground surface showing layers of magnetic chert (mC) and chert-carbonate (CCb) passing into laminated magnetite-chert (M-C). Note continuity of clastic lens (CL) from one type of iron-formation to the other. *D*, Photomicrograph of polished section showing contact between unreplaced chert (C)-siderite (S) and ankeritic carbonate (A) of the transitional zone to magnetitized rock. *E*, Photograph of thin section showing layers of magnetic chert (mC) and magnetic chert-carbonate (mCCb) replaced respectively by laminated and disseminated magnetite-chert (M-C). Transitional zone of secondary cherty carbonate (cCb) is only in layer containing primary carbonate. *F*, Photomicrograph of thin section showing lens of chert-carbonate (CCb) sandwiched between layers of magnetite-chert (M-C) and bordered by marginal zone of relatively coarse-grained carbonate (Cb). In carbonate-bearing layer within the lens, carbonate decreases from *A* to *B*, toward the marginal zone of secondary car-

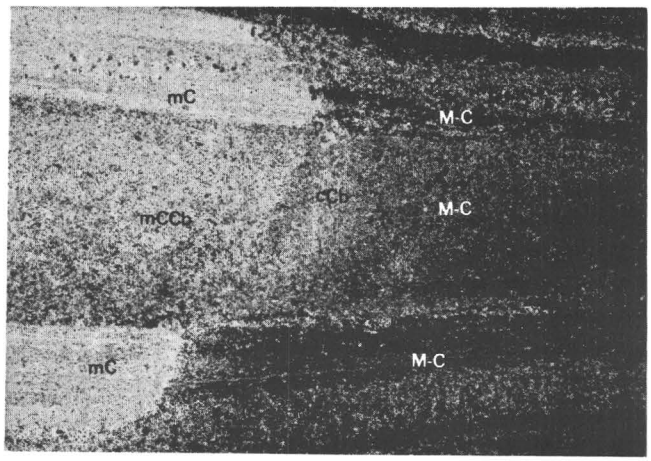

E

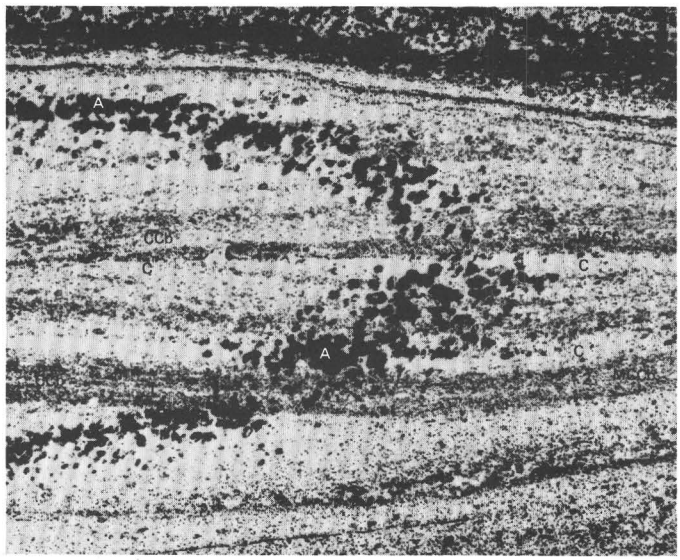

G

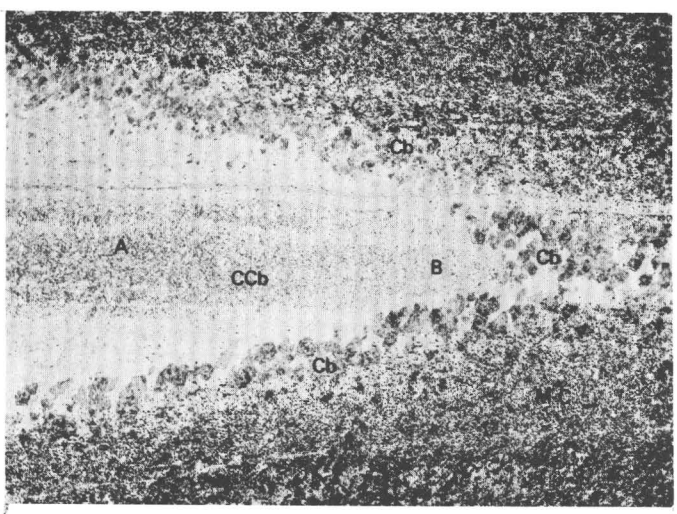

F

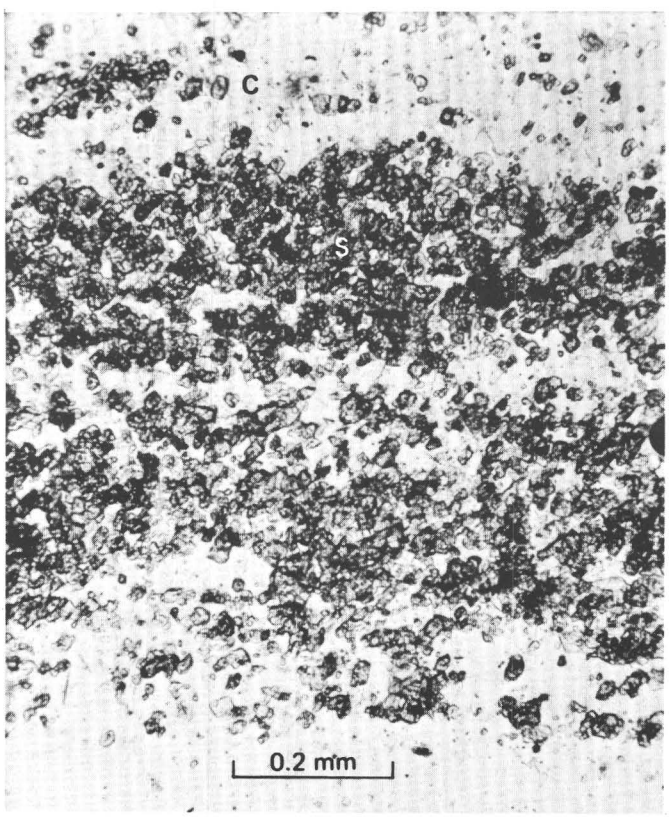

H

bonate. Plane-polarized light. *G*, Photograph of thin section showing lens of laminated chert (C) and chert-carbonate (CCb) on the left, outlined by relatively coarse crystals of oxidized ankerite (A). Laminae pass from the lens across zone of oxidized ankerite to magnetite-bearing chert-carbonate (MCCb). *H*, Photomicrograph of thin section showing layer of sideritic carbonate (S) (from area 1 of *G*), within lens of chert (C) and chert-carbonate. Note lack of magnetite. Plane-polarized light. *I*, Photomicrograph of thin section showing another part of carbonate layer (from area 2 in *G*), in zone of magnetite-bearing siderite (S) and chert (C). Note disseminated magnetite (M). Plane-polarized light. *J*, Finely ground surface showing alteration of chert-carbonate (CCb) to magnetite-chert (M-C), with transitional zone of magnetic chert (mC). Figure continues on following page.

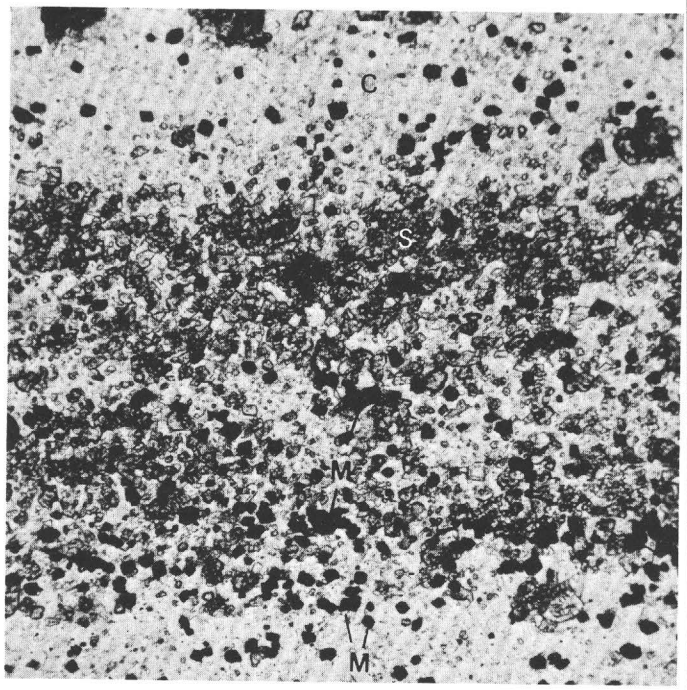

I

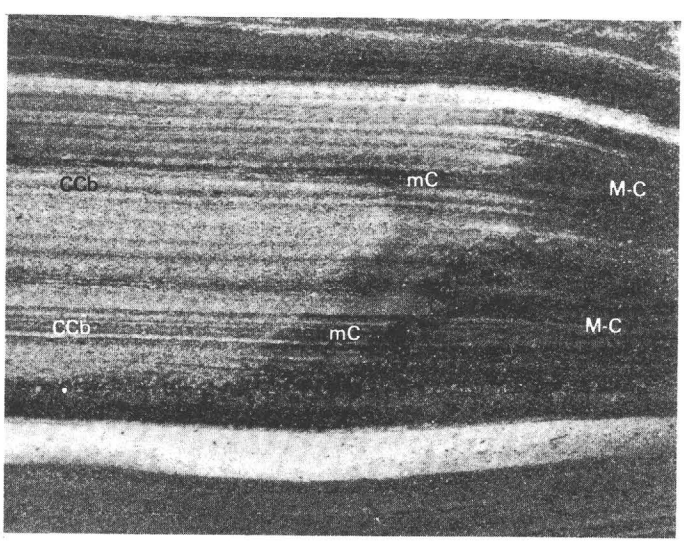

J

FIGURE 51.—Continued.

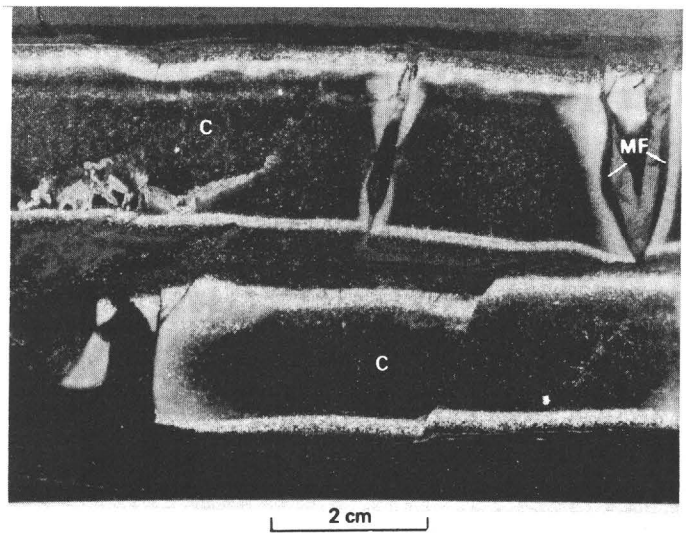

FIGURE 52.—Finely ground surface showing carbonatized brecciated chert (C) sandwiched between undisturbed magnetite-rich layers. Note magnetite filling (MF) in fractures and differences in width of carbonatized rims along chert layers and at broken ends of the beds.

ORIGIN OF MAGNETITE AFTER SEDIMENTATION

Iron-formation layers rich in siderite and layers of magnetitic chert containing magnetite particles only a few microns in size are replaced by magnetite-rich layers as shown above. The fine-grained magnetite of unreplaced parts of layers evidently is primary, but the replacement features clarify the secondary origin of some and perhaps much magnetite at the Empire mine. Unfortunately, the replacement structures indicate little about when the replacements occurred—whether during diagenesis or metamorphism or at another time. In an earlier section of this report (p. 52) it was pointed out that abrupt differences in oxidation state between thin alternate carbonate and magnetite layers should be more readily established during sedimentation or diagenesis than under the equilibrating influence of regional metamorphism. Magnetite at the Empire mine tends to be highly concentrated in laminae that alternate with laminae of chert, iron silicate-chert, siderite-chert, and siderite-iron silicate-chert. Contacts between such laminae commonly are exceedingly sharp and, in accordance with the above theoretical consideration, seem best explained by sedimentation or diagenesis rather than by metamorphism. An origin by sedimentation is ruled out where the magnetite has replaced earlier material.

The uniformly recrystallized fine-grained fabric of magnetite laminae, with grain sizes mainly of 10–30 microns, is similar texturally to sideritic and cherty laminae and seems more likely to result from the metamorphic recrystallization of layers that were already rich in magnetite rather than by re-

placement of other minerals during metamorphism. Hence, such magnetite probably was present at the beginning of metamorphism in smaller grains than now, and where related to replacement structures, most likely formed initially during diagenesis.

Relatively coarse magnetite euhedra up to about 150 microns in size are scattered in some layers of uniformly fine-grained magnetite or in layers of other iron minerals. Such euhedra commonly contain inclusions of chert, siderite, iron silicate, and magnetite in the common small-size range of 5–30 microns. The coarse euhedra are porphyroblasts derived during regional metamorphism from premetamorphic magnetite, or in some cases from siderite.

Replacement structures indicating magnetite that formed after deposition of the iron-formation, such as those illustrated above, are found adjacent to mafic dikes as well as at a distance from dikes. If one judges by obvious features such as layering, magnetite content, megascopic texture, and replacement structures, the iron-formation is essentially the same near dikes as at a distance from them. However, pellet plant recovery data and microscopic study show that the magnetite is fine-grained (5 microns or less) near dikes and is coarser grained (10–30 microns) in the same layers at a distance from dikes. Dikes evidently baked or recrystallized the iron-formation as they were emplaced, making the iron-formation adjacent to dikes impervious or less susceptible to later changes during regional metamorphism than it was at a distance from dikes. If recrystallization was part of the modification of iron-formation near dikes, grains were generally not enlarged to more than 5 microns in size. Later, during regional metamorphism, magnetite grains at a distance from dikes were enlarged to 10–30 microns in size, but in zones bordering dikes the effects of the earlier contact metamorphism inhibited the further growth of magnetite. Adjacent to some dikes, parts of magnetite-rich laminae were replaced during intrusion, by carbonate, chlorite, or pyrite. Such layers clearly contained abundant magnetite at the time of intrusion of the mafic dikes. From the above observations it seems certain that magnetite-rich layers containing replacement structures—hence containing magnetite formed after deposition of the iron-formation—existed at the time of dike emplacement, prior to regional metamorphism. Thus, the evidence here also points to diagenesis as the most likely origin of secondary magnetite.

The processes and changes leading to and encompassing the diagenetic formation of magnetite are envisaged as follows:

1. Deposition of iron-formation containing layers of siderite-chert, magnetitic chert, and magnetitic siderite-chert, by chemical precipitation.
2. Preconsolidation slumping, accompanied and (or) preceded by magnetitization of siderite grains and layers of magnetitic chert and magnetitic siderite-chert.
3. Differential compaction, promoted by the volume reduction inherent in the conversion of siderite to magnetite.
4. Release of CO_2, dehydration of silica, and channeling of oxygen, water, and CO_2, accelerated by slumping, along breaks between slump segments. Further volume reduction and compaction by dehydration of silica.
5. Growth of ankerite near interfaces between replaced and unreplaced zones of iron-formation, utilizing some of the CO_2 released by the conversion of siderite to magnetite.

Postmetamorphic Oxidation

Iron minerals in the magnetite-chert-carbonate iron-formation have been oxidized locally, subsequent to regional metamorphism. Oxidation proceeds inward from grain boundaries. In the same rock, either magnetite may be oxidized to martite while iron carbonate remains comparatively fresh, or the carbonate may be oxidized to hematite or goethite with no change in the magnetite. Generally, however, carbonate can become completely oxidized while some magnetite remains intact. Owing to the fact that the more readily oxidized iron carbonate is subordinate in the magnetite-chert-carbonate iron-formation, the thickness, structure, and texture of oxidized parts are little different from the unoxidized parts. Oxidation possibly is a result of several processes, but most seems to have been caused by the downward circulation of ground water from the existing land surface along fractures, contacts between dikes and iron-formation, and bedding surfaces, and through pore spaces.

Chemical analyses of four partly oxidized samples are listed in table 26. The analyses indicate that the incomplete oxidation produced unappreciable addition or subtraction of elements. However, the oxidation and accompanying leaching did result in the removal of some manganese, magnesium, calcium, and carbon dioxide, a change in the oxidation state of iron from ferrous to ferric, and possibly in small increases in the amount of silica and phosphorus. There was no distinct change in the amount of alumina.

TABLE 26.—*Chemical analyses of partly oxidized magnetite-chert-carbonate iron-formation, Empire mine*

[Analyses by Chemical Laboratory, Cleveland Cliffs Iron Co. Failure of most totals to approximate 100 percent attributed to incomplete measurement of CO_2 and possibly H_2O by loss on ignition (L.O.I.) and to lack of analyses of alkalies]

	Highly oxidized		Moderately oxidized		Unoxidized
SiO_2	45.30	46.30	46.30	47.50	43.71
Al_2O_3	.77	2.20	.79	1.42	1.26
Fe_2O_3	43.33	40.96	37.75	34.32	29.40
FeO	4.63	6.69	12.35	11.58	17.98
MnO	.15	.29	.19	.13	.41
MgO	.42	1.10	.67	1.20	1.25
CaO	.23	.20	.45	1.05	.87
TiO_2	.06	.10	.05	.08	--
P_2O_5	.12	.14	.06	.29	.11
FeS_2	.01	.01	.06	.01	.03
L.O.I.	.68	1.25	--	.83	2.20
Total	95.70	99.24	98.67	98.41	97.22
Magnetite	14.94	21.58	39.84	37.35	42.61
Oxidation ratio	95.24	92.45	85.94	85.56	76.71
CaO/MgO	.55	.18	.67	.88	.69

EFFECT OF DIKES

Chloritic metadiabase dikes [11] crosscut the magnetite-chert-carbonate iron-formation (pl. 2). Contacts between dikes and iron-formation are rather sharp in most places, although brecciation and pyritization obscure some of the contacts. Megascopically, the iron-formation appears to be nearly unaffected by the dikes. However, pellet plant experience and microscope study have shown that the grain size of magnetite adjacent to dikes is substantially less than that at a distance. Also, the mineral content of the iron-formation is significantly modified near some dikes. Adjacent to dikes, magnetite grains typically are 5 microns or less in diameter, whereas at a distance they are 10–30 microns in diameter. The 10–30-micron grains are representative of secondarily magnetitized parts of the iron-formation and are appreciably coarser than unreplaced parts of the same beds. However, they probably attained their present size by recrystallization during regional metamorphism after initially forming grains about 5 microns or less in size during diagenetic replacement. Next to dikes, evidently layers containing magnetite of diagenetic origin, 5 microns or less in size, were baked or welded by the intrusive rock without significant increase in the size of magnetite grains. During the subsequent regional metamorphism of the iron-formation, recrystallization and growth of the fine-grained magnetite in impermeable baked zones adjacent to dikes evidently was inhibited while magnetite at a distance from dikes recrystallized to the 10–30 mesh size.

Mafic dikes have caused some magnetitization, chloritization, and pyritization of the iron-formation, and, as noted above (p. 93), have also produced limited carbonatization in places.

[11] Compositional data on dikes is included in a later section of the quadrangle report, dealing with intrusive rock.

Magnetitization.—Magnetite adjacent to dikes occurs as tiny plates probably pseudomorphous after hematite or iron silicate (fig. 53*A*). Commonly, the magnetite plates are in clusters or granules (fig. 53*B*).

The replacement of hematite by magnetite in the Gogebic Range was reported by James (1954); in

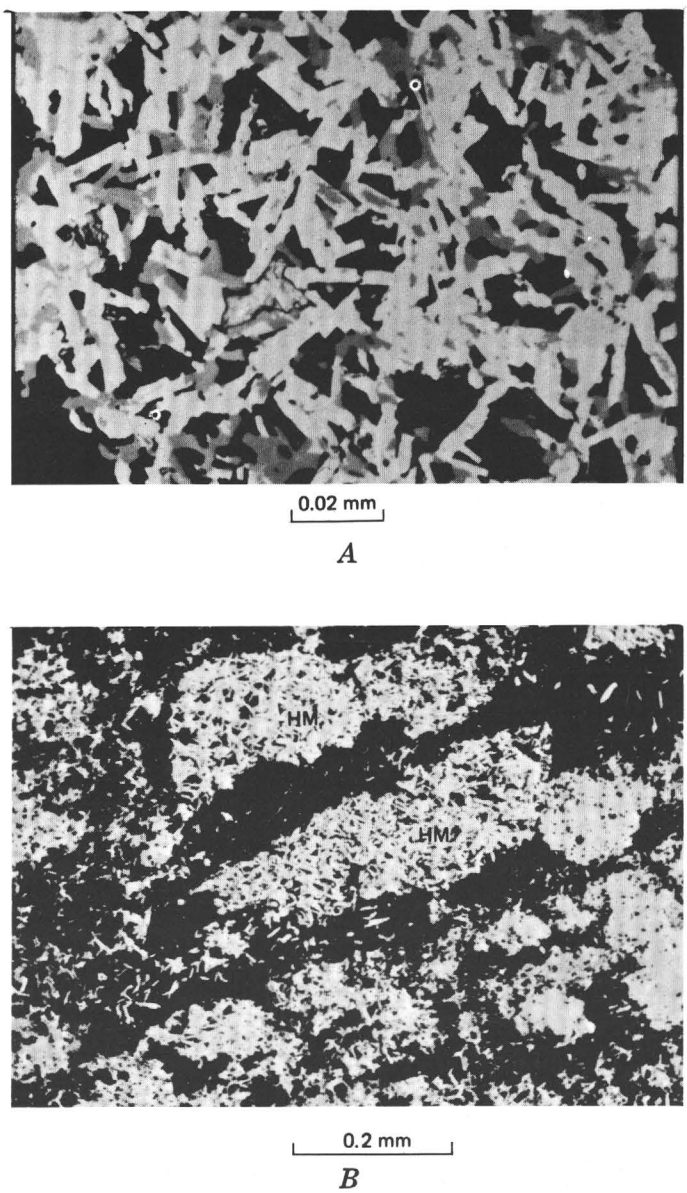

FIGURE 53.—Magnetitization adjacent to dikes, Empire mine. Photomicrographs of polished sections. *A*, Platy grains of magnetite partly to completely replaced by hematite. Original grains probably hematite (or iron silicate that was altered to hematite) prior to magnetitization. Magnetitized grains have been partly oxidized to hematite by weathering. *B*, Granules composed of extremely fine grained platy hematite-magnetite (HM). Granules associated with clastic quartz and some interstitial carbonate.

the Constance Range, Australia, by Whitehead[12]; and in the Albanel and Gunflint Ranges, Ontario, in the Mesabi Range, and in the Tilden area of the Marquette Range by Han (1966). Such magnetite is attributed to slightly reducing conditions during diagenesis and may have resulted from the presence of carbonaceous matter in the original sediments. However, the presence of platy magnetite near dikes in the Empire mine and in the Gunflint Range suggests the local reduction of hematite to magnetite by contact metamorphism. The presence of the platy magnetite in granules, and in granules associated with clastic grains, indicates that the platy grains originally were hematite formed in shallow agitated water at optimum oxidizing potential.

Chloritization.—In one place where iron-formation containing clastic lenses is directly in contact with a 3-foot dike, the iron-formation changes along the same bed in the direction of the dike, from assemblages of magnetite-chert-clastic grains to magnetite-chert-chlorite-clastic grains to chlorite-chert-clastic grains. The progressive change evidently results from the replacement of magnetite by chlorite.

Pyritization.—Pyrite commonly replaces fine-grained magnetite of the iron-formation along dike walls. The pyrite:magnetite ratio tends to increase appreciably toward the dike in the one sample studied. The pyrite is anhedral and coarse and commonly contains some inclusions of magnetite and chert. Where pyritization is greatest, magnetite occurs in small patches within the chert and is rare in the pyrite.

Detrimental effect on concentrating characteristics.—In general, the size, distribution, quantity, and degree of crystallinity of mineral grains are the key factors controlling the concentrating characteristics of the iron-formation. Normal magnetite-chert-carbonate iron-formation gives the best results, generally producing concentrates containing more than 67 percent iron and less than 5 percent silica with an iron unit recovery of approximately 80 percent. The grade drops noticeably if such iron-formation is blended with iron-formation from near dikes. The poorer concentrating qualities of the iron-formation near dikes has been verified by laboratory and plant tests and is explained by the extremely fine grain size of the magnetite and its intergrowth with chert and carbonate.

RIEBECKITE-BEARING IRON-FORMATION

Magnetite-hematitic chert-carbonate iron-formation containing riebeckite and, in places, also aegirinaugite occurs in 1–3 zones in isolated lenses in the upper 150 feet of the magnetite-chert-carbonate unit and near the base of the overlying unit of interbedded iron-formation and clastic rock (pl. 2; fig. 54*A*, *B*). Zones containing riebeckite-bearing beds range from a few feet to about 40 feet thick and extend at least 3,000 feet along strike and 1,400 feet or more downdip from surface and pit exposures. Riebeckite concentrations are irregular within the zones, but collectively they constitute a good stratigraphic marker. A characteristic section of the iron-formation containing riebeckite zones is cut by Empire drill hole 58, in the NW¼ sec. 19 (pl. 2) and is described in table 27.

TABLE 27.—*Log of drill hole 58 showing stratigraphic distribution of riebeckite-bearing zones, Empire mine, NW¼ sec. 19, T. 47 N., R. 26 W.*

Depth (feet)	Lithology
16–408	Magnetite-carbonate-silicate-chert iron-formation. Chloritic dikes at 347–355 and 379–381 ft.
	Top of interbedded unit.
408–552	Interbedded iron-formation and clastic rock.
552–579	Riebeckite-bearing magnetite-hematitic chert-carbonate iron-formation.
579–682	Interbedded iron-formation and clastic rock.
682–703	Riebeckite-bearing magnetite-hematitic chert-carbonate iron-formation.
703–706	Chloritic dike.
706–737	Riebeckite-bearing magnetite-hematitic chert-carbonate iron-formation.
	Bottom of interbedded unit, top of magnetite-chert-carbonate zone.
737–797	Magnetite-chert-carbonate iron-formation.
797–839	Riebeckite-bearing magnetite-hematitic chert-carbonate iron-formation.
839–885	Magnetite-chert-carbonate iron-formation.
885–913	Riebeckite-bearing magnetite-hematitic chert-carbonate iron-formation.
913–1,240	Magnetite-chert-carbonate iron-formation.
1,240–1,390	Carbonate-chert iron-formation.
1,390	End of drill hole.

The riebeckite-bearing zones typically contain (1) slaty iron-formation of magnetite, hematitic chert, scattered clastic quartz grains, and traces of riebeckite; (2) massive iron-formation consisting of unlaminated lenses of magnetite, riebeckite, and chert sandwiched between laminated layers of magnetite, riebeckite-bearing hematitic chert, and carbonate or carbonate-chert; and (3) laminated layers of riebeckite and aegirinaugite-bearing hema-

[12] S. Whitehead, 1962, The petrology of some oolitic iron ores and associated rocks; Petrological report No. M2/62 of Broken Hill Proprietary Co., Ltd., Geological Section, Melbourne, Australia.

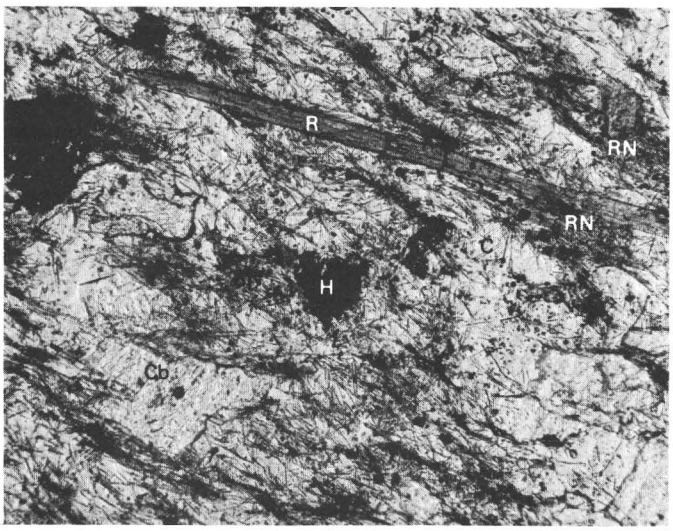

0.1 mm

A

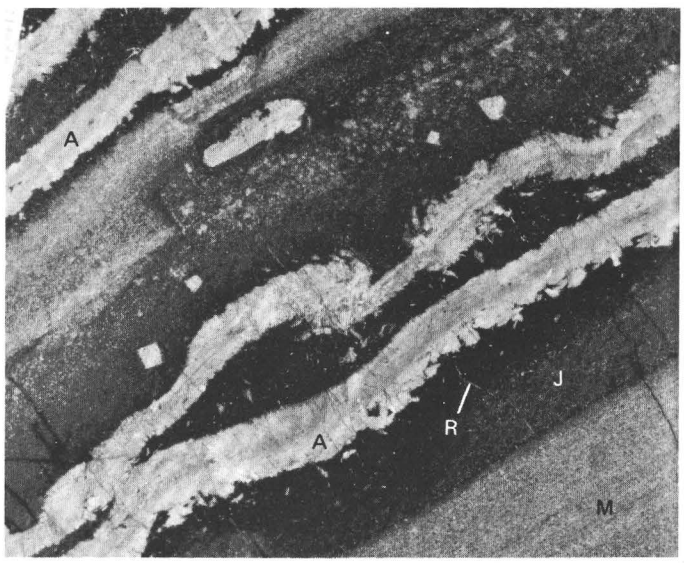

2 cm

C

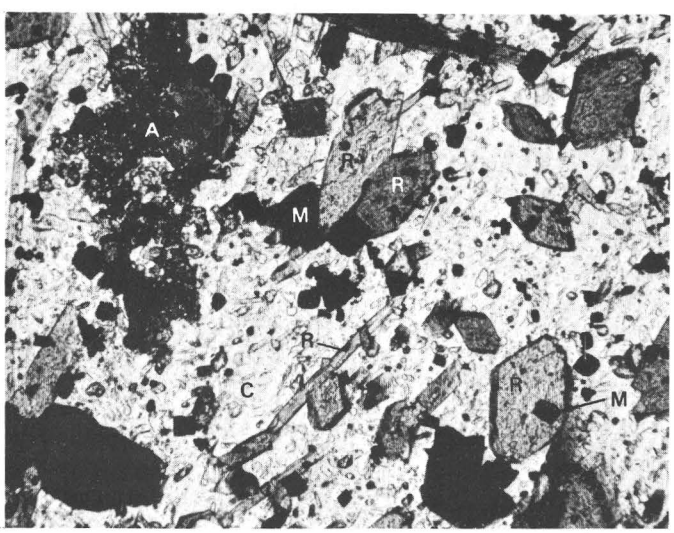

0.1 mm

B

FIGURE 54.—Sodic iron-formation. Empire mine. *A*, Photomicrograph of thin section. Matted clumps of tiny riebeckite needles (RN), and a coarse blade of riebeckite (R) in a matrix of chert (C), carbonate (Cb), and minor hematite (H). Plane-polarized light. *B*, Photomicrograph of thin section. Riebeckite (R), aegirinaugite (A), and magnetite (M) in a matrix of chert (C). Plane-polarized light. *C*, Finely ground surface showing seams of aegirinaugite (A) in layers of riebeckite (R)-chert bounded by layers of partly oxidized magnetite-riebeckite-chert (M) and jasper (J).

titic chert and magnetite-hematitic chert. Most samples of such iron-formation show some secondary oxidation. In general, the order of decreasing susceptibility of secondary oxidation in this rock is aegirinaugite, magnetite, fine-grained riebeckite, coarse riebeckite, and carbonate. Riebeckite-bearing layers and lenses are mainly hematitic chert or carbonate-chert, speckled or tinted by the characteristic blue color of the amphibole; otherwise, they resemble magnetite-chert-carbonate iron-formation. Some riebeckite-bearing lenses are rudely zoned, having mixtures of chert and riebeckite at the centers and chert, porphyroblasts of carbonate, and, in some lenses, minor amounts of riebeckite toward the margins. Remnants or wisps of magnetite laminae and scattered clastic grains are common in the riebeckite-bearing layers.

Riebeckite occurs mainly as randomly directed needles and blades and less commonly as fine fibers (fig. 54*A*), analogous to crocidolite[13]. The fibrous riebeckite (hereinafter called crocidolite) is rather susceptible to oxidation and pseudomorphous replacement by hematite.

In places, pale-green and oxidized brownish-red aegirinaugite occurs in seams as much as 0.5 mm thick sandwiched between and in clusters scattered in riebeckite-bearing cherty layers (fig. 54*C*). Paired laminae rich in aegirinaugite and riebeckite commonly are bounded by red jaspery chert laminae, which in turn may be bounded by laminated beds of magnetite and hematitic chert. Porphyroblasts of

[13] Han, T-M., 1953, Microscopic investigation of core specimens, diamond-drill holes 1 and 2, Empire project, sec. 19, T. 47 N., R. 26 W.: Cleveland Cliffs Iron Co. Metall. Rept. 100.

carbonate commonly are scattered along the contact between jaspery and magnetite-rich beds. The aegirinaugite typically forms large blade-shaped poikiloblasts containing inclusions of chert, carbonate, riebeckite, and magnetite. The most common inclusion, chert, may constitute as much as 30 percent of a poikiloblast.

Chemical analyses of riebeckite-bearing iron-formation are given in table 28, and analyses of two riebeckite concentrates are given in table 29.

TABLE 28.—*Chemical analyses of riebeckite iron-formation and riebeckite-aegirinaugite iron-formation, Empire mine*

[Analyses 1 and 2 by Chemical Laboratory, Cleveland Cliffs Iron Co. Analysis 3 by C. L. Parker, U.S. Geol. Survey. Failure of total for 1 to approximate 100 percent attributed mainly to incomplete measurement of CO_2 by loss on ignition (L.O.I.)]

	1	2	3
SiO_2	48.28	63.92	50.77
Al_2O_3	.33	.31	1.16
Fe_2O_3	27.74	22.87	27.77
FeO	14.28	6.56	11.95
MgO	1.35	.75	1.71
CaO	2.02	.74	1.97
Na_2O	.42	2.37	.53
K_2O	--	--	.23
H_2O^+	--	--	.17
H_2O^-	--	--	.05
TiO_2	.15	.15	.03
P_2O_5	.10	.21	.10
MnO	.40	.40	.39
CO_2	--	--	3.36
F	--	--	.02
S	--	--	.03
L.O.I.	2.35	.84	--
Total	97.42	99.12	100.24

1. Riebeckite-bearing iron-formation.
2. Riebeckite-aegirinaugite-bearing magnetite-hematitic chert iron-formation.
3. Riebeckite-bearing magnetite-chert iron-formation.

TABLE 29.—*Chemical analyses of riebeckite, Empire mine*

[Analysis 1 by Chemical Laboratory, Cleveland Cliffs Iron Co. Analysis 2 by C. L. Parker, U.S. Geol. Survey, n.d., not determined, L.O.I., loss on ignition]

	1	2
SiO_2	57.55	53.88
Al_2O_3	.52	.95
Fe_2O_3	21.29	17.67
FeO	9.26	11.43
MgO	5.85	7.25
CaO	.06	.07
Na_2O	6.14	6.75
K_2O		.07
H_2O^+		1.95
H_2O^-		.00
TiO_2		.08
P_2O_5		.00
MnO		.09
CO_2		n.d.
Cl		.00
F		.05
S		.02
L.O.I.	1.15	
Subtotal	101.82	100.26
Less O for F		.03
Total	101.82	100.23

1. Riebeckite-crocidolite concentrate from cherty iron-formation layer.
2. Riebeckite concentrate from foliated seam of riebeckite in iron-formation.

The value for Na_2O, 0.42 percent in No. 1, table 29, represents about 6.2 percent riebeckite in the rock, which by visual inspection, appears to be a rather typical amount. Silica and ferric iron oxide in No. 1, table 30, the riebeckite-crocidolite concentrate, are considerably higher than they should be in pure riebeckite; the excess is attributed to chert intergrown with crocidolite and to oxidation of some of the crocidolite to hematite. A chemical analysis of aegirinaugite from the Empire mine is abnormally high in silica because of chert inclusions, but when recalculated by assuming a normal silica content, 51.5 percent, the analysis rather closely resembles an acmite analysis from the Cuyuna Range, Minn. (table 30).

TABLE 30.—*Comparison of chemical analyses of aegirinaugite from Empire mine and acmite from Cuyuna iron range, Minnesota*

[L.O.I., loss on ignition]

	Aegirinaugite, Empire mine [1]		Acmite, Cuyana Range, Minn.[2]
	Actual	Recalculated	
SiO_2	62.85	51.50	51.64
Al_2O_3	.54	.71	1.05
Fe_2O_3	23.15	30.29	32.98
FeO	2.06	2.70	.14
MgO	1.15	1.50	.38
CaO	.20	.26	.60
Na_2O 4	9.29	12.15	12.21
L.O.I.	.68	.89	.45
Total	99.92	100.00	99.45

[1] Analysis by chemical laboratory, Cleveland Cliffs Iron Co.
[2] From Grout (1946, p. 129).

Sodium amphibole in iron-formation in the Mesabi Range, Minn. (White, 1954, p. 64–66), and acmite in the Cuyuna Range (Grout, 1946, p. 125) have been attributed to nearby igneous intrusions. Although mafic dikes cut the sodium-bearing iron-formation in the Empire mine, there is no evident relationship between the distribution of the sodium minerals and the dikes. The broad stratabound distribution of riebeckite and aegirinaugite, unrelated to intrusive bodies, and the association of the sodium minerals with hematitic jaspery layers in the dominantly magnetitic iron-formation, the association with hematitic cherty granules in places and with clastic grains of quartz and feldspar, and the gross associations of the sodium-bearing iron-formation with clastic beds all suggest that sodium was deposited syngenetically with the iron-formation in shallow water under strongly oxidizing conditions. Existing grains of sodium amphibole and sodium pyroxene are attributed to growth during diagenesis and (or) low-grade regional metamorphism. Possibly the tinier needles of riebeckite formed during

diagenesis and then in part recrystallized to coarser riebeckite during regional metamorphism simultaneously with a recrystallization of the sodium pyroxene.

UPPER UNIT OF IRON-FORMATION AND INTERBEDDED CLASTIC ROCK

The unit of magnetite-chert-carbonate iron-formation is overlain by a unit of interbedded iron-formation and clastic rock, 200–350 feet thick, extending across the length of the mine (pl. 2). Beds and lenses of clastic material (fig. 55) range in thickness from a few millimeters to about 15 feet, are as much as 100 feet long, and make up as much as 20 percent of the rock in the unit. The beds and lenses of clastic rock are distributed irregularly in the iron-formation and generally cannot be correlated between drill holes that are farther apart than 100 feet. Seams and thin layers of iron-formation are present within some beds of clastic rock, and, locally, fragmented iron-formation is cemented by clastic material. Clastic beds are in contact with iron-formation layers rich in carbonate or magnetite, but none has been seen in direct contact with chert layers. Contacts between clastic rock and iron-formation may be concordant or discordant and are generally sharp. Discordant contacts seem to have resulted from irregular compaction during sedimentation or later, and from the injection of clastic material into cracks in the iron-formation.

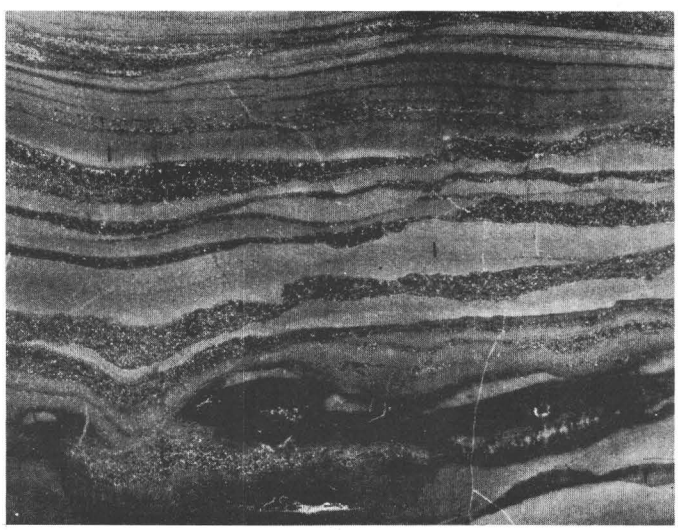

FIGURE 55.—Finely ground surface showing interbedded iron-formation (I) and clastic rock (C), Empire mine.

Iron-formation in the lower part of the interbedded unit consists mainly of magnetite-chert-carbonate similar to that in the underlying unit. Locally, chert-carbonate iron-formation also is present. The contact zone of the interbedded unit and the underlying magnetite-chert-carbonate unit is characterized by riebeckite-bearing magnetite-hematitic chert iron-formation such as described above. Much of the iron-formation in the upper part of the interbedded unit consists of mixtures of magnetite, carbonate, minnesotaite, stilpnomelane, and chert in that order of abundance.

The clastic rock in the interbedded unit is predominantly graywacke and feldspathic quartzite. The graywacke consists essentially of clastic quartz grains and a matrix of one or more of the minerals chlorite, minnesotaite, stilpnomelane, biotite, magnetite, carbonate, and chert. The feldspathic quartzite contains clastic grains of quartz, microcline, orthoclase, and plagioclase, and a subordinate matrix of varying combinations of biotite, chlorite, carbonate, chert, and magnetite.

Typical sections of the unit of interbedded iron-formation and clastic rock are cut by Empire drill holes 18 and 59, respectively in the SW¼ and NW¼ of sec. 19, about 2,000 feet apart (pl. 2); the sections are described in table 31.

TABLE 31.—*Logs of two drill holes cutting upper interbedded iron-formation and clastic rock, Empire mine, sec. 19, T. 47 N., R. 26 W.*

Depth (ft)	Lithology
	Diamond-drill hole 18
4–61	Magnetite-carbonate-chert-silicate iron-formation.
	Upper interbedded unit.
61–75	Magnetite-carbonate-chert-silicate iron-formation with clastic seams.
75–76	Graywacke (chlorite matrix).
76–77	Magnetite-carbonate-chert-silicate iron-formation.
77–78	Graywacke (stilpnomelane matrix).
78–89	Magnetite-carbonate-chert-silicate iron-formation cut by chloritic dikes.
89–92	Graywacke (chlorite-biotite matrix).
92–104	Magnetite-carbonate-chlorite-chert iron-formation with interbedded chloritic graywacke.
104–109	Graywacke (chlorite-magnetite matrix).
109–116	Magnetite-carbonate-chlorite-chert iron-formation with interbedded chloritic graywacke.
116–117	Graywacke (chlorite-biotite matrix).
117–159	Magnetite-carbonate-chert-chlorite iron-formation.
159–176	Graywacke (chlorite-biotite matrix).
176–179	Magnetite-carbonate-chert-chlorite iron-formation.
179–184	Graywacke (chlorite matrix).
184–186	Magnetite-carbonate-chert-chlorite iron-formation (partly oxidized).
186–192	Graywacke (chlorite-magnetite matrix).
192–208	Magnetite-carbonate-chert-chlorite iron-formation.

TABLE 31.—*Logs of two drill holes cutting upper interbedded iron-formation and clastic rock, Empire mine, sec. 19, T. 47 N., R. 26 W.*—Continued

Depth (ft)	Lithology
	Diamond-drill hole 18
208–214	Graywacke (chlorite matrix).
214–241	Magnetite-carbonate-chert-chlorite iron-formation.
241–252	Feldspathic quartzite.
252–288	Magnetite-chert-carbonate iron-formation (locally hematitic).
288–289	Graywacke (chlorite matrix).
289–306	Magnetite-carbonate-chert iron-formation.
306–315	Magnetite-carbonate-chert iron-formation with interbedded chloritic graywacke.
315–320	Graywacke (chlorite matrix).
320–330	Magnetite-carbonate-chert iron-formation.
330–340	Chloritic graywacke with interbedded magnetite-carbonate-chert iron-formation.
340–345	Magnetite-chert-carbonate iron-formation.
345–347	Feldspathic quartzite.
347–360	Magnetite-chert-carbonate iron-formation.
360–405	Riebeckite-bearing magnetite-hematitic chert iron-formation.
Bottom of interbedded unit.	
405–619	Magnetite-chert-carbonate iron-formation.
619	End of drill hole.
	Diamond-drill hole 59
0–290	Carbonate-chert iron-formation.
290–744	Magnetite-carbonate-silicate-chert iron-formation cut by chloritic dikes.
Upper interbedded unit.	
744–778	Magnetite-carbonate-silicate-chert iron-formation with interbedded graywacke.
778–780	Chloritic dike.
780–816	Magnetite-carbonate-silicate-chert iron-formation with interbedded graywacke.
816–821	Graywacke.
821–842	Magnetite-carbonate-silicate-chert iron-formation.
842–893	Graywacke (biotite matrix) with interbedded iron-formation.
893–914	Feldspathic quartzite.
914–919	Magnetite-carbonate-chert iron-formation with some interbedded graywacke (carbonate-rich matrix).
919–922	Graywacke (chlorite-biotite matrix).
922–927	Magnetite-carbonate-chert iron-formation.
927–932	Graywacke (chlorite-biotite matrix).
932–945	Magnetite-carbonate-chert iron-formation.
945–947	Graywacke (chlorite-biotite matrix).
947–972	Magnetite-carbonate-chert iron-formation.
972–1,002	Graywacke (chlorite matrix).
1,002–1,012	Magnetite-carbonate-chert iron-formation.
1,012–1,026	Chloritic graywacke with some beds of iron-formation.
1,026–1,029	Feldspathic quartzite.
1,029–1,049	Chloritic graywacke with some interbedded magnetite-carbonate-chert iron-formation.
1,049–1,075	Magnetite-chert-carbonate iron-formation with some interbedded chloritic graywacke.
1,075–1,112	Riebeckite-bearing magnetite-hematitic chert iron-formation.
1,112–1,125	Magnetite-chert-carbonate iron-formation.
1,125–1,131	Riebeckite-bearing magnetite-hematitic chert iron-formation.
Bottom of interbedded unit.	
1,131–1,560	Magnetite-chert-carbonate iron-formation.
1,560	End of drill hole.

IRON-FORMATION COMPONENT

Iron-formation of the interbedded unit is characterized by wavy-bedded pinch-and-swell structure that is accentuated by the interspersed lenses of clastic rock (fig. 55). Clastic lenses commonly produce load casts in immediately underlying iron-formation. The dominant magnetite-chert-carbonate lithology in the lower part of the unit, the chert-carbonate beds throughout, and the minnesotaite-bearing iron-formation in the upper part are similar compositionally to varieties of iron-formation in the underlying units already described, so in general are not considered further. However, replacement features in the interbedded unit, differing somewhat from those already described in the magnetite-chert-carbonate iron-formation, are discussed below, and additional chemical analyses of four varieties of silicate-bearing iron-formation and one of partly altered hematitic iron-formation are listed (table 32). Spectrographic analyses of 45 drill-core samples indicate that the iron-formation of the interbedded unit contains traces of vanadium, and that the amount of manganese decreases downward in the unit.

TABLE 32.—*Chemical analyses of silicate-bearing and hematitic iron-formation, upper part of interbedded iron-formation and clastic rock*

[Failure of totals for Nos. 1, 3, and 4 to approximate 100 percent attributed to incomplete measurement for CO_2 by loss on ignition (L.O.I.). Analyses by Chemical Laboratory, Cleveland Cliffs Iron Co.]

	1	2	3	4	5
SiO_2	42.12	42.42	28.82	25.08	75.58
Al_2O_3	.55	3.87	1.35	.91	.38
Fe_2O_3	30.31	31.67	30.60	35.40	15.44
FeO	17.23	18.01	27.02	26.24	4.12
MnO	1.26	.09	1.58	2.81	1.15
MgO	.95	1.30	2.08	.56	.14
CaO	.34	.67	.76	.44	.12
TiO_2	.13	.22	.20	.03	.03
P_2O_5	.06	.49	.08	.25	.03
FeS_2	--	.15	.01	--	--
L.O.I.	4.89	.74	3.07	6.08	2.18
Total	97.84	99.63	95.57	97.80	99.17

1. Pit sample, Empire mine; hematite-bearing magnetite-carbonate-silicate-chert iron-formation.
2. Pit sample, Empire mine; magnetite-chert iron-formation.
3. DDH 57 (see pl. 2) footage 563–615; magnetite-silicate-carbonate iron-formation.
4. Pit sample, Empire mine; magnetite-carbonate-chert-silicate iron-formation.
5. Pit sample, Empire mine; hematite-chert-carbonate iron-formation.

REPLACEMENT FEATURES IN IRON-FORMATION COMPONENT

Hematitic layers and lenses.—Near 18,800S–3,600W in the Empire mine (pl. 2), in the upper part of the interbedded unit, lenses and layers of hematite-chert and hematite-chert-carbonate are interbedded and in sharp contact with laminated magnetite-carbonate-chert-silicate iron-formation. Irregular aggregates of hematite coexist with magnetite and granular carbonate, mainly near the tops and

bottoms of layers, and decrease in amount toward the centers of layers. Hematite replaces some carbonate grains pseudomorphously, so all the hematite is believed to have replaced carbonate by oxidation. In some layers of magnetite-carbonate-silicate-chert iron-formation interbedded with the hematitic layers, very selective oxidation has taken place. Coarser carbonate grains, believed to have been ankerite by analogy with similar coarse carbonate in the underlying magnetite-chert-carbonate unit, have been completely replaced by hematite, whereas coexisting finer grained siderite and magnetite have been unaffected by the oxidation.

Magnetite layers.—Magnetite is concentrated along some boundaries between carbonate layers and magnetite-bearing clastic layers and decreases toward the centers of the carbonate layers. Such magnetite is believed to have formed by partial replacement of the carbonate layers.

Carbonate layers.—Carbonate is concentrated along some interfaces between layers of magnetite-chert-carbonate and layers of chert or chert and riebeckite, or between layers of magnetite-chert-silicate-carbonate and layers of minnesotaite and chert or stilpnomelane and chert. Such carbonate is in coarse anhedral to euhedral crystals, contains chert inclusions and, in places, relicts of magnetite-rich laminae, and therefore seems to have formed after deposition, by partial replacement of the bounding layers.

Residual "island" structures.—In places, residual "islands" of laminated iron-formation occur in layers that differ compositionally from the "islands." In general, such "islands" resemble those in underlying units (see figs. 47*A*, *C*). Reaction zones of carbonate and (or) chert envelop the "islands." Layers in which the "islands" occur are interpreted as replacements of earlier layers now represented only by the "islands." Three types of such replacement have been found in the interbedded unit.

(1) "Islands" of magnetite-chert-carbonate in a layer of carbonate-chert iron-formation are bordered by a narrow reaction zone of carbonate and chert. Trains of clastic quartz extend from within some "islands" through the reaction zone into the enclosing layer, similar to the clastic lens shown in figure 51*C*. Magnetite of the original layer evidently has been replaced by carbonate.

(2) "Islands" of magnetite-chert-carbonate-silicate are rimmed by a reaction zone of concentrically arranged coarse-grained carbonate, chert, and coarse-grained carbonate, all enclosed in a layer of carbonate-chert-silicate iron-formation. A layer of silicate-chert bordering the layer containing the "islands" is extensively fractured opposite the "islands," and the fractures are filled with cherty quartz. Possibly compaction and slight arching of the layer around "islands" during replacement produced tension fractures in relatively brittle cherty layers.

(3) "Islands" of hematite-magnetite-silicate-chert occur in a layer of magnetite-chert-carbonate iron-formation. The hematite is fibrous and is a major constituent. The "islands" are surrounded by a shell of chert. Bordering laminae rich in magnetite are bent around the "islands," whereas magnetite laminae in the layer containing the "islands" have been locally replaced by chert of the shell. Evidently silicate in the original layer has been replaced by carbonate, magnetite, and chert, and much of the hematite in the "islands" appears to have been derived from iron silicate.

Growth and alteration of porphyroblasts.—Porphyroblasts of grunerite (drill holes 57 and 66, pl. 2) appear to replace carbonate and magnetite, probably by contact metamorphism during the emplacement of nearby mafic intrusions. Some grains of grunerite in turn have been replaced pseudomorphously by hematite. Grains of carbonate resembling porphyroblasts are scattered in some chert layers and in places have been replaced pseudomorphously by hematite or partly replaced by chlorite. They probably formed during diagenesis or regional metamorphism.

Clastic Component

The clastic component of the interbedded unit consists of graywacke and feldspathic quartzite. Both are irregularly distributed in the unit. Where the two types of clastic rock are in contact, the graywacke generally seems to cut the feldspathic quartzite.

Graywacke.—A large but undetermined proportion of the clastic rock in the interbedded unit can be classified as graywacke—dark-green to gray rock in which silt- and sand-sized angular to rounded quartz and feldspar grains more or less float in a finer grained matrix composed typically of one or more micaceous iron silicate minerals, with or without carbonate, magnetite, and chert. Titaniferous magnetite, tourmaline, zircon, and monazite are minor minerals, found locally. Most of the silty and

sandy clastic grains are quartz, but the matrix is varied. The most common mineral compositions of the matrix are chlorite, chlorite-biotite, chlorite-magnetite-chert, minnesotaite, chlorite-minnesotaite, minnesotaite-magnetite, stilpnomelane, stilpnomelane-magnetite, magnetite-chert-biotite, and magnetite-chlorite-chert-carbonate. The existing matrix minerals have a recrystallized fabric and undoubtedly are a product of reactions and replacements of original ferruginous, siliceous mud. In general, though, because of complete recrystallization, the nature of the original sediment is obscure. Some graywacke beds are graded. Chemical analyses of four graywackes are given in table 33.

TABLE 33.—*Chemical analyses of drill-hole samples of clastic rock, upper interbedded unit, Empire mine*

[Reasons unknown for some totals not approximating 100 percent. L.O.I., loss on ignition. Chemical analyses by Chemical Laboratory, Cleveland Cliffs Iron Co.]

	1	2	3	4	5	6
SiO_2	81.29	83.83	74.93	74.03	52.52	53.03
Al_2O_3	4.00	4.15	5.87	6.10	4.80	4.53
Fe_2O_3	4.86	.57	4.15	5.72	5.00	13.15
FeO	4.50	6.17	7.59	7.59	23.67	18.53
MnO	.27	.15	.19	.12	.48	.37
MgO	1.00	.75	1.45	1.44	3.00	1.90
CaO	1.05	.12	.10	.59	.34	.48
TiO_2	.24	.21	.23	.28	.20	.27
P_2O_5	.02	.03	.04	.02	.02	.02
L.O.I.	2.37	3.16	2.20	1.65	6.03	4.96
Total	99.60	99.14	96.75	97.54	96.06	97.24
Magnetite	6.61	.20	2.28	4.54	3.70	13.69

1. Diamond-drill hole (DDH) 58, at 535 ft; feldspathic quartzite.
2. DDH 59, at 904 ft; feldspathic quartzite.
3. DDH 59, at 886 ft; chlorite-biotite graywacke.
4. DDH 59, at 1,049 ft; chlorite-biotite graywacke.
5. DDH 57, at 580 ft; minnesotaite graywacke.
6. DDH 58, at 68 ft; stilpnomelane graywacke.

Feldspathic quartzite. — Feldspathic quartzite forms part of the clastic component of the upper interbedded unit. The quartzite is massive, pinkish gray, locally crossbedded, and typically occurs in small pockets and irregular lenses. It contains as much as 20 percent feldspar—microcline, orthoclase, and plagioclase in order of abundance—mixed with the clastic quartz. Quartz and feldspar grains are subangular to well rounded, have low to moderately high sphericities, and range in size from 0.005 to 0.25 mm. Quartz grains commonly impinge on one another in sutured contacts. Subordinate amounts of the common matrix minerals of the graywacke are present in the feldspathic quartzite. Chemical analyses of two feldspathic quartzites are listed in table 33.

Replacement Features in Clastic Component

Replacement of margins of clastic grains.—Marginal replacement of clastic grains by chlorite, minnesotaite, stilpnomelane, magnetite, and carbonate is a characteristic feature of the graywacke. Some chlorite occurs in aggregates and granules having shapes like those of clastic quartz grains and may be complete replacements of such clasts. In places, reaction between iron silicate matrix and sand grains in the graywacke has produced reaction rims of feathery and acicular grains of minnesotaite or stilpnomelane on the margins of clasts (fig. 46*C*), or in a shell slightly inside the existing margins (fig. 46*D*). The quartz outside the silicate shell in the latter type of grain may be a secondary overgrowth. Clusters of iron silicate have grown in the cores of some clasts, probably where iron and hydroxyl of the silicate were able to enter clastic grains along minute cracks.

Some layers in the interbedded unit that superficially resemble graywacke consist of quartz clasts that are largely replaced by minnesotaite like those shown in figure 46*E*, and clastlike granules of minnesotaite, as shown in figure 46*F*. Whether the granules are original depositional features or completely silicated grains or clastic quartz is debatable. However, the presence of silicate granules and partly silicated quartz clasts of similar size and shape in the same layer suggests that some silicate granules are pseudomorphs of quartz clasts.

Postdepositional growth of magnetite.—Crystals of magnetite are common in the graywacke (fig. 56). Many such crystals have grown into the margins of clastic quartz grains. These grains may have formed during diagenesis, regional metamor-

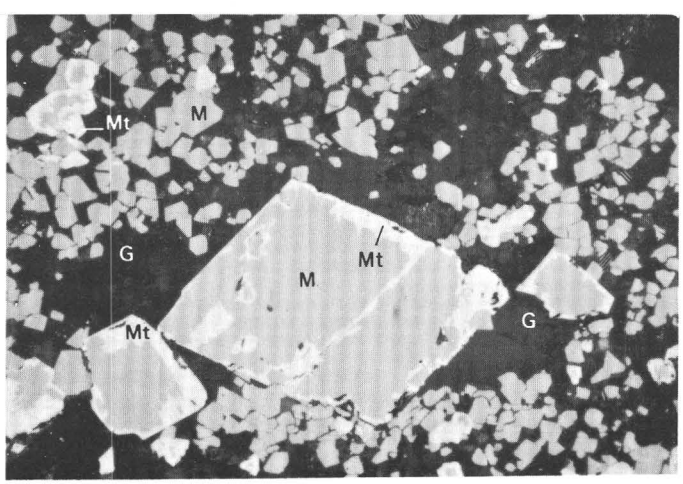

FIGURE 56.—Photomicrograph of finely ground section showing two sizes of magnetite crystals (M) in chloritic graywacke (G). Larger magnetite crystals are partly oxidized to hematite (martite, Mt). The largest magnetite crystal contains several small magnetite inclusions outlined by martite.

phism, or both, so far as can be determined from the evidence. Partial pseudomorphous replacement of such magnetite by hematite (martite) is common (fig. 56).

Clastic grains of intergrown ilmenite-magnetite in some of the graywacke have served as cores for overgrowths of magnetite.

Grunerite porphyroblasts.—Grunerite porphyroblasts occur not only in iron-formation near mafic intrusive bodies, as noted above, but also in some graywacke beds. In Empire drill holes 57 and 66 (pl. 2), grunerite partly replaces quartz clasts.

LITHOLOGY AND STRATIGRAPHY OF IRON-FORMATION IN PALMER BASIN

In the west half of the Palmer basin, south of the Volunteer fault and west of the northwest-trending Richmond fault in the south part of sec. 28, T. 47 N., R. 26 W., the Negaunee Iron-Formation consists largely of jaspilite, magnetite-chert and magnetite-carbonate-chert iron-formation, and altered (oxidized, leached) iron-formation (pl. 3) that was almost certainly derived from the magnetite- and carbonate-rich varieties. Jaspilite occupies much of the stratigraphic section of iron-formation between the Goodrich and Ajibik Quartzites in the SW¼ sec. 29 and the NW¼ sec. 32, and west of there. In the NE¼ sec. 32, a zone of dominantly magnetite-chert and magnetite-carbonate-chert iron-formation as much as several hundred feet thick underlies jaspilite in the basal part of the Negaunee. In that area and to the north in the SE¼ sec. 29, and northeast in sec. 28, jaspilite in the upper and lower parts of the iron-formation is separated by an irregular zone of dominantly rusty brown, red-brown, and yellow-brown altered (weathered, oxidized) hematitic and goethitic iron-formation. Unaltered beds of magnetite-chert and magnetite-carbonate-chert in this zone suggest the derivation of the oxidized iron-formation from such rock. East of the fault that crosses the south part of sec. 28, the iron-formation consists essentially of assemblages of magnetite-chert, magnetite-iron carbonate-chert, magnetite-iron silicate-chert, and iron carbonate-chert. In the east half of the Palmer basin the iron minerals are extensively oxidized to martite, red brown hematite, and goethite in virtually all exposures, and in places the oxidized zone extends downward from the surface through practically the entire thickness of iron-formation. In the deep west-central part of the Palmer basin, north of the Volunteer fault in sec. 29, iron-formation beneath a cover of about 1,000 feet of Goodrich Quartzite has been cut by several drill holes. Iron-formation in the one available drill core consists mainly of magnetite and chert and of jaspery layers of chert, hematite, and magnetite. Carbonate iron-formation is a very minor component of the Negaunee in that area.

Iron-formation containing sideritic carbonate as a major constituent underlies jaspilitic or magnetite-rich varieties beneath parts of the northwest-trending Isabella syncline in the S½SW¼ sec. 29. A drill hole at approximately 770N—820E of the SW. cor. sec. 29 cuts approximately 200 feet of Goodrich Quartzite and 190 feet of underlying jaspilitic and magnetitic iron-formation and then a 50–foot zone of sideritic iron-formation, below which is approximately 130 feet of magnetitic and brownish oxidized iron-formation to the bottom of the hole (pl. 3). Another drill hole about 800 feet to the east-northeast (approximately 1,040N–1,540E of the SW. cor. sec. 29, near the Goodrich-Negaunee contact), passes through approximately 88 feet of the Goodrich, 150 feet of underlying jaspilitic iron-formation, and then 140 feet of dominantly carbonate-facies iron-formation to the bottom of the hole. Drill holes crossing the same section of iron-formation in the central part of the NW¼ sec. 32, 800–1,800 feet updip to the south and south-southeast penetrate jaspilitic, magnetitic, and brown oxidized iron-formation, but virtually no carbonate iron-formation. Some of this iron-formation passes along strike from northeast to north, into brown oxidized iron-formation containing unoxidized remnants of carbonate-facies and chert-magnetite iron-formation in the NW¼NE¼ sec. 32 and the SW¼SE¼ sec. 29. Some of the jaspilitic and magnetitic iron-formation in the center of the NW¼ sec. 32 therefore passes into or is interbedded with carbonate-facies iron-formation both downdip and along strike.

CLASTIC SEDIMENT

Most clastic materials in iron-formation in the Palmer basin are found between the falls of Warner Creek near the SE cor. sec. 30 and the New Richmond mine in the SW¼ sec. 27, T. 47 N., R. 26 W. (see pl. 1). The best exposures are at the old Moore mine in the NE¼ sec. 33, and on the hill due south of the main north-south street in the village of Palmer (street equivalent to Michigan Highway 35), near 200N–350W of SE. cor. sec. 30. Other good exposures are at the falls of Warner Creek immediately west of Michigan Highway 35 in the NE¼ sec. 31; at 4,800N–850E and 4,550N–100E of SW.

cor. sec. 32; near 650S–200E of NW. cor. sec. 33, and at the west end of the Old Richmond mine in the SW¼SW¼ sec. 28. Clastic materials at the old Moore mine include numerous thin sandy and pebbly lenses, a lens of wacke about 50 feet in maximum thickness and 400 feet long, and several short thick lenses of pebbly and cobbly conglomerate, which in the present exposure are probably cross sections of original north-trending, north-sloping filled stream channels or submarine mudflows. Excellent descriptions of the clastic sediments at the Moore mine have been given by Mengel (1956). On the hill in sec. 30, south of the village of Palmer, graywacke-like lenses, varying from about one eighth inch to 6 inches in thickness, alternate quite regularly with laminae of jasper and hematite through a total thickness of about 40 feet just below the conformable and somewhat gradational contact existing between Negaunee Iron-Formation and overlying Goodrich Quartzite in that part of the area. In the northwest wall of the Old Richmond mine, a weathered granitic boulder, 1–2 feet in diameter, and several somewhat smaller rock fragments are isolated in the iron-formation approximately 700 feet above the base of the formation. Near the old Maitland mine, in an exposure at 2,950N–900W of SW. cor. sec. 30, more than half of a thickness of 30–40 feet of interbedded jaspilite and clastic rock consists of lenses, each as much as several inches thick, of ferruginous graywacke and pebbly conglomerate. This rock may be that noted by Tyler and Twenhofel (1952, p. 130–131) as being hundreds of feet above the base of the iron-formation. Isolated outcrops of quartzite and conglomerate 200 feet to the northeast may also be part of the clastic rock in the iron-formation referred to by Tyler and Twenhofel, but in the present study these have been mapped as Ajibik Quartzite just north of the Palmer fault. Clastic sediment in the iron-formation is common in drill holes in the south part of sec. 29 and north part of sec. 32, in the central part of sec. 29 just east of the village of Palmer, along the line between secs. 28–29 and 32–33, and at the southeast end of the Palmer basin in the southeast part of sec. 27 and the southwest part of sec. 26.

Clastic sediment is distributed through much of the iron-formation in the south part of the Palmer basin in sec. 28, 29, and 32 (fig. 57), but evidently is not present through considerable thicknesses of the iron-formation farther east, and north of the Volunteer fault in sec. 29. Although clastic beds are common near the top and bottom of the iron-formation they are not particularly confined to those zones, and some of the thickest layers, or most numerous groupings of thin layers, occur well away from the top and bottom and near the middle of the section.

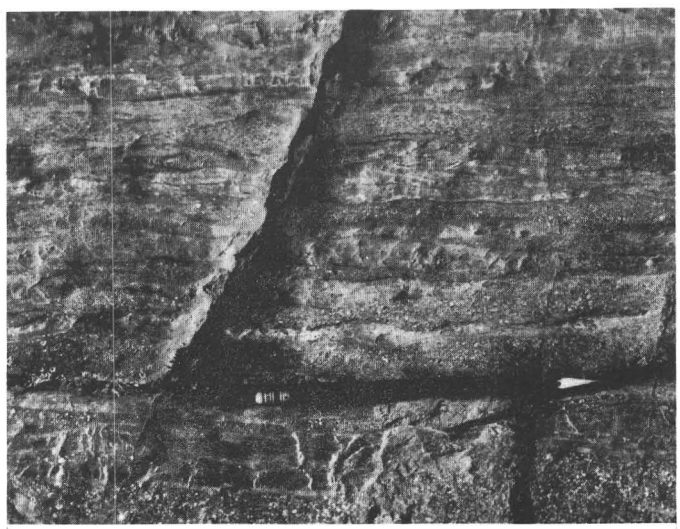

A

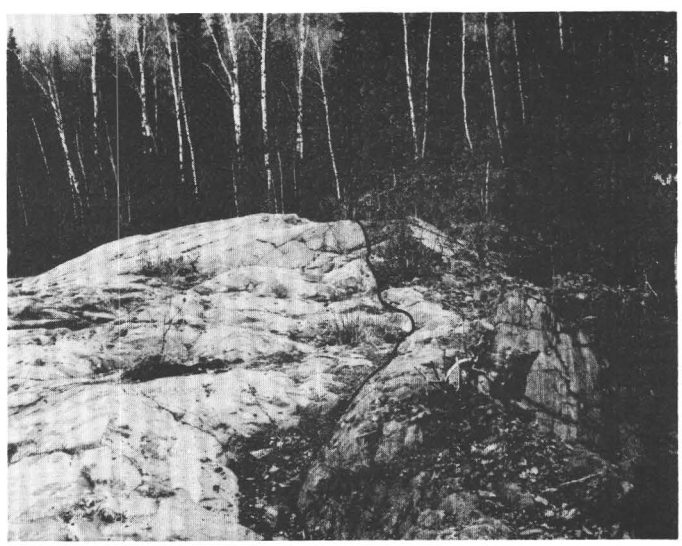

B

FIGURE 57.—Clastic beds in Negaunee Iron-Formation. *A*, Interbedded graywacke and jaspilite, approximately 100 feet stratigraphically below top of Negaunee Iron-Formation, near 150N–380W of SE. cor. sec. 30, T. 47 N., R. 26 W. *B*, Lens of wacke; maximum thickness of lens is about 50 feet. Lower conformable contact of lens with iron-formation marked by inked line. Upper conformable contact of lens is outside photograph to the left. Faint mottling of wacke caused by irregular weathering and oxidation. East end of old Moore mine, Palmer basin, view east, near 100S–1,700W of NE. cor. sec. 33, T. 47 N, R. 26 W.

Mengel (1956) deduced that clastic sediments occur throughout the iron-formation south and east of Palmer. Davis (1965) reached a similar conclusion after finding clastic grains in all but 12 of 300 thin sections made from drill core of 9 or 10 drill holes cutting a large part of the iron-formation in the SE¼ sec. 29 and the NE¼ sec. 32. The distribution of clastic material in the deeper north and central part of the basin is not well known. Drilling done just east of the village of Palmer indicates that clastic beds are spaced through much of the section of iron-formation, but at much greater intervals, generally, than in the south part of the basin.

The total proportion of clastic material in any given stratigraphic section is difficult to assess because of incomplete exposures and scattered quartz grains in the iron-formation, but in three drill holes (fig. 58) cutting nearly the full thickness of the iron-formation—400–700 feet—in the south-central part of the Palmer basin (NW¼ sec. 32), clastic sediment makes up 5–9 percent of the Negaunee, of which 3–6 percent has been measured in discrete layers and an estimated 2–3 percent occurs as scattered grains. The full section of iron-formation in that area contains hundreds of clastic lenses less than one-half inch thick and a few layers greater than 1 foot thick. Layers of iron-formation between clastic beds are generally less than 10 feet thick; a few layers are 30–50 feet thick. Clastic layers can be seen to lense out in outcrops and drill core, and neither thick single layers nor closely spaced groups of layers occurs at consistent distances from the base of the Negaunee in different drill holes, so evidently they are of local extent. One drill hole from which core is available in the central part of the basin just east of Palmer (fig. 58, P–4A) passes through about 1,000 feet of Goodrich Quartzite and then cuts a complete section of iron-formation, about 1,400 feet, down to Ajibik Quartzite. In this section, thin widely spaced clastic laminae form about 1 percent of the section in the upper 800 feet, and in the lower 600 feet several thick beds of graywacke make up about 27 percent of the section.

Most of the detritus in the iron-formation in the Palmer basin is angular and subangular quartz and ranges in size from fine to coarse sand grains, 0.1–2.0 mm in diameter. Detrital materials occur mainly in beds and lenses of graywacke, seams of quartz grains, and quartz grains scattered through laminae of iron-formation (fig. 59). Detrital grains in the graywacke are loosely packed or "float" in a matrix consisting mainly of chlorite, chlorite-magnetite, or hematite. Sericite and chert may be minor matrix minerals. Detrital feldspar, which is abundant in some beds in the Empire mine, is rare in the Palmer basin. Most beds are quartz-chlorite graywacke (fig. 59*B*); the association of chlorite with clastic quartz is exceedingly common, even in isolated clusters containing only a few clasts. Chloritoid of probable metamorphic derivation from aluminous clay has been found in a lens of impure quartzite, one of several such lenses, each a few inches thick, that are interbedded with jaspilitic iron-formation in the NW¼ sec. 32 (fig. 59*A*).

In places, pebbles are mixed with the sand-sized detritus, and elsewhere in the iron-formation are isolated cobbles and boulders of vein quartz, quartzite(?), and granitic rock, as much as 2 feet in diameter. The best examples of such coarse detritus occur toward the southeastern end, south side, of the old Moore mine, near the line between the SE¼ sec. 28 and the NE¼ sec. 33 (Mengel, 1956), and along the northwest wall of the Old Richmond mine in the SW¼SW¼ sec. 28 (Tyler and Twenhofel, 1952).

ORIGIN OF THE IRON-FORMATION

Iron-formation has been widely ascribed to chemical precipitation in lagoons, lakes, or the sea, but vital problems about its origin remain unsolved. Guild (1957, p. 46) summarized the outstanding problems relating to the origin of chert and cherty iron-formation as "(1) the source of the vast quantities of iron and silica; (2) the mode of transportation; (3) conditions which permitted their selective concentration and the exclusion of other materials; and (4) the rhythmic layering of the formations." The Negaunee Iron-Formation has provided additional but inconclusive evidence mainly about the first, third, and fourth of the problems listed by Guild.

The source of iron and silica has been considered by one group of geologists to be volcanic material erupted contemporaneously with the deposition of the iron-formation (for example, Winchell, 1899; Van Hise and Leith, 1911, p. 513–516; Aldrich, 1929, p. 143–144; Goodwin, 1956, p. 589–590; 1962, p. 573–584; Trendall and Blockley, 1970, p. 273–276). Others have maintained that chemical weathering of land areas could have provided sufficient iron and silica, basing this conclusion partly on the lack of evidence for volcanism during periods when several important iron-formations were deposited (for example, Gruner, 1922, p. 459; James, 1954, p. 276–281; White, 1954, p. 50). Inasmuch as alumina must also be an abundant product of the assumed weathering,

the generally insignificant amount of alumina in iron-formation and associated rocks is a serious drawback to the weathering hypothesis.

The Negaunee Iron-Formation contains thick sill-like bodies of metadiabase which metamorphosed parts of the iron-formation during their emplacement, so are younger than the iron-formation. Other thin conformable bodies of highly altered igneous rock are also present in the iron-formation, but are comparatively few and generally are not more than a few feet thick. They could be companion bodies of the thick sills or might have been volcanic flows or ash beds. Therefore, contemporaneous volcanism cannot be ruled out in the Palmer quadrangle during Negaunee time. Even though the volume of volcanic rock extruded near sites of iron-formation deposition was trifling compared with the volume of iron-formation, contemporaneous volcanism at a distance from such sites could have added significant amounts of iron and silicon to the sea water from which the iron-formation precipitated.

The broad area of lower Precambrian mafic rock north of the eastern part of the Marquette synclinorium, and amphibolitic rock in the basement gneiss south of the synclinorium, are possible sources of ferruginous sediments by weathering. Near Palmer, the iron-formation contains some clastic beds containing chloritoid which indicate the deposition of minor amounts of aluminous sediment during Negaunee time.

Thus, the Negaunee Iron-Formation contains evidence of possible contemporaneous volcanism and evidence that at least small amounts of aluminous sediment were present during deposition of the formation. However, neither line of evidence provides unequivocal support for a principal source of iron and silicon by either volcanism or weathering.

Moore and Maynard (1929), Sakamoto (1950), Guild (1957), Trendall and Blockley (1970), and others have discussed the rhythmic layering of iron minerals and silica. Moore and Maynard showed experimentally that layering can be produced from colloidal mixtures of iron and silica in an electrolyte because of the faster precipitation of the iron. Sakamoto concluded that differences in the solubilities of iron and silica caused their precipitation from dilute solutions, in alkaline and acid environments, respectively, and that such environments could be established by variations of pH 5 to pH 9 from wet to dry seasons. Guild noted that such large seasonal changes in pH would be unlikely to occur uniformly across a large depositional basin such as that in which the Brazilian Cauê Itabirite (iron-formation) had been deposited. Using the experimental findings of Moore and Maynard, Guild postulated that the layering of itabirite was caused by periodic fluctuations in the volume of river water carrying iron and silica into the depositional basin. Thicker layers were related to seasonal and longer climatic variations, sharply defined laminae were related to pronounced variations in seasonal rainfall, and layers of mixed silica and hematite were related to periods of year-round rainfall and a constant addition of material to the basin of deposition. Trendall and Blockley proposed seasonal and longer-period climatic controls. The studies just mentioned do not touch on the origin of rhythmic laminations of different iron minerals, which are as characteristic a feature of the Negaunee Iron-Formation as layered iron minerals and chert.

Explanations for layered iron minerals and chert that involve substantial changes in pH and the volume of iron and silica as a result of large seasonal changes in rainfall do not seem to be adequate to account for interlaminations of different iron minerals alone. The practically infinite variety of laminations and the lensing of aggregates of different iron minerals indicate small changes in the concentrations of dissolved iron, silica, oxygen, and carbon dioxide in the depositional or diagenetic environment, almost continuously in time and within short distances laterally. The small sizes of separate chemical environments make it difficult to perceive a direct relationship between the minor chemical variations and controls exerted by large-scale or regionwide factors such as seasonal climatic changes, seasonal changes in the salinity and mineral content of sea water, or fluctuations in the depth of the sea. The innumerable small changes seem to be more readily explained as a direct result of some sort of self-regulating mechanism, taking place almost continuously. Perhaps small widespread fluctuations in the amounts of iron, silica, oxygen, and carbon dioxide dissolved in sea water were caused by continuous or seasonal additions of these components, and these fluctuations were in turn modified locally by currents and the successive precipitation of first one iron mineral and then another. Garrels (1959, p. 33) stated that changes in the composition of a solution as a result of the precipitation of one mineral may cause the solution to become supersaturated in one or more additional solids.

Chert is present in rocks of many areas and geologic periods and evidently formed in several ways involving the replacement of diatomaceous or

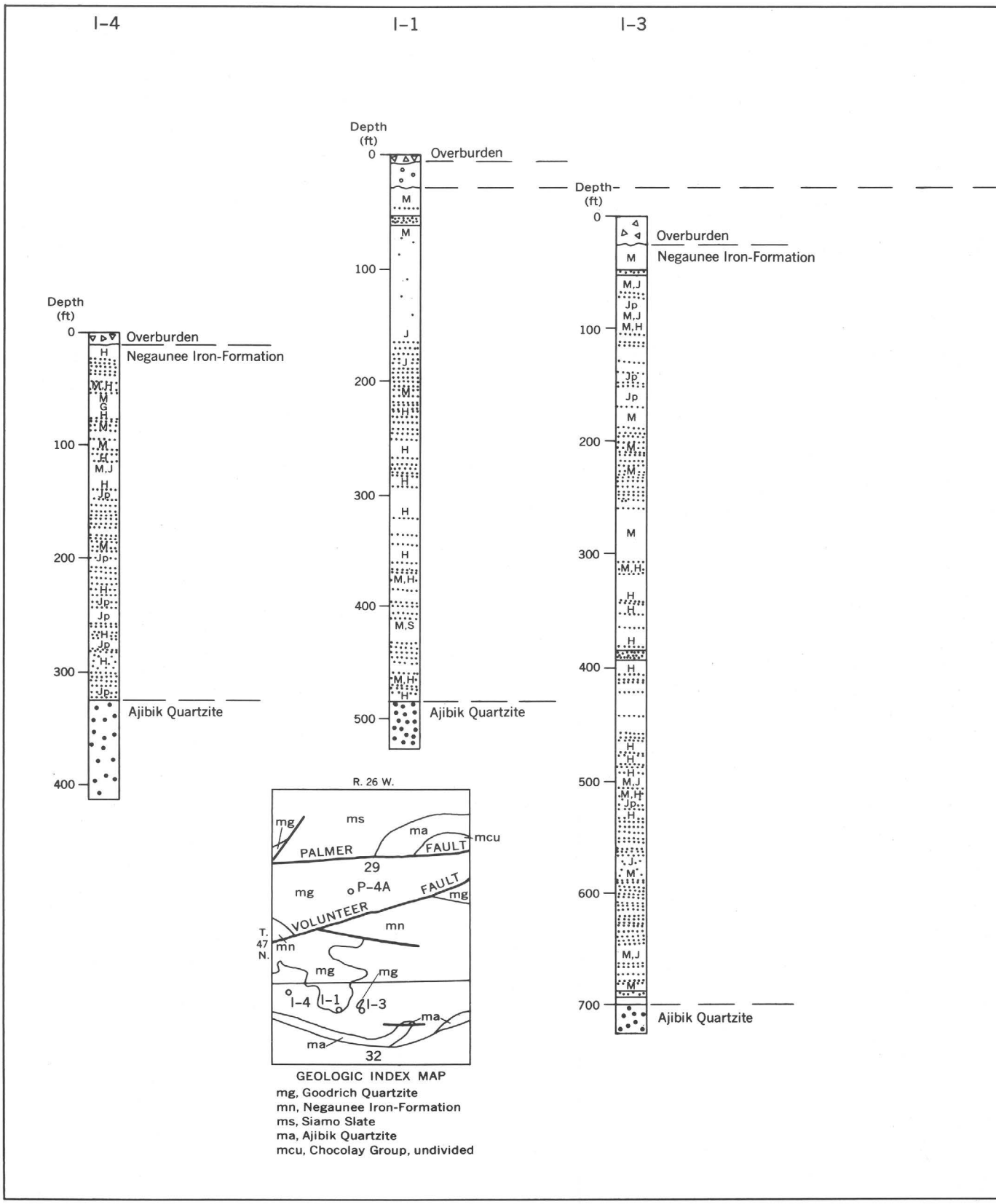

FIGURE 58.—Columnar sections from drill cores showing vertical distribution of clastic sediment in iron-formation, central

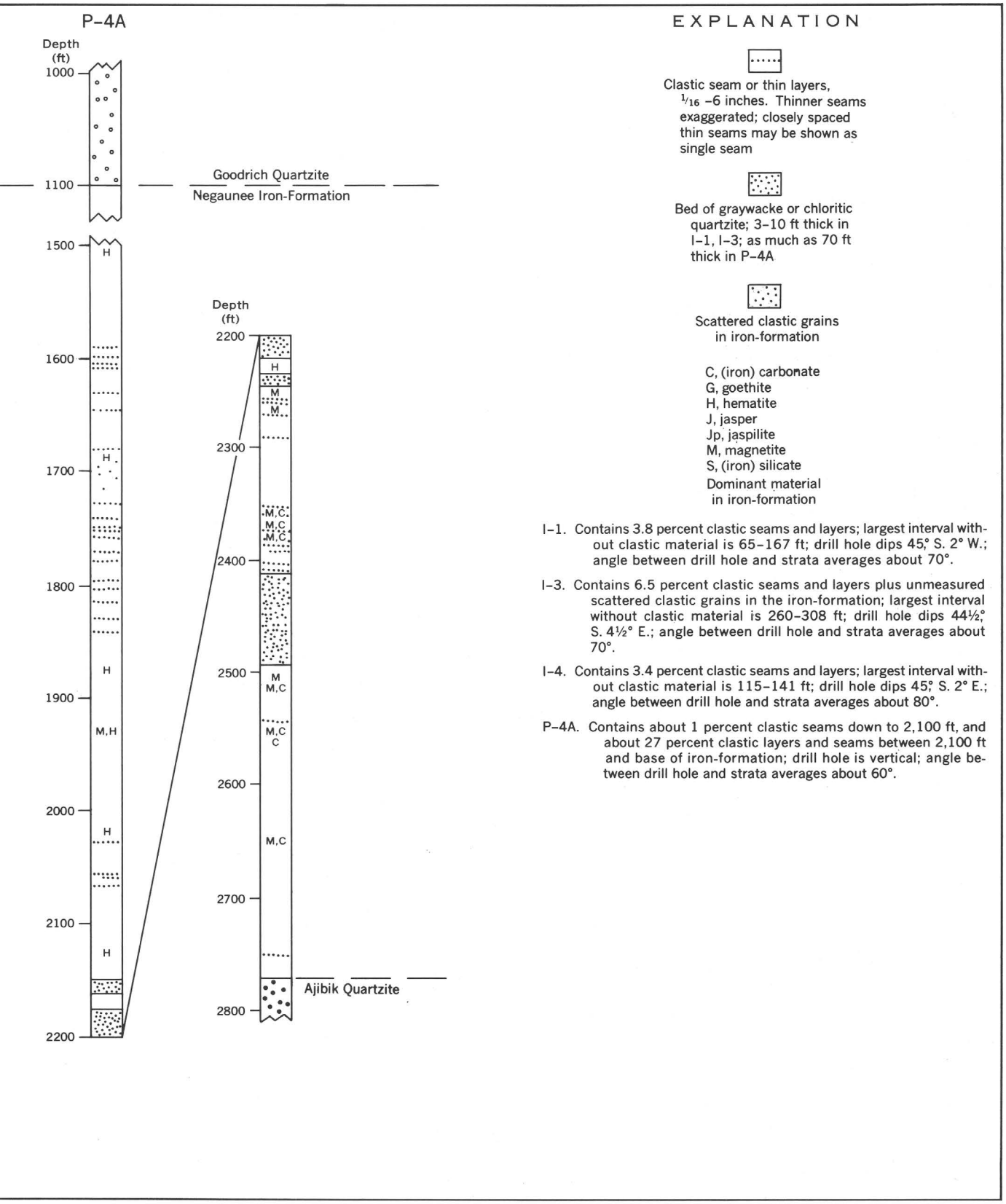

I–1. Contains 3.8 percent clastic seams and layers; largest interval without clastic material is 65–167 ft; drill hole dips 45° S. 2° W.; angle between drill hole and strata averages about 70°.

I–3. Contains 6.5 percent clastic seams and layers plus unmeasured scattered clastic grains in the iron-formation; largest interval without clastic material is 260–308 ft; drill hole dips 44½° S. 4½° E.; angle between drill hole and strata averages about 70°.

I–4. Contains 3.4 percent clastic seams and layers; largest interval without clastic material is 115–141 ft; drill hole dips 45° S. 2° E.; angle between drill hole and strata averages about 80°.

P–4A. Contains about 1 percent clastic seams down to 2,100 ft, and about 27 percent clastic layers and seams between 2,100 ft and base of iron-formation; drill hole is vertical; angle between drill hole and strata averages about 60°.

and south-central parts of Palmer basin, Marquette County, Mich.

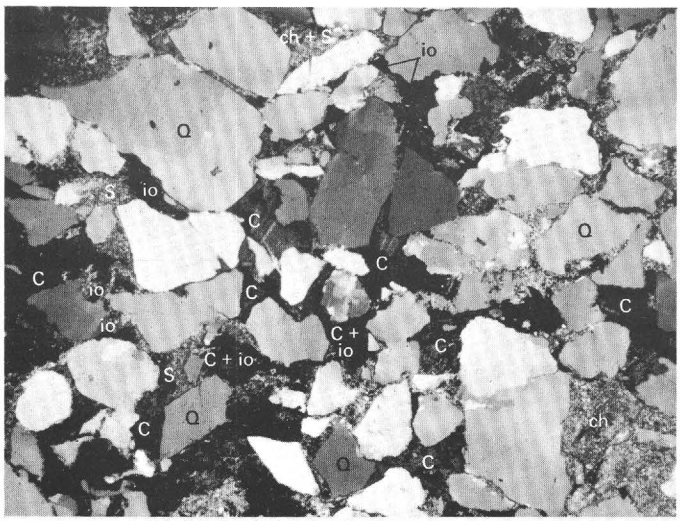

A

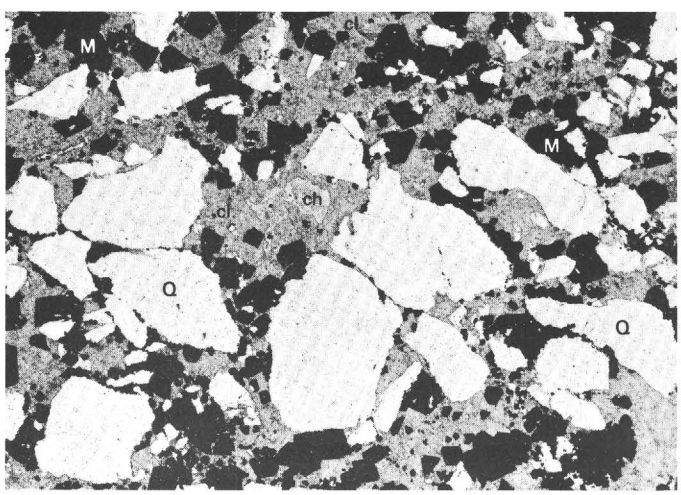

B

FIGURE 59.—Photomicrographs showing detrital materials in Negaunee Iron-Formation. *A*, Chloritoid-rich quartzite, from 5-foot bed in jaspilite, approximately 200 feet stratigraphically above base of Negaunee Iron-Formation. Chloritoid (C) forms large part of matrix between clastic grains of quartz (Q). Sericite (S), chert (ch), and iron oxide (io) also form part of matrix. Surface sample JG–74–64, south part of Palmer basin, near 650S–700E of NW. cor. sec. 32, T. 47 N., R. 26 W. *B*, Magnetite-rich graywacke. Quartz clasts (Q) and magnetite (M) "float" in matrix of chlorite (cl). Irregular area of chert (ch) may be deformed clast or granule. Graywacke interbedded with chert-magnetite through 40-foot zone, roughly 400 feet above base and 350 feet below top of iron-formation, south part of Palmer basin. Drill-core sample JG–106C–64; drill-hole location approximately 670S–2,200E of NW. cor. sec. 32, T. 47 N., R. 26 W. (Drill-hole location 726, sample from 194 ft).

other biogenic silica, or nonsiliceous material, during diagenesis or later, or by direct precipitation during deposition of the rock. Chert in iron-formation generally has been considered to be primary, but a replacement origin is postulated by Lepp and Goldich (1964). The evidence for primary chert summarized by James (1954, p. 273–274) includes features that are common in the Negaunee Iron-Formation.

Chert occurs in the Negaunee in regular layers of even thickness, in relatively thick lenses and pods, and as interstitial material in iron-rich layers. A primary rather than replacement origin is suggested by the even layers, the general absence of cherty layers wedging into or truncating ferruginous layers, and by the usual lack of "ghosts" of ferruginous laminae within cherty layers. Ferruginous laminae adjacent to chert pods tend to be draped against the pods (fig. 35*B* 3, 4), indicating that the pods existed during the early stages of compaction, if not during deposition. Slump structures in chert-rich lenses (figs. 29, 35) probably formed before consolidation of the rock, so they show the early presence of chert. Stylolites are generally considered to be of diagenetic origin. They are rare in chert in the Negaunee; however, their presence as shown in figure 26*A* suggests the diagenetic or earlier origin of the chert, but does not rule out a diagenetic replacement origin for the chert prior to the development of the stylolites.

Grains of clastic quartz are scattered through some ferruginous and cherty layers of the iron-formation, but very commonly in parts of the iron-formation containing detritus, the sandy grains are restricted largely to the ferruginous laminae. In two drill-core samples from about 150 to 400 feet above the base of the iron-formation in the SE¼ sec. 7, T. 47 N., R. 26 W., there is a distinct association of clastic quartz with carbonate-stilpnomelane layers and a sparsity of the detrital grains in beds of chert. Apparently clastic quartz was present at sites of deposition only during the precipitation of carbonate and silicate, or the presence of currents capable of transporting clastic grains somehow inhibited the precipitation of chert. Had the chert replaced sandy ferruginous laminae, vestiges of the sandy grains would probably remain. The deposition of primary chert was more likely to have been somehow directly related to the nondeposition of clastic grains. Possibly influxes of fresh water with the clastic sediment diluted silica in solution and thereby inhibited the precipitation of chert. On the other hand, individual lenses of chert may have coagulated from

supersaturated solutions so rapidly that few slowly arriving sand grains were enclosed in the chert. Experiments on the deposition of silica gel from sols show that a gradual increase in the concentration of colloidal silica in the presence of an electrolyte can be followed by a comparatively rapid coagulation of silica gel in solutions at pH greater than 7, but particularly at pH of 10 or more (Krauskopf, 1956, p. 20). Okamoto and others (1957, p. 129–132) noted rapid coagulation of silica in the presence of small amounts of aluminum. Evidently, the requirement of a basic solution led Krauskopf (1956, p. 25) to conclude that chert cannot be accounted for in marine sediments by inorganic precipitation. Siever (1962, p. 138, 142), however, believes that in restricted marine environments in Precambrian time, when diatoms and most other silica-extracting organisms had not yet developed, silica supersaturation and nonbiogenic precipitation were possible. Thus, the evidence is strong that chert originated as primary deposits of silica, but whether silica was extracted from sea water by inorganic precipitation or by organisms is uncertain. The possibility that purer silica layers were deposited rapidly suggests inorganic precipitation from supersaturated solutions.

Iron-formation rich in iron silicate minerals tends to be poor in chert (table 6). The chert content of such iron-formation commonly is less than 10 percent, whereas other varieties of thinly laminated iron-formation commonly contain 15–50 percent chert. The silica content of cherty iron-formation varies widely. Pure chert-siderite iron-formation having about 61 percent chert contains about 45 percent silica by weight, comparable to the percentage of silica in some of the silicate-rich iron-formation. The silicate iron-formation therefore differs from other thinly laminated iron-formation in the vicinity mainly in having much iron and silica chemically combined, and in lacking chert laminae. This may be a result of the incorporation of silica from original chert into iron silicate minerals after sedimentation. The presence of silicate-rich, chert-poor iron-formation that has about the same range in silica content as other chert-rich iron-formation (for example, see James, 1954, tables 3, 6, 7, 8) therefore may reflect a single process of extracting silica from the sea and a dominant original siliceous product—a protochert.

SIGNIFICANCE OF INTERLAYERED CLASTIC MATERIAL

Interlayered clastic beds and chert-laminated Precambrian iron-formation is a common association in transitional zones near the bottom and top of continuous thick sequences of iron-formation, as at the base of the Negaunee Iron-Formation, or of the Biwabik Iron-Formation of the Mesabi Range (White, 1954, p. 14–16). Plaksenko (1959) has described a cyclic sequence of metashale, magnetitic iron-formation, and hematitic iron-formation from the Kursk district, U.S.S.R., that recurs several times in a typical section, 120–150 m thick, and related it to marine transgressions and regressions. On the other hand, interlayering of clastic beds and iron-formation through thicknesses of hundreds of feet, at a scale of inches for the clastic beds and inches to tens of feet for the intervening iron-formation is not common elsewhere (Govett, 1966, p. 1192; James, 1966, p. W50).

In the Palmer basin, the many individual thin discontinuous beds of graywacke and impure quartzite within the iron-formation and the numerous "showers" of clastic quartz that must have come down during periods of iron-formation deposition are difficult to attribute specifically to minor episodes of transgression or regression. If time surfaces could be drawn through the iron-formation, it seems likely that many would pass repeatedly from iron-formation into lenses of graywacke. The setting seems to have been one of essentially continuous iron-formation (chemical) deposition, masked very locally and briefly from time to time by influxes of clastic material. Clastic material that gave rise to the graywacke must have been rather readily available during much of the time the iron-formation was being deposited and must have been transported and dumped into the iron-silica muds in small amounts at irregular time intervals without fundamentally affecting the chemical precipitation of iron minerals and silica. Any explanation of these mixed rocks, therefore, needs to reconcile relatively quiescent conditions related to the deposition of iron-formation in an environment of restricted circulation, free of clastic sedimentation much of the time, with numerous brief active episodes attended by incursions of poorly sorted clastic sediments.

The Marquette synclinorium and the Palmer basin owe their present configurations largely to folding and faulting during major regional deformation at the end of middle Precambrian time. The orientation of the synclinorium, however, probably was controlled by the trend of foliation, the structural grain, developed in basement rocks prior to middle Precambrian time (Gair, 1964, p. 4; Gair and Thaden, 1968, p. 60–63). Thinning of the Siamo along both north and south flanks of the synclinorium relative

to the axial area (Van Hise and Bayley, 1897, atlas; Boyum, 1964, fig. 7) suggests that the present north and south margins of the synclinorium may roughly parallel the shoreline of an ancient east-west trough in which the middle Precambrian sediments were deposited. If this view is correct, slight crustal deformation initially produced the depositional trough and later became intensified to form the synclinorium.

The increase in coarse clastic sediments in the iron-formation from the axial area toward the south flank of the synclinorium indicates that the clastic sediments came from the south. Furthermore, the widespread occurrence of clastic sediments in the iron-formation in the southern part of the Palmer basin suggests that the south edge of the present basin is near a shoreline of the original depositional basin. Such a shoreline, however, may have been on a local uplift within a depositional basin that extended considerably south of the Palmer basin.

The thinness or absence of the Siamo along the exposed margins of the Palmer basin indicates that during much of Siamo time, while thick slate (mud) and graywacke were deposited ½–3 miles to the north, the Palmer basin was a shallow shelflike embayment off the main Marquette depositional trough. Sericitic quartzite, which is mapped as Ajibik at the exposed margins of the Palmer basin, may have accumulated slowly, starting in Ajibik time and continuing through most of Siamo time. Shortly before the beginning of iron-formation deposition in the area, the Palmer embayment evidently became tectonically active. The floor of the embayment subsided as much as 1,000 feet during Negaunee time while the south margin was raised, probably in part by intermittent movement along faults, in a zone now conspicuously marked by the sheared, altered "Palmer Gneiss." These displacements must have reached their culmination during the regionwide orogeny at the end of middle Precambrian time, but could have started anytime after deposition of the Ajibik. The presence of small lenses of poorly sorted clastic material—mainly graywacke—in the iron-formation indicates numerous minor disturbances of quiet chemical sedimentation during Negaunee time. They are held to be a result of intermittent crustal movements along the south side of the Palmer basin. Continuing fault displacements during deposition and adjacent to the site of iron-formation deposition seems to offer the best explanation for the difference between "normal" clastic-poor iron-formation and the mixed rock of the Palmer area. According to this concept, mixtures of mud and sand accumulated rather continuously at the edge of the embayment, were intermittently dislodged by minor faulting, and flowed down in small turbidity currents over the iron-formation sediments. Clastic material and the iron-formation sediment did not necessarily come from the same source areas.

BARAGA GROUP

GOODRICH QUARTZITE

NAME, LITHOLOGY, STRATIGRAPHIC POSITION, AND THICKNESS

The Goodrich Quartzite was named for exposures of quartzite at the Goodrich mine on the south limb of the Marquette synclinorium, about 7 miles west of Palmer (Van Hise and Bayley, 1895, p. 591). The formation overlies the Negaunee Iron-Formation, generally concordantly or with slight angular discordance, is commonly marked at its base by conglomerate containing fragments of the iron-formation, and has been considered in previous studies to be separated from the Negaunee everywhere by an erosional interval. The Goodrich is the youngest formation of the Marquette Range Supergroup in the Palmer quadrangle, where it occurs principally in the Palmer basin. A small area of Goodrich is also known in the eastern part of the old Jackson mine, near the northwest corner of the quadrangle. In these areas, the Goodrich characteristically is pebbly to cobbly conglomerate or coarse-grained impure quartzite. Quartz-chlorite graywacke and slate evidently are minor components in the Palmer area, although fine-grained pelitic rock is an important part of the formation in the Cliffs Shaft mine, a few miles west of the old Jackson mine. Similar rock may be a significant part of the formation in the Palmer quadrangle but may be unrecognized as such because of poor exposures. Mafic pyroclastic and flow rock in the central part of the Palmer basin is assigned to the Goodrich in this report.

An erosional interval between the deposition of the Negaunee and the Goodrich is indicated by conglomerate containing fragments of the Negaunee at the base of the Goodrich, and erosion may explain some differences in the thickness of the Negaunee from place to place. A gradation between the formations in one place directly south of the village of Palmer indicates that even though parts of the Negaunee were eroded prior to Goodrich time, other parts of the iron-formation remained submerged until then, so that, in places, deposition was essentially continuous from one formation to the other.

The thickness of the Goodrich in the quadrangle is estimated to be as much as 1,400 feet. Drill holes just east of the village of Palmer cut 900–1,000 feet

of the Goodrich. The maximum thickness is estimated by projecting the base of the formation downdip to the north from the drill holes to the Palmer fault at the north boundary of the basin, using the dip established by the drill data. The upper contact of the formation is not present in the quadrangle, however; so the total original thickness in the Palmer area is unknown.

CONGLOMERATE

Outstanding examples of Goodrich conglomerate are present in the Isabella syncline, particularly at the old Isabella mine in an outcrop centering near 400N–1,100E of the SW. cor. sec. 29 (fig. 60), and

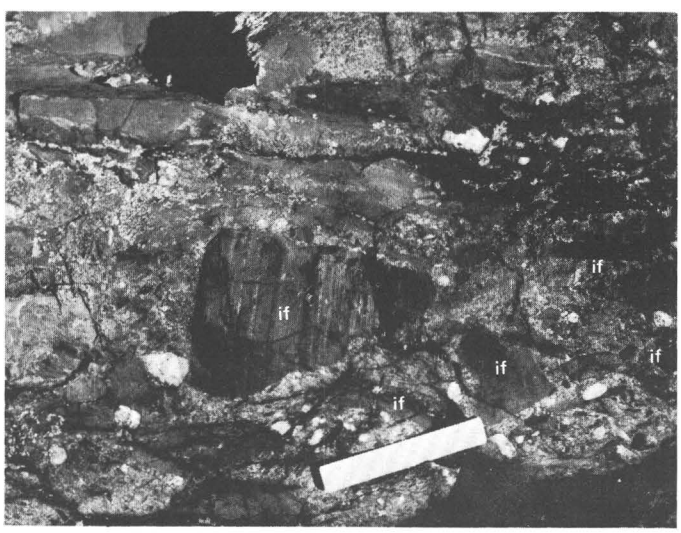

FIGURE 60.—Goodrich conglomerate. Angular cobbles and pebbles of jaspilitic iron-formation (if) and rounded pebbles of vein quartz are set in quartzite matrix. Isabella mine, near 400N–1,100E of SW. cor. sec. 29, T. 47 N., R. 26 W. Length of scale 7 inches.

in a larger outcrop straddling the line between secs. 29 and 32, 1,000 feet to the southeast. Tabular blocks of iron-formation as much as 3 feet long are also present at the Isabella mine, as well as smaller fragments of quartzite and granite(?). Other good examples of the conglomerate are found along the east-west exploration trench following the Goodrich-Negaunee contact north of the old Starwest mine, near 1,600N–2,200W of the SE. cor. sec. 29; on the south side of a drainage trench at the east end of the New Richmond open-pit mine in the S½SW¼ sec. 27; and in two drill holes just north of the New Richmond pit. The maximum thickness of conglomerate in a single exposure is about 50 feet, but as much as 100 feet of conglomerate has been cut in drill holes. The configuration of conglomerate along the base of the Goodrich cannot be observed in separate outcrops, but it is probably lenticular, if one judges by its thinness or absence short distances away, on strike from exposures of conglomerate, in places where quartzite lies directly on or is very close above the iron-formation.

Goodrich conglomerate typically contains pebbles, cobbles, and a few boulders of iron-formation, plus cobbles and smaller pieces of vein quartz, chert, granite, quartzite, and greenstone (metadiabase?). Fragments of hard iron ore have been seen in the conglomerate in other parts of the Marquette iron district. Small pebbles of blue opalescent (vein?) quartz are present in some of the conglomerate. Fragments of iron-formation and chert are generally rather angular and commonly are platy parallel to original bedding; fragments of other types of rock tend to be rounded and without doubt were transported greater distances than the pieces of iron-formation. The rock fragments generally "float" in a matrix consisting of combinations of detrital quartz and feldspar, sericite, and hematite. Coarse sand-sized grains of blue opalescent quartz are common, and minor constituents may include chlorite, magnetite, and monazite (Vickers, 1956).

In places, the matrix consists largely of hematite or hematite and magnetite, which are essentially placer deposits, and the basal Goodrich has been sufficiently rich in iron to be mined. At the Cliffs Shaft, Republic, and Humboldt (Edwards) mines, and reportedly also at the Champion and Old Volunteer mines and elsewhere on the Marquette range, the mining of hematite bodies in the iron-formation beneath the Negaunee-Goodrich contact has been extended into the Goodrich to extract such "detrital," "clastic," or "conglomerate" ore. Most fragments of iron-formation are jaspilitic, and pieces of chert are jaspery, so a characteristic appearance of the conglomerate is of angular red jasper-rich fragments set against a dark-gray to black background.

A 65-foot sequence of the Goodrich cut by a drill hole at 1,220N–550E of the SW. cor. sec. 27, contains several beds or lenses of conglomerate separated by quartzite and ferruginous graywacke and occupies the core of a narrow syncline underlain mainly by the Negaunee Iron-Formation. The conglomerate consists of angular jaspilitic and quartzitic pebbles as much as 4 inches across that are somewhat altered and replaced by brown ferric oxide, smaller pebbles of white softened chert, brown hematite, yellow-brown goethite, and iron-formation with clastic beds, and a matrix of brown hematite, white kaolinized detrital feldspar, and detrital quartz. Some of the smaller pebbles are well rounded.

A few short runs of "conformable" iron-formation in the sequence of clastic beds are interpreted as isolated fragments of iron-formation, which, in flat pieces shaped by original bedding, would have been deposited parallel to bedding of the Goodrich. Near the base of the Goodrich directly south of the village of Palmer, however, thin primary lenses of cherty iron-formation are present in Goodrich Quartzite (fig. 61) and demonstrate a gradational change from

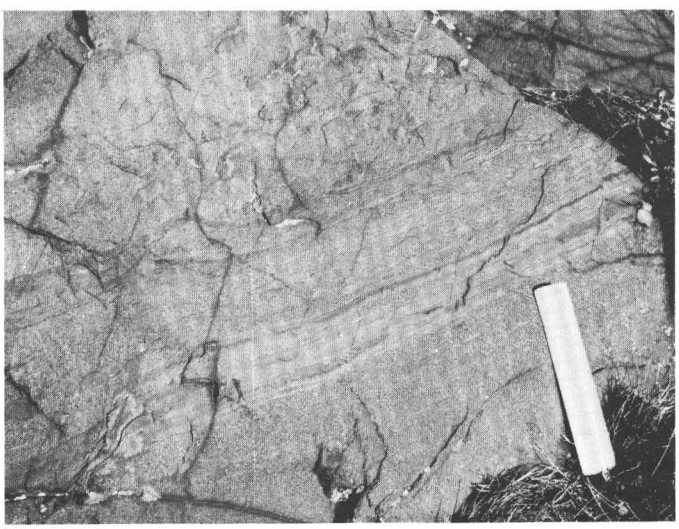

FIGURE 61.—Beds of jaspilitic iron-formation and jasper in quartzite, 10–15 feet above the Goodrich-Negaunee contact. Near 300N–350W of SE. cor. sec. 30, T. 47 N., R. 26 W. Length of scale 7 inches.

the typical chemical sedimentation of the Negaunee to clastic sedimentation of the Goodrich. Therefore, some apparently conformable segments of iron-formation cut by drill core within dominantly clastic beds of the Goodrich in the SW¼ sec. 27 and elsewhere in the Palmer basin may be true beds of iron-formation in the Goodrich.

Probably the alteration of grains and fragments in the conglomerate drilled in the SW¼ sec. 27 is a "weathering" effect produced by ground water moving downward from the present erosion surface and channeled by the synclinal structure. Some Goodrich conglomerate in the area contains little ferruginous material and is gray, light gray-green, or tan on weathered surfaces. In several places in the Palmer basin drill holes cut lenses of conglomeratic graywacke in quartzite—lenses that typically contain angular white fragments of chert or other quartz in a green chloritic matrix.

In the large outcrop 1,000 feet southeast of the old Isabella mine, near 2,100E of SW. cor. sec. 29, rounded cobbles of sericite-chlorite-quartz greenstone (metadiabase?) are common. In the peripheral parts of many such cobbles, concentric layers of magnetite or ferric oxide(?) approximate the shapes of the cobbles and so indicate the secondary concentration of iron in the fragments either shortly before or since their deposition.

It is evident from drilling in the area of the Isabella syncline that through reductions in the proportion and sizes of the coarser fragments, zones of conglomerate commonly grade through dispersed-pebble varieties into graywacke or impure quartzite.

QUARTZITE

Representative samples—all that remains—of some 900–1,000 feet of drill core of the Goodrich from just east of the village of Palmer indicate that the bulk of the formation there consists of ferruginous, sericitic, chloritic, and cherty quartzites. The best exposures of quartzite are found (1) in the vicinity of the old Isabella mine near 500N–900E of SW. cor. sec. 29; (2) near the center of sec. 29; (3) 300N–350W of SE. cor. sec. 30; and (4) in the western part of the Old Volunteer mine property at 200S to 700S–1,400E to 2,100E of NW. cor. sec. 31, and at 0 to 100N–2,100E to 2,200E of SW. cor. sec. 30. Quartzite as well as conglomerate is also exposed at the east end of the New Richmond mine in the SW¼ sec. 27. Small but significant exposures of quartzite, which demonstrate the presence of the Goodrich north of the Richmond fault in sec. 28, occur between 1,250 and 1,400 feet south of the center of the section, and at 950N–1,250W of SE. cor. of the section.

Goodrich Quartzite is generally light gray, light reddish gray, or gray green, and weathers dark gray, reddish brown, reddish gray, or buff-tan. The quartzite almost invariably contains poorly sorted detrital quartz, as much as about 5 mm in diameter, and matrix sericite, and may also contain detrital chert and feldspar (microcline, perthite, sodic plagioclase), scattered grit and pebbles, matrix chert, chlorite, biotite, carbonate, and hematite, and minor amounts of monazite (Vickers, 1956), magnetite, chloritoid, and andalusite. The detrital quartz commonly is light blue and opalescent, which is a factor in correlating some isolated occurrences with the Goodrich, such as those in sec. 28. With variations in the proportions of coarser detritus to matrix minerals, impure quartzite grades locally to wacke or graywacke. Red-brown biotite occurs in small books in the matrix and is plastered on the surfaces of detrital quartz and

feldspar grains in gritty ferruginous feldspathic quartzite exposed at 2,350S–1,950W of the NE. cor. sec. 29. Greenish biotite is present in the quartzite south of the center of sec. 28. It is uncertain whether the biotite reflects the level of regional metamorphism after deposition or is clastic and derived from lower Precambrian gneiss. The chloritoid and andalusite have been seen only in one sample from the exposure near the center of sec. 29, from a narrow zone of shearing and brecciation impregnated by quartz veinlets, so may have originated during metamorphism after deposition of the Goodrich.

MAFIC PYROCLASTIC AND FLOW ROCK

Metamorphosed mafic pyroclastic and flow rock extends east-southeast in a narrow belt across the south half of sec. 28, T. 47 N., R. 26 W., and is here correlated temporally with the Goodrich Quartzite. The belt is bounded on the north largely by the Richmond fault, and on the south entirely by Negaunee Iron-Formation. A single outcrop of iron-formation occurs north of the metavolcanic rock, on the north side of the road east from the village of Palmer, at 1,630N–1,200E of the SW. cor. sec. 28. The metavolcanic rock was considered to be a unit within the iron-formation by Tyler and Twenhofel (1952, p. 123) and by Davis (1965, p. 63), possibly because of its position between the one outcrop of iron-formation on the north and the belt of iron-formation on the south. However, evidence obtained during the present mapping suggests the stratigraphic equivalency of the metavolcanic rock and the Goodrich.

West of the north-south midline of sec. 28, the exposed metavolcanic rock is pyroclastic, and east of there is altered vitrophyric(?) flow rock. The pyroclastic rock consists mainly of loosely packed cobble-sized and smaller fragments of green altered vitrophyric(?) flow rock and a cherty selvage between fragments. A few 6-inch cobbles near 1,600N–350E of the SW. cor. sec. 28, weather to a salmon color and evidently are fragments of felsic volcanic rock. Most fragments are angular, less than 3 inches in size, and tend to be flattened and have ragged terminations. Such fragments consist largely of fine-grained chlorite representing the original probably glassy groundmass; some fragments also contain altered carbonate-rich lath-shaped pseudomorphs of plagioclase phenocrysts. Chemical analyses (table 34) indicate a rather mafic basaltic composition, but differing from those of typical basalt in having a high K_2O content.

TABLE 34.—*Chemical analyses of mafic pyroclastic rock, Goodrich Quartzite, sec. 28, T. 47 N., R. 26 W.*

[Standard chemical analyses by S. M. Berthold, U.S. Geol. Survey]

	1	2
SiO_2	47.86	44.76
Al_2O_3	15.68	17.05
Fe_2O_3	5.44	2.43
FeO	10.30	12.58
MgO	9.92	9.76
CaO	.55	1.30
Na_2O	.01	.01
K_2O	2.14	2.44
H_2O^+	6.36	5.88
H_2O^-	.20	.12
TiO_2	1.56	1.76
P_2O_5	.27	.30
MnO	.16	.18
CO_2	.03	1.44
Total	100.48	100.01

1. JG–14–67; drill-hole location 693; approx. 1,500 N. of SW. cor. sec. 28 (1–2 ft composite sample).
2. JG–15–67; drill-hole location 740; approx. 1,150N–3,000E of SW. cor. sec. 28 (1–2 ft composite sample).

A 1-foot bed of graywacke, a few inch-thick sandy lenses, and several fragments of iron-formation occur in the pyroclastic rock near 1,550N of the SW. cor. sec. 28, and a few small granitic pebbles have been seen in the metavolcanic rock near 1,000N–1,900E of the SW. cor. sec. 28. The graywacke is composed of coarse sand-sized clasts of feldspar and quartz and pebble-sized and smaller pieces of volcanic rock set in a matrix of sericite, chert, iron oxide, and carbonate (fig. 62).

Vitrophyric(?) flow rock evidently occurs in place in several small outcrops in the SE¼ sec. 28.

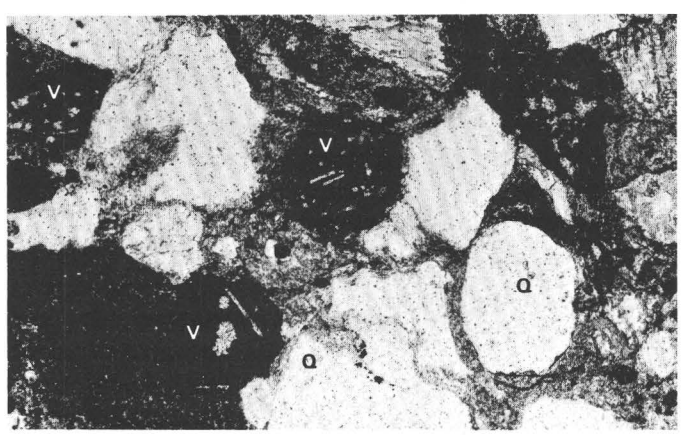

FIGURE 62.—Photomicrograph of graywacke from 1-foot bed in pyroclastic rock, Goodrich Quartzite, surface sample JG–49–64, near 1,550N of SW. cor. sec. 28, T. 47 N., R. 26 W. Clastic grains are quartz (Q) and altered vitrophyric(?) rock (V). Note lath-shaped pseudomorphs of plagioclase phenocrysts in fragments of volcanic rock. Plane-polarized light.

Whether these occurrences are representative of the entire east half of the volcanic belt or are intercalated with unexposed pyroclastic rock is unknown. The vitrophyric(?) rock is virtually identical with the rock composing most of the pyroclastic fragments in the western half of the volcanic belt and present in the graywacke shown in figure 62.

Structural attitudes in the iron-formation a short distance west of the belt of metavolcanic rock, near the center of the SE¼ sec. 29, indicate that the metavolcanic rock lies along the axis of a syncline, the northwest end of which terminates (closes) near the line between secs. 28 and 29; therefore, the iron-formation north of the metavolcanic rock is stratigraphically beneath the rock—on the north limb of the syncline. The metavolcanic rock evidently is younger than all the iron-formation. Near the west end of the westernmost outcrop in the volcanic belt, a boulder about 15 inches in diameter and smaller pieces of cherty jaspilitic iron-formation occur in pyroclastic rock, 1,550N of the SW. cor. sec. 28, just west of a 1-foot lens of feldspathic graywacke and a few thinner sandy lenses that are interlayered with the pyroclastic rock. Platy pieces of chert beds lie in the pyroclastic rock about parallel to the graywacke lens, and the graywacke contains fragments of the volcanic rock. The graywacke and probably the nearby fragments of iron-formation must be products of erosion, water transport, and subaqueous deposition during the time of volcanism. The iron-formation must have been at least partly consolidated at the time of volcanism. The position of the metavolcanic rock adjoining and overlying the iron-formation, in a stratigraphic relation to the iron-formation analogous to that of the Goodrich, and the presence in the metavolcanic rock of fragments of the iron-formation are the evidence on which the correlation of the metavolcanic rock and the Goodrich is based.

The presence of an apparently isolated volcanic deposit of such limited extent as that in sec. 28 is not readily explained. Approximately 9–15 miles west-northwest of the area, mafic coarsely pyroclastic rock of the Clarksburg Volcanics Member (Van Hise and Bayley, 1897, p. 460–487) overlies the Greenwood Iron-Formation Member of the Michigamme Slate, and is as much as 2,900 feet stratigraphically above the base of the Goodrich Quartzite (W. F. Cannon, U.S. Geol. Survey, oral commun., 1968). The Clarksburg contains the only other known mafic pyroclastic rock of middle Precambrian age in the Marquette Range with which the isolated occurrence in the Palmer basin might be correlated. There is no direct evidence on which to base such a correlation and no support for it in the stratigraphic sequence if the deposition of the uppermost Negaunee, the Goodrich, and the Michigamme are assumed each to be essentially synchronous throughout the area. The Clarksburg overlies and is separated from vitreous Goodrich Quartzite by as much as 2,500 feet of underlying metasedimentary rock, whereas the pyroclastic rock near Palmer underlies vitreous Goodrich Quartzite. If the pyroclastic rock near Palmer were correlative with the Clarksburg—both presumably having been deposited in the same relatively short span of time—a transgression of the Goodrich, and also at least the upper part of the Negaunee Iron-Formation, would be indicated from the western part of the Marquette district toward the east during middle Precambrian time. Vitreous Goodrich Quartzite would have been deposited long before the Clarksburg volcanism in the Clarksburg area and just after the volcanism in the Palmer area. Such a drastic change in sedimentation in a short distance is not beyond possibility and is not overruled by known evidence, but the general similarity of lithology and thickness of both the Negaunee and Goodrich in the Palmer and Clarksburg areas tends to support an intuitive conclusion that they were deposited more or less simultaneously, hence that the volcanic rocks are not correlative.

EROSION OF NEGAUNEE BEFORE DEPOSITION OF GOODRICH QUARTZITE

Conglomerate containing fragments of underlying Negaunee Iron-Formation occurs at the base of the Goodrich Quartzite along the Marquette Range and in the Republic trough south of the west end of the Marquette district over distances of about 20 miles The conglomerate undoubtedly represents broad erosion of the Negaunee prior to or coincident with the initial stages of Goodrich deposition. The hiatus between the Negaunee and Goodrich formations was recognized in early geologic studies of the area and was the basis for dividing the metasedimentary rocks—the Marquette series of Van Hise and Bayley (1897)—into lower and upper parts which were correlated at the time with lower and upper Huronian rocks on the north shore of Lake Huron, 200 miles to the east. Although the pre-Goodrich erosion occurred over much of the Marquette district and may have been one

cause of present variations in the thickness of the Negaunee Iron-Formation, beveling of the Negaunee is slight in most places, and the two formations, where in juxtaposition, have accordant or nearly accordant attitudes.

On the hill immediately south of the village of Palmer, near 300N–350W of the SE. cor. sec. 30, the contact between the Goodrich and the Negaunee is conformable, and the two formations are somewhat intergradational. Clastic lenses, 2 inches or less thick, are abundant in the upper 50 feet of jaspilitic iron-formation (fig. 57*A*), and the iron-formation is overlain by a thick bed of (Goodrich) quartzite in which a few thin jaspilitic and jaspery lenses are interlayered within about 15 feet above the base of the quartzite (fig. 61). Coarse Goodrich conglomerate (fig. 60) rests on the iron-formation as close as 1,300 feet east of this gradational zone. The Negaunee was not everywhere raised above the erosional base level before Goodrich time. Locally, the deposition of clastic sediment and iron-formation of the Negaunee gave way virtually without interruption to the deposition of only clastic sediment of the Goodrich.

In the Menominee district, 50–60 miles south of the Marquette Range, the Vulcan Iron-Formation, which is equivalent to the Negaunee in the Menominee Group (James, 1958, p. 35), evidently was irregularly eroded before deposition of the overlying Michigamme Slate (Bayley and others, 1966, p. 62). The lower part of the Michigamme in that area is locally conglomeratic and is probably equivalent to the Goodrich Quartzite. Reasons for believing that the Michigamme rests unconformably on the Vulcan are: "(1) the present limited distribution of the Menominee Group, (2) the apparent discordancies between post-Vulcan and post-Michigamme folds, (3) the regional aspect of the post-Vulcan but pre-Michigamme diastrophism, and (4) the presence of Michigamme basal conglomerates" (Bayley and others, 1966, p. 62). Despite the probability that erosion completely removed the iron-formation in parts of the Menominee district before deposition of the Michigamme, it is interesting that on Keel Ridge east of Iron Mountain, Bayley and his coworkers found basal sericite slate of the Michigamme resting conformably on the Brier Slate Member of the Vulcan Iron-Formation. Two younger members of the Vulcan evidently were eroded before the Michigamme was deposited, yet the uplift and tilting preceding erosion was not sufficient to prevent a conformable relation between the Michigamme and the Brier Slate Member.

In the Gogebic district, Michigan, 100–150 miles west of the Marquette district, Tyler Slate directly overlies Ironwood Iron-Formation, in a relation analogous to that of the Michigamme on the Vulcan and the Goodrich Quartzite on the Negaunee Iron-Formation. The Tyler Slate rests conformably on the Ironwood (Van Hise and Leith, 1911, p. 233).

It is concluded here that local, slight, and somewhat variable uplift of parts of the Marquette-Menominee area occurred in immediate pre-Goodrich time but died out to the west toward the present Gogebic Range. Within short distances, areas of pre-Goodrich iron-formation that were subject to erosion passed into still-submerged iron-formation. The erosion of parts of the Negaunee before Goodrich time, therefore, was not a result of a uniform regionwide uplift related to a sweeping diastrophism, but rather appears to have been related to local, generally slight, and irregular uplifts which took place at about the same time over a large region. Such a region might have been characterized by irregular shorelines and numerous islands and embayments.

LOWER OR MIDDLE PRECAMBRIAN INTRUSIVE ROCKS

Lower or middle Precambrian intrusive rocks in the quadrangle are metadiabase (grading to metagabbro) and pegmatite (grading to granite). Large masses of granite that form an integral part of the Compeau Creek Gneiss have been described earlier in the report and are not considered here

Metadiabase occurs in sills and dikes, cutting lower Precambrian gneiss and middle Precambrian metasedimentary formations. Some is of middle Precambrian age and some may be older. Pegmatite forms thin dikes, conformable pods, and small irregular bodies in the lower Precambrian gneiss, but is not abundant and has not been mapped separately from the gneiss. It is similar to pegmatite in the Sands quadrangle to the east (Gair and Thaden, 1968, p. 55) and is not further described here.

METADIABASE

OCCURRENCE AND DISTRIBUTION

DIKES IN COMPEAU CREEK GNEISS

Metadiabase cuts Compeau Creek Gneiss in the south half of the quadrangle in a number of thick east- to southeast-trending dikes and in thinner probably connecting dikes that trend north-northeast. Some of the latter dikes appear to be truncated by middle Precambrian rocks at the south edge of the Palmer basin, so probably are of early

Precambrian age. On available evidence, most of the dikes in the gneiss could be of early or middle Precambrian age.

DIKES IN MIDDLE PRECAMBRIAN ROCKS

Dikes of highly altered green to light-colored rock, now rich in chlorite, sericite, or clay minerals cut the Negaunee Iron-Formation in many places. Most or all of them were probably diabase originally, were changed to metadiabase during regional metamorphism, and later may have been altered again during oxidation-leaching of the iron-formation. The more highly altered of the dikes are commonly referred to in the mines as "soapstone." Such dikes are common in the east half of sec. 7, T. 47 N., R. 26 W., in all the underground mines, and in most drill holes cutting oxidized iron-formation. Dikes of altered metadiabase cut the iron-formation in the Empire mine and southwest of there in the New Volunteer mine in the NE¼NE¼ sec. 18, and in the south part of the New Richmond mine in SW¼ sec. 27, T. 47 N., R. 26 W., in the old Jackson mine in sec. 1, T. 47 N., R. 27 W., and south of the Old Richmond mine in the south-central part of the Palmer basin. Most of the dikes trend between west-southwest and northwest. Detailed mapping in underground mines by geologists of the Cleveland Cliffs Iron Co. and the Jones and Laughlin Steel Corp. has shown that most of the highly altered dikes occur along faults, so the presence of such dikes supports a strong probability of faults where other evidence is lacking

A few thin dikes of metadiabase or other altered igneous rock have also been found in the Kona Dolomite in the south-central part of sec. 13, in the Ajibik Quartzite in the SW¼ sec. 21, and in the Siamo Slate in the SE¼ sec. 5, north of the center of sec. 8, a short distance north of the W¼ cor. sec. 11, and in the N½ sec. 30, T. 47 N., R. 26 W.

BELLEVIEW "SILL" IN SIAMO SLATE AND NEGAUNEE IRON-FORMATION

The Belleview "sill" occurs mainly in Siamo Slate in the north half of the quadrangle and is named for outcrops at the prominent topographic gap just east of Belleview in the west-central part of sec. 17. The "sill" is locally conformable with bedding in the slate and roughly follows the structural trend of adjoining formations, but mapping shows that in parts of the area it cuts across bedding at a small angle. The "sill" has a length along strike of about 7 miles and a maximum thickness of about 900 feet. It pinches out to the south in the NE¼ sec 19 and ends to the north just north of the quadrangle (W. P. Puffett, U.S. Geol. Survey, oral commun., 1968). In the downdip direction, west from the outcrop in sec. 10, and northwest in secs. 15–17, the "sill" apparently dips more gently than the Siamo Slate, cuts upward in the stratigraphic section, and crosses the Siamo-Negaunee contact at a depth of about 2,000 feet in the northeastern part of sec. 7, T. 47 N., R. 26 W. (see pl. 1, section *B–B'*, drill-hole locs. 137, 178, 191, 196, and 201). At the topographic gap east of Belleview, the "sill" crosses a fault and passes south into the lower part of the Negaunee Iron-Formation. In the northeast part of the quadrangle, the "sill" is extensively sliced by faults in the axial part of the Marquette synclinorium. The "sill" may be cut off near the north edge of the quadrangle by east-trending faults. Isolated exposures of metadiabase just west and north of the center of sec. 3, T. 47 N., R. 26 W., may be segments of the "sill," displaced eastward from the north end of the main body.

The Belleview "sill" grades from fine-grained metadiabase at its margins to coarse-grained metadiabase in its interior but gives only minor evidence of crystallization differentiation. Pegmatitic or granophyric segregations not exceeding 1 foot in thickness are present within 50 feet below the top of the "sill" near 1,550N–1,300E and 550N–1,950E of the SW. cor. sec. 3, and 4,500N–2,750E of the SW. cor. sec. 10, and a 4-inch syenite vein cuts the mafic rock near 2,500N–1,000E of the SW. cor. sec. 17.

The Belleview "sill" was emplaced before late middle Precambrian metamorphism after early faulting in the deformation of the Marquette synclinorium and was later subjected to additional faulting.

BRECCIA ZONES

In sec. 17, conspicuous dikelike breccia zones as much as 30 feet wide cross the "sill" at Belleview gap and extend east-northeastward from there for about 2,500 feet, parallel to the strike of the "sill." About 1,100 feet south of the gap, an east-striking zone of breccia crosses almost the full exposed thickness of the "sill." The breccia consists mainly of rounded and angular cobbles and blocks of coarse metadiabase in a fine-grained slaty chloritic matrix interpreted here as mylonitized metadiabase. Sparse fragments of granitic rock, 2–4 inches in maximum diameter, are in the breccia near 3,050N–2,100E, 2,800N–1,900E, and 3,700N–3,900E from the SW. cor. sec. 17. The first two of these localities are

at or close to the lower contact of the "sill" and Siamo Slate where the "sill" bends from a north to an east trend. There is no evident fault displacement of the walls of the breccia zones. The metadiabase fragments appear to be identical to nearby coarse-grained phases of the "sill," but the mechanism for emplacement of the granitic fragments in their midst is unknown. It seems obvious that pieces of granite have been carried up long distances from the basement. The most reasonable analogy is with a type of autobreccia dike in volcanic terranes in which comminuted wall rock is injected into contiguous rocks. In part of the breccia zone on the south wall of Belleview gap, very angular cobbles of coarse-grained metadiabase are suspended in a matrix of medium-grained metadiabase, which evidently was intruded after brecciation of the coarser rock.

SILLS IN NEGAUNEE IRON-FORMATION

TRACY SILL

The Tracy sill is the lowest of several thick conformable bodies of metadiabase contained entirely within the Negaunee Iron-Formation. The name is derived from a prominent outcrop in the NE¼ sec. 7 and the NW¼ sec. 8, T. 47 N., R. 26 W., a short distance south of the Tracy mine (J. W. Avery, Jones & Laughlin Steel Corp., oral commun., 1964; Gair and Simmons, 1970).

The Tracy sill has a maximum thickness of about 250 feet and its base is 1,100–1,200 feet above the base of the Negaunee; in this report it has been traced from the north edge of the quadrangle (and beyond to the north and northwest by others) south to the vicinity of the N¼ cor. sec. 19, T. 47 N., R. 26 W. From drill data alone, it appears to extend southwest across the NW¼ sec. 19, but to pinch out beyond there to the southwest and updip to the southeast. The sill probably was emplaced at an early stage in the deformation of the Marquette synclinorium, and later in the deformation was extensively sliced by faults in the axial part of the synclinorium in sec. 7. The sill is projected across the faulted zone between the Tracy mine near the SW. cor. sec. 5, and the Athens mine, one-half mile to the north, from drill data and from its established distance from the base of the Negaunee.

SUMMIT MOUNTAIN SILL

The Summit Mountain sill intrudes Negaunee Iron-Formation, next in sequence above the Tracy sill, and is separated from that body by 120–340 feet of iron-formation. The sill has been named from occurrences on Summit Mountain, a short distance west of the quadrangle in secs. 24–25, T. 47 N., R. 27 W. (Gair and Simmons, 1970). Within the quadragle the sill has a maximum thickness of about 500 feet and forms a belt trending northeast to north to northwest between the south-central part of sec. 24 and the center of sec. 12, T. 47 N., R. 27 W. The curving belt is concave to the west and marks the closure of a major west-plunging syncline. This sill was probably emplaced at the same time as the Tracy sill. It has been cut in the S½ sec. 18, T. 47 N., R. 26 W., and the SE¼ sec. 13, T. 47 N., R. 27 W., by faults that probably developed during deformation of the Marquette synclinorium. At the west edge of the quadrangle just south of the center of sec. 24, the upper part of the sill cuts upward across the iron-formation and may merge with the overlying sill.

PARTRIDGE CREEK SILL

The Partridge Creek sill is confined within the Negaunee Iron-Formation; its base is 70–140 feet above the Summit Mountain sill. It has been named from large exposures in the ridge northeast of Partridge Creek in the SE¼ sec. 12, T. 47 N., R. 27 W. (Gair and Simmons, 1970). At the west edge of the quadrangle in sec. 12 the sill has a thickness of about 400 feet. To the southeast across the SE¼ sec. 12, it splits into two layers, the lower of which is about 100 feet thick and the upper, about 200 feet thick. The layers are separated by about 150 feet of iron-formation. They extend southeast into the W½ sec. 18, T. 47 N., R. 26 W., and pinch out. Near the SE. cor. sec. 12, the upper layer thickens markedly and passes into an irregular dike that cuts upward across the iron-formation and may connect with the overlying Suicide sill. The upper layer has been extended south of the west-northwest-trending fault in the NW¼ sec. 18 by drill data only.

SUICIDE SILL

The Suicide sill is the uppermost conformable metadiabase in the Negaunee Iron-Formation within the quadrangle. It has been named for exposures in the upper part of the Suicide Hill ski jump on the ridge south of Partridge Creek, a few hundred feet west of the quadrangle in the south-central part of sec. 12, T. 47 N., R. 27 W. (Gair and Simmons, 1970). The broad belt of metadiabase that includes the type location is along the trough of a northwest-plunging syncline occupying most of the NE¼ sec. 13, T. 47 N., R. 27 W., and parts of adjoining

sections. The maximum thickness of iron-formation between the Suicide and Partridge Creek sills is about 900 feet. Because of the pinchout of the Partridge Creek sill, the Suicide sill is next above the Summit Mountain sill in the SW¼ sec. 18, T. 47 N., R. 26 W., and in the SE¼ sec. 13, T. 47 N., R. 27 W. The thickness of the iron-formation between the Suicide and Summit Mountain sills in that area ranges from roughly 150 to 800 feet, but it cannot be determined to what extent this variaion is caused by squeezing out or thickening of the iron-formation between the sills during folding, or by crosscutting of the iron-formation by the sills during their emplacement. Both the Summit Mountain and Suicide sills are disrupted by faults in the SE¼ sec. 13. Much of the Suicide sill extends west of the quadrangle, and mapping in the Palmer quadrangle alone cannot establish the continuity of the sill south of the faults. However, the sill is projected south of the faults in secs. 13 and 24 on the basis of stratigraphic position above the Summit Mountain sill. The thickness of the Suicide sill cannot be determined in the main belt because the top of the sill is not present in the synclinal trough in the eastern part of sec. 13. The metadiabase body next above the Summit Mountain sill in sec. 24, which is interpreted as the Suicide sill, has a thickness of about 400 feet, assuming a dip of 30°. As noted above, the Summit Mountain and Suicide sills may merge at the west edge of the quadrangle near the center of sec. 24.

DESCRIPTION

The metadiabase is widely variable in appearance, mineralogy, and chemical composition. Thin sills and dikes originally were fine grained, and many dikes in the iron-formation in particular were sheared along faults during or after emplacement, and as a result were greatly altered. Thick dikes in the gneiss and sills in the middle Precambrian metasedimentary rocks, on the other hand, crystallized originally to relatively coarse grains or porphyritic fabrics, except at chilled margins, and have been relatively resistant to modification. Original minerals are rare, however. Original textures are well preserved in most dikes that cut the gneiss and in large sills in the middle Precambrian metasedimentary rocks. Mineral changes in such bodies have taken place largely by pseudomorphous replacement.

Metadiabase that intrudes the gneiss is generally dark green and contains saussuritized albitic plagioclase, blue-green or deep-green amphibole, and scattered magnetite and ilmenite(?), the latter rimmed by leucoxene. Amphibole may be partly altered to biotite and (or) chlorite. Pale-green actinolitic amphibole is present in some samples, but the prevalence of darker amphibole indicates that much of the lower Precambrian gneiss in the south half of the quadrangle was at the level of the lower epidote amphibolite facies during late middle Precambrian metamorphism.

Most metadiabase in the metasedimentary rocks in the north half of the quadrangle is dark green to medium gray green. Thin dikes and sills in oxidized iron-formation may be shades of red, red brown, red green, or light gray. Diabasic texture generally is obscure or destroyed entirely in dikes or sills less than 10 feet thick, but coarse diabasic and ophitic textures are very well preserved in the thicker bodies, particularly in the Belleview "sill" and the main sills in the iron-formation. Plagioclase is saussuritic and albitic, particularly in the larger bodies, or is variably replaced by carbonate, chert, chlorite, sericite, biotite, and clay minerals; in one place, replacement is by an unusual mixture of biotite and epidote. Original pyroxene commonly is replaced by pale-green tremolite-actinolite and minor chlorite or biotite, or entirely by chlorite-biotite. Pyroxene cores remain within amphibole in some coarse-grained parts of the Belleview "sill." Leucoxene dust, plates, and rims (on ilmenite?) are common.

Thin mafic dikes that cut the iron-formation in general are more highly altered than dikes of comparable thickness that cut other formations. It is concluded that reactants derived from the iron-formation during emplacement of the intrusive rock, metamorphism, and(or) postmetamorphic oxidation-leaching of the iron-formation account for the thorough breakdown of minerals and textures in such dikes. The dikes now consist of various nondescript mixtures of carbonate, sericite, chert, epidote, biotite, clay minerals, and dusty opaque minerals or leucoxene. Such extreme alteration has produced a light-colored sericitic dike rock in one part of the old Jackson mine in the SE¼ sec. 1, T. 47 N.. R. 27 W., which in turn is partly replaced by hematite evidently derived from weathering at the present erosion surface. In general, it is impossible now to distinguish alterations that may have been deuteric, metamorphic, or postmetamorphic in such dikes. The original composition of dikes that are now highly altered is not definitely known but is thought to have been mafic because (1) dikes that are sufficiently unaltered to identify

primary composition are all mafic, and (2) light-colored highly altered dike rock in places grades into greenish mafic dike rock.

Some highly altered sericite-rich igneous rock in the northwest part of the quadrangle that is not definitely crosscutting in the iron-formation contains rare round amygdulelike aggregates of cherty quartz which suggest that such rock, and similarly altered igneous bodies that are definitely conformable, might be of volcanic origin and contemporaneous with the iron-formation. However, the altered condition of the amygdular rock probably precludes a positive determination of volcanic or near-surface intrusive origin.

Chemical analyses of two samples of the Tracy sill substantiate the textural evidence that the original rock was diabase (table 35). Both samples are chemically equivalent to basalt or gabbro, but sample 1, from the fine-grained upper chilled zone, about 30 feet below the top of the sill, contains less SiO_2 and more total iron oxide and MgO (is more mafic) than sample 2 from the coarse-grained interior, roughly 125 feet below the top and 230 feet above the bottom of the sill.

Analyses of highly altered dike rock from the Jackson mine area, in the SE¼ sec. 1, T. 47 N., R. 27 W. (table 35, Nos. 3 and 4) show great enrichment in Al_2O_3 and, if the original rock was mafic, also in K_2O (fixed in sericite). If it had an original mafic composition, the altered dike rock has probably also been enriched in TiO_2 in at least sample 3 and has had an extreme loss of FeO, MgO, CaO, and Na_2O.

An average analysis derived from 12 chemical analyses of moderately altered mafic dikes from the Empire mine (table 35, column 5) shows substantial losses in SiO_2 and CaO from typical mafic compositions, and a small increase in Al_2O_3. K_2O and Na_2O were not reported in the analyses.

TABLE 35.—*Chemical analyses of sills and dikes in Negaunee Iron-Formation*

[Standard rock analyses. Analysts: G. O. Riddle (Nos. 1 and 2) and S. M. Berthold (Nos. 3 and 4), U.S. Geol. Survey; Chemical Laboratory of Cleveland Cliffs Iron Co. (No. 5)]

	1	2	3	4	5	
					Average of 12 samples	Standard deviation
SiO_2	45.81	48.11	43.94	51.03	39.70	10.71
Al_2O_3	16.13	15.05	35.74	26.29	18.35	2.67
Fe_2O_3	1.00	2.37	2.05	9.36	6.31	2.64
FeO	12.69	9.81	.35	.40	16.74	4.24
MgO	8.21	6.03	.34	.47	8.33	1.82
CaO	4.24	8.99	.13	.53	.48	.48
Na_2O	3.35	3.18	.42	.39	--	--
K_2O	1.11	1.08	8.77	4.07	--	--
H_2O^+	4.78	2.66	5.55	5.93	--	--
H_2O^-	.13	.08	.04	.05	--	--
TiO_2	1.59	1.95	2.97	1.14	1.80	.45
P_2O_5	.17	.19	.07	.48	.26	.14
MnO	.09	.19	.03	.02	.14	.09
CO_2	.47	.19	.00	.00	--	--
Cl	.00	.01	--	--	Loss on ignition 7.58	1.57
F	.05	.05	--	--		
Subtotal	99.82	99.94	--	--		
Less O for F	.02	.02	--	--		
Total	99.80	99.92	100.40	100.16		

1. JG–132A–66; fine-grained metadiabase; drill hole location 232, 1-ft composite from 247–252 ft., 2250N.–1100E. of SW. cor. sec. 7, T. 47 N., R. 26 W.
2. JG–132B–66; coarse-grained metadiabase; drill hole location 232, 1-ft composite from 339–348 ft.
3. JG–30–67; highly altered dike; 600S.–750E. of NW. cor. Palmer quadrangle.
4. JG–31–67; highly altered dike; 500S.–1600E. of NW. cor. Palmer quadrangle.
5. Chloritic dikes, Empire mine. Data furnished by Tsu-Ming Han, Cleveland Cliffs Iron Co.

UPPER PRECAMBRIAN INTRUSIVE ROCKS—KEWEENAWAN SERIES

DIABASE

East-northeast-trending diabase dikes intrude lower Precambrian gneiss in the southern part of the quadrangle and middle Precambrian metasedimentary rocks in the Palmer basin and axial part of the Marquette synclinorium (secs. 4, 5, 7, and 10, T. 47 N., R. 26 W.). The only known Keweenawan dike in the gneiss crosses the entire quadrangle and extends another 20 miles to the west. The Isabella dike in the Palmer basin and the North Buffalo and Prince of Wales dikes near the north edge of the quadrangle cross bodies of soft iron ore (mined out). Thin unexposed diabase has been cut by drill holes in the eastern part of sec. 18, T. 47 N., R. 26 W., and mafic dike rock reported along the Volunteer fault in an old drill log is probably diabase (see section on magnetic surveys, p. 129).

The dike rock is massive, dark gray, and medium to fine grained and has characteristic diabasic texture grading to vitrophyric at chilled contacts (fig. 63). Calcic plagioclase and pyroxene are essential minerals, and magnetite is a minor constituent—less than 10 percent. Spots of serpentine in places, not more than a few percent of the constituents, are probably pseudomorphs of olivine. Grain margins of pyroxene commonly have altered deuterically to tremolite-actinolite, chlorite, chlorite-carbonate, or biotite, and plagioclase may be partly replaced by sericite, chlorite, epidote, or carbonate. Parts of the Isabella and North Buffalo dikes have been extensively altered—argillized—where they cross areas of strong oxidation of the iron-formation or bodies of soft ore. Original minerals have been replaced largely by montmorillonite, kaolinite, quartz, and hematite,[14] but even in thoroughly argillized parts of the diabase, gross texture is fair-

[14] X-ray identification by T. E. C. Keith, U.S. Geol. Survey.

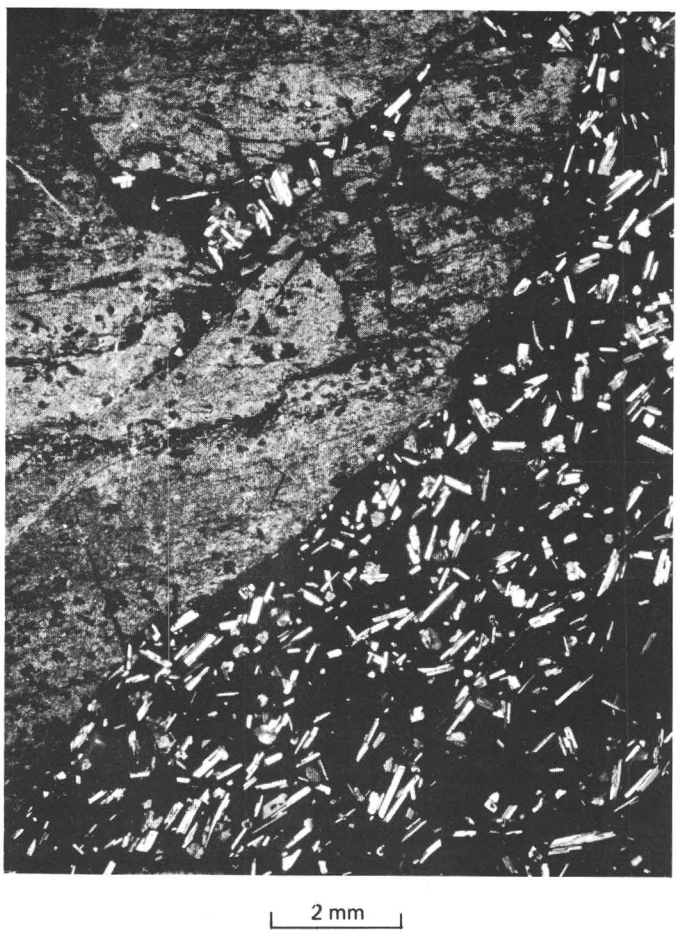

FIGURE 63.—Photomicrograph of diabase apophysis in iron-formation. Plane-polarized light.

ly well preserved. Argillization of the diabase quite clearly resulted from the action of the same solutions that caused oxidation-leaching of adjacent iron-formation and the growth of bodies of soft ore; so the diabase itself is preore in age, and possible solutions given off during its emplacement were not the principal oxidizing agent of the iron-formation.

QUARTZ VEINS AND SILICIFIED ROCK

Quartz veins occur notably along faults and fracture zones. Vein quartz is generally light gray to milky white and brecciated. In mapping, some faults were extended or connected with one another solely because of the existence of linear belts of brecciated vein quartz between them.

The most conspicuous occurrences of vein quartz are: (1) a thick vein trending east-southeast near the west edge of the quadrangle at the line between T. 46 N. and T. 47 N.; (2) in quartzite, mainly, along the Palmer fault near the east edge of the quadrangle, near the SE. cor. sec. 22, in the north-central part of sec. 27, and in the NW¼ sec. 28, T. 47 N., R. 26 W.; (3) in a northwest-trending zone in slate in the Chocolay Group in the W½ sec. 22, T. 47 N., R. 26 W.; (4) in numerous narrow zones trending west to west-northwest in slate and silicified Kona Dolomite in the N½ sec. 23 and the west-central part of sec. 24, T. 47 N., R. 26 W.; (5) in the Summit Mountain sill about 700 feet south of the center of sec. 18, T. 47 N., R. 26 W.; and (6) at the edge of a thick metadiabase dike about 1,500N–300E of the SW. cor. sec. 15, T. 46 N., R. 26 W.

Cherty silicified rock is a common part of the Palmer Gneiss in the NE¼ sec. 33, T. 47 N., R. 26 W., and underlies a half-mile-long east-trending ridge in the area of the Compeau Creek Gneiss in the central part of sec. 1, T. 46 N., R. 26 W., partly in the Palmer quadrangle and partly in the Sands quadrangle to the east (Gair and Thaden, 1968, p. 23–25). Boulders of silicified Compeau Creek Gneiss are abundant on a low topographic rise near 1,400N–1,700E of SW. cor. sec. 10, T. 46 N., R. 26 W.; their concentration here suggests a nearby source.

The quartz vein at the line between T. 46 N. and T. 47 N. near the west edge of the quadrangle is larger by far than any other in the area—as much as 170 feet thick and at least 5,500 feet long—and has an unusual fine, even-grained sugary texture. The vein is along a well-defined topographic lineament (depression) which continues east-southeast beyond outcrops of the quartz for about 2½ miles. The lineament probably represents an important fracture zone—possibly a fault—in the basement, but displacement cannot be detected because of the absence of marker beds.

The quartz veins are generally devoid of metallic minerals, except along some of the brecciated veins in the undivided Chocolay Group, mainly in the western half of sec. 24, T. 47 N., R. 26 W., which contain small concentrations of specular hematite. Several such hematitic quartz veins were prospected by test pits sometime in the past.

DOLOMITE-QUARTZ VEINS

Veins and pods of dolomite or dolomite-quartz are found in the Palmer Gneiss and Compeau Creek Gneiss mainly in the NE¼ sec. 33 and at the east end of the mapped belt of Palmer Gneiss in sec. 34, T. 47 N., R. 26 W. The rock is tan to brown, grain sizes vary widely, irregular areas of quartz are characterized by flamboyant and comb

structures, and pods in the Palmer Gneiss are cut by abundant veinlets (Gair and Simmons, 1968, p. D191). Separate deposits in the Palmer Gneiss have a maximum length of about 20 feet and width of about 3 feet, and in the Compeau Creek Gneiss, an undetermined length and maximum width of about 5 feet. The CaO, MgO, and SiO_2 of the veins probably were derived from surrounding gneiss and mobilized during crushing of the gneiss along shear-fracture zones.

PYRITE AND PYROPHYLLITE-QUARTZ CONCENTRATIONS

Traces of pyrite are present in many of the rocks in the quadrangle, particularly metadiabase, but noteworthy concentrations are known only in two places: in Ajibik Quartzite at the south margin of the Palmer basin at 3,900N–2,900E of the SW. cor. sec. 32, and in Compeau Creek Gneiss at the edge of a northwest-trending dike of metadiabase at 4,900N–3,750E of the SW. cor. sec. 16, T. 46 N., R. 26 W.

Within 10–20 feet on the north side of the outcrop in sec. 32, pyrite is somewhat concentrated in 1–3-inch patches. The pyrite content of the mineralized zone is probably less than 5 percent. Thin veinlets of pyrophyllite-quartz are present in the pyritiferous quartzite. The pyrite and pyrophyllite-quartz probably were deposited by locally derived hydrothermal solutions during shearing-faulting of the south margin of the Palmer basin.

The pyrite near the edge of the dike in sec. 16 is in scattered rich concentrations (estimated grade of concentrates, 10–20 percent), 1–4 inches in diameter within irregular masses of salmon-colored syenite. The area in which pyrite concentrations occurs is about 50 by 100 feet, occupying much of the north half of the nominal outcrop of Compeau Creek Gneiss. Possibly the unusual concentration of pyrite and feldspathic rock is related to the intersection of diabase and metadiabase dikes about 300 feet north of the exposure.

STRUCTURE

GENERAL PATTERN

The west-trending Marquette synclinorium and relatively uplifted basement rocks to the south are major structural divisions in the quadrangle. The axial part of the synclinorium contains large folds and is extensively sliced by faults (fig. 64). On the south flank of the synclinorium, the Palmer basin is a downfaulted remnant of a large doubly plunging syncline. Faults bound the synclinorium and the Palmer basin on the south and divide the Palmer basin into several wedge-shaped blocks. The structural trend of basement rocks in the south half of the quadrangle is generally east-southeast, and major dike trends in that area are northwest, north-northeast, east, and east-southeast.

FOLDS

Within the synclinorium, in the eastern half of the quadrangle, the Kona Hills and Wewe Hills are broad anticlinal uplifts separated by the Goose Lake syncline, the axis of which plunges northwest (fig. 64). Basement rock is exposed at the core of the Wewe Hills anticline. The broad Kona Hills and Wewe Hills anticlines are characterized by small internal folds. Those in the Wewe Hills generally lack consistent trends and probably reflect irregular relief on the top of basement rocks at shallow depths in the subsurface. In the north part of secs. 28 and 29, T. 47 N., R. 26 W., en echelon from the Wewe Hills anticline to the east-northeast, the faulted remnant of a companion anticline underlies the Ajibik Hills. The axis of the intervening syncline plunges northwest from near the northwest corner of sec. 28, past the northeast end of the Empire mine in sec. 19, and loses definition in an extensively faulted area near the southwest corner of sec. 18.

In the west half of the quadrangle, the axial part of the synclinorium contains broad west-plunging synclines separated by narrow anticlines or by faults in secs. 7 and 18, T. 47 N., R. 26 W., and sec. 13, T. 47 N., R. 27 W. The Suicide sill lies along two northwest-trending synclines in the NE¼ sec. 13, and in the NE¼ sec. 12, a small faulted segment of the Summit Mountain sill lies along a syncline between two major exposures of the sill. Several tight fault-bounded synclines are between broader anticlines in secs. 5 and 8, T. 47 N., R. 26 W. The two largest of such fault-bounded troughs, the Athens syncline in secs. 4–5 and the syncline just north of the Tracy fault in sec. 8 (fig. 64), are sites of the major Athens and Tracy ore bodies.

The central part of the Palmer basin is uplifted along faults which divide the overall syncline into several distinct structural units. The eastern part of the basin is occupied by a poorly defined east-west syncline, which is recognized mainly because of the presence along its axis of Goodrich conglomerate and quartzite (seen in only a few outcrops and drill holes) and a corresponding magnetic low (p. 130, this report). The synclinal axis

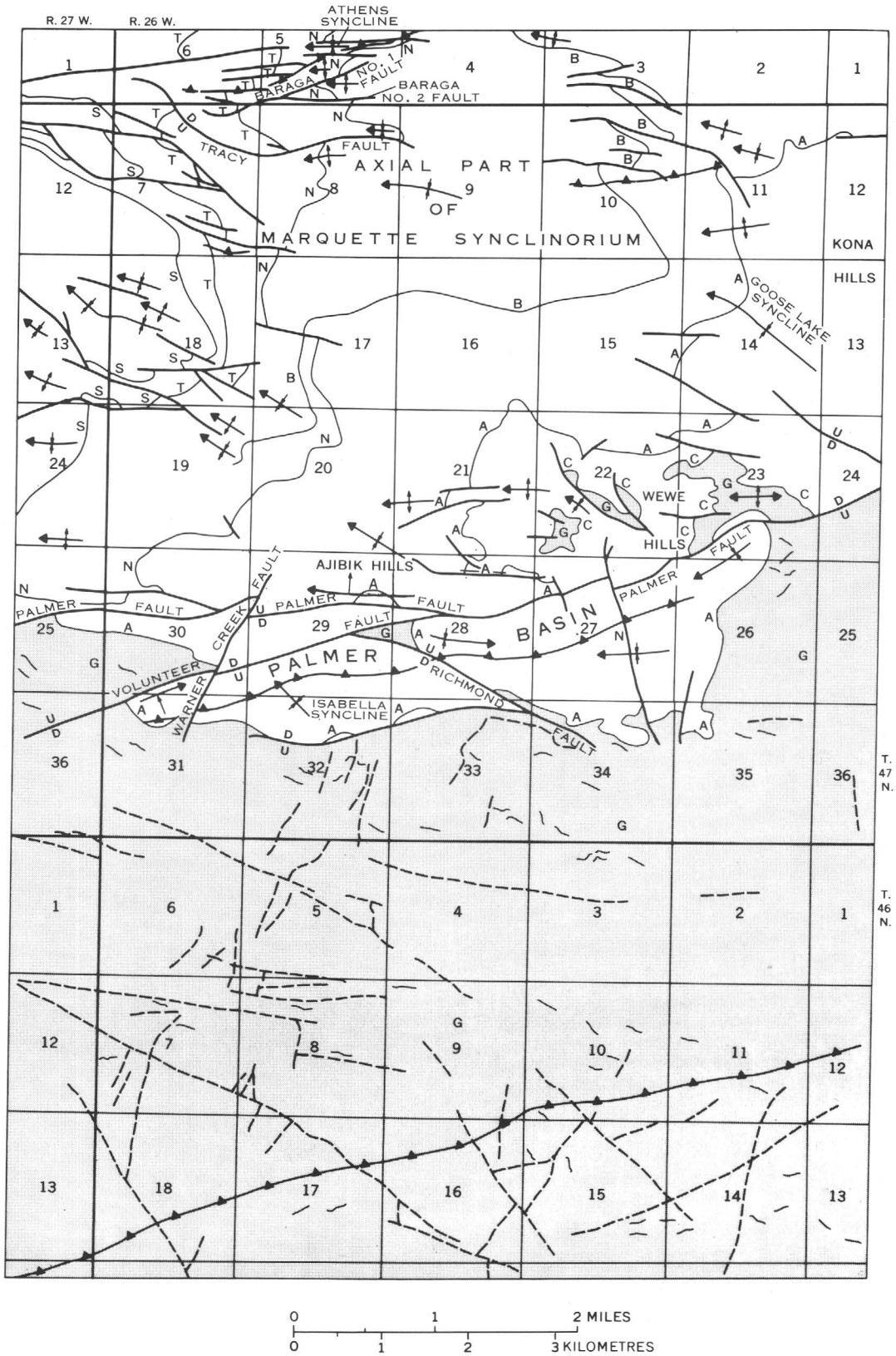

FIGURE 64.—Sketch map showing major structures in the Palmer quadrangle.

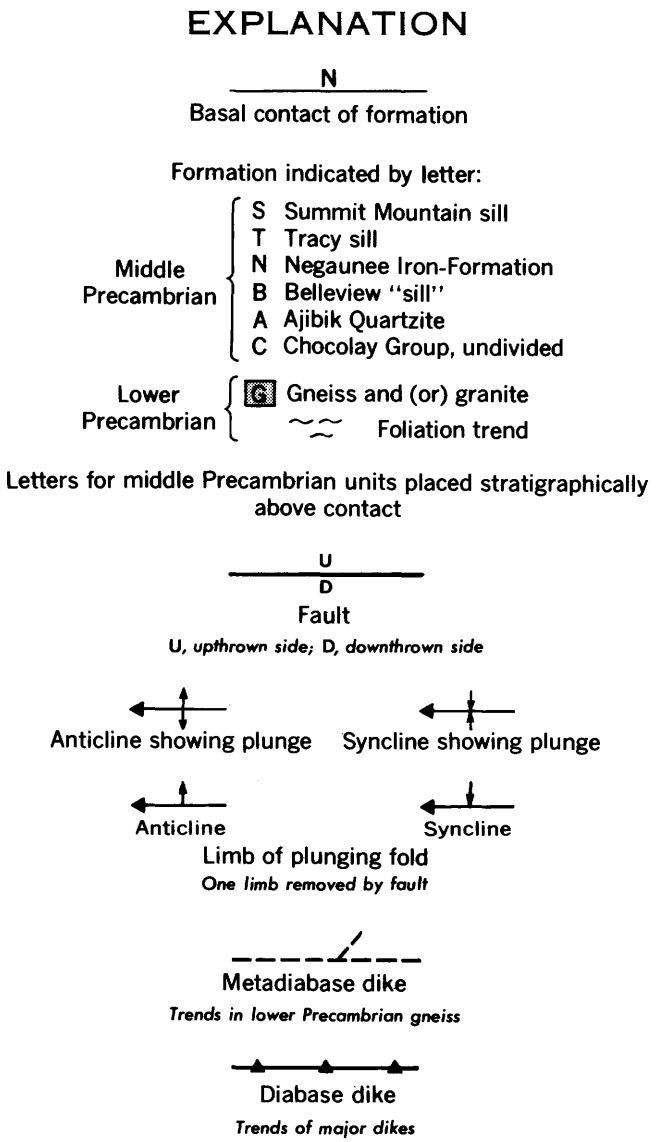

passes a short distance north of the New Richmond mine in the SW¼ sec. 27, and the axial plunge of the syncline in the vicinity of the mine is generally eastward. However, the south limb of the syncline is complexly folded into a second-order doubly plunging syncline in the southwest part of the New Richmond mine (pl. 4). Immediately west of the Richmond fault in the central part of the Palmer basin, the axis of the syncline has a west-northwest orientation, and along the axial zone, the Negaunee Iron-Formation is overlain by mafic meta-agglomerate correlated with Goodrich Quartzite. The Palmer basin closes on the west in the SE¼ sec. 30 and the NW¼ sec. 31, T. 47 N., R. 26 W. The structure of the west third of the basin is dominated by the northwest-plunging Isabella syncline in secs. 29 and 32 and by a deep fault-bounded trench across the central part of sec. 29.

FAULTS

The Marquette synclinorium is a result of folding and faulting that were related in time and cause. Faults can be grouped into those that formed contemporaneously with folds and have in general a west, west-northwest, or west-southwest trend, and those, much less numerous, that formed later in folding or afterwards and have north-northwest or north-northeast trends. Virtually the entire south margin of the synclinorium and Palmer basin are bounded by faults, and most large folds in the axial part of the synclinorium are cut by a fault along one limb. The Tracy and Baraga faults and the fault along the north side of the Athens syncline are outstanding examples of faults along the flanks of folds.

Faults are recognized by mapped offsets and truncations of stratigraphic units, by juxtaposition of rock units not in normal sequence with one another, and by elongate zones of brecciated and silicified rock (fig. 64). Thin mafic dikes are so common along faults cutting the iron-formation that the presence of such a dike anywhere in the iron-formation justifies a strong presumption of faulting.

The Palmer fault is the major fault in the quadrangle and is part of the regional fault bounding the south side of the Marquette synclinorium for many miles to the east and west (Gair and others, 1961; G. C. Simmons and W. F. Cannon, U.S. Geol. Survey, oral communs., 1969). The fault, which was first reported by Hotchkiss (1903), separates the Palmer basin on the south from the rest of the Marquette synclinorium. Regional displacement along the fault east and west of the Palmer basin is north side down, but between the basin and the synclinorium it is north side up with a stratigraphic offset of about 3,500 feet north of the center of sec. 29.

The Palmer basin is envisaged during sedimentation as an embayment that extended south of the main Marquette depositional basin and that subsequently was sharply downfolded and downdropped into basement rocks bordering on the east, west, and south as they were uplifted relative to the Marquette basin. The floor of the Palmer basin is upfaulted on the south side of the Volunteer fault and on the north side of the Richmond fault, which branches from the Volunteer. The Volunteer fault, which branches from the Palmer fault was first recognized by Hotchkiss (1903), and the Richmond fault evidently was first recognized by Vickers (1956, pl. 9). The Palmer basin and the major Palmer and Volun-

teer faults have been offset by later northward-trending faults, notably the Warner Creek fault near the west end and unnamed faults near the east end of the basin. The northward-trending faults are symmetrically oriented to a north line about midway between the east and west ends of the basin, which was probably a major stress axis of the late faulting.

Near the northwest corner of the quadrangle, faults apparently isolate a block containing the upper part of the Negaunee Iron-Formation (jaspilite) and Goodrich Quartzite from stratigraphically much lower parts of the Negaunee (near the horizon of the Tracy sill) to the north and south.

FOLIATION IN COMPEAU CREEK GNEISS

Foliation in most of the area of Compeau Creek Gneiss in the south half of the quadrangle trends east to southeast and dips vertically to moderately north and northeast. Only in a few limited areas, principally in the SE¼ sec. 33, T. 47 N., R. 26 W., and the north-central part of sec. 3, T. 46 N., R. 26 W., does the trend of foliation change from normal directions to a northeastward orientation.

In general, foliation trends in the gneiss are discordant with the south edge of the Marquette synclinorium and Palmer basin in the quadrangle, which emphasizes the role of faulting in establishing the south margin at an angle to the grain of the basement. The regional synclinorial axis, however, is close to the trend of foliation (Gair and Thaden, 1968, p. 63) and also is discordant to the Palmer fault.

DIKE PATTERNS

IN COMPEAU CREEK GNEISS

Metadiabase dikes in the Compeau Creek Gneiss are mainly in two roughly perpendicular sets trending southeast to east-southeast and northeast to north-northeast (pl. 1, fig. 64). The dikes trending south of east generally are several times thicker than those trending east of north, although both sets evidently were emplaced almost simultaneously. In secs. 32 and 33, dikes in the north-northeast-trending set apparently are truncated by middle Precambrian rocks in the Palmer basin; so they probably were emplaced in early Precambrian time. At that time a major axis of crustal tension was evidently alined northeast to north-northeast, and arching of the crust may have taken place along an east-southeast axis.

A diabase dike of Keweenawan age trends east-northeast through the gneiss in the south part of the quadrangle. A negative magnetic anomaly over this dike indicates that the dike extends west on the same trend for about 20 miles from the southwest corner of the quadrangle (Case and Gair, 1965).

IN MIDDLE PRECAMBRIAN METASEDIMENTARY ROCKS

Metadiabase dikes that cut middle Precambrian rocks are largely in the Negaunee Iron-Formation, and most are along faults at trends varying from slightly north to slightly south of east. A northwest trend is evident locally, as in the Foley dike in the NE¼ sec. 7 and in unnamed dikes in the east third of sec. 19, T. 47 N., R. 26 W. The trends south of east are similar to those of metadiabase dikes in the gneiss, but the east-northeast trends differ markedly from the north-northeast set in the gneiss, which suggests a fundamental discordance between dikes in the two areas. The control exerted on dikes by fold-related faults indicates that they were emplaced sometime after the onset of folding at the end of middle Precambrian time, before or during regional metamorphism.

Widely separated diabase dikes of Keweenawan age in the metasedimentary rocks have trends of east to east-northeast, essentially the same as the trend of the diabase dike in the gneiss. The most conspicuous of these dikes are the Isabella dike in the Palmer basin, an unnamed dike a mile northwest of Goose Lake, and the North Buffalo dike in secs. 4–6, T. 47 N., R. 26 W.

MAGNETIC SURVEYS

The aeromagnetic map of the Marquette iron district and bordering areas (Case and Gair, 1965) broadly delineates major magnetic and structural-stratigraphic units within the Palmer quadrangle. Ground magnetic surveys have facilitated tracing the Goose Lake Member of the Siamo Slate and contacts of other units, and major faults, in parts of the north half of the quadrangle having few or no outcrops (pl. 5). The most conspicuous magnetic zone, marking the Negaunee Iron-Formation in the northwest part of the quadrangle, has not been surveyed on the ground during the present work because the extent of the iron-formation in that area is well known from outcrops, drill data, and the aeromagnetic survey.

AEROMAGNETIC SURVEY

The aeromagnetic survey that included the Palmer quadrangle was flown in 1950, along north-south lines spaced at intervals of one-quarter mile, 500 feet above the ground, in a DC–3 airplane equipped with an AN/ASQ fluxgate magnetometer (Case and

Gair, 1965). J. R. Balsley supervised the survey, and F. A. Petrafeso, the compilation. The aeromagnetic survey showed the dominant magnetic features in the quadrangle to be (1) highs over the Negaunee Iron-Formation in northwest part, referred to, above; (2) a linear high above the Goose Lake Member of the Siamo Slate, extending northeastward from a short distance northeast of the village of Palmer to near the middle of the north boundary; (3) highs over the Negaunee Iron-Formation in the Palmer basin; and (4) a linear low above a diabase dike from the southwest corner eastnortheastward to the east boundary.

GROUND MAGNETIC SURVEYS

Ground magnetic surveys in the north half of the quadrangle (pl. 5) have been made principally to trace the poorly exposed Goose Lake Member of the Siamo Slate and the corresponding trend of the slate across the axial part of the Marquette synclinorium (Gair and Wier, 1964), and to locate magnetic zones and delineate the structure of the Palmer basin (Gair, 1965).

Fieldwork was done during the summer of 1963, sporadically during winter months between January 1965, and April 1967, and in May-June 1968. Magnetic measurements were made generally at paced intervals of 100 feet along sundial compass traverses spaced 200–400 feet apart. Most stations shown in the figure are believed to be located with an error of less than 100 feet. Isomagnetic contours shown in the figure are for gamma values relative to an arbitrary zero datum. The approximate absolute vertical-intensity gamma value of the arbitrary zero datum is 56,800 (Bath, 1951; Gair and Wier, 1964). Corrections for diurnal variations and mild magnetic storms were controlled by base-station readings generally made at intervals of 2–3 hours. The change in successive base-station readings was rarely greater than 90 gammas, and the variation for an entire day was seldom as much as 150 gammas. The average gamma error at any given station relative to the arbitrary datum was probably less than 30 gammas, the value of 1 scale division on the most commonly used number 2 calibration scale of the Jalander magnetometer.

The Negaunee Iron-Formation and the Goose Lake Member of the Siamo Slate are essentially the only magnetic rocks in the surveyed area. The Isabella dike in the Palmer basin, and an unnamed diabase dike in the central part of sec. 10, T. 47 N., R. 26 W. are negatively polarized, locally; linear lows in the SE¼ sec. 30 probably represent unexposed diabase dikes, one of them along the Volunteer fault. Metadiabase and mafic pyroclastic rock in the surveyed area have magnetic values corresponding to the magnetic background. Low magnetic values over the iron-formation north of the center of sec. 25, T. 47 N., R. 27 W. are a result of a decrease in primary or diagenetic magnetite and of secondary oxidation on the south flank of the Marquette synclinorium.

The positive magnetic anomalies shown on plate 5 are related to (1) the Goose Lake Member of the Siamo Slate, (2) the Negaunee Iron-Formation in the Palmer basin, and (3) a small segment of the Negaunee beneath the Belleview "sill"—referred to below as the Belleview zone.

ZONE OF GOOSE LAKE MEMBER

A strong linear anomaly follows an irregular course from the central part of sec. 10 southwestward to the northern part of sec. 29, T. 47 N., R. 26 W., reflecting a thin folded layer of magnetic rock—the Goose Lake Member of the Siamo Slate. The highest magnetic values, between 80,000 and 90,000 gammas, are where the iron-formation is in contact with metadiabase near the NE. cor. sec. 15, and probably result from enrichment in magnetite by the contact metamorphism of siderite. The anomaly is interrupted and apparently displaced from the central part of sec. 10 northwestward to the SW¼ sec. 3 by faulting of the iron-formation. Oxidation of the iron-formation adjacent to faults may explain the absence of the anomaly in the faulted zone. From the SW¼ sec. 3, the linear anomaly passes east-southeast to east, and near the SE. cor. sec. 2, it breaks up into small highs that continue the eastward trend into the Sands quadrangle. The iron-formation member lenses out or becomes weakly and irregularly magnetic a short distance east and northeast of the quadrangle (W. P. Puffett, U.S. Geol. Survey, oral commun., 1964). The linear anomaly ends to the southwest, apparently by lensing out, a short distance north of the Palmer fault.

PALMER BASIN

Magnetite-rich iron-formation and magnetite-bearing jaspilite in the Palmer basin form a general east-west magnetic high greater than 2,000 gammas along the south and southeast margins, interrupted only by the northwest-trending Richmond fault near the SE. cor. sec. 28, and by the north-northwest-trending fault in the SE¼ sec. 27 and the adjacent part of sec. 34. For much of its extent the anomaly exceeds 10,000 gammas, locally

is 20,000–90,000 gammas, and reaches 148,000 gammas at one station about 800 feet south-southwest of the NE. cor. sec. 32, corresponding generally with variations in magnetite concentration, by enrichment or relative decreases in oxidation. The anomaly in general decreases gradually northward because of the northward dip of the iron-formation beneath the Goodrich Quartzite. The virtually unexposed southeast margin of the Palmer basin is sharply defined by the large northeast-trending anomaly over magnetite-rich iron-formation near the SE. cor. sec. 27. A right-lateral offset in the anomaly in the south part sec. 30, and a left-lateral offset near the SE. cor. sec. 28, reflect movements along the Volunteer and Richmond faults, respectively. The large magnetic low near the middle of the south edge of sec. 29 apparently was caused largely by oxidation in the Isabella syncline. An elongate east-west magnetic low extends across sec. 27 just south of the center of the section and across the south half of sec. 28. The low crosses a few known occurrences of Goodrich Quartzite and is interpreted as caused by a narrow belt of Goodrich along the major synclinal axis in the east half of the Palmer basin.

BELLEVIEW ZONE

A sharply defined magnetic high extends northeast from the SE¼ sec. 19 to just north of the center of sec. 20, and from there north to near the center of sec. 17. The anomaly is caused by a segment of the Negaunee Iron-Formation beneath the Belleview "sill." The abrupt termination of the anomaly near the center of sec. 17 is attributed to faulting which displaced the iron-formation upward to the north and, in effect, westward because of the west dip. The Belleview "sill" was emplaced after faulting and crosses the fault from Siamo Slate on the north to the iron-formation on the south, west of the center of sec. 17.

ORE DEPOSITS

IRON

GENERAL CHARACTER AND DISTRIBUTION

Iron ore has been mined in the Palmer quadrangle area since about 1848. The deposits occur entirely within the Negaunee Iron-Formation. Ore bodies mined during the first hundred years consisted invariably of iron oxide concentrated by natural processes that took place after deposition and lithification of the iron-formation. Since World War II, the development of economic methods of concentrating iron oxide artificially has resulted in a changed concept of iron ore (James and others, 1961, p. 79) marked by a gradually increasing utilization of "taconitic" and jasper iron-formation in which little or no natural concentration has occurred. Most natural ore may be classified by chemical composition and physical structure—chemically as Bessemer and non-Bessemer ore, manganiferous ore, and siliceous ore, and physically as soft and hard ore (Marsden, 1968, p. 495, 501). Total production from the Palmer quadrangle has been about 65 million tons of natural ore, including 14 million tons of low-grade siliceous ore, and (at the end of 1972) about 25 million tons of pellets made from taconite ore. Shipments and types of ore from mines in the quadrangle through 1966 are listed in table 36.

Ore bodies (containing principally soft and hard ore) concentrated by natural processes, resulted from large transfers of material within the original iron-formation—influxes and residual concentrations of hematite or goethite, and the removal of silica and (or) carbon dioxide. In effect, such ore bodies represent localized end stages of widespread alteration and oxidation of the iron-formation.

Bodies of soft ore are encased in brown partly altered iron-formation; in the partly altered rock, prealteration iron carbonate, iron silicate, and magnetite have been more or less entirely oxidized and replaced by hematite or goethite, but chert is intact or only partly replaced by the secondary iron oxide. Hard ore almost invariably is bordered by jaspilitic iron-formation, corresponding chemically (in terms of ferric oxide) with the brownish, partly altered and oxidized iron-formation that surrounds soft ore. The iron-formation surrounding and giving rise to bodies of soft ore was recrystallized during regional metamorphism before being altered into ore. Iron-formation bordering hard ore, on the other hand, apparently was altered, and most of the iron of the ore bodies was concentrated before regional metamorphism, so that recrystallization acted on material already altered and concentrated.

Deposits of soft ore are mainly just above the base of the iron-formation; on plunging structures, such deposits in the quadrangle reach depths of 2,500 feet below the surface. Soft ore also occurs adjacent to faults and dikes and well above the base of the formation, above moderately dipping mafic sills. Large bodies of "siliceous ore" have resulted from partial postmetamorphic alteration and

TABLE 36.—*Production from iron mines in Palmer quadrangle*

[U, underground mine; OP, open-pit mine; OPU, open-pit mine initially and then developed underground]

Name of mine	Type of mine	Company	Location	Dates operated	Type(s) of ore	Tonnage shipped
Athens	U	Cleveland Cliffs	SE¼ 6-47-26	1918-51	Soft red non-Bessemer hematite	11,614,630
Blue	U	Queen Mining	SW¼ 5-47-26		do	Included in Queen total.
Breitung-Hematite	U		Parts of SE¼ and SW¼ 6-47-26.	1901-20	Soft hematite and goethite	Included in Tracy mine total.
Buffalo	U	Queen Mining	SE¼ 5-47-26		Hard and soft dark-red non-Bessemer hematite.	Included in Queen total.
Bunker Hill (adjoins Athens).	U	Cleveland Cliffs	SE¼ 6-47-26	1952-64	Soft red non-Bessemer hematite	[1]4,611,569
Carr	U	Mexican Iron	NW¼ 33-47-26	1872-74	Hard siliceous hematite?	2,380
Chicago			S½SE¼ 7-47-26	1879-83		9,012
East Buffalo; includes Lackawanna.	U	Queen Mining	SE¼ 5-47-26	1886-88	Hard and soft dark-red non-Bessemer hematite.	17,780
East Chicago Forty				1879-83		Included with Chicago total.
				1942-47		Included with Mary Charlotte total.
Empire (New)	OP	Cleveland Cliffs for Empire Iron Mining.	19-47-26	1963-present	Magnetic taconite (pellets)	[2]25,832,134
Empire (Old)	OP	Oglebay Norton; M. A. Hanna; Empire Quinn.	S½SW¼ 19-47-26	1907-28	Hard red siliceous hematite	768,474
Isabella; includes Watson.	U	Pickands Mather for Youngstown Mines; Steel & Tube of America; Cascade Mining.	SW¼ 29-47-26	1912-34	Soft red Bessemer and non-Bessemer hematite.	1,965,929
Jackson	OPU	Jackson Mining; Jackson Iron; Jackson Ore.	1-47-27	1846-1924	Hard hematite (specular, granular, slate) and soft red siliceous hematite.	[3]4,357,256
Lucy; includes East Jackson, McComber, Pendill.	OPU		SW¼SW¼ 6-47-26 NW¼NW¼ 7-47-26.	1870-1913	Soft red siliceous and manganiferous, non-Bessemer hematite.	622,797
Maitland (New) (see Volunteer, New).	OP		NW¼NW¼ 30-47-26			
Maitland Shaft (Old); includes Palmer Lake.	U		S½NW¼ 30-47-26	1908-28	Soft brown Bessemer and non-Bessemer, and siliceous hematite.	Included with Volunteer (Old).
Manganese; includes Aetna.	U		NE¼NW¼ & N½NE¼ 7-47-26.	1871-86		35,072
Mary Charlotte[4]; includes Breitung-Hematite 1 and 2, Himrod, Orion.	OPU	Himrod Hematite; Green Bay Iron; North Range Mining.	NE¼SE¼ 7-47-26 NW¼SW¼-SW¼NW¼ 8-47-26.	1872-1948	Soft red hematite; hard red siliceous hematite.	6,916,598
Milwaukee-Davis; includes Grand Rapids.	OP	Milwaukee Iron	SE¼NW¼ 7-47-26	1879-1915	Red soft to semihard Bessemer hematite.	533,022
Moore; includes Consolidated, Gribben, Mesaba's Friend, Royal.	OP	Gribben Iron; Consolidated Mining; American Steel and Wire; Oliver Iron Mining.	SE¼ 28-47-26	1873-1904	Red specular hematite and siliceous hematite-goethite.	87,769
New York Hematite	U		SE¼SW¼-SW¼SE¼ 4-47-26 6-47-26	1870-82		(37,587) included with Tracy mine total.
Palmer (adjoins Volunteer, Old); includes Bagaley, Emma, West End.	OPU	Cascade Iron; Palmer Iron; Pittsburgh & Lake Superior; Volunteer Iron.	NW¼ 31-47-26	1871-87	Specular slaty hematite and granular specular hematite.	Included with total for Volunteer (Old).
Pioneer	OPU		NW¼SW¼ 4-47-26	1886-88		15,409
Pittsburgh & Lake Superior (adjoins Palmer).		Pittsburgh & Lake Superior	NW¼ 31-47-26	1872-74	Specular slaty hematite	24,020
Platt	U	Donora Iron	NW¼NE¼ 32-47-26	1891-96		73,844
Primrose; includes Joyce, Primrose Valley.	OP	Oliver Iron Mining	SE¼SW¼ 28-47-26	1896	Siliceous hematite	6,040
Prince of Wales	U	Queen Mining	SW¼ 5-47-26		Soft hematite	Included with Queen total.
Queen; includes Regent Group.[6]	U	Queen Mining	SW¼ 5-47-26	1886-1917	Hard and soft dark-red non-Bessemer hematite.	[5]8,195,123
Richards (adjoins Moore).	OP	Richards Land & Iron	NE¼ 33-47-26	1887-97	Siliceous hematite	8,261
Richmond (New)	OP	M. A. Hanna for Richmond Iron.	SW¼ 27-47-26	1927-55	Hard red siliceous hematite	4,224,437
Richmond (Old)	OP	M. A. Hanna for Richmond Iron; Oliver Iron Mining.	SW¼SW¼ 28-47-26	1896-1927	do	3,604,913
Rolling Mill	OPU	Rolling Mill	S½NE¼ 7-47-26	1871-1935	Soft hematite and goethite	2,997,802
South Buffalo	U	Queen Mining	SE¼ 5-47-26		Soft hematite	Included with Queen total.
Star West; includes Home, Prout, Wheat.	OPU	Wheat Iron Mining; Home Iron Mining; Starwest Mining; Corrigan McKinney.	SE¼SE¼ 29-47-26		Soft blue siliceous Bessemer hematite.	209,115
Tracy[7]	U	Jones & Laughlin	SW¼ 5-47-26 NW¼ 8-47-26	1955-1971	Soft hematite and goethite	[8] 9,665,854
Volunteer (New)	OP	Pickands Mather	NW¼ 25-47-27. NW¼ 30-47-26.	1926-60	Hard gray-red siliceous hematite and siderite.	5,377,223
Volunteer (Old)	OPU	Donora Iron; Volunteer Iron; Volunteer Ore.	S½S½ 30-47-26 N½N½ 31-47-26.	1871-1916		[9]1,705,971
Total						93,482,434

[1] Included shipments from combined Athens and Bunker Hill mines operated as a unit; most of this production from Bunker Hill mine just north of Palmer quadrangle.
[2] Tonnage pellets to end of 1972.
[3] Jackson mine is mainly in Ishpeming quadrangle; so most of tonnage not from Palmer quadrangle.
[4] Includes Allen and Bay State or Green Bay pits not listed separately in table.
[5] Includes tonnage for so-called Queen group of mines—Buffalo, South Buffalo, Blue, Prince of Wales, and Queen.
[6] Regent Group includes Prince of Wales and parts of Queen and Blue mines.
[7] Includes Tracy, Baraga, and Lucky Star ore bodies in mining done since 1955, and Breitung, New York Hematite, and Lucky Star of period 1870–1937.
[8] Tonnage through 1971, includes 1,784,851 tons shipped from Breitung, New York Hematite, and Lucky Star mines between 1870 and 1937.
[9] Includes shipments from Palmer and Maitland Shaft (Old) mines.

oxidation, attended by some concentration of goethite or hematite, but by little removal of chert.

Hard ore and bordering jaspilite apparently occur at different stratigraphic levels in the iron-formation in different localities, but invariably just below the erosional contact with overlying Goodrich Quartzite.

MAJOR CATEGORIES OF IRON ORE

The major categories of natural iron ore on a basis of physical structure, namely hard and soft ore and the intermediate semihard ore, encompass the major compositional varieties, Bessemer and non-Bessemer ore, siliceous ore, and manganiferous ore. Bessemer ore contains less than 0.045 percent phosphorus; non-Bessemer ore contains more than 0.045 percent phosphorus, but commonly less than 0.3 percent, siliceous ore contains more than 18 percent silica; and manganiferous ore, 2–10 percent manganese.

SOFT ORE

Soft ore is red, bluish red, red brown, yellow brown, or yellow, and is earthy, friable, vuggy, porous, and semiplastic to locally compact and lumpy. Compact layers of iron oxide several inches thick to nearly paper-thin plates, generally pass irregularly into less coherent ore. Principal ore minerals are reddish and red-brown hematite, red-blue martite, and brown, yellow-brown, and yellow goethite. Hematite in polished sections typically is finely pitted and may be hydrated (variety lepidocrocite?). Gypsum is present in some ore from the Tracy mine and vicinity, and manganite and possibly other manganese minerals are present in vugs and veins in oxidized iron-formation near the Tracy ore body.

Most soft ore from the Palmer quadrangle is a low-phosphorus, non-Bessemer type. Chemical analyses of ore shipments averaged for a number of years for different ore bodies are listed in table 37. Average iron content in the major bodies of soft ore ranges from about 54 to 60 percent; silica, about 6 to 15 percent; phosphorus, 0.05 to 0.13 percent; and manganese, 0.2 to 0.5 percent.

HARD ORE

Hard ore is blue black, steel gray, or reddish blue to reddish black, and compact, lumpy, and massive. Original iron-formation laminations are preserved in some hard ore, and remnants of layers of red chert (jasper) and gray chert are incorporated in the ore in places. Principal ore minerals are specular hematite and martite. Chemical analyses of shipments of hard ore, specifically, are not available from the mined-out deposits in the Palmer quadrangle. Most such ore was taken during the early years of mining at the Jackson and Old Volunteer mines or was included and analyzed with other ores from those mines. Similar ore from the Cliffs Shaft mine a few miles west of the northwest corner of the quadrangle, has had a compositional range over the years of about 58–62.5 percent in iron, 5–7 percent in silica, 0.09–0.13 percent in phosphorus, and 0.2–0.8 percent in manganese.

SILICEOUS AND MANGANIFEROUS ORE

Siliceous ore in general contains more than 18 percent silica, but most has been mined to yield 38–44 percent silica (Marsden, 1968, p. 495). Siliceous ore is red, reddish brown, or reddish to bluish black, and semihard, with a high proportion of compact platy ferruginous and cherty material and minor earthy ferruginous material. Principal ore minerals are hematite (or lepidocrocite?) and goethite. Siliceous ore from the Palmer quadrangle, as indicated by averages of yearly shipments (table 37), generally has contained 36–43 percent iron and 30–43 percent silica. Manganese ranges from 0.09–0.3 percent in most deposits. Ore in the contiguous Lucy and South Jackson ore bodies near the SE. cor. sec. 1, T. 47 N., R. 27 W., is both siliceous and manganiferous, and contains 2.5–3.5 percent manganese. The manganiferous ore apparently reflects the higher-than-normal manganese content of the iron-formation near the SE. cor. of sec. 1. Secondary manganese minerals in oxidized iron-formation indicate that the manganiferous iron-formation extends for about a mile east across the north part of sec. 7, T. 47 N., R. 26 W., from the manganiferous siliceous ore at the Lucy mine.

TACONITE ORE

Taconite ore, as of 1972, was being mined in the Palmer quadrangle only at the Empire mine. The taconite ore is gray to dark-gray, magnetite-rich, cherty sideritic iron-formation from which commercial concentrations of iron are prepared artificially by crushing and magnetic separation. Normal grain sizes of 5–35 microns necessitate crushing of 95 percent of the taconite ore to sizes less than 500 mesh to free the magnetite from the cherty quartz and carbonate. Some—perhaps a large part—of the existing magnetic iron oxide probably was deposited as iron carbonate and converted to oxide during diagenesis of the iron-formation. The taconite ore ap-

TABLE 37.—*Average chemical analyses for annual shipments of iron ore from major ore bodies, Palmer quadrangle*

[Compiled from annual publications of the Lake Superior Iron Ore Association, 1911–1952 (incomplete), and the successor organization, the American Iron Ore Association, 1961–1968 (incomplete), Cleveland, Ohio]

Ore body	Year of shipment (yearly averages are averaged again by groups of years)	Fe	P	SiO_2	Mn	Al_2O_3	CaO	MgO	S	Loss on ignition	Moisture[1]
Soft ore											
Athens	1919, 1921–23, 1925–27, 1929, 1931.	60.35	0.130	6.85	0.50	2.85	0.88	0.77	0.014	1.61	12.62
Do	1934, 1937, 1951	58.56	.098	10.64	.36	2.39	.50	.51	0.11	1.33	10.78
Isabella	1916, 1919, 1922–23, 1925–27, 1929, 1931, 1934.	57.69	.064	13.32	.16	2.30	.40	.33	.012	1.16	8.68
Maitland (Old)	1913	57.40	.047	12.46	.63	1.34	.48	.37	.051	1.57	10.66
Mary Charlotte:											
Mary grade	1910, 1913, 1916, 1919, 1921–23, 1925–27.	58.62	.107	9.25	.23	2.72	.80	.77	.087	1.85	13.55
Charlotte grade	1910, 1913, 1916, 1919, 1921–23, 1925.	54.46	.098	15.09	.25	2.69	.93	.85	.089	1.82	12.81
Milwaukee-Davis	1910, 1913	60.62	.124	5.93	.41	1.12	1.28	1.04	.033	2.24	10.62
Queen	1910, 1915–16	57.18	.109	6.44	[2].47	---	---	---	---	---	----
Rolling Mill	1910, 1913, 1916	58.16	.107	7.07	---	---	---	---	---	---	----
Do	1919, 1921, 1925–27, 1929, 1931, 1935.	58.41	.228	8.54	.42	2.67	1.53	.79	.119	2.80	12.03
Star West	1913	55.15	.036	15.60	.15	.90	1.40	1.22	.003	1.00	2.60
Tracy	1961–66, 1968	59.15	.095	6.99	.39	2.92	---	---	.419	---	11.23
Siliceous ore											
Empire (Old)	1910, 1916	40.91	0.080	39.00	0.095	0.98	0.28	0.30	0.016	0.90	3.55
Jackson Bessemer	1910	50.30	.042	24.50	.10	2.00	.35	.08	.015	1.00	2.00
Lucy[3]	1910, 1912	46.07	.067	27.75	3.46	2.57	.39	.26	.019	2.64	9.95
Maitland (Old)	1919, 1928	42.97	.065	31.01	.25	1.20	.42	.96	.013	4.45	3.89
Richmond (Old)	1910, 1916, 1919, 1922–23, 1925–26	40.32	.048	38.79	.11	1.03	.51	.46	.012	1.50	3.16
Richmond (New)	1927, 1929, 1931–32	36.78	.058	43.05	.09	1.51	.72	.51	.007	1.06	3.08
Rolling Mill siliceous	1919	41.50	.076	36.47	.32	2.52	1.32	.67	.020	2.14	6.25
South Jackson[3]	1910, 1913, 1916, 1919, 1922–23	39.78	[4].006	34.57	2.61	1.53	.46	.28	.016	2.74	7.35
Volunteer (New)	1926–27, 1929, 1931	36.04	.044	42.40	.19	1.76	.26	.27	.014	2.93	3.38
Taconite ore (after concentration and pelletization)											
Empire (New)	1964–66, 1968	64.26	0.011	7.35	0.07	0.33	---	---	0.003	---	1.39

[1] Measured before drying.
[2] No data for 1910; represents average for 1915–1916.
[3] Also classified as manganiferous ore.
[4] Phosphorus for 1913 shipments was 1.03 percent; listed average is for shipments during the other 5 years.

parently has sustained little absolute increase in iron content since deposition, and virtually none since regional metamorphism. The raw taconite ore typically contains 30–35 percent iron, 35–45 percent SiO_2, 0.2–0.35 percent manganese, and 0.03–0.05 percent phosphorus. Pellets made from the magnetite concentrates contain about 64 percent iron, 7 percent silica, 3 percent Mn, and 0.01 percent P (table 37).

BRIEF HISTORY OF MINING

Iron was first discovered in the Lake Superior region in 1844, in sec. 1, T. 47 N., R. 27 W., a few hundred feet west of the quadrangle boundary. The next year the Jackson Mining Company was organized and in 1848 commenced mining hard ore at the Jackson mine near the discovery site. More than 100 other mining companies were formed during the 2 years after the first discovery, but most of them soon failed. Operations during the first 2 decades apparently proceeded mainly at the Jackson mine and at several other properties west of there. No mining at other locations in the quadrangle has been recorded until 1870. Between 1870 and 1872, the mining of soft ore began in the east and southeast environs of the present city of Negaunee, at the Lackawanna (later East Buffalo), Lucy, Manganese, Mary Charlotte, New York Hematite (later, Breitung Hematite and, still later, Tracy), and Rolling Mill mines (fig. 65). During the same years the mining of hard ore started at the Old Volunteer mine and contiguous properties just west of the present village of Palmer, and small amounts of siliceous ore were taken east of Palmer at the Carr property. Over the years, mines in the east and southeast environs of Negaunee—principally the Athens mine, the Queen group, and the Tracy mine—have continued to be the main source of soft ore in the quadrangle; the Jackson and Old Volunteer mines provided virtually all the hard ore mined. The last mining of hard ore in the quadrangle was at the Old Volunteer mine in 1916. About 43 million tons of soft ore have been taken from the mines in the quadrangle, and roughly 2 million tons of hard ore.[15] Mines near Palmer—principally the Old and New Richmond mines to the

[15] 4,357,250 tons of ore from Jackson mine includes hard siliceous ore and is mainly from the Ishpeming quadrangle.

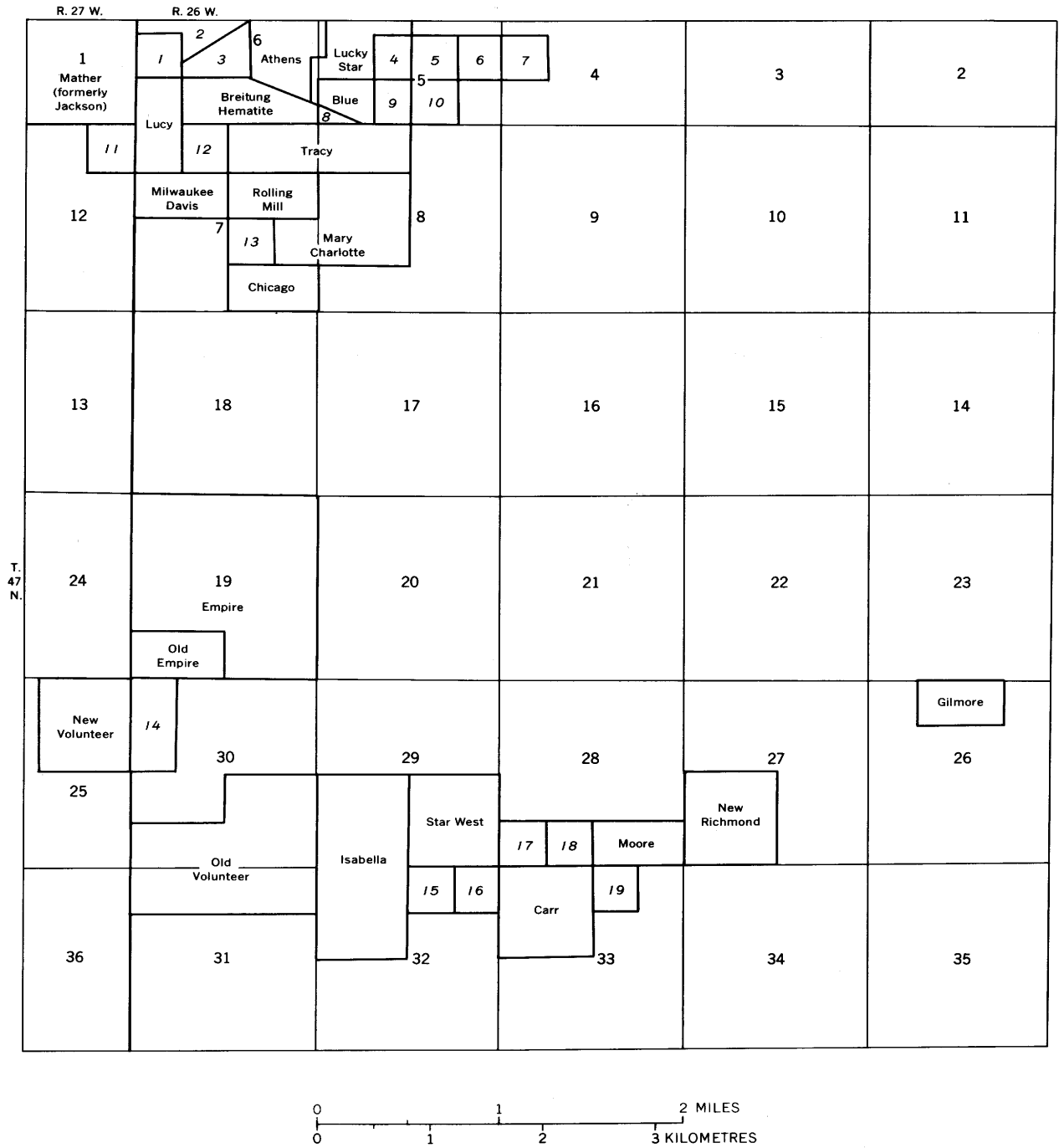

FIGURE 65.—Index map of mining properties in the Palmer quadrangle. Property too small to list name on map: *1*, Pendill; *2*, Cliffs Arctic; *3*, Bunker Hill; *4*, Prince of Wales; *5*, Buffalo; *6*, East Buffalo (formerly Lackawanna); *7*, Pioneer; *8*, Sundry Parcel 1; *9*, Queen; *10*, South Buffalo; *11*, Section 12; *12*, Manganese; *13*, Himrod; *14*, Maitland-Volunteer; *15*, Platt; *16*, Wicks; *17*, Old Richmond; *18*, Primrose; *19*, Richards.

east and the Old Empire and New Volunteer to the northwest—have been the sources of almost all the siliceous ore mined, some 14 million tons. The production of pellets from taconite ore began at the (new) Empire mine in 1963 and through the 1972 season totalled about 25.8 million tons. The production rate of pellets since the completion of a plant expansion in 1967 has been a little more than 3 million tons per year, making the Empire mine the largest single iron mine in Michigan at the time this report was written.

Iron mines in the Palmer quadrangle, their dates of operation, types of ore, and production are listed in table 36.

DESCRIPTION AND GEOLOGIC SETTING OF SOFT-ORE DEPOSITS

Soft ore bodies formed in the Negaunee Iron-Formation after consolidation, metamorphism, and deformation of the rock. They are a culmination of alteration types that can be seen in earliest stages in most natural exposures. Bodies of soft ore occur at different stratigraphic levels within the iron-formation. Iron-formation in which soft ore formed apparently contained iron minerals that could be readily oxidized. Chert, where present, must have been in grains of sufficiently small size to be dissolved by natural aqueous solutions in reasonable intervals of geologic time (James, 1955, p. 1478–1480). Parts of the iron-formation that have given rise to bodies of soft ore are floored by relatively impermeable rock—commonly slate or mafic igneous rock, but in places evidently only by less permeable iron-formation. Favorable sites for ore bodies are where dipping beds flatten or are interrupted by a barrier that produced an upward-opening structural trap.

Large volumes of iron-formation beneath the Tracy sill in the axial part of the Marquette synclinorium show various stages of alteration between pristine postmetamorphic iron-formation and soft ore. Samples of such rock collectively provide virtually a panorama of the change. Sideritic carbonate and iron silicates have been oxidized to earthy red hematite, to goethite, and probably also to hydrated hematite; magnetite octahedra have been oxidized to martite; manganite and possibly other unidentified manganese oxides formed locally, probably from manganese-bearing sideritic carbonate or from kutnahorite; and chert has been softened to milky white silica or has been replaced by iron oxide (figs. 66, 67) and in places has been leached, leaving small voids. Original carbonate and silicate, once oxidized, may be indistinguishable. In the earliest stages of oxidation, isolated rhombs of carbonate and flakes or needles of silicate become slightly rusted; later, the single crystals may be totally replaced pseudomorphously by hematite or goethite, and oxidation advances into aggregates of the carbonate and silicate. Original laminations tend to be obscured or destroyed in the red, ocherous yellow, or mottled red and yellow rock derived from pale-gray, yellow-gray, and green varieties of carbonate or silicate iron-formation. On the other hand, oxidation of dark-gray magnetite-rich iron-formation generally produces a well-laminated rock finely speckled with blue-black martite. During the earliest stage of martitization, the outer margins of magnetite crystals are replaced by hematite, with perfect preservation of original crystal faces (fig. 56). The boundary between martite and magnetite is irregular, and it moves into the magnetite during succeeding stages of replacement. Eventually, an octahedron of magnetite may become a sharply defined octahedron of hematite in which there may remain only tiny remnant patches, or no vestige, of magnetite. The simultaneous, side-by-side development of two forms of ferric oxide, of martite from magnetite and earthy hematite or goethite from carbonate or silicate, is extremely selective, as shown in polished sections by the remarkable preservation of grain boundaries of magnetite-martite.

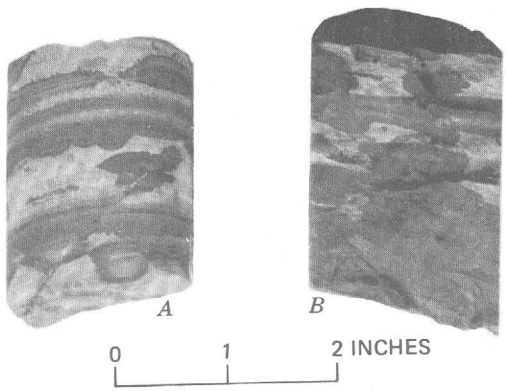

FIGURE 66.—Drill-core samples showing partial oxidation-replacement of carbonate-magnetite iron-formation. Siderite, magnetite, and chert replaced by hematite and goethite (dark). Drill-core sample JG–93B–66; drill-hole location approx. 1,400N–1,150W of SE. cor. sec. 7, T. 47 N., R. 26 W. (drill-hole location 256, sample from 109 ft).

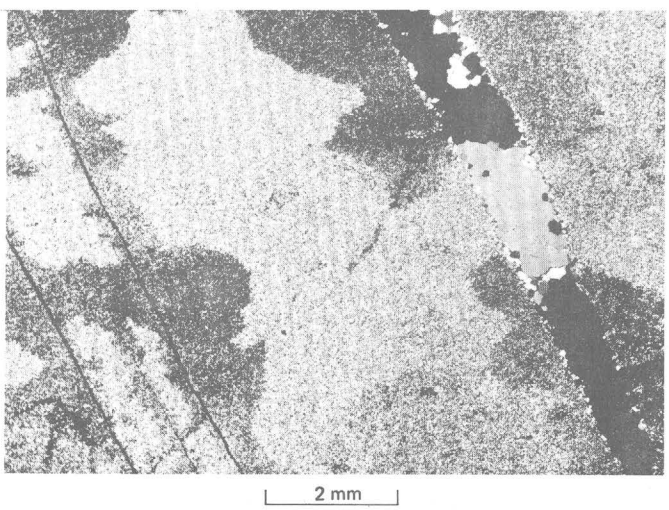

FIGURE 67.—Photomicrograph of thin section showing irregular replacement of chert by goethite (dark). Surface sample JG–8A–64, Moore mine, 500N–2,600E of SW. cor. sec. 28, T. 47 N., R. 26 W. Crossed polarizers.

During oxidation of the iron minerals, chert typically was softened by leaching and tended to be replaced by secondary iron oxides. Nodular concentrations of goethite or hematite that have replaced chert produce a spotted pattern or "leopard texture" in parts of the oxidized iron-formation; the essential control for such texture remains unknown. In places, finely pitted bedded white chert many feet thick, although replaced by irregular patches of hematite and goethite, is virtually free of iron minerals between the patches of replacing hematite or goethite. Projection of the iron-free beds of chert into the adjacent patches of replacing iron oxides suggests the original existence of continuous beds of chert-rich iron-formation many feet thick, prior to replacement. Beds of chert of comparable thickness, however, are not known from unoxidized parts of the iron-formation. During oxidation-leaching of such rock, disseminated grains of iron minerals may have been removed entirely from original positions within individual laminae, and the resulting oxidation products may have replaced parts of the remaining cellular chert, or silica leached from the iron-formation updip may have been redeposited in and replaced leached oxidized iron-formation at a lower level owing to local ponding of ground-water solutions. At the same time or later, small vugs formed at boundaries between chert and secondary iron oxide and within patches of secondary iron oxide. Some vugs are now partly filled with manganite and goethite (D. F. Hewett, U.S. Geol. Survey, written commun., 1967), nacrite, dickite, kaolinite, and other clay minerals (Bailey and Tyler, 1960), and with quartz.

Although iron silicates theoretically could be a prime source of soft ore, they are not the necessary preoxidation iron mineral, as suggested by Tyler (1949) and Mann (1953), and in fact are most abundant in iron-formation at a distance from enriched (nontaconite) ore bodies. Gradational changes from soft ore to partly oxidized carbonate show that soft ore in the Palmer quadrangle is derived from carbonate-rich iron-formation, as in the Iron River-Crystal Falls district, Michigan (James and others, 1968, p. 115). However, the widespread occurrence in the Negaunee Iron-Formation, and near some ore bodies, of mixed facies, rich in carbonate but also containing magnetite (martite) and small amounts of silicate, indicates that oxidation of these less abundant iron minerals gave rise to some of the hematite or goethite in soft ore. Once hematite has formed, whether as a primary sediment or later, it is inert to oxidation, is relatively insoluble, and is subject to further concentration, mainly residually, by the removal of chert in solution.

Most bodies of soft ore lie along and rise into the iron-formation from the contact of the iron-formation with the underlying Siamo Slate. Favored sites are synclinal troughs and other upward-opening structures that result from slate faulted against, or dikes cutting, the tilted iron-formation-slate contact. The favorable conditions for the accumulation of soft ore near the base of the iron-formation and in structural troughs are well illustrated by major occurrences of such ore in the axial part of the Marquette synclinorium east and southeast of the city of Negaunee (pl. 6).

The bottoms of some now largely exhausted ore bodies in the Mary Charlotte mine, shown in the south part of the isometric cross section diagram, are 100–300 feet above the base of the iron-formation and apparently were only in part floored by intrusive rock.

ORE BODIES RELATED TO FOLDS

SYNCLINAL ORE BODIES

Synclinal ore bodies are limited downward by a relatively impermeable layer or formation—commonly the top of the Siamo Slate—which is an integral part of the fold configuration. Only the upper few feet of the slate at most have been touched by oxidation. Locally, the base of an ore body may be above the impermeable floor, over patches of incompletely altered iron-formation. The upper surface of ore bodies typically is irregular, grades into oxidized iron-formation, and may be defined only by chemical analyses of samples. It may be depressed above the axis of the syncline, giving the entire ore body a synclinal form, or it may pass from limb to limb more or less horizontally, or it may even arch upward somewhat across the axial part of the syncline. Ore commonly builds up higher on one limb than the other. Synclinal ore bodies include a variant formed on structural terraces where dipping beds on the flank or broad nose of a large syncline are locally flattened but do not reverse in dip.

The combined Athens-Bunker Hill-Lucky Star-Prince of Wales ore body and its extension to the east (pl. 6) represents the outstanding synclinal ore body in the Palmer quadrangle. The ore body follows the synclinal trough within about 100 feet stratigraphically above the base of the iron-formation, from near the land surface at the old Pioneer property (fig. 65) about 2,100 feet north of the

SE. cor. sec. 5, T. 47 N., R. 26 W., westward for about 8,200 feet, plunging in that distance to a depth of about 2,600 feet below the surface. The ore body is relatively narrow in the tight eastern part of the syncline (pl. 6), cross sections 2,200E, 2,000E, 1,720E) but widens westward, as the south limb flattens and the syncline opens, to a maximum of about 700 feet (cross sections 200W, 1,000W, 1,400W). The axial part of the syncline evidently was a favorable site for the emplacement of dikes parallel and subparallel with the axial plane. The dikes too are highly altered adjacent to ore, so clearly were emplaced before the ore. They may have facilitated the formation of soft ore by fragmenting the iron-formation and thus increasing its porosity, and by subdividing the syncline into smaller more confined troughs. However, evidently only locally, as on the south limb in cross section 200W, do the dikes account for a significant buildup of soft ore apart from the synclinal trough as a whole.

The blue ore body, 1,000–1,200 feet south of the Lucky Star ore body is localized in a west-plunging syncline cut by steep dikes crossing the axial trend at a small angle (pl. 6, cross sections 600E, 800E, 970E, 1,100E). As in the Athens-Bunker Hill-Lucky Star-Prince of Wales ore body, the syncline evidently channeled ground-water circulation and played a critical role in the accumulation of soft ore, whereas dikes were only of minor significance.

ANTICLINAL ORE BODIES

No soft ore bodies related essentially to anticlines are known in the Palmer quadrangle. However, in places, second-order anticlines on the flanks of synclines have been overridden by a buildup of soft ore in the syncline, as in the Athens ore body (cross section 600W) and in the Blue ore body (cross section 1,100E). Ore at these places is thinner over the crest of the anticline than in the bordering first-order syncline on one side and second-order syncline on the other. It seems likely that ore accumulated first in the synclines and eventually coalesced above the anticline when the second-order syncline was filled. If this interpretation is correct, the anticlines were only of incidental importance.

ORE BODIES RELATED TO DIKES

Mafic dikes played a critical part in the localization of many ore bodies by forming barricades and structural troughs at their intersections with beds of iron-formation or iron-formation and slate, and thus serving as a floor or retaining wall for at least part of the ore body. Where dikes are along faults bounded by iron-formation on one side and slate on the other, as is common, the dikes apparently served the same function as slate faulted against iron-formation where dikes were absent; so the fault is of more significance than the dike in the localization of the ore.

The Baraga ore body (pl. 6, cross sections 200E, 300W, 600W), part of the Tracy ore body (pl. 6, cross sections 200E, 00), many of the ore bodies in the Mary Charlotte mine (pl. 6, cross sections 890E, 160W; fig. 68), parts of the Lucy ore body (fig. 69), and the Isabella ore body in the south part of the Palmer basin (pl. 3) rest on floors or against walls of dike rock. In the Mary Charlotte mine, a network of dikes effectively subdivides the iron-formation into blocks (fig. 68). Within a block, an irregular isolated body of soft ore may extend upward vertically or at an inclined angle into the iron-formation from a structural trough or floor made by the dike bounding the lowermost part of the block. In mine workings and structure sections through such an ore body, above the level of the dike-rock floor, the ore may be in contact only with iron-formation and appear to be unrelated to a structural trough or dike. At the Isabella mine, soft ore accumulated in a structural trap where the northwest-plunging trough of the Isabella syncline is blocked by a vertical dike cutting east-northeast across the syncline (pl. 3). Ore collected in three favorable bedding zones in the iron-formation—zones evidently having a suitable combination of composition and permeability—on the southeast side and up the plunge of the synclinal axis from the dike (Stephen Royce, private report to Volunteer Ore Co., 1942). The ore was said to improve in grade and thickness as it approached the dike and the three zones coalesced close to the dike. Exploration both outside the synclinal trough and down the plunge of the trough immediately northwest of the dike found no ore. The localization of the soft ore thus is attributed to the structural trap at the intersection of the syncline and the dike.

The western part of the Tracy ore body rests on the top of a thick flat-lying sill-like dike of metadiabase (pl. 6, cross sections 1,875W, 2,255W), which cuts gradually upward to the west across the west-plunging Siamo Slate and Negaunee Iron-Formation and is correlated with the Belleview "sill" mapped at the surface to the east.

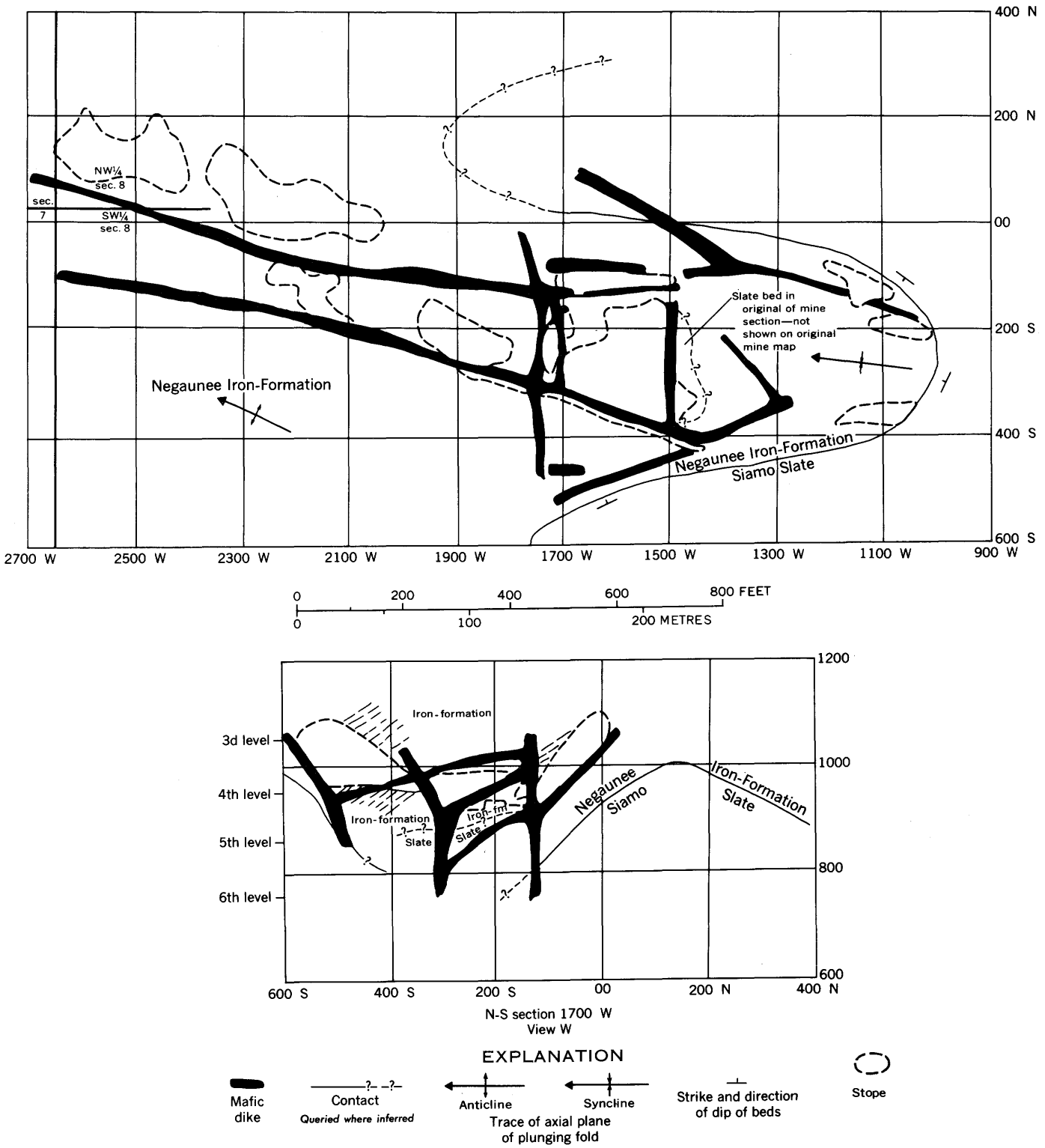

FIGURE 68.—Geologic map of part of the 4th level and section of the Mary Charlotte mine. Modified slightly from map of North Range Mining Co. Coordinates 00–00 at center of sec. 8, T. 47 N., R. 26 W.

Old structure sections of the Lucy mine provide an incomplete three-dimensional picture of the ore bodies and a somewhat equivocal picture of the relationship of dike rock to ore (fig. 69). The ore clearly is underlain by dike rock in places, but locally dike rock also is in vertical contact with

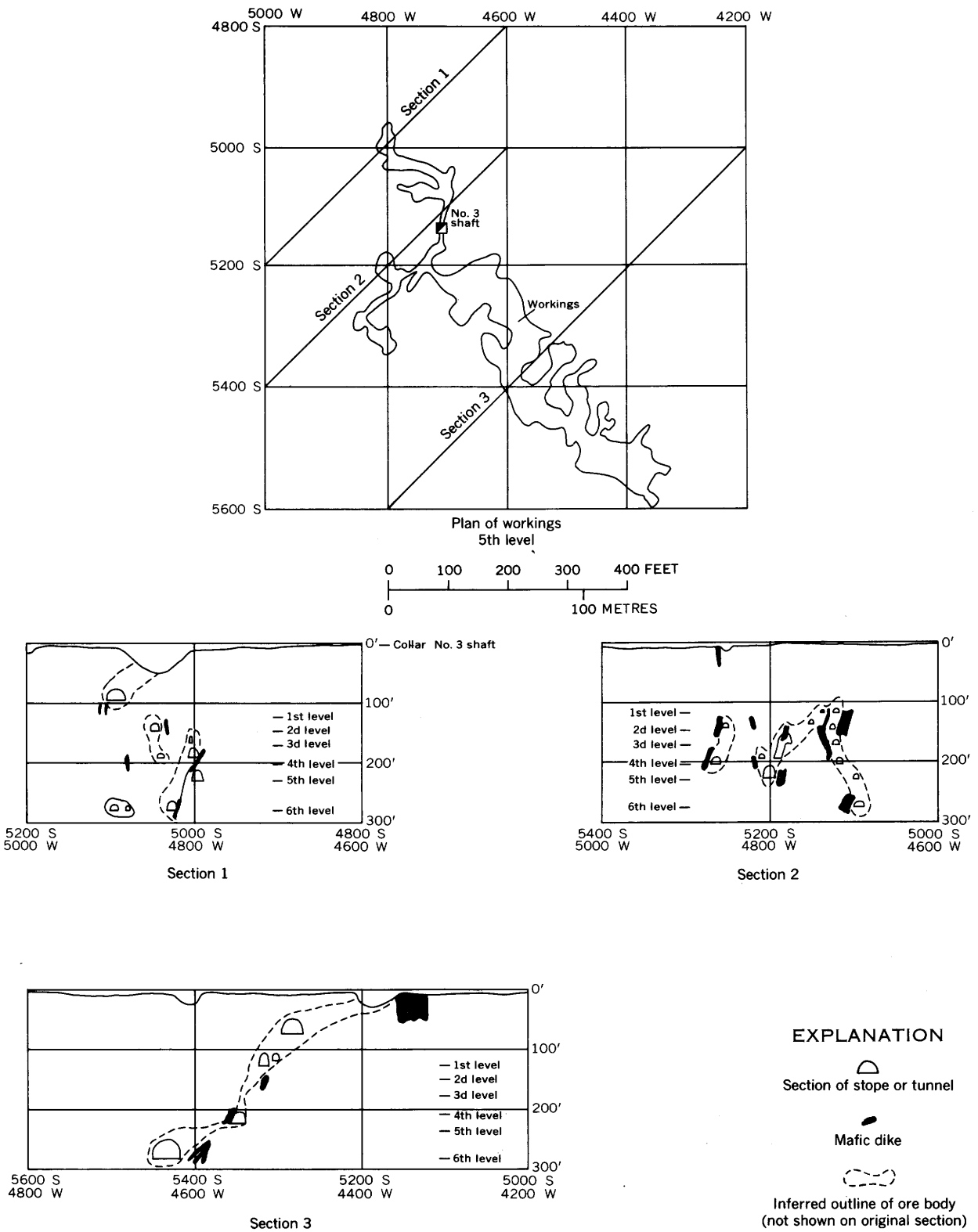

FIGURE 69.—Map and sections of the Lucy mine, SW¼SW¼ sec. 6, T. 47 N., R. 26 W.; Coordinates 00–00 at NE. cor. sec. 6. Map and sections modified slightly from maps of Cleveland Cliffs Iron Co.

or overlies ore. A possible explanation is that ore that began accumulating above a steeply dipping dike-rock floor continued to accumulate upward even where the dip of the dike became vertical or relatively overturned, although such a relationship would be contrary to the observation in the Iron River-Crystal Falls district that ore ends abruptly on the overturned overhanging limbs of synclines (James and others, 1968, p. 118).

ORE BODIES RELATED TO FAULTS

Some bodies of soft ore in the axial part of the synclinorium rest on a floor of Siamo Slate but are bounded on one side by a fault along which the iron-formation has been downdropped against the slate. The ore occupies troughs which are truncated synclines or monoclines, outlined by the interesecting sedimentation and fault contacts of the iron-formation and slate. Dikes along some of the faults apparently fulfill the same function as the slate block on one side of the dike, as noted above; consequently, in such situations they are not critical to the formation of the ore body. The Baraga ore body (pl. 6, cross sections 00, 300W, 600W, 800W) and the Tracy ore body (cross sections 800E, 200E, 00, 500W, 1,300W, 1,875W) provide outstanding examples of ore bodies thus related directly or indirectly to faults.

ORIGIN OF SOFT ORE

Three theories—the meteoric, hydrothermal, and modified hydrothermal—have been posed in recent times to explain the oxidation of iron minerals and the leaching of chert that necessarily took place during the conversion of iron-formation to soft ore of the Lake Superior type (James and others, 1968, p. 120). The alteration of iron-formation accordingly is envisaged as having taken place through the agency of (1) meteoric or supergene water "carrying oxygen and carbon dioxide from the atmosphere" (Van Hise and Leith, 1911, p. 544–545; Leith and others, 1935, p. 24–25); (2) hydrothermal or hypogene solutions given off by deep magmatic bodies (Gruner, 1930); or (3) mixtures of meteoric and hydrothermal solutions (Gruner, 1937).

The meteoric theory is consistent with the minerals and assemblages in oxidized iron-formation and soft ore, with the occurrence of ore in upward-opening structures, with the continuation of most ore bodies and all known areas of oxidation to the land surface, and with the decrease in oxidation downward from the surface. Objections to the meteoric theory have been based largely on an assumed inadequacy of (1) cold water to dissolve large amounts of chert, and (2) surface-derived ground water to circulate effectively to the depths of several thousand feet at which oxidation is known to occur.

The hydrothermal and modified hydrothermal theories offered apparently more likely processes for removing chert on a large scale and achieving deep oxidation. However, serious doubts exist about the validity of the hydrothermal theories because of (1) the general absence of typical hydrothermal minerals or assemblages within and beneath areas of oxidized iron-formation and soft ore; (2) the usual unaltered condition of footwall rock at distances greater than a few feet beneath ore bodies; and (3) the virtual absence of soft ore in downward-opening traps, which condition is almost impossible to reconcile with hypogene solutions. James and others (1968, p. 115–124) show that existing data best support an eclectic explanation relying entirely on meteoric water, but on meteoric water that circulated irregularly in the zone of aeration in an arid environment above a deep water table, in a partly artesian system. Using a model consistent with reasonable physico-chemical conditions and dimensions of known ore bodies (solubility of silica, 100 ppm at 25°C; oxygen dissolved in water, 9.3×10^{-6} g/cc at 20°C; permeability of iron-formation, 10 millidarcys; parallelopiped of iron-formation, 1 $cm^2 \times$ 2,000 meters long), James and others (1968, p. 120–121) deduced that 5.4×10^9 cc of unheated water could bring in sufficient oxygen and remove enough silica to convert 2×10^5 cm^3 of iron-formation to soft ore in 2×10^6 years. Thus, doubts about the chemical efficacy of meteoric water to produce the soft ore bodies seem to be without valid basis.

The postulated arid epoch is neither proved nor disproved by existing evidence. However, a later Precambrian arid epoch is consistent with the presence along the south shore of Lake Superior of red sandstones of late Keweenawan age (Leith and others, 1935, p. 24–25; Harold Hubbard, U.S. Geol. Survey, oral commun., 1969) and late Keweenawan or Cambrian age (Hamblin, 1958), containing angular clasts of fresh feldspar. A zone of deep oxidation related to a late Precambrian arid epoch might conform roughly and appear to be related to the present land surface if the surface did not undergo major dissection during the long ensuing period of crustal stability. The proposed arid epoch is likened by James (1968, p. 115–124) to present conditions in Australia that are thought to result in deep chemical weathering and are known to result in artesian circulation at a depth of 4,000 feet. Thus, he suggests that similar

conditions and effects in the Lake Superior area could have produced deep irregularly distributed oxidation in late Precambrian time, followed by buildups of soft ore in the lower parts of structural traps through the accumulations, stagnation, and expulsion of water during periodic wet cycles. The groundwater system as a whole is considered to have been essentially unconfined, but local artesian systems were critical in flushing out structural traps.

It is clear that large volumes of the Negaunee Iron-Formation in the Palmer quadrangle have been attacked by aqueous solutions, resulting in extensive oxidation, leaching, redeposition of iron, replacement of chert by iron minerals, and deposition of manganite, goethite, quartz, gypsum, and clay minerals in vugs and cracks. James and others (1968, table 18, p. 110) showed that in the conversion of carbonate iron-formation to soft ore, FeO is changed to Fe_2O_3, and SiO_2 and CO_2 are largely removed. In the example cited, the concentration of iron increases from 0.786 g/cc to 1.751 g/cc, that of SiO_2 decreases from 1.030 g/cc to 0.228 g/cc, and that of CO_2 decreases from 0.794 g/cc to 0.010 g/cc. Most manganite has been deposited within 700 feet down from the land surface, and most gypsum from 1,000 to 1,400 feet below the surface. Evidence favors a supergene origin for the aqueous solutions, although some small-scale alterations may be better explained as a product of minor and local hypogene solutions.

Beneath the Tracy sill in the axial part of the synclinorium south from Negaunee to the NE¼ sec. 18, T. 47 N., R. 26 W., oxidation of original carbonate, magnetite, and silicates in the iron-formation is nearly complete down to 1,000–1,500 feet but tends to die out at greater depths. Locally, however, oxidation reaches downward even farther, especially along west-plunging troughs, to depths of 3,000 feet and more, some 1,500 feet below present sealevel. A supergene origin for the oxidizing solution is suggested by the localization of soft ore in upward-opening structures floored by impermeable rock (pl. 6), and by the tendency of alteration to decrease from the surface down the dip of inclined beds of iron-formation.

Gypsum is irregularly but widely distributed in soft ore and oxidized iron-formation in a rather flat zone approximately between sea level and several hundred feet above sea level (Anderson, 1968, p. 512). The sulfur content of gypsiferous rock is 0.2–3.0 percent. In underground drill holes in the Tracy mine, gypsum occurs sporadically in cracks and vugs in oxidized iron-formation or soft ore at the following elevations above sea level (in feet): 106, 110, 112, 159, 164, 193–258, 260, 284–289, 310–475. The gypsum-bearing zone must project across local folds or other structures. The nearly parallel position of the zone both to sea level and to the existing land surface suggests that it formed parallel to a water table. The location of the gypsiferous zone more than 1,000 feet below the surface thus indicates an effect of surface-derived ground water at substantial depths. If the formation of gypsum is a result of the same process that oxidized the iron-formation and produced soft ore, as the widespread association suggests, then solutions responsible for the alteration of the iron-formation must have been supergene or principally supergene. The flatness of the gypsum zone is consistent with a derivation along an ancient water table, inasmuch as the presence in northern Michigan of flat-lying sandstone of late Keweenawan or early Paleozoic age indicates little tilting in the area since near the beginning of Paleozoic time.

The passage of hypogene solutions through the iron-formation has been inferred from occurrences of dickite and nacrite in vugs (Bailey and Tyler, 1960, p. 156), from extreme alteration of mafic dikes to the "soapstone" of miners, next to ore bodies (Mann, 1953), and from manganite fillings of vugs and cracks in association with crystals of goethite and quartz (D. F. Hewett, U.S. Geol. Survey, written commun., 1967). If the inferences are correct, the question remains as to how significant such solutions might have been in causing the widespread oxidation and soft ore. Theoretically, at least, hypogene solutions could have deposited clay, manganese, and iron minerals long after the epoch of oxidation and ore formation.

Although there is no doubt that mafic dikes in oxidized parts of the iron-formation are much more argillized than elsewhere, the argillization itself tells us little about the temperature or source of the solutions that caused it. Sericite and chlorite are common products of regional metamorphism in the metadiabase dikes; so the origin of these minerals in the argillized metadiabase dikes is ambiguous. X-ray data indicate that thoroughly argillized upper Precambrian diabase—the North Buffalo dike—in the north part of the Tracy mine consists largely of montmorillonite, kaolinite (illite and sericite), and questionable gibbsite.[16] These clay minerals can be attributed either to hypogene or supergene solutions (see Meyer and Hemley, 1967, p. 185). A comparison of chemical analyses of highly altered mafic dike rock, originally probably metadiabase, and typical metadiabase (table 35)

[16] X-ray identification by T. E. C. Keith, U.S. Geol. Survey.

shows that leaching of bases is a major aspect of the dike alteration. According to Meyer and Hemley (1967, p. 214), hydrolytic base leaching would require at least a mildly acid environment. Superficially, this requirement seems to be inconsistent with the association of argillized dikes with leached-oxidized iron-formation, because aqueous solutions, even those initially made acidic by the addition of atmospheric CO_2, should become basic upon reacting with and dissolving sideritic (carbonate) iron-formation (Garrels, 1960, p. 50–58).

However, the association of argillized dikes principally with areas of greatest alteration of the iron-formation and with bodies of soft ore indicates that argillization is probably more related to areas of long-continued changes in the iron-formation than to areas where only initial alterations of siderite have taken place. In thin sections, oxidation of siderite is the earliest change that can be seen in the alteration of fresh carbonate iron-formation to thoroughly oxidized iron-formation and soft ore. The carbonate can be eliminated entirely or greatly reduced in amount well before completion of the ore-forming process. With early elimination of the carbonate and a resulting increase in porosity of the rock and with an accelerated circulation of ground water from the surface through the oxidized (ferric) and partly leached iron-formation, the new influxes of ground water mixed with atmospheric CO_2 might remain acidic. Garrels (1960, p. 50–52) has shown that the addition of CO_2 to the system, water-calcium carbonate, has a marked effect on lowering the pH, even though the equilibrium pH is not lowered below 7 if the supply of carbonate is unlimited. A simple mixing of rain water and atmospheric CO_2 gives a pH of 5.7 (Garrels, 1960, p. 57). Ground water of that acidity could have argillized the dikes. Mildly acid hydrothermal solutions undoubtedly cause argillization more rapidly than mildly acid cold solutions, but time probably was not a critical factor, inasmuch as the changes could have taken place throughout the 300-million year Keweenawan-Paleozoic interval.

The occurrences of drusy manganite are only within about 700 feet down from the land surface near Negaunee, but this relationship does not necessarily indicate supergene solutions, because manganese transported in hypogene solutions may be capable of being precipitated by oxidation only near or at the surface (Hewett and Fleischer, 1960, p. 51). Hewett has found (written commun., 1967) that manganite and drusy quartz are deposited from supergene solutions mainly in arid regions above deep-lying water tables. Hewett's inference that the manganite near Negaunee is not supergene, therefore, appears to be based on an assumption that it did not form while the climate was arid, which is reasonable if the oxidation is related to a land surface formed in later geologic time. On the other hand, supergene manganite would fit nicely into the model of late Precambrian arid conditions and deep chemical weathering proposed by James.

A source for hypogene water in amounts adequate to have produced the extensive oxidation and leaching is problematical. The only post-iron-formation igneous intrusive rocks known in the area are the present bodies of metadiabase of late middle Precambrian age and diabase dikes of Keweenawan age. Major alteration of the iron-formation postdated the emplacement of the metadiabase, and all or most of it probably also postdated the Keweenawan dikes, inasmuch as such a dike within a major area of oxidized and replaced iron-formation in the Tracy mine is itself thoroughly altered. Hypogene solutions, if any, therefore, must have come from a remote source in late-Keweenawan or post-Keweenawan time. The lack of evidence for derivation of hypogene solutions from a nearby igneous source supports the idea that the tremendous volume of water required to accomplish most of the alteration of the iron-formation came downward from the land surface. At most, it seems likely that hypogene solutions could have produced only minor effects, the precipitation of late minerals in vugs and perhaps the dissolving out of some vugs sometime after the onset of major supergene alteration.

DESCRIPTION AND GEOLOGIC SETTING OF HARD-ORE DEPOSITS

Since the early days of mining in the area, bodies of hard ore have been known to be localized in the iron-formation within 100–200 feet beneath the Goodrich Quartzite, and the Goodrich-Negaunee contact has served as a prospecting guide to hard ore. Some hard-ore deposits outside the Palmer quadrangle pass upward across the contact into conglomerate ore—a combination of typical lower Goodrich detritus and hematite matrix. Hard ore generally has a recrystallized metamorphic fabric; so iron apparently was concentrated largely or entirely before metamorphic recrystallization of the rock. Jaspilite iron-formation almost invariably underlies and partly encases bodies of hard ore, and since its grains of quartz and iron oxide were locked together during late middle Precambrian metamorphism, has remained virtually intact, save possibly for the martiti-

zation of magnetite, with no change in total iron content and texture.

Jaspilite occurs in fragments in basal Goodrich Quartzite and is identical with bedrock jaspilite, indicating that prejaspilite iron oxide-chert rock existed as such during the Negaunee-Goodrich erosion interval. In general, jaspilite is underlain by carbonate-rich iron-formation, and the zone of jaspilite is irregular. In a few places in the Cliffs Shaft mine in the Ishpeming quadrangle, jaspilite beds grade along strike into chert-siderite beds, and small "islands" of chert-carbonate iron-formation are surrounded by jaspilite. In the Palmer quadrangle, jaspilite underlying hard ore at the Jackson mine in sec. 1, T. 47 N., R. 27 W., and in the Old Volunteer mine in secs. 30–31, T. 47 N., R. 26 W., is hundreds of feet thick; indeed near the border between the Old Volunteer and Isabella properties (fig. 65), the entire section of iron-formation, several hundred feet thick, is jaspilite. In that area, seams and beds of unoxidized graywacke are interlayered with some of the jaspilite. Five miles west of the quadrangle at the old Saginaw mine in the central part of sec. 19, T. 47 N., R. 27 W., hard ore is separated from underlying oxidized goethitic iron-formation (which presumably was sideritic iron-formation before weathering) by a zone of jaspilite only a few feet thick.

Hard ore commonly overlies or abuts against intrusive greenstone in the Cliffs Shaft and Champion mines west of the Palmer quadrangle, and in the Cliffs Shaft mine it occurs both in synclines and anticlines. However, little can be said of such relationships in the Palmer quadrangle, mainly because of a lack of detailed information about subsurface geology in the long-defunct Jackson and Old Volunteer mines. Dikes of highly altered mafic rock cut and may floor parts of the Jackson ore body, but their spatial relationship to specific concentrations of hard ore is largely unknown. Cobbles of intrusive greenstone are present in Goodrich conglomerate south of Palmer, on the boundary between secs. 29 and 32, near the apparent truncation by the conglomerate of a dike that cuts the iron-formation. It is therefore highly probable that at least some dikes were emplaced in the iron-formation before Goodrich time and could have served as barriers or floors for accumulations of secondary iron oxide during the pre-Goodrich erosion interval. The Old Volunteer ore body dips north against the Volunteer fault below the Goodrich-Negaunee unconformity and ends against the fault (pl. 1, *C–C′*), but it is not known whether the ore body increased in size or improved in grade downdip toward the fault.

ORIGIN OF HARD ORE

The origin of hard ore has been explained principally by two theories: (1) weathering-metamorphic theory, according to which premetamorphic weathering, oxidation, and enrichment of (principally) carbonate iron-formation by meteoric solutions occurred during the erosion interval at the beginning of Goodrich time and was followed by metamorphic recrystallization of oxidized iron-formation and soft ore to jaspilite and hard ore (Van Hise, 1892; Van Hise and Bayley, 1897, p. 404–405; Van Hise and Leith, 1911, p. 278–279, 555–557; Leith and others, 1935, p. 24–25); (2) hydrothermal theory, according to which alteration of iron-formation and concentration of iron was accomplished by hypogene water sometime after regional metamorphism had taken place (Crump, 1948; Marsden, 1968, p. 504).

Data available in the Palmer quadrangle are not adequate for a comprehensive evaluation of the two theories. However, the weathering-metamorphic theory is favored by (1) the location of bodies of hard ore at the folded erosion surface, beneath the Goodrich Quartzite and above and extending into jaspilite; (2) the presence in basal Goodrich of fragments of jaspilite and hard ore; (3) the recrystallized fabric of the ore; and (4) the almost total absence of evidence of the passage of hydrothermal solutions in iron-formation below the hard ore. The lack of evidence of hydrothermal solutions from an extraneous source does not rule out hydrothermal solutions formed during regional metamorphism by the heating of water contained within premetamorphic iron-formation, oxidized iron-formation, or soft ore, although such an origin has not been suggested by advocates of the hydrothermal theory.

There can be no doubt of a relationship between hard ore and jaspilite. Either they are coproducts of the same process, or the iron of the hard-ore bodies was concentrated selectively from a premetamorphic form of the jaspilite. Van Hise and his coworkers advocated the derivation of all jaspilite by essentially the same process envisaged in their weathering-metamorphic theory for the origin of hard ore, that is, the metamorphism of weathered oxidized carbonate iron-formation. Oxidation of the iron-formation and enrichment to ore grade took place more or less simultaneously. James (1954, p. 259), on the other hand, interpreted much if not all of the jaspilite as primary oxide-facies iron-formation that had recrystallized during regional metamorphism. Evidence cited earlier in this report indicates that some jaspilite was a primary oxide facies and some was

derived by the premetamorphic weathering of sideritic iron-formation, but no determination can be made of the relative importance of these processes. If the parent rock of hard ore was primary oxide-facies iron-formation, the ore-forming process would have entailed the dissolving and transporting of substantial amounts of ferric iron oxide, whether by meteoric solutions before regional metamorphism or by hydrothermal solutions during or after metamorphism. Likewise, if jaspilite derived by Van Hise's weathering-metamorphic process later gave rise to hard ore through the action of hydrothermal solutions, the ore-forming process would have required the dissolving, transport, and redeposition of large amounts of hematite. Existing jaspilite near hard ore does not bear witness to such action. Chert layers were replaced by ferric iron oxide during the formation of hard ore, but the low solubility of ferric iron (Hem, 1960) makes it unlikely that much of the secondary hematite (or goethite) was derived by the dissolving of primary ferric oxide while underlying sideritic iron-formation was not altered at all. The problem of accounting for selective enrichment of primary or secondary hematitic iron-formation with no corresponding effects in nearby sideritic iron-formation is obviated if the hematitic iron-formation and ore are themselves seen as alteration products of carbonate iron-formation. Perhaps one of the strongest arguments for the derivation from carbonate iron-formation is that, allowing for the effects of regional metamorphism, jaspilite and hard ore are closely analogous to oxidized iron-formation and soft ore known to be derived from carbonate iron-formation.

Hard ore generally is several percent richer in iron than most existing bodies of soft ore. Proponents of the hydrothermal theory consider the higher grade of hard ore to be a result of the more effective dissolving and concentrating action of hot water than cold water (Anderson, 1968, p. 516). However, there is no inherent reason why premetamorphic soft ore could not have been enriched additionally during metamorphism by the heating and driving off of ground water and the bonded water of hydrated iron oxide. Or, if the atmosphere and dissolved gases in ground water were richer in CO_2 in middle Precambrian time than later, premetamorphic soft ore initially might have been more enriched in iron than were bodies of soft ore formed in later Precambrian time. A CO_2-rich atmosphere was postulated by MacGregor (1927) and has been invoked by him and others as the unique conditions that restricted the development of iron-formation to Precambrian time. While primary oxide iron-formation and oxidation during the pre-Goodrich erosion interval testify to an oxidizing atmosphere in middle Precambrian time, the atmosphere then may have been richer in CO_2 than in later Precambrian time and now (James, 1954, p. 256). Consequently, ground water charged with atmospheric gases in middle Precambrian time may have been more effective in concentrating iron in bodies of soft ore than during later Precambrian time. Thus, features that favor the hydrothermal theory are not particularly inconsistent with the weathering-metamorphic theory, whereas many of the features supporting the latter theory are virtually insupportable under the hydrothermal theory.

THORIUM

Abnormal radioactivity was discovered in dump-fragments of Goodrich Quartzite at the Old Volunteer and Old Maitland mines near Palmer by Robert Reed in 1951, and the discovery led to Vickers' (1956) study of the Goodrich. Vickers determined that the radioactivity is caused by thorium present in detrital monazite. Monazite is irregularly distributed and is concentrated in beds of pebble conglomerate that are a few inches to a few feet thick. The monazite content of the Goodrich ranges from about 2.9 pounds per ton in the lower 200–300 feet of the formation to as much as 110 pounds per ton in glacial erratics probably derived from parts of the formation that are more than 300 feet above the base (Vickers, 1956, p. 185). The thorium content of the rock locally therefore is as high as 0.37 percent.[17] Vickers concluded that the Goodrich Quartzite is a potential low-grade source of monazite.

In the present report an effort is made to evaluate thorium resources in the Goodrich near Palmer, although the evaluation is hampered by a lack of drilling in more favorable parts of the Goodrich since Vickers's work. Also, much of the drill core studied by Vickers that represented parts of the Goodrich having the largest amounts of monazite is no longer available. The evaluation made here is based on volume estimates of the Goodrich derived from the recent mapping and on a correlation of scintillometer readings over outcrops of the Goodrich with the measured thorium content of samples from four of the outcrops (pl. 7, fig. 70) in conjunction with Vickers' data.

Scintillometer readings at the sample sites represent virtually the total range of radioactivity over

[17] Thorium constitutes approximately 6.6 percent of chemically analyzed monazite cited by Vickers (1956, p. 180).

outcrops of the Goodrich. The thorium content of the samples was measured by Carl A. Bunker of the U.S. Geological Survey, using a gamma-ray spectrometer. Comparisons of the radioactivity at each sample site with the thorium content of the respective samples are shown in fig. 70. Discrepancies in linearity between measured radioactivity and thorium content are attributed to the cone effect in measuring radioactivity plus the irregular distribution of monazite in the quartzite, which means that the radioactivity measured at a sample site unavoidably includes emissions from rock containing different amounts of monazite from the sample. Total radioactivity at each site is also influenced by the configuration of the outcrop and adjacent unexposed rock and possibly also by the presence of uranium and radioactive potassium in the rock, although the generally linear relationship shown in the graph suggests that most of the radioactivity is related to thorium.

By the use of the interpolated curve for thorium content versus radioactivity and mean values of radioactivity in outcrops, weighted in accordance with the mapped area of outcrops, average grades of thorium have been determined in three distinct areas that encompass nearly all the outcrops and the bulk of the Goodrich Quartzite near Palmer (pl. 7). The three areas are (1) the block between the Palmer and Volunteer faults in the central part of the Palmer basin (NW¼ sec. 28, center sec. 29, east-center sec. 30), here called the central area; (2) the Isabella syncline and vicinity south of the Volunteer fault (SW¼ sec. 29, NW¼ sec. 32, SE¼ sec. 30); and (3) the Old Volunteer mine area at the west end of the Palmer basin south of the Volunteer fault and west of the Warner Creek fault (S½ S½ sec. 30,

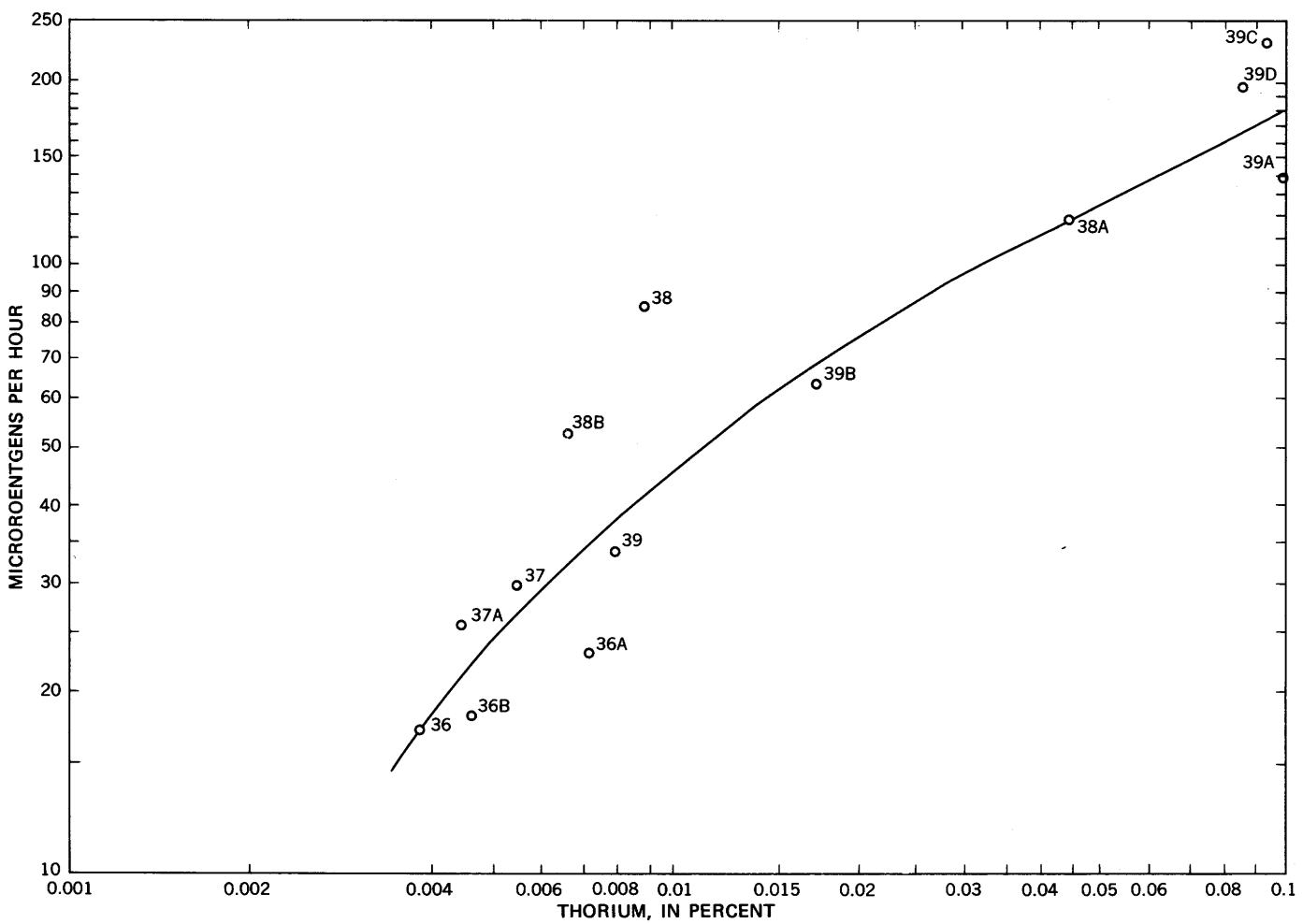

FIGURE 70.—Thorium content of samples of Goodrich Quartzite versus radioactivity (log-log plot, curve fitted by eye). Localities shown on plate 7.

N½ N½ sec. 31). The lower 200–300 feet of the Goodrich is contained in the Isabella syncline, and the lower 500–600 feet, in the Old Volunteer mine area. In the central area, probably all the Goodrich at the bedrock surface is between 300 and 1,400 feet above the base of the formation. Unfortunately, the most abundant exposures and widespread data on grade are found where the thorium content evidently is lowest, in the lower 200–300 feet of the Goodrich in the Isabella syncline. The average radioactivity of outcrops in the Isabella syncline is 22.2 microroentgens/hour, from which an average thorium content of 0.092 pounds/ton is deduced (fig. 70, table 38). In the Old Volunteer mine area, average radioactivity is 74.6 microroentgens/hour, suggesting an average thorium content of 0.38 pounds/ton. In the central area, the average thorium content of the upper part of the Goodrich, more than 300 feet above the base of the formation, is considered to be 1.06 pounds/ton, derived by averaging the thorium content of the outcrop near the center of sec. 29—1.04 pounds/ton—and the computed thorium content of drill core studied by Vickers (1956, p. 184)—1.09 pounds/ton, with a range of 0.26 to 3.56 pounds/ton. The lower 300 feet of the Goodrich in the central area is arbitrarily assigned the grade of the corresponding part of the formation in the Isabella syncline to the south—0.092 pounds/ton.

TABLE 38.—*Correlation of thorium content and radioactivity*

Percent Th	Pounds Th/ton	Radioactivity (microroentgens/hour)
0.004	0.08	18.3
.005	.10	24.3
.006	.12	30.0
.007	.14	34.0
.008	.16	38.0
.009	.18	43.0
.01	.20	47.0
.015	.30	62.0
.02	.40	77.0
.025	.50	88.0
.03	.60	100.0
.035	.70	107.0
.04	.80	115.0
.045	.90	122.0
.05	1.0	126.0
.055	1.1	133.0
.06	1.2	135.0
.07	1.4	147.0
.08	1.6	162.0
.09	1.8	170.0
.10	2.0	182.0

To estimate thorium resources, the thorium grade for each of the three principal areas of Goodrich Quartzite near Palmer has been multiplied by the estimated tonnage of quartzite in the corresponding area. In the absence of extensive drilling to determine the configuration of the base of the Goodrich, estimates of volume and tonnage are subject to errors of perhaps as much as 25 percent. The surface area of the Goodrich Quartzite in each of the three bodies was measured by planimeter and multiplied by estimated thicknesses to determine volume. The estimated tonnages are given on plate 7, based on an assumed specific gravity of 2.7 for the quartzite. Much of the large thorium resource may never be recoverable because of its wide dispersion and deep burial in the Goodrich Quartzite.

DRILL-HOLE DATA AND LOCATIONS

[See pl. 8; numbered by sections, from west to east, starting at northwest corner of quadrangle. DHL, drill hole location. Coding scheme explained on pl. 8]

DHL	Data
Secs. 1 and 12, T. 47 N., R. 27 W.	
1	Cj 4 nf–365 nl (45S)
2	Cj 8 42–926 "jp" (90)
3	Cj 20 28–701 "jp" (65S)
4	Cj 13 0–163 "sr" (20S)
5	Cj 131 nf "hoj" (nd)
6	Cj 107 nf "soj" (nd)
7	Cj 119 nf "soj" (nd)
8	Cj 108 nf "soj" (nd)
9	Cj 126 nf "soj" (nd)
10	Cj 125 nf "soj" (nd)
11	Cj 124 nf "soj" (nd)
12	Cj 112 nf "soj" (nd)
13	Cj 111 nf "soj" (nd)
14	Cj 110 nf "soj" (nd)
15	Cj 109 nf "soj" (nd)
16	Cj 117 nf "soj" (nd)
17	Cj 106 nf "soj" (nd)
18	Cj 101 nf "soj" (nd)
19	Cj 120 nf "soj" (nd)
20	Cj 100 nf "soj" (nd)
Secs. 1 and 12, T. 47 N., R. 27 W.—Continued	
21	Cj 99 nf "lo" (nd)
22	Cj 97 nf "lo" (nd)
[2] 22A	Cj 98 nf "soj" (nd)
23	Cj 103 nf "lo" (nd)
[2] 23A	Cj 105 nf "soj" (nd)
24	Cj 104 nf "soj" (nd)
25	Cj 90 nf "soj" (nd)
26	Cj 83 nr
27	Cj 69 10–50 "mjp" (90)
28	Cj 91 nr
29	Cj 70 8–50 "mjp" (90)
30	Cj 92 nf "soj" (nd)
31	Cj 82 nf "soj" (nd)
32	Cj 81 nf "soj" (nd)
33	Cj 79 nf "soj" (nd)
34	Cj 135 nf "soj" (nd)
35	Cj 134 nf "soj" (nd)
36	Cj 133 nf "soj" (nd)
37	Cj 80 nf "soj" (nd)
38	Cj 71 10–50 "mjp" (90)
Secs. 1 and 12, T. 47 N., R. 27 W.—Continued	
39	Cj 87 nf "soj" (nd)
40	Cj 84 nf "soj" (nd)
41	Cj 72, Cj 73 nr
42	Cj 85 nf "soj" (nd)
43	Cj 93 nf "soj" (nd)
44	Cj 86 nf "soj" (nd)
45	Cj 74 5–55 "mjp" (90)
46	Cj 75 nf "soj" (nd)
47	Cnj 9 5–135 "smj" (90)
48	Cj 76, 77 nf "soj" (nd)
49	Cj 78 nf "soj" (nd)
50	Cnj 8 10–87 "dk" (4 S18W)
51	Cnj 10 5–135 "smj" (90)
52	Cnj 11 5–68 "smj" (90)
53	Cj 121 nf "soj" (nd)
54	Cj 122 nf "soj" (nd)
55	Cj 123 nf "soj" (nd)
56	Cj 128 nf "soj" (nd)
57	Cj 115 nf "soj" (nd)
Secs. 1 and 12, T. 47 N., R. 27 W.—Continued	
58	Cj 116 nf "soj" (nd)
59	Cj 117 nf "soj" (nd)
60	Cj 129 nf "soj" (nd)
61	Cj 130 nf "soj" (nd)
62	Cj 96 nf "soj" (5 S25W)
63	Cj 88 nf "soj" (nd)
64	Cj 89 nf "soj" (nd)
Sec. 6, T. 47 N., R. 26 W.	
65	Cpl 100–105 (six drill holes) nr
66	Cp J_3 69–332 "jp" (90)
67	Cp I_3 52–393 "di" (90)
68	Cp K_3 62–282 "o" & "pr" (90)
69	Cn 21 nr
70	Ca 11 57–1818 "dk" (90)
71	Ca 4 56–2086 "jp" (90)
72	Ca 9 64–1166 "jp" (90)
73	Ca 5 61–1882 "jp" (90)
74	Ca 10 55–1883 "jp" (90)

DHL	Data
	Sec. 6, T. 47 N., R. 26 W. —Continued
75	Ca 3 63–1934 "jp" (90)
76	Cp A 14–1570 "jp" & "sr" (90)
77	Cbt 18 nf nl (90)
78	Cbt 9 nr
79	Cbt 10 nr
80	Ca 8 57–2295 "jp" (90)
81	Ca 2 55–2418 "jp" (90)
82	Ca 6 86–1930 "jp" (90)
83	Cbt E 52–2410 "jp" (90)
84	Cbt 11 nf–2700 nl (nd)
85	Cbt G 60–2336 "jp" (90)
86	Cbt 12 nr
87	Ca 1 0–2260 "jp" (90)
88	Cbt K 20–1601 "chl sch" (90)
89	Cbt 17–1 nr
90	Ca 7 49–2103 "jp" (90)
91	Cbt J 32–984 "jp" (90)
92	Cbt I 31–2045 "chl sch" (90)
93	Cbt 14–1 nf–1420 nl (nd)
94	Cn 16 nr
95	Cbt L 28–2150 "jp" (90)
96	Cbt 8 nr
97	Cbt 7 nr
98	Cbt D 58–2233 "jp" (90)
99	Cbt 6 nf–1900? nl (nd)
100	Cbt F 36–1186 "jp" (90)
101	Cbt 13–1 nf–1300 nl (nd)
102	J 605 nr
103	Cbt 20 37–2240 "jp" (90)
104	Cbt W 8–2090 "jp" (90)
105	Cbt 20 100?–2020? nl (90)
106	Cbt 5 nf–2400 nl (nd)
107	J 612 94–1604 "oxid h mar ch i.f." (90)
108	Cbt 26 nf nl (90)
109	Cbt 27 nf–1400 nl (90)
110	Cbt 92 55–1662 "jp" (90)
111	J 609 48–942 "taconitic i.f. with leop" (45N) J 610 42–1374 "chy mar i.f." (90)
112	Cbt 15 nf–1240 nl (90?) Cbt H 34–1224 "chl sch" (90)
113	Cp D 8–1060 "jp" (90)
114	Cbt 19 nf–>1900 nl (90)
115	Cbt R 10–2072 "jp" (90)
116	Cp B 20–520 "pr" (90)
117	Cbt 17–2 17–831 "jp" (90)
118	Cbt 4 nr
119	Cbt 0 15–412 "jp" (90)
120	Cbt Z 45–1804 "sch" (90)
121	J 604 35–1461 "di" (90)
122	Cbt 36 nf–1300 "soj"? (90)
123	B 160 15–1220 "jp" (90)
124	Cbt 32–1 nf–<400 nl (90)
125	Cbt 14–2 28–1079 "lo" (90)
126	Cbt 13–2 10–176 "chl sch" (53NE)
127	Cbt 25 nf–600 nl (90)
128	Cbt A 50–1226 "jp" (90)
129	J 608 73–496 "di" (45N)

DHL	Data
	Sec. 6, T. 47 N., R. 26 W. —Continued
130	Cbt 117 58–1701 "jp" (90)
131	J 607 53–807 "taconitic h ch i.f." (45N)
132	J 601 55–1587 "i.f." (90)
133	J 606 21–1413 "di" (90)
134	B 162 15–1376 "jp" (90)
135	Cbt 37 nf–1355 nl (90)
136	Cbt 131 3–1132 "jp" (86S)
137	J 614 15–2021 "oxid h lim i.f." (90)
138	J 602 24–356 "ch h i.f." (50 S50W)
139	J 603 29–1947 "oxid h leop i.f." (90)
140	J 611 43–483 "oxid h i.f." (nd)
141	Cbt 101 nf–1002 "chl sch" (90)
142	Cbt 29 nr
143	Cbt 33 90–nf nl (90)
144	Cbt 34 46–800 "dk" (90)
145	Cbt 35 nf–1400 nl (75 N45W)
146	Cbt 145 23–1336 "gs" (70 N52W)
	Sec. 5, T. 47 N., R. 26 W.
147	Cn 22 nr
148	Cs 1 73–753 "jp" (90)
149	Cls 105 51–394 "sch" (90)
150	Cls 110 86–719 "di" (90)
151	Cls shaft nr
152	Cls Q 60–1182 "jp" (90)
153	Cn 14 55–55 nl (90)
154	Cun 12 45–1554 "soj" (90 to 73 N28E)
155	Cls Y 52–310 "jp" (90)
156	Cls V 64–1385 "jp" (90)
157	Cls U 60–1272 "jp" (90)
158	Cls F 73–1222 "jp" (90)
159	Cls T 82–1357 "jp" (90)
160	Cn 16 104–1159 "jp" (90)
161	Cls M 0–1082 "jp" (90)
162	Cls P 55–1005 "jp" (90)
163	Cn 7 139–1014 "cg–sl–jp" (90)
164	Cn 11 100–561 "jp" (90)
165	Cn 15 36–36 nl (90)
166	Cls X 24–699 "jp" (90)
167	Cls N 32–940 "jp" (90)
168	C? 152 nr
169	C? 153 nr
170	I 28 nr
171	I 30 nr
172	I 35 nr
173	I 34 nr
174	I 37 nr
175	I 33 nr
	Sec. 7, T. 47 N., R. 26 W.
176	J 733 24–465 "di" (90) J 734 24–607 "di" (45N)
177	J 752 17–778 "i.f." (45N)
178	J 738 31–2054 "oxid h lim i.f." (90)
179	J 773 38–96 i.f.-md (45 S60W)
180	J 762 69–1800 "alt h i.f." (90)

DHL	Data
	Sec. 7, T. 47 N., R. 26 W. —Continued
181	Ish 141 44–755 "jp" (86S)
182	Ish 142 23–1118 "jp" (90)
183	J 728 24–224 "i.f." (45N)
184	J 727 21–428 "i.f." (nd)
185	J 769 43–93 "oxid i.f. and lho" (55 N70E)
186	J 761 90–237 "soft to hard h" (90)
187	J 767 29–80 "oxid h i.f." (90) J 768 30–91 "oxid h i.f." (50S)
188	J 763 77–156 "soft to hard h" (47N)
189	J 765 64–121 "goet h i.f." (90) J 766 nf "i.f." (90)
190	J 730 30–762 "oxid chy lim leop i.f." (45N)
191	J 735 5–2486 "di" (90)
192	J 760 38–1710 "alt di or ash bed" (90)
193	J 732 32–647 "i.f." (45N)
194	J 736 12–2578 "oxid goet i.f." (90)
195	J 729 36–666 "i.f." (45N)
196	J 718 20–2564 "oxid lim leop i.f." (90)
197	J 756 19–1145 "oxid lim i.f." (90)
198	J 759 33–1789 "h mar i.f." (90)
199	J 731 33–588 "di" (45N)
200	J 720 20–1120 "oxid db" (90)
201	J 757 25–1673 "h lim i.f." (90)
202	J 745 34–355 "di" (50 N65E) J 746 15–2000 "di" (90)
203	J 754 25–518 "oxid h mn i.f." (45N)
204	J 719 23–2074 "oxid chy h mn i.f." (90)
205	J 711 21–1861 "i.f." (90)
206	J 739 28–668 oxid h mar i.f. (45N)
207	J 713 15–2483 oxid goet i.f. (90)
208	J 710 18–1546 "oxid chy jp" (nd)
209	J 709 3–1424 "di" (90)
210	J 744 34–579 oxid h mar ch i.f. (50N)
211	J 725 18–1640 "i.f." (90)
212	J 716 13–1177 "di" (90)
213	J 721 63–1016 oxid i.f. (90)
214	J 724 10–1095 "hard h i.f." (90)
215	J 714 20–1108 "mar h lim i.f." (90)
216	J 712 14–826 "i.f." (90)
217	J 786 44–357 mt sil cb ch i.f. (50N)
218	J 723 18–1817 oxid mar h ch i.f. (90)
219	J 722 35–954 oxid h ch i.f. (90)

DHL	Data
	Sec. 7, T. 47 N., R. 26 W. —Continued
220	J 717 21–882 oxid h goet ch i.f. (90)
221	J 715 20–855 md (90)
222	J 708 13–260 "i.f." (45 N32E)
223	J 701 24–272 "h spec chy granular i.f." (45 N32E) J 704 25–316 "i.f." (90)
224	J 705 12–445 oxid mt mar h i.f. (90)
225	J 784 7–555 "gy grn intr" (70N)
226	J 750 36–772 "oxid h goet leop i.f." (45N)
227	J 740 26–1051 "mar i.f." (45N)
228	Mhm 104 20–720 "jp" (85 S45E)
229	Mhm 29 6–706 "jp & lo" (90)
230	J 790 17–57 "oxid chy mar i.f." (60 N60E)
231	J 789A 20–80 "mixed oxid di and mar i.f." (90) J 789B 15–50 "alt di" (90)
232	J 706 67–2133 md (90)
233	J 781 25–349 mt sil ch cb i.f. (50N)
234	J 755 19–626 partly oxid mar mt chy i.f. (45N)
235	J 703 10–1057 "oxid chy i.f." (90)
236	J 747 12–844 "oxid mar i.f." (45N)
237	J 741 11–467 mar i.f. (60N)
238	B? 27 nf "i.f." (90)
239	J 788 63–141 "oxid goet i.f." (90)
240	J 779 0–750 md (50N)
241	J 707 23–1190 oxid h mar ch i.f. (90)
242	Mhm 133 22–826 "lo" (90)
243	Mhm 36 4–873 "lo" (90)
244	Mhm 32 24–670 "lo" (90)
245	Mhm 127 5–813 "lo & sl" (90)
246	J 748 32–824 "oxid chy h i.f." (45N)
247	J 742 26–815 oxid h mar i.f. (45N)
248	Mhm 40 4–144 "jp & lo" (90)
249	Mhm 119 7–792 "lo & o" (90)
250	Mhm 123 20–696 "jp" (90)
251	Mhm 28 22–988 "lo" (90)
252	J 774 19–486 md (45E)
253	J 776 90–329 md (45E)
254	J 702 10–1328 "di" (90)
255	J 777 9–647 md (50E)
256	J 751 20–744 partly oxid mt mar ch sil i.f. (45N)
257	J 785 32–403 mt sil cb ch i.f. (45E)
258	Mhm 188 51–924 "jp" (90)
259	Mhm 174 25–845 "jp" (90)
260	Mhm 175 15–830 "lo" (90)
261	Mhm 186 nf–882 "lo" (90)

DHL	Data
	Sec. 7, T. 47 N., R. 26 W. —Continued
262	J 743 25–865 oxid mar i.f. (45N)
263	Ich 173 20–725 "jp" (90)
264	J 778 12–249 mt sil i.f. (50E)
265	J 772 13–651 md (53E)
266	J 764 9–640 md (50E)
	J 770 7–167 md (90)
267	J 749 36–527 "oxid h chy i.f." (40N)
268	J 775 22–700 md (45E)
269	J 780 18–749 md (50E)
270	J 782 0–608 sil mt ch i.f. (50E)
271	J 783 0–369 "mt chy i.f." (45E)
	J 787 3–284 mt ch sil i.f. (45S)
272	J 753 20–756 oxid h goet chy leop i.f. (45N)
	Sec. 8, T. 47 N., R. 26 W.
273	J 841 15–1125 "i.f." (90)
274	J 827 20–892 "i.f." (90)
275	J 826 30–990 "i.f." (90)
276	J 828 28–908 "i.f." (90)
277	J 825 29–1031 "i.f." (90)
278	J 842 16–1326 "oxid i.f." (90)
279	J 824 26–1251 "i.f." (90)
280	J 820 31–1103 "i.f." (90)
281	M 12 nf–623 nl (90)
282	J 819 13–1024 "i.f." (90)
283	J 818 20–965 "h spec i.f." (90)
284	Mtr 163 30–689 "lo" (90)
285	J 816 39–293 "i.f." (90)
286	J 823 16–1387 "di" (90)
287	J 821 21–1390 "chy i.f." (90)
288	J 822 23–1132 "lim ch i.f." (90)
289	J 850 20–529 "oxid h mar i.f." (60S)
290	M 194 nf–1002 "jp" (90)
291	M 193 38–906 "jp" (80S)
292	J 817 25–950 h spec ch i.f. (90)
293	Mtr 191 36–843 "jp" (90)
294	M 192 40–706 "jp" (90)
295	J 801 57–238 "i.f." (45S)
296	J 815 40–478 "i.f." (90)
297	J 813 56–440 "i.f." (90)
298	J 811 65–340 "i.f." (90)
299	J 809 48–165 "i.f." (90)
300	J 814 40–345 "i.f." (90)
301	J 812 55–446 "i.f." (90)
302	J 812 55–446 "i.f." (90)
303	J 808 55–311 "i.f." (90)
304	J 807 40–306 "i.f." (90)
305	J 803 35–435 "i.f." (90)
306	J 802 67–183 "transition i.f. to sl" (90)
307	J 806 75–160 "i.f." (45S)
308	J 804 44–276 "i.f." (90)
309	J 805 16–120 "transition sl i.f. to sl" (90)

DHL	Data
	Sec. 8, T. 47 N., R. 26 W. —Continued
310	J 830 3–1257 "di" (90)
311	J 829 28–1456 "i.f." (90)
312	Mtr 161 37–1050 "jp" (90)
313	J 832 17–1336 "di" (90)
314	J 831 0–883 "di" (90)
315	J 833 10–677 "di" (90)
316	J 838 18–519 "oxid leop i.f." (90)
317	J 834 18–462 "oxid h ch i.f." (90)
318	J 837 32–597 "oxid h ch i.f." (90)
319	Bgb 107 20–553 "lo & jp" (90)
320	Bgb 38 50–278 "jp" (90)
321	J 836 53–583 "oxid h ch i.f." (90)
322	Bgb 39 46–648 "jp" (90)
323	J 843 60–643 "di" (45N)
324	Bgb 41 54–492 "lo" (90)
325	Blt 22 60–678 "jp–lo" (90)
326	J 835 23–510 "oxid h ch i.f." (90)
327	Bgb 11 92–434 nl (90)
328	J 839 11–320 "h ch mar
329	Blt 23 68–798 "jp" (90)
330	Blt 24 58–708 "jp" (90)
331	J 844 90–555 "oxid h i.f." (90)
332	Blt 31 36–464 "lo" (90)
333	Blt 30 56–214 "jp" (90)
334	Blt 33 88–148 "jp–lo" (90)
335	J 845 80–604 "partly oxid slightly mt i.f." (65N)
336	Blt 109 33–549 "jp" (90)
337	NR 511 45–490 "dk or sill" (90)
338	J 839 11–320 "h ch mar i.f." (90)
339	Blt 112 53–648 "lo" (90)
340	J 846 97–789 "oxid lim h i.f." (45N)
341	J 840 76–492 "oxid leop i.f." (90)
342	J 847 53–574 "ch lim h i.f." (90)
343	J 848 46–612 oxid mar h ch pc i.f. (90)
344	J 849 25–301 cb sil i.f. (90)
	Sec. 13, T. 47 N., R. 27 W.
345	Ccd 6 9–365 "intr" (90)
346	Ccd 18 25–500 mt–grun i.f. (85E)
347	Ccd 9 5–860 "intr" (90)
348	Ccd 12 10–1061 "mt chy sil cb i.f." (85E)
349	Ccd 13 11–508 md (85W)
350	Ccd 20 6–724 mt ch i.f. (90)
351	Ccd 5 2–498 "mt chy i.f." (90)
352	Ccd 8 0–1056 mt chy sil i.f. (45 N49E)
353	Ccd 21 33–425 "mt chy sil i.f." (90)
	Ccd 22 44–612 "mt chy i.f." (70W)

DHL	Data
	Sec. 13, T. 47 N., R. 27 W. —Continued
354	Ccd 19 8–512 md (85E)
355	Ccd 11 2–602 "mt chy i.f." (90)
356	Ccd 17 3–40 "i.f." (nd)
357	Ccd 16 0–40 "i.f." (nd)
358	Ccd 15 6–40 "i.f." (nd)
359	Ccd 14 0–40 "mt chy i.f." (nd)
360	Ccd 7 10–249 "mt chy i.f." (90)
361	Ccd 10 0–488 "intr" (90)
362	Ccd 23 4–300 mt chy i.f. (90)
363	Ccd 38 nf md (60 S83E)
364	Ccd 39 16–785 md (60 S89E)
365	Ccd 35 28–1315 cb i.f. (60 N89E)
366	Ccd 36 88–1110 md (60 S88E)
367	Ccd 37 66–815 oxid h chy i.f. (90)
368	Ccd 33 51–60 md (90)
369	Ccd 32 20–27 oxid h ch i.f. (90)
370	Ccd 40 73–1137 md (60 S84E)
371	Ccd 31 15–1260 md (60 S87E)
372	Ccd 3 didn't reach ledge Ccd 3A 76–612 "h chy i.f." (55 S84E)
373	Ccd 34 60–65 md (90)
	Sec. 18, T. 47 N., R. 26 W.
[1]374	Ccdpl 24 24–67 mt i.f. (90)
[2]374A	Ccd 63 40–585 "intr" (60 S87E)
374B	Ccd 64 13–633 "intr" (60 S88E)
374C	Ccd 65 15–663 "intr" (60 S86E)
374E	Ccd 68 5–923 "mt chy cb i.f." (60 N89E)
374F	Ccd 67 22–1292 "intr" (60 S89E)
374G	Ccd 60 13–895 "mt ch cb i.f." (60 S84E)
374H	Ccd 66 25–1060 "mt chy cb i.f." (60 N87E)
374I	Ccd 69 0–1000 "mt chy cb i.f." (60E)
374J	Ccd 57 5–749 "mt ch i.f." (90)
374K	Ccd 59 5–543 "cg mt ch i.f." (90)
374L	Ccd 61 200–450 "earthy h i.f." (90)
374M	Ccd 62 6–700 "intr" (90)
375	Cb 41 0–753 mt sil ch i.f. (60 S82E)
376	Cb 46 24–480 mt ch i.f. (50E)
377	Cb 22 14–44 "mt sid sl" (90)
378	Cb 23 44–644 "mt chy cb i.f." (54E)
379	Cb 19 32–225 "soj" (90)

DHL	Data
	Sec. 18, T. 47 N., R. 26 W. —Continued
380	Cb 24 22–717 ch mt cb sil i.f. (54 S86E)
381	Cb 40 22–359 mt i.f. (50E)
382	Cb 39 0–947 md (50 S86E)
383	Cb 20 11–125 "soj" (90)
384	Cb 29 15–781 "di" (60 N88E)
385	Cb 21 7–132 "soj" (90)
386	Cb 25 24–587 "partly oxid mt ch cb i.f." (58 S86E)
387	Cb 51 22–611 mt i.f. (62 S86E)
388	Cb 42 10–939 "intr" (50E)
389	Cb 12 6–594 "soj" (90)
390	Ccd 37 20–523 "mt chy i.f." (50 S88E)
391	Cb 27 16–804 "mt chy sil i.f." (59 N85E)
392	Cb 44 8–700 "intr" (50 S87E)
393	Cb 26 25–775 "h goet ch i.f." (58 N86E)
394	Cb 11 6–166 "soj" (90)
395	Cb 10 5–196 "soj" (90)
396	Cb 9 11–95 "soj" (90)
397	Cb 8 4–240 "soj" (90)
398	Cb 4 0–760 "mt sid" (90)
399	Cb 16 15–390 "soj" (90)
400	Cb 1 20–325 "jp" (90)
401	Cb 15 15–477 "soj" (90)
402	Cb 13 7–362 "soj" (90)
403	Cb 17 17–392 "soj" (90)
404	Cb 14 13–525 "sid" (90)
405	Cb 2 18–497 "di" (90)
406	Cb 35 6–1106 "intr" (90)
407	Cb 52 41–755 mt i.f. (62 N89E)
408	Cb 43 3–749 mt chy sil i.f. (50 N88E)
409	Cb 54 5–861 mt ch i.f. (60 N87E)
410	Ccd 38 6–519 "mt chy i.f." (45 N83E)
411	Cb 30 10–799 gs (60E)
412	Cb 18 18–298 "mt sid sl" (90)
413	Cb 3 22–154 "jp" (90)
414	Cb 28 20–630 "mt h goet chy i.f." (74 S69E)
415	Ccd 36 7–891 "mt chy sil i.f." (90)
416	Cb 53 11–531 mt i.f. (62 S88E)
	Cb 55 8–412 "mt chy cb i.f." (90)
417	Cb 5 17–85 "grun" (90)
418	Cb 45 16–752 "mt h chy i.f." (50E)
419	Cb 6 38–109 "grun" (90)
420	Cb 31 7–645 partly oxid mt i.f. (59 S88E)
421	Cb 7 11–127 "grun" (90)
422	Cb 50 12–630 "mt chy i.f." (54 S88E)
423	Cb 47 36–520 mt ch i.f. with local sil zones (45 N85E)

DHL Data

Sec. 18, T. 47 N., R. 26 W. —Continued

424 Cb 49 10–673 ch mt i.f. (60 S82E)
425 Cb 32 28–771 mt ch sil i.f. (45 S85E)
426 Cb 48 27–580 gs (55 S89E)

427 Ccd 56 7–1190 md (nd)
428 Cb 33 38–830 ch mt sil i.f. (42 N89E)
[3]429 P 2 11–300 "cb h i.f." (90)
430 Cb 34 41–750 mt sil ch i.f. (47 N72E)

Sec. 24, T. 47 N., R. 27 W.

431 Ccd 38 nf–1132 "intr" (60 N87E)
[2]431A Ccd 36 62–857 md (60 S89E)
432 Ccd 37 7–609 mt cb ch i.f. (60 S89E)
433 Ctn 6 105–456 "h ch i.f." (45 N89E)
434 Ctn 10 12–614 "h ch i.f." (90)

435 Ctn 5 80–409 "h ch i.f." (45E)
436 Ctf 23 114–905 "intr" (50 S87E)
437 Ccdpl 30 33–47 mt i.f. (90)
438 Ccdpl 31 54–71 md (90)
439 Ccdpl 28 94–100? oxid chy h i.f. (90)

440 Ccdpl 32 49–60 md (90)
441 Ccdpl 26 78–85 oxid h i.f. (90)
442 Ctf 21 43–1605 "intr" (50E)
443 Ccdpl 34 5–17 md (90)
444 Ccdpl 33 38–43 h chy i.f. (90)

445 Ccdpl 25 112–130 chy h i.f. (90)
446 Ctf 22 68–1072 "h ch i.f." (50E)
447 Ccdpl 35 46–54 md (90)
448 Ccdpl 27 145–148 chy h i.f. (90)
[2]448A Ccd 39 18–800 "mar h ch i.f." (45 S3W)
448B Ccd 40 22–800 "mar ch i.f." (45 S2W)

Sec. 19, T. 47 N., R. 26 W.

449 P 3 31–72 "di" (90)
450 P 5 15–360 "cb i.f." (90)
451 Ce 63 7–723 "mt h chy sil i.f." (90)
452 P 12 16–355 "cb i.f." (90)
453 Ce 57 11–700 gs (90)

454 Ce 45 39–700 "mt ch sil i.f." (45E)
455 Ce 61 2–649 "chy cb sil mt i.f." (90)
456 Ce 67 15–441 "mt chy cb sil i.f." (90)
457 Ce 60 13–442 "mt cb chy i.f." (90)
458 P 13 2–370 "cb i.f." (90)

459 P 9 5–295 "cb i.f." (90)
460 Ce 65 28–448 "mt chy cb clastic i.f." (90)

DHL Data

Sec. 19, T. 47 N., R. 26 W. —Continued

461 Ce 68 49–283 "mt chy cb clastic i.f." (90)
462 Ce 39 40–639 "mt ch i.f." (90)
463 P 8 11–181 "cb i.f." (90)

464 Ce 59 0–1560 "cb mt i.f." (90)
465 CM 52 nl–88 "ch Fe cb" (nd)
466 Ce 66 21–1535 "chy cb sil mt i.f." (90)
467 P 6 nr
468 Ce 36 38–1002 "mt ch sil i.f." (41 S82E)

469 Ce 37 13–17 "mt chy sil i.f." (90)
470 Ce 42 18–382 "mt ch i.f." (90)
471 Ce 56 0–631 "cb mt i.f." (90)
472 CM E–2 3–427 "jp & lbo" (nd)
473 Ce 58 16–1475 mt chy cb i.f. (90)

[2]473A Ce 71 116–1130 "mt chy cb i.f." (90)
474 Ce 38 30–57 "mt ch sil i.f." (90)
475 Ce 50 0–621 "mt chy cb i.f." (90)
476 Ce 40 15–432 "intr" (45 S80E)
477 P 14 61–405 "chy h i.f." (90)

478 CM 53 nl–364 "jp" (nd)
479 P 11 nr
480 Ce 69 69–356 "chl dk" (58S)
481 P 7 nr
482 Ce 62 105–260 "chl dk" (90)
[2]482A Ce 70 36–1517 "mt chy cb clastic i.f." (90)
483 Ce 10 14–563 "gw" (90)
484 Ce 8 6–507 "mt ch sil i.f." (90)
485 Ce 12 18–479 ch cb i.f. (90)
486 Ce 13 14–193 "mt ch cb i.f." (90)

487 Ce 28 28–197 "mt ch sil i.f." (90)
488 Ce 54 86–1298 "mt chy cb i.f." (90)
489 Ce 64 117–401 "h chy cb sil i.f." (90)
490 P 4 nr
491 P 10 nr

492 Ce 19 4–612 "gw" (90)
493 P 1 nr
494 Ce 9 20–500 "mt ch cb i.f." (90)
495 Ce 5 16–546 "mt ch sil i.f." (90)
496 Ce 29 85–236 "mt h ch i.f." (90)

497 Ce 53 46–431 "mt chy cb i.f." (90)
498 Ce 55 70–661 "chl dk" (90)

DHL Data

Sec. 19, T. 47 N., R. 26 W. —Continued

[2]498A Ce 72 0–495 "mt chy sil i.f." (90)
499 CM 54 nl–373 "ch Fe cb" (nd)
500 CM 56 14–361 "jp" (nd)

501 CM 57 68–533 "jp" (nd)
502 CM 58 89–244 "ch Fe cb" (nd)
503 Ce 18 9–619 "mt ch cb i.f." (90)
504 Ce 1 3–1773 "h mt cb ch i.f." (90)
505 Ce 2 8–1411 "mt ch cb i.f." (90)

506 Ce 6 22–500 "mt ch sil i.f." (90)
507 Ce 32 22–188 "mt ch sil i.f." (90)
508 CM 51 9–207 "lbo" (nd)
509 Ce 52 12–431 "mt chy cb i.f." (90)
510 CM E–1 19–164 "jp & lbo" (nd)

511 CM 59 10–331 "jp & lbo" (nd)
512 Ce 3 63–400 "mt ch sil i.f." (90)
513 Ce 27 86–212 "mt ch sil i.f." (90)
514 Ce 14 2–671 "mt ch cb i.f." (90)
515 Ce 4 16–640 "mt ch cb i.f." (90)

516 Ce 11 30–581 "mt ch sil i.f." (90)
517 Ce 7 26–485 "intr" (90)
518 Ce 35 26–225 "mt h ch i.f." (90)
519 CM 55 40–330 "jp" (nd)
520 CM 60 20–216 "jp" (nd)

521 Ce 24 56–145 "qzit" (90)
522 Ce 16 19–663 "mt h ch i.f." (90)
523 Ce 41 18–27 "mt ch i.f." (90)
524 Ce 20 29–212 "mt ch sil i.f." (90)
525 Ce 46 5–397 "h chy i.f." (90)

526 Ce 21 17–373 "mt ch sil i.f." (90)
527 CM 61 10–273 "chy Fe cb with sl seams" (nd)
528 CM 62 10–40 "chy Fe cb with sl seams" (nd)
529 Ce 17 18–513 "mt ch sil i.f." (90)
530 Ce 15 14–690 "mt ch cb i.f." (90)

531 Ce 49 0–400 "mt chy cb i.f." (55 S45E)
532 Ce 48 0–55 "h i.f." (65 S88E)
Ce 48A 0–176 "dk" (65 N79E)
533 Ce 30 15–631 mt ch cb i.f. (90)
534 Ce 23 23–145 "mt ch sil i.f." (90)

DHL Data

Sec. 19, T. 47 N., R. 26 W. —Continued

535 Ce 22 63–269 "partly oxid mt ch sil i.f." (90)

536 Ce 47 2–188 "mt chy cb i.f." (55 S45E)
537 Ce 43 9–19 "mt ch sil i.f." (90)
538 Ce 25 15–38 "gw" (90)
539 Ce 26 38–63 "sil i.f." (90)
540 Ce 33 27–37 "gw" (90)

541 Ce 51 28–315 "h mt chy cb i.f." (90)
542 Coe 3 20–400 "lo & jp" (nd)
543 Coe 2 30–320 "jp" (nd)
544 Coe 1 16–35 "sl" (nd)
545 Cep 44 15–17 "qzit" (90)
546 Ce 31 33–41 "mt gw" (90)
547 Ce 34 24–32 "gw" (90)

Sec. 20, T. 47 N., R. 26 W.

548 Ce 5 31–232 "mt sil i.f." (90)
549 CM A nf "db or di" (35 approx. SE)
550 CM 152 nr
551 Ce 2 5–443 "sil mt i.f." (55E)
552 Ce 1 57–624 "sil i.f." (90)

553 Ce 3 11–610 sil mt i.f. (60S)
554 Ce 4 188–468 "sil mt i.f." (60S)
555 CM 1 nr
556 CM 151 141–551 "jp" (90)
557 CM 22 46–127 "sl–jp" (90)
558 CM 20 21–105 "sl–pr–q" (nd)

Sec. 25, T, 47 N., R. 27 W.

559 V 6 32–917 "jp" (90)
560 V 9 35–1110? "jp" (90)
561 V 5 25–591 "gs" (90)
562 V 8 35–621 "jp" (nd)
563 V 7 31–674 "jp" (90)

564 V 4 39–521 "lo" (90)
565 V 3 9–544 "jp–lo" (90)
566 V 2 22–33 "qzit" (90)
567 V 1 25–106 "jp" (90)
568 Clpv 3 75–128 "gn" (nd)

Sec. 30, T. 47 N., R. 26 W.

569 Cep 38 10–20 "qzit" (90)
570 Cep 21 19–27 "qzit" (90)
571 Cep 22 26–36 "qzit" (90)
572 Cep 23 20–29 "qzit" (90)
573 Cep 24 10–20 "qzit" (90)

574 Cep 25 9–19 "qzit" (90)
575 Cep 31 29–39 "arg–qzit" (90)
576 Cep 28 16–26 "qzit" (90)
577 Cep 37 13–23 "qzit" (90)
578 Cep 26 26–36 "qzit" (90)

579 Cep 6 30–38 "mt ch sil i.f." (90)
580 Cep 7 15–33 "qzit" (90)
581 Cep 8 18–28 "qzit" (90)
582 Cep 9 24–34 "qzit" (90)
583 Cep 10 5–15 "qzit" (90)

DHL Data

Sec. 30, T. 47 N., R. 26 W. —Continued

584_____Cep 32 13–23 "arg–qzit" (90)
585_____Cep 34 22–32 "arg-qzit" (90)
586_____Cep 35 25–35 "qzit" (90)
587_____Cep 29 12–22 "qzit" (90)
588_____Cep 36 10–20 "qzit" (90)

589_____Cep 27 9–19 "qzit" (90)
590_____Cep 11 0–10 "arg" (90)
591_____Cep 12 7–17 "qzit" (90)
592_____Cep 13 5–15 "qzit" (90)
593_____Cep 14 9–19 "qzit" (90)

594_____Cep 15 0–28 "qzit" (90)
595_____Cep 33 16–26 "fer arg–qzit" (90)
596_____Cep 4 50–53 "qzit" (nd)
597_____Clp 1 4–318 "jp" (nd)
598_____V 23 nr

599_____V 2–2 nr
600_____V 1–2 nr
601_____Cep 5 20–1200 "qzit" (90)
602_____Cep 39 0–10 "qzit" (90)
603_____Cep 30 18–28 "qzit" (90)

604_____Cep 40 12–22 "qzit" (90)
605_____Cep 16 12–22 "qzit" (90)
606_____Cep 17 5–15 "qzit" (90)
607_____Cep 18 5–15 "qzit" (90)
608_____Cep 19 4–14 "qzit" (90)

609_____Cep 20 5–15 "aren arg" (90)
610_____Cep 1 32–159 "qzit" (90)
611_____V 22 nr
612_____V 21 nr
613_____V 30 14–762 "sr" (90)

614_____Cep 2 54–59 "qzit" (90)
615_____Cep 3 61–80 "qzit" (90)
616_____V 2–3 nr
617_____V 11 20–550 approx. "i.f." (90)
618_____V 19 25–570 approx. "i.f." (90)

619_____V 16 28–585 approx. "i.f." (90)
620_____V 3–2 nf nl (90)
621_____V 28 20–520 approx. "qzit" (90)
622_____V C2 60–475 "cg qzit" (90)
623_____V C2–1 72–120 "qzit" (90)

624_____V 18 15–360 approx. "i.f." (90)
625_____V 14 25–473 approx. "i.f." (90)
626_____V 20 20–500 approx. "i.f." (90)
627_____V 8 25–440 approx. "i.f." (90)
628_____V 13 20–280 approx. "i.f." (90)

629_____V 10 10–330 approx. "i.f." (90)
630_____V 5 22–248 approx. "i.f." (90)
631_____V 12 20–388 approx. "i.f." (90)

DHL Data

Sec. 30, T. 47 N., R. 26 W. —Continued

632_____V 7 30–52 approx. "i.f." (90)
633_____V 15 20–380 approx. "i.f." (90)

634_____V 2–3 nf "i.f." (90)
635_____V 27 15–52 "qzit" (90)
636_____V 26 0–6 "qzit" (90)
637_____V 17 20–225 approx. "i.f." (90)
638_____V Qzit Hole nf (nd)

639_____V 25 15–180 approx. "i.f." (90)
640_____Clpv 2 60–220 "gn" (nd)
641_____V 6 nr
642_____V 4 nr
643_____V V6 nf–1100 approx. "gn" (90)
644_____V V7 37–253 "qzit" (nd)
645_____V C1 29–1090 "qzit" (90)
646_____V C1–1 34–1220 "cg qzit" (65S)
647_____WK 5 40–428 "db" (90)
648_____WK 6 60–147 "qzit" (90)

649_____WK 1 70–nf "qzit" (90)
650_____V V1 nf–269 "cg" (90)
651_____V 6–2 nr
652_____V 32 58–871 "qzit" (63 nd)
653_____V 4–2 nf "jp" (SW)

654_____V 7–2 nf "qzit" (SW)
655_____V 29 51–940 "ch" (60 nd)
656_____WK 2 40–nf "qzit" (90)
657_____WK 3 55–nf "qzit" (90)
658_____WK 4 0–nf "qzit" (52 nd)

Sec. 31, T. 47 N., R. 26 W.

659_____Dv All 86–149 "sh qzit" (90)
660_____Dv A14 33–64 "i.f." (90)
661_____V 3 nr
662_____V 5 nr
663_____O 2 nf nl (52SE)

664_____Dv A6 0–160 "i.f." (90)
665_____O 3 nf nl (90)
666_____V 4 nr
667_____Dv A13 14–535 "db" (90)
668_____V 1 11–184 "jp" (90)

669_____V 2 17–541 "jp" (90)
670_____O 1 nf "db" (70SW)
671_____Dv A12 21–171 "gn or qzit" (90)

Sec. 29, T. 47 N., R. 26 W.

672_____Cc 101 7–2363 "qzit" (90)
673_____U C3 18–956 "qzit" (90)
674_____PL K1 40–nf "qzit" (75S)
675_____CM 103 22–1148 "qzit" (90)
676_____PL K5 nr

677_____U C1 57–431 "qzit" (44 NNW)
678_____U C6 43–714 "qzit" (90)
679_____U C7 23–493 "qzit" (90)
680_____Cp 4 36–1153 "qzit" (90)
Cp 4A 937–2927 (80–85 nd)
681_____U C5 12–32 "qzit" (65S)

682_____PL K4 nf "qzit" (75S)
683_____PL K2 nf "qzit" (74SSW)
[2]683A___U C2 15–1454 "qzit" (90)
684_____U C4 74–607 "qzit" (65S)
685_____PL K3 nf "qzit" (75S)

DHL Data

Sec. 29, T. 47 N., R. 26 W. —Continued

686_____CM 104 46–450 "qzit" (90)
687_____U C105 70–500 alt gn (51S)
688_____Cp 3 18–2037 "qzit" (63S)
689_____Cp 2 22–2898 "h mt jp i.f." (90)
690_____Cp 1 21–2072 "h chy i.f." (90)

691_____U C111 0–754 qzit (45S)
692_____U C107 58–350 pyc (51S)
693_____U C104 8–696 pyc & i.f. fragments (48S)
694_____U C106 24–234 i.f. (51S)
695_____U C103 15–728 i.f. (48S)

696_____Ci 8 50–390 qzit cg (46 S1W)
697_____Ci 7 46–594 gw (44½ S5W)
698_____CM 108 3–772 "qzit" (60SE)
699_____CM 114 11–582 "qzit" (78 SSE)
700_____CM 120 7–455 "qzit" (60 SSE)

701_____U C113 15–1012 i.f. (90)
702_____CM 115 10–433 "i.f." (70S)
703_____CM 102 25–766 "di" (60 S38E)
704_____CM 118 22–850 "qzit" (90)
705_____CM 116 16–407 "qzit" (90)

706_____CM 119 19–970 "ore" (90)
707_____CM 117 27–254 "di" (60 N38W)
708_____CM 105 15–1151 "qzit" (90)
709_____Ci 6 15–637 qzit & local cg (45 S1E)
710_____CM 113 11–581 "qzit" (75 SSW)

711_____Ci 5 9–514 gw cg (90)
712_____U C114 6–1153 "i.f." (90)
713_____U C102 15–521 "i.f." (48S)

Sec. 32, T. 47 N., R. 26 W.

714_____Ci 4 14–415 jp i.f. (45 S2E)
715_____CM 107 23–67 "di" (90)
716_____CM 109 33–187 "jp–lbo" (90)
717_____CM 110 26–706 "jp–lbo" (90)
718_____Ci 2 10–606 sly h i.f. (45 S9E)

719_____CM 106 6–953 "cg" (90)
720_____CM 111 16–1345 "dk" (90)
721_____CM 112 6–1110 "qzit" (90)
722_____U C112 15–906 "i.f." (90)
723_____U C110 12–586 "i.f." (45S)

724_____U C101 2–343 i.f. (50S)
725_____Ci 1 5–526 cg (45S)
726_____Ci 3 27–724 mt ch i.f. (44½ S4E)
727_____CM B_2 17–291 "jp–lbo" (90)
728_____CM B_1 12–455 "jp–lbo" (58S)

DHL Data

Sec. 28, T. 47 N., R. 26 W.

729_____Ccl 9 12–55 massive h (90)
730_____Ccl 3 38–51 soft oxid i.f. (90)
731_____Ccl 4 26–43 oxid chy h i.f. (90)
732_____Ccl 2 7–10 oxid chy h i.f. (90)
733_____Ccl 1 16–22 oxid chy h i.f. (90)

734_____Ccl 10 7–35 oxid i.f. (90)
735_____Cc 11 24–1738 oxid mar i.f. (90)
736_____Ccl 8 17–27 oxid mar i.f. (90)
737_____Ccl 6 36–45 arg clastic rk & oxid i.f. (90)
738_____Ccl 7 38–66 oxid chy mar i.f. (90)

739_____Ccl 5 45–66 oxid chy h mar i.f. (90)
740_____U C109 53–373 clastic rock–cg (45S)
741_____U C108 20–667 pyc with ch & h fragments (45S)

Sec. 27, T. 47 N., R. 26 W.

742_____Cc 2 16–150 oxid ch lim h i.f. (90)
743_____Cce 39 46–2070 oxid i.f. (90)
744_____Cce 32 16–1630 oxid h ch & granular oxid mt ch i.f. (90)
745_____Cce 34 53–1167 mar i.f. (47 N7W)
Cce 37 43–1336 oxid h i.f. (90)
746_____Cce 41 77–1028 oxid chy h goet i.f. (90)

747_____Cc 31 13–72 oxid chy h i.f. (90)
748_____Cce 48 29–2413 oxid goet leop i.f. (90)
Cce 48A 2353–2442 (90)
749_____Cc 3 16–150 oxid h ch i.f. (45S)
750_____Cc 4 18–147 hard chy h i.f. (45S)

751_____Cc 5 21–150 chy h i.f. (45S)
752_____Cce 33 21–1728 oxid chy h i.f. (90)
753_____Cce 35 38–220 oxid chy h i.f. (90)
Cce 36 23–1552 db (80S)
754_____CM 101 24–515 "jp" (70S)
755_____Cc 6 ledge not reached–10 (90)
756_____Cc 29 12–31 db (90)
757_____Cc 30 15–70 soft h (90)
758_____Cce 42 10–2122 oxid h i.f. (90)
759_____Cce 38 13–1436 oxid h goet i.f. (90)
760_____Cce 40 18–1111 oxid h i.f. (90)

761_____Cce 43 17–136 "h chy i.f." (43 N51E)
762_____Cce 44 20–66 "h chy i.f." (45 N3E)
763_____CM 102 32–220 "dk" (60S)
764_____Cc 27 8–90 oxid chy goet h i.f. (90)

DHL	Data
	Sec. 27, T. 47 N., R. 26 W. —Continued
765	Cc 28 4–62 chy h goet leop i.f. (90)
766	Cce 86 4–1005 oxid h mar i.f. (90)
767	CM 103 28–356 "jp" (60S)
768	Cce 51 34–744 oxid chy h mar i.f. (90)
769	Cce 54 56–1675 oxid h mar i.f. (90)
770	Cce 58 66–647 oxid h goet leop i.f. (90)
771	Cce 50 32–675 oxid chy goet i.f. (90)
772	Cc 25 18–95 oxid chy goet i.f. (90)
	Cce 47 24–1022 "h goet chy i.f." (90)
	Cce 47A 954–2026 (90)
773	Cc 26 14–92 oxid chy h i.f. (90)
774	MH 207 49–119 "qzit" (45S)
775	CM 104 20–267 "jp–lo" (60S)
776	Cce 56 25–746 qzit–gw–cg (90)
777	MH 211 18–100 "i.f.–qzit" (45S)
778	Cce 55 13–750 gw with i.f. fragments (90)
779	MH 205 17–190 "lim chy ore" (45S)
780	Cce 53 20–755 oxid h mar ch i.f. (90)
781	MH 212 16–125 "sil o" (45S)
782	Cce 46 19–724 mixed gw & oxid i.f. (90)
783	Cc 24 13–45 md–intr (90)
784	Cc 23 5–69 oxid h goet i.f. (90)
785	Cce 87 4–1160 oxid i.f. (90)
786	Cce 84 49–863 oxid h mt i.f. (90)
787	MH 208 21–190 "sil o" (45S)
788	MH215 20–150 "sil o with grn sly bands" (45S)
789	MH 203 17–190 "sil o" (45S)
790	Cc 21 10–72 oxid chy h i.f. (90)
791	Cce 59 20–1544 oxid h goet chy leop i.f. (90)
792	Cc 19 5–84 oxid chy h i.f. (90)
793	Ccel 80 16–18 "h chy i.f." (90)
794	Cc 22 14–92 oxid chy h i.f. (90)
795	Cce 88 0–1011 oxid h chy i.f. (90)
796	MH 206 8–190 "sil o" (45S)
797	MH 216 22–150 "sil o" (45S)
798	MH 213 11–125 "sil o" (45S)
799	MH 219 24–150 "chy i.f." (45S)
800	MH 210 14–150 "i.f.–qzit" (45S)
801	Ccel 69 11–15 "h chy i.f." (90)
802	Ccel 68 7–8 "h chy i.f." (90)
803	Ccel 67 8–10 "h chy i.f." (90)
804	Cc 18 4–44 "dk" (90)
805	Ccel 82 2–4 "h chy i.f." (90)
806	Ccel 81 12–13 "h chy i.f." (90)
807	Cce 57 9–725 oxid h mar i.f. (90)
808	MH 217 20–150 "chy i.f." (45S)
809	Cce 52 12–1209 oxid h mar i.f. (90)
810	MH 202 18–190 "sil o" (45S)
811	MH 214 11–125 "sil o" (45S)
812	MH 209 5–100 "sil o" (45S)
813	Ccel 70 13–16 "h chy i.f." (90)
814	Cc 11 5–25 "soj" (90)
815	Ccel 71 5–6 "h chy i.f." (90)
816	Ccel 66 7–10 "h chy i.f." (90)
817	Ccel 72 5–6 "h chy i.f." (90)
818	Cce 85 10–839 oxid i.f. (45 S1W)
819	Cce 83 24–790 partly oxid mt mar i.f. (90)
820	CM 105 13–442 "jp–lo" (60S)
821	CM 106 17–104 "jp" (60S)
822	MH 201 13–190 "sil o" (45S)
823	Cce 49 0–720 oxid h i.f. (90)
824	Cce 45 9–727 oxid h goet i.f. (90)
825	Cc 9 15–85 gw (90)
826	Ccel 73 12–14 "h chy i.f." (90)
827	Ccel 60 7–10 "h chy i.f." (90)
828	Ccel 65 7–10 "h chy i.f." (90)
829	Cc 14 6–64 "soj" (45S)
830	Ccel 62 6–9 "h chy i.f." (90)
831	Ccel 64 10–14 "h chy i.f." (90)
832	Cc 15 11–88 "sil ho" (45S)
833	CM 108 13–505 "jp–lo" (60S)
834	MH 204 15–190 "lim i.f.–qzit" (45S)
835	CM 107 9–806 "jp–lbo" (60S)
836	MH 218 19–100 "qzit–chy i.f." (45S)
837	CM 113 14–500 "jp–lo" (60S)
838	Ccel 74 1–3 "h chy i.f." (90)
839	CM 111 4–800 "jp–lbo" (60S)
840	CM 112 6–728 "jp–lo" (60S)
841	Cc 8 13–100 oxid h ch i.f. (90)
842	Ccel 61 3–5 "h chy i.f." (90)
843	Cc 12 12–106 "oxid i.f.–lo" (45S)
844	Ccel 63 12–18 "h chy i.f." (90)
845	Cc 17 5–93 "sil lbo" (90)
846	Ccel 75 10–12 "h chy i.f." (90)
847	Cc 7 18–100 chy h i.f. (90)
848	Cc 13 24–96 "hoj" (45S)
849	Ccel 79 9–12 "h chy i.f." (90)
850	Cc 20 11–20 "soj"–gw (90)
851	Ccel 76 14–16 "h chy i.f." (90)
852	Cc 10 17–179 chy h i.f. (45S)
853	Ccel 77 21–23 "h chy i.f." (90)
854	Ccel 78 26–27 "h chy i.f." (90)
	Sec. 26, T. 47 N., R. 26 W.
855	Ch 3 16–585 "oxid i.f.–lo" (90)
856	Ch 2 95–485 "lo" (60SE)
857	Cce 1 107–591 oxid h mar ch i.f. (90)
	Ch 7 111–380 "oxid i.f.–lo" (60SE)
858	Cce 2 85–366 oxid goet i.f. (90)
859	Ch 1 128–679 "lo" (60SE)
860	Ch 5 87–155 "qzit" (90)
861	Ch 4 45–88 "qzit" (90)
862	Cce 4 nf nl (90)
863	Ch 6 70–250 "i.f.–sl" (60SE)
864	Cce 5 nf nl (90)
865	Cce 3 nf nl (75 S75E)
866	Ch 9 163–168 "gr" (90)
867	Ch 8 131–140 "gr–sl" (90)
	Sec. 35, T. 47 N., R. 26 W.
868	Ch 1 120–nf "gr" (90)

[1] Plotted in Sec. 24, T. 47 N., R. 27 W. on company map.

[2] Lettered numbers plotted after preparation of rest of index map. (Drill hole Ccd 63 listed in Sec. 18 in company records, but plots in adjacent part of Sec. 7.)

[3] Shown at north edge of Sec. 19, T. 47 N., R. 26 W., in company records.

REFERENCES CITED

Aldrich, H. R., 1929, The geology of the Gogebic iron range of Wisconsin: Wisconsin Geol. and Nat. History Survey Bull. 71, 279 p.

Alling, H. L., 1947, Diagenesis of the Clinton hematite ores of New York: Geol. Soc. America Bull., v. 58, no. 11, p. 991–1018.

American Commission on Stratigraphic Nomenclature, 1961, Code of stratigraphic nomenclature: Am. Assoc. Petroleum Geologists Bull., v. 45, no. 5, p. 645–665.

Anderson, G. J., 1968, The Marquette district, Michigan, *in* Ridge, J. D., ed., Ore deposits of the United States, 1933–1967 (Graton-Sales Volume): New York, Am. Inst. Mining, Metall., and Petroleum Engineers, v. 1, p. 507–517.

Bailey, S. W., and Tyler, S. A., 1960, Clay minerals associated with the Lake Superior iron ores: Econ. Geology, v. 55, no. 1, p. 150–175.

Barghoorn, E. S., and Tyler, S. A., 1965, Microorganisms from the Gunflint Chert: Science, v. 147, no. 3658, p. 563–577.

Bath, G. D., 1951, Magnetic base stations in Lake Superior iron districts: U.S. Bur. Mines Rept. Inv. 4804, 16 p.

Bayley, R. W., Dutton, C. E., Lamey, C. A., and Treves, S. B., 1966, Geology of the Menominee iron-bearing district, Dickinson County, Michigan, and Florence and Marinette Counties, Wisconsin: U.S. Geol. Survey Prof. Paper 513, 96 p.

Becke, F., 1909, Ueber diaphthorite: Mineral. Petrog. Mitt., v. 27, p. 369–375.

Bissell, H. J., 1959, Silica in sediments of the upper Paleozoic of the Cordilleran area, *in* Ireland, H. A., ed., Silica in sediments—A symposium: Soc. Econ. Paleontologists and Mineralogists Spec. Pub. 7, p. 150–185.

Boyum, B. H., 1964, The Marquette mineral district, Michigan: Inst. Lake Superior Geology, 10th Ann., Ishpeming, Mich., May 1964, Guidebook, p. 17–37.

Cannon, W. F., and Gair, J. E., 1970, A revision of stratigraphic nomenclature for middle Precambrian rocks in northern Michigan: Geol. Soc. America Bull., v. 81, no. 9, p. 2843–2846.

Case, J. E., and Gair, J. E., 1965, Aeromagnetic map of parts of Marquette, Dickinson, Baraga, Alger, and Schoolcraft Counties, Michigan, and its geologic interpretation: U.S. Geol. Survey Geophys. Inv. Map GP–467.

Clark, S. P., Jr., 1961, A redetermination of equilibrium relations between kyanite and sillimanite: Am. Jour. Sci., v. 259, no. 9, p. 641–650.

Clark, S. P., Jr., Robertson, E. C., and Birch, A. F., 1957, Experimental determination of kyanite-sillimanite equilibrium relations at high temperatures and pressures: Am. Jour. Sci., v. 255, no. 9, p. 628–640.

Collins, W. H., 1925, North shore of Lake Huron: Canada Geol. Survey Mem. 143, 160 p.

Crowell, J. C., 1957, Origin of pebbly mudstones: Geol. Soc. America Bull., v. 68, no. 8, p. 993–1010.

Crump, R. M., 1948, Origin of hard ore of the Marquette district: Univ. Wisconsin, unpub. Ph.D. thesis, 87 p.

Curtis, C. D., and Spears, D. A., 1968, The formation of sedimentary iron minerals: Econ. Geology, v. 63, no. 3, p. 257–270.

Davis, J. F., 1965, A petrologic examination of iron-formation and associated graywackes and pyroclastic breccias within the Negaunee Formation of the Palmer area, Marquette district, Michigan: Univ. Wisconsin, unpub. Ph.D. thesis, 179 p.

Deer, W. A., Howie, R. A., and Zussman, J., 1962–1963, Rock-forming minerals: New York, John Wiley & Sons, 5 v.

Dzulyński, Stanislaw, and Walton, E. K., 1965, Sedimentary features of flysch and graywackes (Developments in sedimentary 7): New York, Elsevier Pub Co., 274 p.

Gair, J. E., 1964, Structures in the eastern part of the Marquette synclinorium [abs.]: Inst. Lake Superior Geology, 10th Ann., Ishpeming, Mich., May 1964, Program, p. 3–4.

——— 1965, Magnetic surveys of east and west ends of Palmer (Cascade) district, Marquette County, Michigan: U.S. Geol. Survey open-file map.

——— 1967, Influence of faulting on deposition of clastic interbeds in Negaunee Iron-Formation near Palmer, Michigan [abs.]: Inst. Lake Superior Geology, 13th Ann., East Lansing, Mich., May 1967, Program, p. 11–12.

——— 1968, Preliminary geologic map of the Palmer 7½-minute quadrangle, Marquette County, Michigan, 1:12,000: U.S. Geol. Survey open-file map.

Gair, J. E., and Simmons, G. C., 1968, Palmer Gneiss—an example of retrograde metamorphism along an unconformity: U.S. Geol. Survey Prof. Paper 600–D, p. D186–D194.

——— 1970, Metadiabase sills in Negaunee Iron-Formation south of Negaunee, Michigan: U.S. Geol. Survey Bull. 1324–A, p. 24–30.

Gair, J. E., and Thaden, R. E., 1968, Geology of the Marquette and Sands quadrangles, Marquette County, Michigan: U.S. Geol. Survey Prof. Paper 397, 77 p.

Gair, J. E., Thaden, R. E., and Jones, B. F., 1961, Folds and faults in the eastern part of the Marquette iron range, Michigan: U.S. Geol. Survey Prof. Paper 424–C, p. C76–C78.

Gair, J. E., and Wier, K. L., 1956, Geology of the Kiernan quadrangle, Iron County, Michigan: U.S. Geol. Survey Bull. 1044, 88 p.

——— 1964, Geologic and magnetic survey of a part of the Palmer 7½-minute quadrangle, Michigan: U.S. Geol. Survey open-file map.

Garrels, R. M., 1959, Rates of geochemical reactions at low temperatures and pressures, *in* Abelson, P. H., ed., Researches in geochemistry: New York, John Wiley & Sons, p. 25–37.

——— 1960, Mineral equilibria—At low temperature and pressure: New York, Harper & Bros., 254 p.

Goodwin, A. M., 1956, Facies relations in the Gunflint iron formation: Econ. Geology, v. 51, no. 6, p. 565–595.

——— 1962, Structure, stratigraphy, and origin of iron formations, Michipicoten area, Algoma District, Ontario, Canada: Geol. Soc. America Bull., v. 73, no. 5, p. 561–586.

Govett, G. J. S., 1966, Origin of banded iron-formations: Geol. Soc. America Bull., v. 77, no. 11, p. 1191–1212.

Grout, F. F., 1946, Acmite occurrences in the Cuyuna Range, Minnesota: Am. Mineralogist, v. 31, nos. 3–4, p. 125–130.

Gruner, J. W., 1922, Organic matter and the origin of the Biwabik iron-bearing formation of the Mesabi range: Econ. Geology, v. 17, no. 6, p. 407–460.

——— 1930, Hydrothermal oxidation and leaching experiments; their bearing on the origin of Lake Superior hematite-limonite ores: Econ. Geology, v. 25, no. 7, p. 697–719; no. 8, p. 837–867.

——— 1937, Hydrothermal leaching of iron ores of the Lake Superior type; a modified theory: Econ. Geology, v. 32, no. 2, p. 121–130.

——— 1944a, The structure of stilpnomelane reexamined: Am. Mineralogist, v. 29, nos. 7–8, p. 291–298.

——— 1944b, The composition and structure of minnesotaite, a common iron silicate in iron formations: Am. Mineralogist, v. 29, nos. 9–10, p. 363–372.

——— 1946, Mineralogy and geology of the taconites and iron ores of the Mesabi Range, Minnesota: St. Paul, Minn., Iron Range Resources and Rehabilitation Comm., and Minnesota Geol. Survey, 127 p.

Guild, P. W., 1957, Geology and mineral resources of the Congonhas district, Minas Gerais, Brazil: U.S. Geol. Survey Prof. Paper 290, 90 p.

Gundersen, J. N., and Schwartz, G. M., 1962, The geology of the metamorphosed Biwabik Iron Formation, eastern Mesabi district, Minnesota: Minnesota Geol. Survey Bull. 43, 139 p.

Halferdahl, L. B., 1961, Chloritoid—Its composition, X-ray and optical properties, stability, and occurrence: Jour. Petrology, v. 2, no. 1, p. 49–135.

Hall, A. L., 1930, Asbestos in the Union of South Africa: 2d ed., South Africa Geol. Survey Mem., v. 12, 324 p.

Hallimond, A. F., Dunham, K. C., Hemmingway, J. E., Taylor, J. H., Davies, W., Dixie, R. J. M., and Bannister, F. A., 1951, The constitution and origin of sedimentary iron

ores—A symposium: Yorkshire Geol. Soc. Proc., v. 28, pt. 2, p. 61–101.

Hamblin, W. K., 1958, The Cambrian sandstones of northern Michigan: Michigan Geol. Survey Div. Pub. 51, 146 p.

Han, T.-M., 1962, Diagenetic replacement in ore of the Empire mine of northern Michigan and its effect on metallurgical concentration [abs.], *in* Inst. Lake Superior Geology, 8th Ann., 1962, Program: Houghton, Mich., Michigan Coll. Mining and Technology, p. 7.

——— 1966, Textural relations of hematite and magnetite in some Precambrian metamorphosed oxide iron-formations [abs.] *in* Inst. Lake Superior Geology, 12th Ann., 1966, Program: Sault Ste. Marie, Mich., Michigan Technol. Univ., p. 10.

Hem, J. D., 1960, Restraints on dissolved ferrous iron imposed by bicarbonate redox potential, and pH: U.S. Geol. Survey Water Supply Paper 1459–B, p. 33–55.

Hewett, D. F., and Fleischer, Michael, 1960, Deposits of the manganese oxides: Econ. Geology, v. 55, no. 1, p. 1–55.

Hotchkiss, W. O., 1903, Some changes in the geology of the area about Palmer, Michigan: Univ. Wisconsin, unpub. B.S. thesis, 55 p.

——— 1919, Geology of the Gogebic Range and its relation to recent mining developments: Eng. and Mining Jour., v. 108, pt. 1, p. 443–452; pt. 2, p. 501–507; pt. 3, p. 537–541; pt. 4, p. 557–582.

Jackson, T. A., 1965, Power-spectrum analysis of two "varved" argillites in the Huronian Cobalt series (Precambrian) of Canada: Jour. Sed. Petrology, v. 35, no. 4, p. 877–886.

James, H. L., 1954, Sedimentary facies of iron-formation: Econ. Geology, v. 49, no. 3, p. 235–293.

——— 1955, Zones of regional metamorphism in the Precambrian of northern Michigan: Geol. Soc. America Bull., v. 66, no. 12, pt. 1, p. 1455–1488.

——— 1958, Stratigraphy of pre-Keweenawan rocks in parts of northern Michigan: U.S. Geol. Survey Prof. Paper 314–C, p. 27–44.

——— 1966, Chemistry of the iron-rich sedimentary rocks, chap. W *in* Data of geochemistry, 6th ed.: U.S. Geol. Survey Prof. Paper 440–W, 61 p.

James, H. L., Clark, L. D., Lamey, C. A., and Pettijohn, F. J., 1961, Geology of central Dickinson County, Michigan: U.S. Geol. Survey Prof. Paper 310, 176 p.

James, H. L., Dutton, C. E., Pettijohn, F. J., and Wier, K. L., 1968, Geology and ore deposits of the Iron River-Crystal Falls district, Iron County, Michigan: U.S. Geol. Survey Prof. Paper 570, 134 p.

Klein, Cornelis, Jr., 1966, Mineralogy and petrology of the metamorphosed Wabush Iron Formation, southwestern Labrador: Jour. Petrology, v. 7, no. 2, p. 246–305.

Knopf, E. B., 1931, Retrogressive metamorphism and phyllonitization: Am. Jour. Sci., 5th ser., v. 21, no. 121, p. 1–27.

Krauskopf, K. B., 1956, Dissolution and precipitation of silica at low temperatures: Geochimica et Cosmochimica Acta, v. 10, nos. 1–2, p. 1–26.

Krotov, B. P., 1940, On the occurrence in the Khalilovo iron ore deposits of magnetite formed from solutions of superficial origin at a low temperature: Akad. Nauk SSSR Doklady, v. 26, no. 8, p. 801–803.

Kuenen, P. H., and Migliorini, C. I., 1950, Turbidity currents as a cause of graded bedding: Jour. Geology, v. 58, no. 2, p. 91–127.

LaBerge, G. L., 1964, Development of magnetite in iron formation of the Lake Superior region: Econ. Geology, v. 59, no. 7, p. 1313–1342.

——— 1967, Microfossils and Precambrian iron-formation: Geol. Soc. America Bull., v. 78, no. 3, p. 331–342.

Lamey, C. A., 1931, Granite intrusions in the Huronian formations of northern Michigan: Jour. Geology, v. 39, no. 3, p. 288–295.

——— 1933, The intrusive relations of the Republic granite: Jour. Geology, v. 41, no. 5, p. 487–500.

——— 1934, Some metamorphic effects of the Republic granite: Jour. Geology, v. 42, no. 3, p. 248–263.

——— 1935, The Palmer gneiss: Geol. Soc. America Bull., v. 46, no. 7, p. 1137–1162.

Leith, C. K., 1925, Silicification of erosion surfaces: Econ. Geology, v. 20, no. 6, p. 513–523.

Leith, C. K., Lund, R. J., and Leith, Andrew, 1935, Pre-Cambrian rocks of the Lake Superior region: U.S. Geol. Survey Prof. Paper 184, 34 p.

Lepp, Henry, and Goldich, S. S., 1964, Origin of Precambrian iron formations: Econ. Geology, v. 59, no. 6, p. 1025–1060.

Lovering, T. G., 1962, The origin of jasperoid in limestone: Econ. Geology, v. 57, no. 6, p. 861–889.

MacGregor, A. M., 1927, The problem of the Precambrian atmosphere: South African Jour. Sci., v. 24, p. 155–172.

Mann, V. I., 1953, Relation of oxidation to the origin of soft iron ores of Michigan: Econ. Geology, v. 48, no. 4, p. 251–281.

Marsden, R. W., 1968, Geology of the iron ores of the Lake Superior region in the United States, *in* Ridge, J. D., ed., Ore deposits of the United States, 1933–1967 (Graton-Sales Volume): New York, Am. Inst. Mining, Metall., and Petroleum Engineers, p. 489–506.

Mengel, J. T., Jr., 1956, The relationship of clastic sediments to iron-formation in the vicinity of Palmer, Michigan: Univ. Wisconsin, unpub. M.S. thesis, 98 p.

Meyer, Charles, and Hemley, J. J., 1967, Wall rock alteration, *in* Barnes, H. L., ed., Geochemistry of hydrothermal ore deposits: New York, Holt, Rinehart and Winston, p. 166–235.

Miles, K. R., 1942, The blue asbestos-bearing banded iron formations of the Hamersley ranges, Western Australia: Western Australia Geol. Survey Bull. 100, p. 5–37.

Milton, Charles, and Eugster, H. P., 1959, Mineral assemblages of the Green River formation, *in* Abelson, P. H., ed., Researches in geochemistry: New York, John Wiley & Sons, p. 18–150.

Miyashiro, Ahiko, 1961, Evolution of metamorphic belts: Jour. Petrology, v. 2, no. 3, p. 277–311.

Moore, E. S., and Maynard, J. E., 1929, Solution, transportation, and precipitation of iron and silica: Econ. Geology, v. 24, no. 3, p. 273–303; no. 4, p. 365–402; no. 5, p. 506–527.

Nanz, R. H., 1953, Chemical composition of pre-Cambrian slates, with notes on the geochemical composition of lutites: Jour. Geology, v. 61, no. 1, p. 51–64.

Okamoto, G., Okura, T., and Goto, K., 1957, Properties of silica in water: Geochimica et Cosmochimica Acta, v. 12, no. 1–2, p. 123–132.

Ovenshine, A. T., 1965, Sedimentary structures in portions of the Gowganda Formation, north shore of Lake Huron, Canada: Univ. Calif., Los Angeles, unpub. Ph.D. thesis, 213 p.

——— 1970, Observations of iceberg rafting in Glacier Bay, Alaska, and the identification of ancient ice-rafted deposits: Geol. Soc. America Bull., v. 81, no. 3, p. 891–894.

Owens, J. S., 1965, [Discussion of "Origin of the Precambrian iron formations" by Lepp and Goldich, Econ. Geology, September-October, 1964, and "Development of magnetite in iron-formation of the Lake Superior region" by LaBerge, Econ. Geology, Nov., 1964]: Econ. Geology, v. 60, no. 8, p. 1731–1734.

Peacock, M. A., 1928, The nature and origin of the amphibole asbestos of South Africa: Am. Mineralogist, v. 13, p. 241–285.

Pettijohn, F. J., 1943, Basal Huronian conglomerates of Menominee and Calumet districts, Michigan: Jour. Geology, v. 51, no. 6, p. 387–397.

——— 1949, Sedimentary rocks: 1st ed., New York, Harper & Bros., 526 p. (2d ed., 1957).

Pettijohn, F. J., and Bastron, Harry, 1959, Chemical composition of argillites of the Cobalt series (Precambrian) [Ontario] and the problem of soda-rich sediments: Geol. Soc. America Bull., v. 70, no. 5, p. 593–599.

Plaksenko, N. A., 1959, O nekotorykh osobennostyakh stroeniya tolshchi metamorficheskikh porod dokembriya KMA, prichinakh izh vezniknoveniya i ikh stratigraficheskom znachenii [Certain structural features of Precambrian metamorphics of the Kursk magnetic anomaly, their causes and stratigraphic significance]: Akad Nauk SSSR Izv., Ser. Geol., 1959, no. 3, p. 46–64 [In Russian; Engl. translation pub. by Am. Geol. Inst., 1960].

Puffett, W. P., 1969, The Reany Creek Formation, Marquette County, Michigan: U.S. Geol. Survey Bull. 1274–F, p. 1–25.

——— 1974, Geology and ore deposits of the Negaunee 7½-minute quadrangle, Marquette County, Michigan: U.S. Geol. Survey Prof. Paper 788, 53 p.

Rezak, Richard, 1957, Stromatolites of the Belt series in Glacier National Park and vicinity, Montana: U.S. Geol. Survey Prof. Paper 294–D, p. 127–154.

Riedel, Alfredo, 1953, Remarques sur la systematique et la valeur stratigraphique de quelques stromatolithes du Moyen-Congo: Soc. Géol. France Bull., ser. 6, v. 3, pt. 7–8, p. 667–675.

Sakamoto, T., 1950, The origin of the pre-Cambrian banded iron ores: Am. Jour. Sci., v. 248, no. 7, p. 449–474.

Schreyer, W., and Yoder, H. S., Jr., 1959, Cordierite-water system: Carnegie Inst. Yearbook 58, p. 100–104.

Semenenko, J. P., Polovko, N. I., Zhukov, G. V., Ladieva, V. D., and Makukhina, A. A., 1957, Petrografiya zhelezisto-kremnistykh formatsii Ukrainskoi SSR [Petrography of siliceous iron-formation of the Ukrainian SSR]: Kiev, Akad. Nauk Ukrainskoi SSR, Inst. Geol. Nauk, 536 p. [Partial English translation by M. Blake, U.S. Geol. Survey, in James, 1966].

Shrock, R. R., 1948, Sequence in layered rocks: New York, McGraw Hill Book Co., 507 p.

Siever, Raymond, 1962, Silica solubility, 0°–200°C., and the diagenesis of siliceous sediments: Jour. Geology, v. 70, no. 2, p. 127–150.

Thompson, J. B., Jr., 1955, The thermodynamic basis for the mineral facies concept: Am. Jour. Sci., v. 253, no. 2, p. 65–103.

Trendall, A. F., and Blockley, J. G., 1970, The iron formations of the Precambrian Hamersley group, Western Australia (with special reference to the associated crocidolite): Western Australia Geol. Survey Bull. 119, 366 p.

Twenhofel, W. H., 1919, Pre-Cambrian and Carboniferous algal deposits: Am. Jour. Sci., 4th ser., v. 48, p. 339–352.

Tyler, S. A., 1949, Development of Lake Superior soft iron ores from metamorphosed iron-formation: Geol. Soc. America Bull., v. 60, no. 7, p. 1101–1124.

Tyler, S. A., and Barghoorn, E. S., 1954, Occurrence of structurally preserved plants in pre-Cambrian rocks of the Canadian Shield: Science v. 119, no. 3096, p. 606–608.

Tyler, S. A., Marsden, R. W., Grout, F. F., and Thiel, G. A., 1940, Studies of the Lake Superior pre-Cambrian by accessory-mineral methods: Geol. Soc. America Bull., v. 51, no. 10, p. 1429–1538.

Tyler, S. A., and Twenhofel, W. H., 1952, Sedimentation and stratigraphy of the Huronian of upper Michigan, Pts. 1, 2: Am. Jour. Sci., v. 250, no. 1, p. 1–27; no. 2, p. 118–151.

Van Hise, C. R., 1892, The iron ores of the Marquette district of Michigan: Am. Jour. Sci., 3d ser., v. 43, p. 116–132.

Van Hise, C. R., Adams, F. D., Bell, J. M., Hayes, C. W., and Leith, C. K., 1905, Report of the special committee for the Lake Superior region: Jour. Geology v. 13, p. 89–104.

Van Hise, C. R., and Bayley, W. S., 1895, Preliminary report on the Marquette iron-bearing district of Michigan: U.S. Geol. Survey, 15th Ann. Rept., p. 477–650.

——— 1897, The Marquette iron-bearing district of Michigan: U.S. Geol. Survey Mon. 28, 608 p., atlas.

Van Hise, C. R., and Leith, C. K., 1911, The geology of the Lake Superior region: U.S. Geol. Survey Mon. 52, 641 p.

Vickers, R. C., 1956, Geology and monazite content of the Goodrich Quartzite, Palmer area, Marquette County, Michigan: U.S. Geol. Survey Bull. 1030–F, p. 171–185.

Wadsworth, M. E., 1892, Subdivisions of the Azoic or Archaean in northern Michigan: Science, v. 20, p. 355; Am. Jour. Sci., 3d ser., v. 45, p. 72–73.

——— 1893, Report of the State Geologist for 1891–82: Michigan Geol. Survey Rept. 1891–1892, p. 59–73.

Walcott, C. D., 1914, Pre-Cambrian Algonkian algal flora: Smithsonian Misc. Colln., v. 64, no. 2, p. 77–156.

White, D. A., 1954, The stratigraphy and structure of the Mesabi Range, Minnesota: Minnesota Geol. Survey Bull. 38, 92 p.

Winchell, N. H., 1899, The geology of Minnesota: Minnesota Geol. and Nat. Hist. Survey, Final Rept., v. 4.

Wygant, T. C., and Mancuso, J. J., 1969, Organic structures from Negaunee (iron) formation, Marquette Range, Michigan [abs.], *in* Inst. Lake Superior Geology, 15th Ann., 1969, Program: Oshkosh, Wis., Wisconsin State Univ., p. 42.

INDEX

[Italic page numbers indicate major references]

☆U.S. GOVERNMENT PRINTING OFFICE: 1975 O—585-476/132